5-2017

# Reversible silencing of spinal neurons unmasks a left-right coordination continuum.

Amanda Marie Pocratsky
*University of Louisville*

# REVERSIBLE SILENCING OF SPINAL NEURONS UNMASKS A LEFT-RIGHT COORDINATION CONTINUUM

By

Amanda Marie Pocratsky
B.S., Purdue University, 2010
M.S., University of Louisville, 2013

A Dissertation
Submitted to the Faculty of the
School of Medicine at the University of Louisville
in Partial Fulfillment of the Requirements
for the Degree of

Doctor of Philosophy
in Anatomical Sciences and Neurobiology

Department of Anatomical Sciences and Neurobiology
University of Louisville
Louisville, Kentucky

May 2017

REVERSIBLE SILENCING OF SPINAL NEURONS UNMASKS A LEFT-RIGHT COORDINATION CONTINUUM

By

Amanda Marie Pocratsky
B.S., Purdue University, 2010
M.S., University of Louisville, 2013

A Dissertation Approved on

February 24, 2017

by the following Dissertation Committee:

_____
Dissertation Co-Director: Dr. David S. K. Magnuson

_____
Dissertation Co-Director: Dr. Scott R. Whittemore

_____
Dr. Martha Bickford

_____
Dr. Dena Howland

_____
Dr. Nicholas Mellen

DEDICATION

This dissertation is dedicated to my parents,

Mark and Carol Pocratsky,

who have always been and always will be my biggest supporters.

Thank you.

ACKNOWLEDGEMENTS

First, I would like to thank my committee members, Drs. Martha Bickford, Dena Howland, and Nick Mellen, for their guidance and support throughout my graduate research experience. I would like to thank the Kentucky Spinal Cord Injury Research Center core personnel: Darlene Burke, Johnny Morehouse, Christine Yarberry, and Jason Beare. Without their expertise and support, none of this work would have been possible. I would also like to extend my appreciation to all the Magnuson and Whittemore lab members as they have truly become a part of my scientific family.

Finally, I would like to express my deepest gratitude to my two mentors: Dr. David S.K. Magnuson and Dr. Scott R. Whittemore. They have profoundly changed my life. I am forever indebted to them. Thank you.

ABSTRACT

REVERSIBLE SILENCING OF SPINAL NEURONS UNMASKS A LEFT-RIGHT COORDINATION CONTINUUM

Amanda Marie Pocratsky

February 24, 2017

This dissertation is focused on dissecting the functional role of two anatomically-defined pathways in the adult rat spinal cord. A $Tet^{On}$ dual virus system was used to selectively and reversibly induce enhanced tetanus neurotoxin expression in L2 neurons that project to L5 (L2-L5) or C6 (long ascending propriospinal neurons, LAPNs). Results focus on the changes observed during overground locomotion.

The dissertation is divided into four chapters. Chapter One is a focused introduction to locomotion, including its broad description, the central mechanisms of its expression, how genetic-based approaches defined these mechanisms, and the limitations in these approaches. It concludes with details of the silencing paradigm used here and a summary of the main findings.

Chapter Two describes the functional consequences of silencing L2-L5 interneurons. The focus is on selective disruption of hindlimb coordination during overground locomotion, revealing a continuum from walk to hop. These changes are independent of speed, step frequency, and other spatiotemporal features of gait. Left-right alternation was restored during swimming and stereotypic

exploration, suggesting a task-specific role. Silencing L2-L5 interneurons partially uncoupled the hindlimbs, allowing spontaneous shifts in coordination on a step-by-step basis. It is proposed this pathway distributes temporal information for left-right hindlimb alternation, securing effective coordination in a context-dependent manner.

Chapter Three focuses on the consequences of silencing LAPNs.Three patterns of interlimb coupling are disrupted: left-right forelimb, left-right hindlimb, and contralateral hindlimb-forelimb coordination. Observed again was a context-dependent continuum from walk-to-hop, irrespective of step frequency, speed, and the salient features that define locomotion. However, instead of spontaneous shifts in coordination as observed from L2-L5 interneuron silencing, the breadth of coupling patterns expressed were maintained on a step-by-step basis. It is proposed that this ascending, inter-enlargement pathway distributes temporal information required for left-right alternation at the shoulder and pelvic girdles in a context-dependent manner.

Collectively, these data suggest that L2-L5 interneurons and LAPNs are key pathways that distribute left-right patterning information throughout the neuraxis. The functional role(s) of these pathways are exquisitely gated to the context at hand, suggesting that the locomotor circuitry undergoes functional reorganization thereby endowing or masking the silencing-induced disruptions to interlimb coordination.

TABLE OF CONTENTS

PAGE

LIST OF FIGURES

LIST OF TABLES

TABLE PAGE

# CHAPTER I

# A FOCUSED INTRODUCTION TO LOCOMOTION

## An introduction to locomotion

Locomotion is a fundamental behavior that allows animals to move in order to satisfy their needs, whether it is searching for food, escaping predators, or simply traversing through various environments. It can take the form of swimming, flying, and overground stepping across various species. While its expression appears effortless, locomotion is a complex motor behavior that reflects the coordination of numerous muscles throughout the body. How this movement is governed can be understood at multiple levels.

From a broad perspective, locomotion can be described by the stereotypic, repeated patterns of stepping, called gait. Walking, trotting, and galloping are traditional gaits; however, alternation is the preferred gait observed across insects, amphibians, reptiles, birds, and mammals[1-7]. As a function of speed, gait can be quantitatively described by a set of spatiotemporal parameters (Figure 1)[8]. This interrelationship is well-documented across as well as within various taxa[1,7,9-17] with studies revealing that not only do animals have a broad repertoire of locomotor gaits, but there are also preferred methods to switch between them[16].

## Central control of locomotion: a historical perspective

The planning and initiation stages of locomotion originates in supraspinal centers, including the cortex, basal ganglia, midbrain, and hindbrain[18-21]. However, the neuronal elements required to express locomotion are contained entirely within the spinal cord[7,22-24]. It is in the spinal cord that the two salient features which define locomotion are generated: rhythm and pattern[25]. Rhythm and pattern are inextricably linked, but functionally distinct phenomena.

Rhythm is the locomotor “clock.” It is the strong, regular, and repeated sequence of steps that defines the various gaits (e.g. repeating step sequence 1-2-3-4). Alternatively, pattern is the locomotor “tempo” or how quickly the limbs move within the defined step sequence. Both intra- and left-right limb movements generate this patterned behavior[25]. As a whole, the spinal networks that secure rhythm and pattern are called locomotor central pattern generators (CPGs)[26] with the cervical and lumbar spinal enlargements serving as hubs for the forelimbs and hindlimbs, respectively[25]. The hindlimb CPG is of particular interest, in part due to its major role in generating the propulsive forces required for movement[27-29] and its clinical significance for functional recovery after spinal cord injury[30]. Therefore, research focused intensely on two key questions: (1) where are the neuronal components that form the CPG located within the lumbar spinal cord and (2) how does this network, as an integrated unit, control the precise timing and pattern of hindlimb movements?

Studies performed in the spinalized cat or isolated neonatal rodent spinal cord revealed that the hindlimb CPG network is distributed throughout the caudal

thoracic and lumbar spinal cord, with the rostral lumbar segments showing enhanced capacity for rhythmic activity[23,31-39]. Throughout this rostrocaudal distribution, the putative CPG neurons are concentrated in ventral gray matter of the spinal cord[33,37,40-43]. After establishing the positional framework of the hindlimb CPG network, scientists then set out to determine how this unit produced the rhythm and pattern characteristic of locomotion.

Rhythm generation likely stems from ipsilateral-projecting neurons that directly excite motor neurons[25]. These neurons are distributed throughout the lumbar neuraxis and appear to act as one rhythmic network when locomotion is induced. Alternatively, intralimb coordination is secured through ipsilateral inhibitory neurons that coordinate stereotypic alternation between flexor and extensor motor neurons[32,44-48]. By default, commissural interneurons that anatomically interconnect the two sides of the spinal cord govern left-right coordination[25]. This diverse class of neurons is further described below.

There are two types of commissural interneurons: (1) intrasegmental neurons which likely coordinate segmental, homonymous muscles[49,50] and (2) intersegmental neurons, which have long axons that project at least two spinal segments in either ascending or descending directions[51-54]. While ascending commissural interneurons have been shown to play an important role in coordinating left-right activity in the neonatal mouse[55], descending commissural interneurons are more involved in finer aspects of pattern generation (e.g. crossed flexor-extensor coordination) instead of strict left-right alternation[56-59].

The depth of these studies were at the network-level using traditional methods such as electrophysiological recordings and basic anatomical tracing. While these results have built our foundational understanding of the hindlimb CPG architecture, one fundamental issue remains: how do distinct neurons within this network secure specific motor behaviors? To address this question, more discrete methods that provide increased specificity are required.

**Genetic dissection of the locomotor circuitry**

Cracking of the genetic code that programs neuronal identity in the developing mouse spinal cord[60] has enabled unparalleled insight into the functional role of transcriptionally-specified neurons during locomotion[61]. This genetic-based approach affords two primary advantages, the ability to (1) target specific neuronal subpopulations within the central nervous system and (2) reproducibly perform complex manipulations[62].

To summarize, ipsilateral and excitatory neurons that express the transcription factor short stature homeoprotein 2 (SHOX2) constitute one component of the rhythm generating circuitry[63]. Currently, the molecular identification of other core, rhythmic neurons remains elusive. Intralimb coordination is expressed through the synergistic actions of ipsilateral, inhibitory V1 and V2b neurons[64,65] ("V" indicates a ventrally-derived class of neurons). With additional input from V2a neurons[66,67], left-right coordination is secured through the ascending commissural V0 interneurons[68,69]. Conversely, the descending commissural V3 interneurons are dispensable in left-right alternation[70]. From this body of work, we now understand at the transcriptional level the formation and

function of discrete spinal circuits. The next goal was to apply this knowledge at the systems level to determine how these pathways create the traditional locomotor gaits.

Emerging from this analysis was the modular organization hypothesis, which suggests dedicated neuronal ensembles encode distinct gaits[17,61] (summarized in Figure 2). Central to this hypothesis is the following: (1) locomotor gaits are expressed through distinct neuronal ensembles, which are (2) recruited in a speed-dependent fashion. These ensembles are genetically defined and engaged in an ascending order (as a factor of speed) to ensure the limbs maintain effective left-right coordination. Therefore, the walk-trot ensemble secures the limbs in alternation at low-to-moderate speeds and step frequencies (Figure 2, lower quadrant). With increasing speed, the locomotor network is reconfigured to generate asynchronous left-right movements indicative of galloping (Figure 2, middle quadrant). The bounding ensemble is selected at greatest speeds to produce left-right synchrony (Figure 2, upper quadrant). Importantly, this hypothesis upholds the well-defined relationship between gait-associated spatiotemporal parameters and locomotor speeds[10]. While the manipulation of genetically-encoded neurons has transformed our understanding of how the locomotor circuitry creates various behaviors, there are fundamental concerns endemic to this approach that must be addressed.

**Fundamental concerns regarding genetic-based approaches**

First, each “distinct” class of genetically-encoded neurons is actually comprised of multiple subpopulations (e.g. 30 subtypes for the V1 class alone)[62,71].

This is substantiated by a mixed phenotype of excitatory/inhibitory, ipsilateral/commissural, and ascending/descending projections[60,72]. Thus, each class is not pure, but instead the amalgamation of numerous traits. Further confounding this are documented functional differences between (as well as within) subtypes[67-69,73,74], an important caveat to consider as it relates to the issues described below.

Second, ablating progenitor domains that give birth to neuronal classes (and their subclasses) concurrently alters the non-targeted spinal circuitry. For example, when one domain is removed the neighboring domains trans-specify or adopt the identity of what is lost[61,68,75]. This makes it difficult to determine whether the functional changes observed are due to the actual loss of neurons or the *de novo* function of the trans-specified, "hybrid" neurons.

Third, ablating neurons born from the progenitor domains in the embryonic or postnatal spinal cord results in developmental compensation[76]. As the animal matures, the spinal cord will offset this neuronal loss through the formation of new circuits or connections. Moreover, there are striking differences in both morphology and functional role between the postnatal and adult genetically-encoded classes[77,78]. To circumnavigate this issue, some researchers have conditionally ablated neuronal classes after the animal has fully matured[67]. However, these studies are few and far between.

Fourth, these genetically-identified neurons are not enriched in the lumbar enlargement. Instead, they are distributed throughout the entire spinal cord as well as supraspinal centers[71]. Therefore, genetic ablations theoretically remove a

substantial component of the entire neuraxis. In an attempt to increase specificity, recent effort has been made to selectively knockout neurons within confined segments[67]. Nonetheless, these studies are limited in number and scope.

Finally, the significant majority of these studies were performed using isolated embryonic or neonatal spinal cords[72]. While this technique provides exquisite control in teasing out network perturbations in response to genetic ablations, it also removes two omnipresent regulators of the locomotion: supraspinal drive and sensory feedback. Therefore, the conclusions drawn from these studies are profoundly dependent on the following: the neuronal ensembles that elicit fictive, “locomotor-like” behavior faithfully recapitulate the neuronal ensembles (and their dynamics) that execute stereotypic locomotion. Of the few *in vivo* studies performed, nearly all used treadmill-based locomotion as the primary functional readout[67]. Although the treadmill produces a consistent number of steps over a large (and controllable) range of speeds[14], it is a fundamentally different stepping environment compared to the more natural overground setting[16,17]. Unsurprisingly, this impacts the emergence of gaits due to conflicting input from visual, vestibular, and proprioceptive sources[7,14,16,79].

In light of these limitations, to what level of confidence can we say a genetically-encoded class of neurons sub-serves a specific physiological role in the natural expression of locomotion? Shockingly, this question is rarely addressed. To avoid these pitfalls, the ideal method would be to acutely and reversibly silence spinal pathways in the mature, naïve animal while it freely steps during overground locomotion[76].

**Acute and reversible silencing of spinal neurons in the naïve adult**

Recently, Kinoshita *et al* developed an innovative dual virus approach to silence anatomically-defined pathways independent of cell-specific promoters[80]. This is an inducible $Tet^{On}$ system consisting of two viral constructs (AAV2-rtTAV16, lenti-eTeNT) (Figure 3). Through intraspinal injections, neurons are doubly infected at the level of their cell body with AAV2-rtTAV16 and at their synaptic terminal field with lenti-eTeNT. Giving *ad libitum* doxycycline in the drinking water induces eTeNT (enhanced tetanus neurotoxin) expression, which prevents synaptic vesicle release at the terminal field thereby silencing neurotransmission. This system is described in more detail below (refer to Table 1 and **Error! Reference source not found.** for additional detail).

The lentiviral HiRet-TRE-EGFP.eTeNT is based on the HIV-1 vector, which is pseudotyped with a fusion envelope glycoprotein to increase (and sustain) viral gene transduction[81-83]. The lentiviral vector is injected at the terminal field where it is then retrogradely transported ("HiRet" = "highly-efficient retrograde") to cell body for subsequent neuronal infection. The second construct is AAV2-CMV-rtTAV16, which is a neurotropic virus that expresses the doxycycline activated $Tet^{On}$ sequence, a variant of the reverse tetracycline transactivator (rtTAV16)[84]. Without doxycycline, neurons will constitutively express rtTAV16 alone. Doxycycline permits rtTAV16 to bind to its promoter TRE (tetracycline responsive element), which induces EGFP.eTeNT transgene expression. EGFP.eTeNT is a fusion protein which permits fluorescent detection of silenced terminals (enhanced green fluorescent protein, EGFP). At the terminal, eTeNT proteolytically cleaves vesicle-

associated membrane protein 2 (VAMP2) to block exocytosis of synaptic vesicles and suppress neurotransmission. Removing doxycycline restores neurotransmission. Importantly, the expression of eTeNT does not affect cell survival, morphology, or anatomical distribution of infected neurons[85].

Here, we use this $Tet^{On}$ system to acutely and reversibly silence pathways in the adult rat spinal cord with overground locomotion as the primary functional outcome measure. This dissertation is focused on the consequences of silencing two distinct pathways: (1) spinal L2 neurons that project to L5 (L2-L5 interneurons) and (2) spinal L2 neurons that project to C6 (long ascending propriospinal neurons, LAPNs). Results from these studies are described in Chapters Two and Three, respectively, followed by an inclusive discussion that briefly highlights parallels found between them. The main conclusions drawn from this body of work are as follows.

Silencing L2 neurons that project to either L5 or C6 disrupts left-right coordination. Here, we observed a continuum of interlimb coupling patterns ranging from walking to hopping. These changes occurred independently from the fundamental principles of locomotion: rhythm, intralimb coordination, speed, and its relationship to spatiotemporal gait indices (stance, swing, stride, etc). Strikingly, the functional consequences of silencing these spinal pathways are exquisitely gated towards the behavioral context at hand. Specifically, when animals were stepping in a “non-exploratory, going from A to B mode,” we saw profound changes in interlimb coordination. However, if the animal stepped in an “exploratory mode,” the silencing-induced effects were immediately abolished. Even after taking into

account the speed at which these behaviors were expressed, we still saw a “stepping mode” modulation of the silencing-induced phenotype. Moreover, hindlimb alternation was immutable to silencing-induced perturbations when the limbs were unloaded during swimming. Collectively, these data indicate that L2-L5 interneurons and LAPNs are key distributors of left-right patterning information to secure effective coordination during overground locomotion, but perhaps in a task-specific manner.

In light of these findings, we believe that the conditional silencing of spinal pathways has unmasked a context-driven reconfiguration of the lumbar central pattern generating circuitry. During certain conditions, the “functional demand” for these L2 projection pathways is high. The nervous system calls upon them to distribute temporal information throughout the neuraxis immediately. Therefore, when these neurons are not functionally available to do so, the consequences are profound. However, when the behavioral context changes such that the functional demand for these pathways is low, the locomotor behavior is not impaired. This multifunctional reorganization of the lumbar locomotor circuitry endows the system with incredible flexibility, allowing a breadth of motor actions to be expressed on a moment-by-moment basis. From a clinical perspective, the lumbar locomotor circuitry is the gateway to walking. Therefore, understanding how this circuitry governs effective stepping is tantamount to harnessing its intrinsic functional capacity as a powerful substrate for locomotor recovery after spinal cord injury.

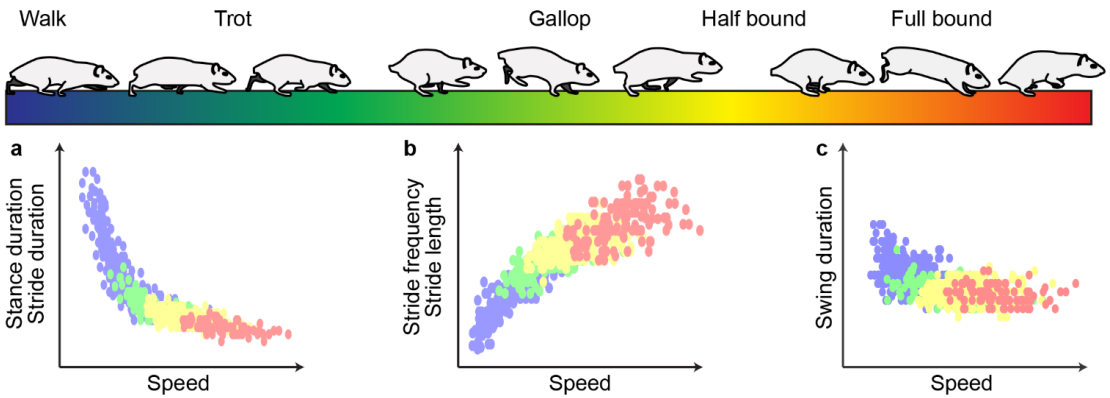


**<u>Figure 1</u>. The Relationship Between Gait, Speed, And The Spatiotemporal Indices That Govern Locomotion.** The top panel illustrates the traditional locomotor gaits schematically (half-bound not shown, but is typified by the forelimbs "galloping" and the hindlimbs "bounding"). (**a**) During slower speeds when the animals are walking or trotting (blue), the stance duration (time the paw is in contact with the ground) and stride duration (sum of stance and swing durations) are increased. When animals transition to other gaits with increased speed (gallop=green, half-bound=yellow, full-bound=red), these durations will exponentially decrease. (**b**) There is a linear relationship between speed and stride frequency (the number of strides taken per unit time) as well as stride length (the distance the paw travels with each step). Therefore, as animals increase their speed and switch between gaits, the stride frequency and length will increase as well. (**c**) Swing duration (the amount of time the paw is in the air) does not change substantially with speed between the various gaits. Plots were generated from a sampling of preliminary hindlimb data (Chapter Three).

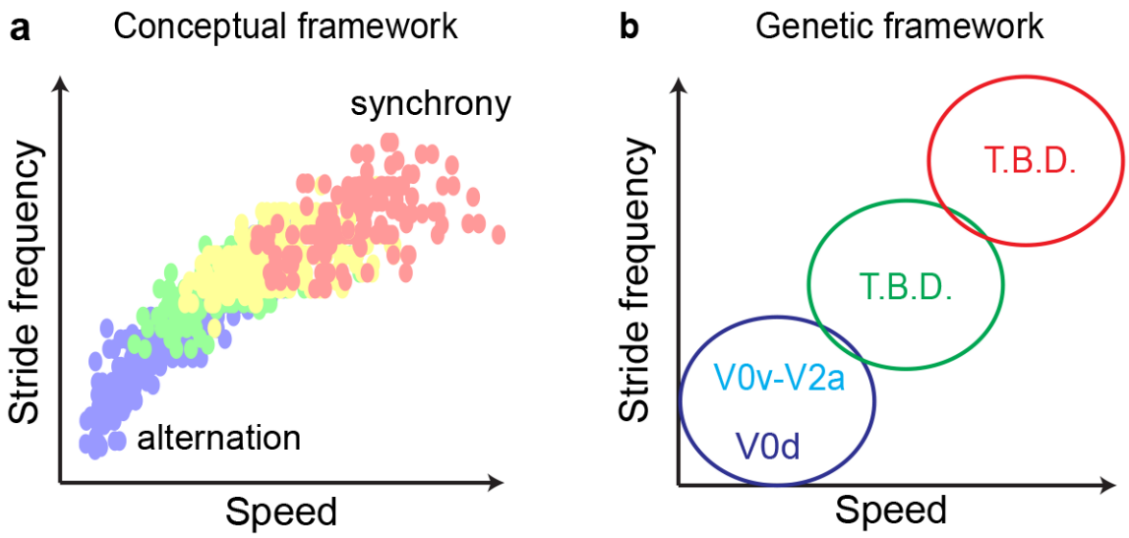




**Figure 2. Modular Organization Of Locomotor Circuitry.**

(**a**) The conceptual framework for the genetic-based modular organization hypothesis. Here, discrete pathways are selectively recruited in a speed and step-frequency dependent fashion in order to express the various gaits (shown in color). (**b**) Schematic illustrating the principles behind the modular organization hypothesis. Each circle represents a locomotor gait. Within each circle are the genetically-identified pathways that have been implicated in expressing that particular gait. To date, the V0d interneurons are directly involved in the slower, alternating gait (walk)[17]. The V0v-V2a microcircuit governs the faster alternating gait (trot)[17]. Genetically-encoded pathways responsible for the more synchronous gaits (green=gallop; red=bound) have not been identified.

*Figure 3*

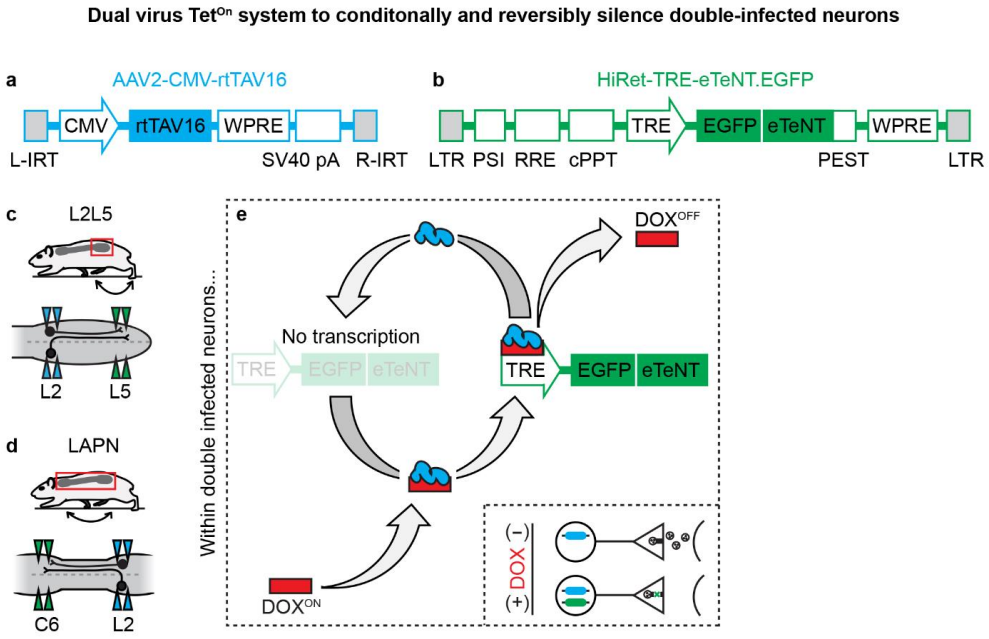


**<u>Figure 3</u>. Tet$^{On}$ approach to silence spinal pathways in the adult rat.**

(**a**) AAV2 construct constitutively expresses reverse tetracycline transactivator, VP16 ("AAV2-rtTAV16"). (**b**) Lentiviral construct expresses eTeNT.EGFP upon activation of Tetracycline Responsive Element promoter (TRE; "lenti-eTeNT"). (**c**) Injections to silence L2-L5 interneurons (bilateral L2 injections of AAV2-rtTAV16; L5 injections of lenti-eTeNT). (**d**) Injection protocol to silence LAPNs (bilateral L2 injections of AAV2-rtTAV16; C6 injections of lenti-eTeNT). (**e**) Within double infected neurons, rtTAV16 (blue) is constitutively expressed. rtTAV16 is activated by doxycycline (red), allowing it to bind to TRE promoter. TRE induces eTeNT.EGFP expression, which cleaves vesicle associated membrane protein 2 thereby suppressing neurotransmission. Removing doxycycline reverse rtTAV16 binding from TRE promoter, shutting off expression of eTeNT to restore neurotransmission. Refer to Tables 1 and 2 for further detail on constructs.

**Table 1. AAV2-CMV-rtTAV16 construct features.**

This construct constitutively expresses reverse tetracycline transactivator 16 (rtTAV16) under the control of the cytomegalovirus promoter (CMV)[80]. When activated by doxycycline, rtTAV16 binds to its promoter (Tetracycline Responsive Element, TRE). “AAV2-rtTAV16” is injected at the level of the cell bodies (refer to Figure 3).

*Table 1*

| Construct feature | Description | Purpose |
|---|---|---|
| L/R-IRT | Left/right inverted terminal repeat sequences | Used to insert genetic sequence into host genome |
| CMV | Human cytomegalovirus immediate-early promoter | Drive constitutive expression of transgene rtTAV16 |
| rtTAV16 | Reverse tetracycline transactivator, variant 16<br>This is a fusion protein of the tetracycline repressor with herpes simplex virus activation domain VP16<br>Variant 16 confers 7-fold increase in transcriptional activity and 100-fold increase in DOX sensitivity | A fusion protein that is activated by doxycycline<br>When activated, it will bind to its promoter (Tetracycline Responsive Element; TRE) |
| WPRE | Woodchuck hepatitis virus post-transcriptional regulatory element | Enhances the viral titer and transgene expression |
| SV40 pA | Simian virus 40 polyadenylation termination signal | Used to define the end of a transcriptional unit (transgene rtTAV16), thereby facilitating the release of the newly synthesized RNA |

**Table 2. HiRet-TRE-eTeNT.EGFP construct features.**

Construct inducibly expresses eTeNT.EGFP when rtTAV16 binds to TRE promoter (only after activation via doxycycline; described in Table 1)[80]."Lenti-eTeNT" is injected at the terminal field (Figure 3).

*Table 2*

| Construct feature | Description | Purpose |
|---|---|---|
| LTR | Long terminal repeat sequences | Used to insert genetic sequence into host genome |
| PSI | Packing | Required for transgene mRNA packing and delivery |
| RRE | Rev response element | Accessory protein; allows the mRNA to be exported from the nucleus to the cytoplasm for translation |
| cPPT | Central polypurine tract | Increases transduction efficiency and eTeNT.EGFP expression |
| TRE | Tetracycline responsive element | Promoter for transgene expression (eTeNT.EGFP) only when activated by doxycycline-activated rtTAV16 |
| EGFP.eTeNT | Enhanced tetanus neurotoxin, light chain fragment (eTeNT) that is fused with enhanced green fluorescent protein (EGFP) | eTeNT cleaves vesicle associated membrane protein 2 (VAMP2), a protein required for presynaptic docking/fusion of vesicles |
| PEST | Peptide sequence rich in protein (P), glutamic acid (E), serine (S), and threonine (T) | Signal peptide for protein degradation through ubiquitination |
| WPRE | Woodchuck hepatitis virus post-transcriptional regulatory element | Enhances the viral titer and transgene expression |

# CHAPTER II

# SILENCING SPINAL INTERNEURONS: A CONTINUUM OF WALKING TO HOPPING

## Introduction

Locomotion is a behavior that reflects the interaction between supraspinal, spinal, and sensory systems[21]. While supraspinal structures control its initiation, the spinal cord coordinates the muscles distributed throughout the body into regular patterns of stepping[61]. This complex behavior is based on two principles: rhythm and pattern[25]. Together, these features are functionally organized into a hierarchical network that governs locomotion[21]. Most central to movement is rhythm, which sets the step cycle period and its two defining components: swing and stance duration[86]. Within this rhythm, patterned movements must be precisely controlled to secure effective stepping[25]. Specifically, flexion and extension must be exquisitely timed to allow limb segments to shift around joints (intralimb coordination)[25] while movements between limb pairs must be coordinated (interlimb coordination)[7]. These sequences of interlimb movement are the defining features of gait[87]. As a function of speed, each gait is characterized by a distinct set of stepping rhythms and patterns[17]. Therefore, not only are these principle features precisely controlled, but they are also adaptable to the speed. The spinal

networks that collectively produce this behavior are called central pattern generators, with cervical and lumbar spinal enlargements serving as hubs for the fore- and hindlimbs, respectively[25]. Understanding how locomotion is governed through this hierarchical network occurs at various levels and complexity. At the systems level, emphasis is placed on describing the overall behavior of the animal during locomotion[88]. A more in-depth approach to determine how specific pathways functionally integrate into the system occurs at the network level[88]. Finally, the intrinsic and dynamic properties of individual neurons and synapses is investigated at the cellular level[88]. In this study, we explored the functional consequences of silencing an anatomically-defined spinal pathway in an otherwise intact system in the freely behaving adult rat.

Using a dual virus $Tet^{On}$ system originally developed by Tadashi Isa and colleagues[80], we targeted L2 descending interneurons that project ipsi- or contralaterally to L5 in the adult rat spinal cord. A potential analog of the commissural pathway silenced here has been previously studied in the isolated neonatal rodent spinal cord[56-58]. Using electrophysiological techniques, contralateral L2-L5 interneurons were shown to be rhythmically active throughout all phases of the locomotor cycle leading the investigators to suggest that this pathway likely coordinates the actions of various muscles required for multi-joint movements during stepping[52,54,57,59]. Therefore, it is hypothesized that conditionally silencing ipsi- and contralaterally-projecting L2-L5 interneurons in the alert, behaving animal would affect flexor-extensor coordination across the joints, disrupting hindlimb kinematics during locomotion.

## Materials and methods

Procedures were performed in accordance with the Public Health Service Policy on Humane Care and Use of Laboratory Animals, as well as the University of Louisville Institutional Animal Care and Use and Institutional Biosafety Committees. A total of N=16 adult, female, Sprague-Dawley rats (200-220g) were used. Animals were housed two per cage with *ad libitum* food and water under 12 hour light:dark cycle. This project utilized Kentucky Spinal Cord Injury Research Center Neuroscience core facilities that are supported by P30 GM103507.

### *Viral vector production*

Plasmid vectors were provided by Dr. Tadashi Isa and colleagues[80]. HiRet-TRE-EGFP.eTeNT ($1.6x10^7$ vp/ml) and AAV2-CMV-rtTAV16 ($4.8x10^{12}$ vp/ml) were built following previously described methods[89,90].

### *Intraspinal injections of viral vectors*

Power analysis of previously obtained gait data revealed N=6-8 was sufficient to detect a significant difference with 90-99% power. N=6 rats were anesthetized (sodium pentobarbital, 50 mg/kg i.p.) and received a T13 laminectomy (rostral half) to expose spinal L5. HiRet-TRE-EGFP.eTeNT was bilaterally-injected (0.5 µl/site, 1.5 mm rostrocaudal, four sites total) into the intermediate gray matter (0.4 mm mediolateral, 1.4 mm dorsoventral) using a stereotaxic device (World Precision Instruments, FL, USA)[91]. Injections were given in two, 0.25 µl boluses. Three minute incubations following each bolus were allotted to facilitate viral uptake. Following injections, the incision site was sutured in layers and surgical staples were applied to close the wound. Animals received

traditional post-operative care, including gentamicin (20 mg/kg, s.c.), glycopyrrolate (0.02 mg/kg, s.c.), and lactated Ringer's solution (10 c.c, s.c.). Buprenorphine (10mg/kg, s.c.) was given every 12 hours for the first 48 hours post-surgery for pain management while prophylactic doses of gentamicin was administered for 7 days. Animals recovered voluntary bladder control within 24 hours post-surgery.

One week later, animals were re-anesthetized (ketamine:xylazine; 80 mg/kg:4 mg/kg, i.p.) and received a T12 laminectomy (rostral half) to expose spinal L2. Animals then received two sets of bilateral injections of AAV2-CMV-rtTAV16 (0.5 µl/site, 1.5 mm rostrocaudal; 0.6 mm mediolateral, 1.5 mm dorsoventral, four injections total). The injection protocols and post-operative care were followed as described above. After suturing, the animals received the reversal agent Yohimbine (0.1 mg/kg, i.m.) to counteract the effects of xylaxine. Animals recovered for 9 days before pre-doxycycline assessments. No animals were excluded from the study based on *a priori* criteria of normal gait at Pre-DOX1.

***Experimental design***

Doxycycline hydrochloride (DOX, 15 mg/ml; Fisher Scientific BP26531; NH, USA) was dissolved in 3% sucrose water and provided *ad libitum* for 5-8 days. Approximate volumes of consumption were recorded and replenished daily.

Functional testing was performed prior to injections (Baseline), before DOX (Pre-DOX1), during DOX ($DOX1^{ON}$D1-D8), and one week post-DOX ($DOX^{OFF}$). Assessments were repeated one month later (Pre-DOX2, $DOX2^{ON}$D1-D5) to assess the reproducibility of locomotor changes. Before Baseline, animals were

acclimated to the stepping/swimming chamber. Stepping was spontaneous and volitional. Animals did not receive task-specific or positive/negative reinforcement training. The order of animal testing was random. Due to the overt change in behavior during silencing, it was impossible to blind the experimenters to control versus $DOX^{ON}$ time points. Raters were blinded to animal-specifics across time points. Each animal served as its own control based on the following: (1) each surgery is unique concerning the proportion of total L2-L5 interneurons that are double-infected, (2) there is inherent variability in transgene expression across animals, and (3) there exists normal inter-animal variability in behavior. Control (Baseline, Pre-DOX1, $DOX^{OFF}$, Pre-DOX2) versus experimental ($DOX1^{ON}$D1-8, $DOX2^{ON}$D1-5) time point comparisons were made on an individual and group basis. Group data are shown.

***Three-dimensional hindlimb kinematics***

Hindlimb kinematic analysis was performed as described[92,93]. Briefly, the skin overlying the anterior rim of the pelvis (iliac crest; I), head of the greater trochanter (hip; H), lateral malleolus of the ankle (A), and the metatarsophalangeal joint of the toe (T) was marked thereby describing hindlimb movement using three segments (I-H, H-A, A-T) and two angles (I-H-A, H-A-T). Animals freely walked in a plexiglass walkway tank while high-speed (100 frames/sec) videos were acquired from one ventral and two sagittal viewpoints. Videos were analyzed using MaxTraq, MaxMate, and MaxTraq3D software (Innovision Systems; MI, USA). A minimum of 2 stepping passes per hindlimb were analyzed that met the following criteria: (1) animal walked at least ¾ the length of the tank, or approximately 1

meter, (2) continuous walking with no distracted behavior, (3) trajectory was relatively straight with minimal lateral deviations, and (4) visually representative of the animals overall locomotor behavior.

To quantify vertical hip movements ("hip height") during stepping, the difference in hip peak-to-trough excursion was calculated on a step-by-step basis. Each hindlimb was analyzed separately to confirm no significant side differences. Thereafter, both hindlimbs were averaged and then normalized to Baseline. The average angular excursion of the proximal (IHA) and distal (HAT) joint angles were analyzed for each hindlimb separately. The coordination of the HAT and IHA joint angles for each hindlimb was calculated from the time of peak IHA divided into peak-to-peak HAT. These coordination values (0 to 1) were then plotted on a circular graph with a phase of 0 (or 1) indicating coordinated intralimb movements.

***Volitional overground gait analysis***

Ventral recordings were used to analyze the timing of individual paw contacts and lift offs. A minimum of 4 passes (or 8 step cycles, defined as stance + swing) were analyzed per animal following the previously defined criteria. Stereotypic exploratory behavior was qualitatively defined as frequent-to-consistent pausing/hesitation that was concomitant with either visual distractions or interactions with the external environment (e.g. sniffing, licking). Stepping passes displaying these overt behaviors were not analyzed.

To quantify hindlimb coordination, the time of initial contact for the left hindlimb was divided into the length of time for one complete stride cycle of the reference right hindlimb. The following are potential issues with regard to phase

analysis in freely stepping animals: (1) interchangeability in lead limb and (2) basal level of variability in alternation. To account for the first issue, the circular 0-1 phase data was transformed to a linear scale of 0.5-1.0 (convert <0.50 to its reciprocal >0.50) thereby normalizing the limbs to account for any inter-animal variability. Next, to quantify silencing-induced changes in coordination beyond normal variability observed, all control time points (Baseline, Pre-DOX1, $DOX^{OFF}$, and Pre-DOX2) were averaged (hindlimb mean= 0.55; forelimb mean=0.54). Any phase value >2 S.D. from this mean is irregular (hindlimb: >0.63; forelimb: >0.62). The proportion of phases >2 S.D. were compared across time for forelimbs and hindlimbs during stepping. The raw phase data was used for circular statistics.

To quantify the absolute stride-by-stride changes in coordination, phases were first calculated from the time of initial contact for the left hindlimb divided into the length of time for one complete stride cycle of the reference right hindlimb. Next, the absolute change in phase was calculated on a step-by-step basis and then plotted over time. Any value >2 S.D. from the control mean change is plotted in the shaded area (hindlimb mean=0.043, S.D.>0.113; forelimb mean=0.066; S.D.>0.131).

Multiple comparisons were made with the transformed phases to determine if silencing-induced changes correlated with speed or the following gait parameters: stance time, swing time, stride time, stride (or step) frequency, and stride distance. For the instantaneous data (reflects individual steps), phases were compared to the instantaneous speed (distance traveled per step over time, centimeters/second), step frequency (inverse of the time for one stride cycle,

Hertz), or stride length (distance traveled per step, centimeters) for all control and all $DOX^{ON}$ time points, respectively. Individual time point comparisons were also made. These data were plotted as three-dimensional scatter graphs as well as two-dimensional contour plots with speed shown in color. Additionally, the frequency of hindlimb phases were analyzed with respect to speeds ≤90 centimeters/second (walk-trot) and >90 centimeters/second (gallop-bound) at individual as well as collapsed control and $DOX^{ON}$ time points[94-98]. Thereafter, the instantaneous datasets were averaged and then processed for correlations with and without controlling for speed.

***Swim phase analysis***

The walking tank was filled with 7-8 inches of 25-28ºC water and a neoprene-covered exit ramp was attached to one end. As the animal swam in both directions, a high-speed camera set up 18 inches from the tank recorded 6-7 complete stroke cycles per pass. A minimum of 4 passes (or 8 stroke cycles) were analyzed per animal following the previously defined criteria. The peak downward extension of the toe was digitized for both hindlimbs to determine the phase relationship during swimming. To quantify this relationship, the time of peak extension of the left toe was divided into the length of time for one complete stroke cycle of the reference right hindlimb. Values were transformed as described above and the proportion of phases >2 S.D. from transformed control mean were compared across time (mean=0.54; 2 S.D. >0.64). The stroke-by-stroke change in hindlimb coordination was calculated as described above (mean=0.033; 2 S.D. >0.098).

***Viral tissue processing and EGFP.eTeNT immunohistochemistry***

Animals were euthanized during DOX2$^{ON}$-D5 with an overdose of sodium pentobarbital then transcardially perfused with 0.1 M PBS (pH 7.4) and 4% paraformaldehyde. Spinal cords were dissected, post-fixed overnight, and transferred to 30% sucrose for 3-4 days at 4ºC. Spinal segments L1-L6 were dissected, embedded in tissue freezing medium, cryosectioned at 30 µm in 5 sets, and stored at -20ºC. Fluorescent immunohistochemical detection of EGFP.eTeNT-positive terminals at L5 was performed following previously described methods[99] with rabbit anti-GFP (abcam ab290, 1:5,000; UK) and guinea pig anti-NeuN (Millipore ABN90P, 1:500; MA, USA) as primary antibodies. Secondary antibodies (anti-rabbit AlexaFluor 488, -guinea pig AlexaFluor 594 from Jackson Immunoresearch; PA, USA) were used at 1:200 dilutions. Negative controls include non-immune sera as well as mid-thoracic spinal cord for absence of labeling (data not shown). Images were captured using an Olympus FluoView 1000 confocal microscope with the oil immersion 100x objective using 488 and 543 lasers (Olympus; PA, USA). Z-stacks acquired were 53-68 slices at 0.4 µm optical steps. The raw .oif files were imported into Amira 3D software (FEI; OR, USA) for volume rendering to qualitatively assess the relative density and distribution of EGFP.eTeNT-positive terminals onto neurons throughout laminae V-IX at spinal L4-5. The 3D images were rotated about the x-, y-, and z-axes to verify close apposition of eTeNT-positive terminals onto NeuN-positive somata and primary dendrites.

***Intraspinal fluorescent dextran injections, light sheet fluorescence microscopy, and absolute L2-L5 interneuron counts***

N=5 rats were anesthetized with ketamine/xylazine (80mg/kg; 4mg/kg; i.p.). The surgical methods and injection coordinates used for the fluorescent dextrans were identical to that of the lentiviral vector. 10% FluoroEmerald (in sterile water; ThermoFisher; MA, USA) and 10% FluoroRuby were injected on the left and right sides of the spinal L5 with respect to the dorsal viewpoint. After 2 weeks of retrograde transport, animals were sacrificed and spinal cords dissected as described above. The L5 segment was processed for histology as described above. Slides were hydrated in 0.1 M TBS, coverslipped, and imaged for a priori inclusion criteria of injection site accuracy (spinal level, laminae VII-VIII). Images were captured using a Nikon TiE 300 inverted microscope with the 10x objective and GFP and TexRed filter settings (Nikon; Tokyo, Japan). Thereafter, the entire L2 segment was isolated and optically cleared following previously described methods100. Images were acquired using a LSFM microscope using 488 and 594 lasers (La Vision, Germany) and were imported into Bitplane (Imaris) for analysis. Counts of FluoroRuby and FluoroEmerald-labelled neurons were performed manually, blinded to ipsi- and contralateral designation. Of the 4,783 L2-L5 interneurons counted, none had dual ipsi- and contralateral projections. Data shown is from N=3. For clarity, FluoroEmerald is shown alone. Power analysis revealed that N≥38 animals would have been necessary to detect a significant difference between ipsi- and contralateral L2-L5 interneurons (power ≥80%).

Figure 4 schematics and definition of ipsi- and contralateral are with respect to the in vivo injection site as opposed to the dorsal viewpoint during surgery.

***CTB-AlexaFluor injections, immunohistochemistry, and proportional cell counts***

Power analysis demonstrated N=3-5 animals was sufficient to detect a significant difference (power >99%) in the number of L2-L5 interneurons that were positive versus negative for local projections. N=5 rats were anesthetized with ketamine/xylazine and received a complete T12-T13 laminectomy to expose spinal L1 through L5. Cholera toxin beta subunit (type B, 1% solution in 0.1M PBS at pH 7.4; Molecular Probes; OR, USA) conjugated to the following AlexaFluors were used for intraspinal injections (with respect to dorsal viewpoint): CTB-488 at right L1 (0.5 mm mediolateral; 1.3 mm dorsoventral), CTB-594 at left L4-5, and CTB-647 at right L4-5 (both at 0.5 mm mediolateral and 1.4 mm dorsoventral). Two different CTB fluorophore conjugates were used in order to distinguish between ipsi- and contralateral L2-L5 interneurons (ipsi-CTB 594, contra-CTB 594, ipsi-CTB 647, and contra-CTB 647). We chose to use L1 as our injection site to identify local L2-L5 interneuron collaterals for the following reasons: (1) the rostral lumbar circuitry is critical for locomotor generation[35,37,38,101], (2) it is well-documented that local collaterals typically branch off within 1.5 segments of their cell body[50,52], and (3) injecting at L1 would permit bilateral counts at L2. Injecting at-level with the L2-L5 interneurons would have greatly limited our analyses. Note that this labelling strategy does not implicate a relatively small population of neurons, called ascending-descending commissural interneurons (adCINs), whose axons

bifurcate and project approximately 1.5 segments rostrocaudally[52]. Instead, the two branches labelled here are highly asymmetrical with one spanning ≤1 segment while the other is ≥2-3 segments. Each injection site received a total of 0.5 µl given in 0.25 µl boluses over 4 minutes. After 2 weeks of retrograde transport, animals were sacrificed following methods described above. Spinal T13-L6 was dissected and post-fixed in 4% paraformaldehyde for one hour followed by cryopreservation in 30% sucrose. The cords were embedded and sectioned at 30 µm in 5 sets such that adjacent sections were 150 µm apart rostrocaudally. All animals met *a priori* inclusion criteria for injection site accuracy. Co-localization of CTB-488 with CTB-594 or CTB-647 was confirmed using an Olympus FluoView 1000 confocal microscope with a water immersion 20x objective and 488, 543 and 647 lasers. The z-stacks acquired (10-15 slices at 2 µm optical steps) were imported into Nikon NIS-Elements software and rendered using the slice view with orthogonal crosshairs to illustrate co-localization. After confirmation of co-localization, one complete set was hydrated, stained with Hoechst, coverslipped, and imaged using the 10x objective on the inverted microscope using the DAPI, GFP, TexRed, and CY5 filters. Power analysis showed that analyzing n=5-7 sections/animal could detect a significant difference (94-99% power) for the following: (1) %L2-L5 positive versus negative for local projections; (2) %L2-L5 positive for local projections –ipsilateral versus contralateral; (3) %ipsi-L2-L5 positive for ipsilateral-local versus contralateral-local; (4) %contra-L2-L5 positive for ipsilateral-local versus contralateral-local. CTB-labeled neurons were counted in 7 randomly-selected sections per animal throughout spinal L2 as defined by Rexed laminae.

Counts were performed in a blinded fashion. The following *a priori criteria* were used: (1) the CTB-positive neurons must be located in laminae V-X (we saw no CTB signal in lamina IX), (2) must co-localize with the nuclear marker Hoechst or have an overt nucleolar space, and (3) the strength of the CTB signal should be approximately two-times greater than the immediate background shown quantitatively with the horizontal intensity profile function. The following CTB labelled-neurons were counted: $488^{+}$, $594^{+}$, $647^{+}$, $488^{+}/594^{+}$, $488^{+}/647^{+}$. A total of 5,884 L2-L5 interneurons and 2,961 resident L2 neurons (488 alone) were counted. Similar to the tissue clearing and LSFM cell counts, no $594^{+}/647^{+}$ L2 neurons were found (data not shown). As previously stated, respect is paid to the *in vivo* injection site with regard to schematics and ipsi- and contralateral categorization. Images shown are representative. Data shown are proportional counts of L2-L5 interneurons.

***Statistical analyses***

Statistical analyses were performed using IBM SPSS v22 software package. Parametric and non-parametric comparisons were performed accordingly[102-107]. Differences between groups were considered statistically significant for p values ≤0.05.

Step and swim phase analysis

For the raw and transformed phase data as well as the absolute step-by-step (or stroke-by-stroke for swim) change in coordination, significant differences in frequency of phase values >2 S.D. from control mean were detected using the Binomial Proportion Test[106]. Levene's Test for Equality of Variances was used to

test for a normal distribution of the phase data. Note that at control time points, e.g. Baseline, the data had a non-normal distribution (highly clustered at 0.5). No outliers (any value >3 S.D. from the time point average) were detected.

Circular statistics was performed on the raw phase data to analyze phase distribution. Classically, parametric tests are used determine whether the circular data is from a uniform distribution. These analyses are based on strict assumptions regarding the data distribution and are restricted to either uniform or unimodal patterns[102,103]. Our data did not fit these criteria. Furthermore, we had no evidence to support a unimodal distribution with the same degree of concentration (e.g. relative concentration at each of the four control time points). Instead, we used non-parametric circular statistics to test the null hypothesis that the two time points being compared had the same phasic direction (concentrated or clustered)[103]. Time point comparisons were performed using the non-parametric two-sample $U^2$ tests. Thereafter, all control time points and $DOX^{ON}$ time points were respectively grouped and compared as well. The length of the vector *r*, an indicator of the amount of concentration or clustering of phases in one direction, was averaged for all control and all $DOX^{ON}$ time points, respectively, and compared using the independent t-test between means with equal variance. Angular deviation *s*, or the circular standard deviation, was also compared using these methods. For reference, angular deviation is equivalent to 1 S.D. Two-tail p values are reported.

The non-parametric Kolmogorov-Smirnov (KS) Test was used to compare differences in the cumulative frequency distributions of raw and transformed hindlimb phase values over time (data not shown). The KS test was also used to

compare cumulative frequency distributions of transformed hindlimb phases at speeds ≤90 cm/sec (walk-trot) and >90 cm/sec (gallop-bound) over time.

Instantaneous phase comparisons were made with the Spearman Rank correlation test against the following gait parameters: stance time, swing time, stride time, stride frequency, stride length, and speed. The 95% prediction intervals were used as a visual aid for distribution of speed-stride length and speed-stride time. Prediction intervals were calculated from each control dataset and then superimposed onto the corresponding DOX panels. The relative percentage of swing and stance durations were compared between two speed groups (≤90 cm/s or >90 cm/s) during $DOX^{ON}$ using the paired t-test. At speeds ≤90 cm/s, the relative percent of swing and stance durations were compared between all control and all $DOX^{ON}$ time points using the independent t-test between means of equal variance. Statistical analyses of control time points at speeds >90 cm/s were not possible due very few animals stepping at this velocity. Pearson and part correlations (controlling for speed) followed by the Bonferroni correction for Type I errors were used on the averaged datasets.

Step sequence pattern[108] data is shown as the percent of total patterns observed and was analyzed using repeated measures analysis of variance (ANOVA) with groups as a factor followed by Tukey honest significant difference (HSD) *post hoc* t-test for DOX1 and DOX2 separately (data shown is mean ± S.D.).

Hindlimb kinematics

Joint angular excursion of each hindlimb was analyzed using mixed model ANOVA followed by Bonferroni post hoc t-test (data shown as mean joint excursion

± S.D.). After determining no significant side difference, the hip height data was normalized to Baseline followed by Pre-DOX1 versus DOX1ON and Pre-DOX2 versus DOX2ON comparisons using paired t-test for means of equal variance (data shown is mean hindlimb hip excursion ± S.D.; two-tail p value reported). Left and right hindlimb HAT-IHA phase values were analyzed using circular statistics as described above. Right hindlimb is shown.

Cell counts

Absolute L2-L5 interneuron cell counts from cleared L2 segments were analyzed using the independent t-test between means of equal variance. Proportional counts of L2-L5 interneurons differentially labelled with CTB were analyzed using one-way ANOVA followed by Tukey's post hoc t-test as well as independent t-tests between means with equal variance (data shown as mean ± S.D.; two-tail p values reported).

## Results

### *L2-L5 interneurons likely do not participate in intralimb coordination during overground locomotion*

We performed bilateral injections at the L2 and L5 spinal cord segments to silence both the ipsilateral and contralateral projections (Figure 4a). In double-infected neurons that constitutively express rtTAV16, doxycycline (DOX) induces enhanced tetanus neurotoxin (eTeNT) expression (Figure 4b). eTeNT is then transported to the terminal field where it prevents exocytosis of synaptic vesicles thereby silencing neurotransmission. Removing DOX from the drinking water restores neurotransmission, thereby allowing us to acutely and reversibly silence

this anatomically-defined pathway in the otherwise intact adult rat. The data shown are from kinematic and gait assessments of animals stepping overground at control time points when neurotransmission was intact and during two rounds of $DOX^{ON}$-induced silencing (Figure 4c).

To determine the functional consequences of silencing L2-L5 interneurons on flexor-extensor coordination across the hindlimb joints, we marked the skin overlying the iliac crest, hip, ankle, and toe in order to describe limb movement using three segments (**Error! Reference source not found.**a,b) and two angles **Error! Reference source not found.**c,d). At control time points, animals displayed stereotypic and coordinated flexor-extensor activity across the joints. This is illustrated by the characteristic excursions of limb segments (**Error! Reference source not found.**a, bottom), normal hindlimb range-of-motion (Figure 11, supplementary to **Error! Reference source not found.**), and coordinated movements in the proximal and distal joint angles (**Error! Reference source not ound.**c, circular plot, 0= coordinated). Unexpectedly, when we silenced L2-L5 interneurons we saw a disruption in left-right hindlimb alternation during stepping (Video 1). The severity of this disruption ranged from mild changes in alternation to hindlimb “hopping” where the hindlimbs moved synchronously (shown kinematically in **Error! Reference source not found.**b). Despite the silencing-nduced effects on left-right alternation, intralimb coordination persisted as seen by the characteristic pattern of flexor-extensor activity across the limb joints (**Error! eference source not found.**b) and between the proximal-distal limb angles (**Error! Reference source not found.**d). Collectively, these data suggest that L2-

5 interneurons are likely not involved in intralimb, flexor-extensor coordination during overground locomotion.

***Silencing L2-L5 interneurons alters the overall locomotor stepping pattern***

We next analyzed how silencing L2-L5 interneurons affected the step sequence pattern[108]. Traditionally, the primary pattern used by rodents is called alternate. It is characterized by alternation of the hind- and forelimbs with each step (Figure 6a, left panel) and has a “zig-zag” appearance in limb recruitment graphs (right panel). Prior to silencing, the alternate step pattern dominated (Figure 6d). When we silenced L2-L5 interneurons, animals significantly increased their use of the cruciate step pattern (Figure 6e), which reflects the sequential movements of the homologous limb pairs as opposed to alternation between the shoulder and pelvic girdles (Figure 6b,c). Removing DOX from the drinking water reversed this pattern shift (Figure 6d,e) and silencing one month later reproduced the effects (Figure 6f,g). Together, these data suggest that silencing L2-L5 interneurons produces a quadrupedal stepping behavior that is primarily forelimb-leading, hindlimb-trailing as opposed to the stereotypic alternation between the two girdles.

***Silencing L2-L5 interneurons selectively disrupts hindlimb alternation during stepping, revealing a continuum of coordination from walking-to-hopping***

The salient observation from silencing L2-L5 interneurons is a change in hindlimb alternation during stepping (Video 1). However, quadrupedal mammals will naturally express various patterns of interlimb coordination. These distinct,

repeated patterns are defining features of the classic gaits[87]. Therefore, we set out to determine if the interlimb coordination expressed during silencing reflected these stereotypic gait patterns.

Traditionally, walking and trotting are slower gaits wherein the hindlimbs alternate (Figure 7a, lower-panel). This temporal relationship can be expressed as a coordination (or phase) value by dividing the initial contact time of the left hindlimb by the right hindlimb stride time (stance + swing). These phase values, ranging from 0 to 1, are plotted on a circular graph to illustrate interlimb coordination (Figure 7a, lower-right). For walking and trotting, the phase value is close to 0.5 (180°), indicating left-right alternation with out-of-phase hindlimb movements[17]. With increasing speed, the gait switches from walk-trot to gallop where there is a phase-shift with increased overlap between left and right stance (or swing) phases (Figure 7b, phase≈0.25 or 0.75, depending on the lead limb)[17]. At even higher speeds, some animals will switch their gait to bounding where the hindlimb movements are in-phase (Figure 7c, phase≈0/1). These gait-specific coordination changes also occur in the forelimbs.

First, to control for inter-animal variability in lead limb (illustrated in Figure 6)[12,13], we transformed hindlimb phase values <0.5 to the reciprocal >0.5 and found the mean phase of all control time points (Figure 7d). Any value >2 S.D. from this mean is beyond control (or normal) variability and was considered “irregular”. Prior to silencing, left-right hindlimb alternation was the overt stepping pattern (Figure 7e). Silencing L2-L5 interneurons significantly disrupted this alternation, but the changes observed were not clustered at the coordination values reflective of the

traditional gaits. Instead, we saw the emergence of a coordination continuum from hindlimb walking to hopping (Figure 7e). Notably, the silencing-induced effects were not all-or-none as seen by the preponderance of phase values within the normal range. Removing DOX restored hindlimb alternation while re-silencing one month later once again significantly disrupted it. These perturbations to hindlimb alternation did not influence or “spread” to the forelimbs as alternation persisted (Figure 7f). Despite the significant change in hindlimb coordination, the animals maintained a 1:1 stepping relationship between the fore- and hindlimbs (Figure 7g).

We also investigated hindlimb coordination during swimming (Figure 7h), a bipedal locomotor behavior where the limbs are unloaded and the proprioceptive and cutaneous feedback associated with plantar stepping is altered. Strikingly, hindlimb alternation remained intact (Figure 7h; Video 2), suggesting that L2-L5 interneurons do not participate in hindlimb alternation during a task where afferent feedback associated with stepping is altered/removed. Collectively, these data suggest that silencing L2-L5 interneurons selectively disrupts hindlimb alternation in a context-specific manner, without affecting the overall stepping ability of the animal.

***Silencing L2-L5 interneurons partially uncouples the hindlimbs, allowing spontaneous shifts in left-right coordination with each step***

Typically, the pair of limbs at each girdle work together as a coupled unit during stepping[87]. This functional coupling ensures that they step in a consistent fashion, regardless of the gait. This characteristic feature of locomotion raises an

important question: does the silencing-induced disruption of hindlimb alternation reflect a functional uncoupling of the left and right limbs? To address this issue, we performed circular statistics on the raw dataset to quantify the amount of concentration (Figure 8) and dispersion (Figure 12, supplementary to Figure 8) in the phase data[103]. Limb coupling is exemplified by a high degree of concentration in one direction (Figure 8a, top). Alternatively, complete uncoupling indicates that the left and right hindlimbs are stepping independently from each other, with different frequencies, giving a uniform phase distribution around the circular plot (Figure 8a, bottom)[102].

Prior to silencing, the hindlimbs were coupled at alternation with the preponderance of phases near 0.5 and with normal variability (Figure 8b, top). During silencing, this concentration was significantly reduced. Instead, the coordination values became distributed around the circular plot (Figure 8b, bottom, Table 3). Removing DOX restored the concentration of phase values towards alternation and silencing one month later replicated the effects. As anticipated, the forelimb phases remained concentrated at alternation (Figure 8c) as did the hindlimbs during swimming (Figure 8d) (Table 4). Complementary to concentration is the amount of dispersion and circular variance in the phase data, both of which are typically low when the limbs are coupled. Silencing L2-L5 interneurons significantly increased these parameters in the hindlimbs alone (Figure 12, supplementary to Figure 8). Once again, the effects were not all-or-none and did not produce a uniform distribution indicative of complete uncoupling. Therefore, we contend that silencing L2-L5 interneurons results in the partial uncoupling of

the hindlimbs during overground stepping. Moreover, this uncoupling does not impact the forelimbs nor translate to a non-weight bearing locomotor task.

Thus far we have examined the effect of silencing L2-L5 interneurons on the overall stepping performance. We next wanted to explore how the disruption in left-right alternation influenced dynamic coordination on a step-by-step basis. To do this, we quantified the absolute change in phase per step and used this as an indicator for the relative consistency in hindlimb coordination (Figure 8e, example shown in left panel, steps 1-3 with respective |changes|). Consistent hindlimb coordination is typified by minor changes in phase on a stride-by-stride basis, which suggests the limbs are stepping in a regular, repeated fashion. Conversely, large changes in coordination per stride would indicate increased variability between the hindlimbs as they are stepping.

Figure 8f summarizes the absolute change in left-right hindlimb coordination, per step, for the individual locomotor bouts of each animal across all time points (example shown in Figure 8e). Any sequence of steps with a change in hindlimb coordination beyond the normal stride-by-stride variability is plotted in the shaded area. Prior to silencing, there were minor changes in step-by-step coordination with approximately 96% of all steps taken falling within the normal variability observed at control time points (Figure 8h). These small changes were primarily concentrated around 0.5 (Figure 13, supplementary to Figure 8). Silencing L2-L5 interneurons significantly increased the step-by-step variability in hindlimb coordination, as seen by the large spikes in absolute phase change (Figure 8f, red bars in top panel). This included step sequences with dramatic

changes in coordination per step as well as instances of drift where the hindlimbs started in-phase and then drifted out-of-phase (Figure 13, supplementary to Figure 8). Removing DOX restored the consistency in step-by-step coordination while re-silencing one month later replicated the increased variability. Once again, this was exclusive to hindlimb stepping as forelimb stepping and hindlimb swimming remained normal (Figure 13, supplementary to Figure 8).

In addition to analyzing the silencing-mediated effects on dynamic hindlimb coordination, we also examined the per step changes in stride time, which is the duration of the stance and swing phase for one step cycle. We calculated changes in stride time and matched them to the corresponding changes in hindlimb coordination. Surprisingly, the hindlimbs continued to step with stride durations that fell within the normal range despite the large shifts in left-right coordination (Figure 8f, bottom). Together, these data suggest that silencing L2-L5 interneurons partially uncouples the hindlimbs during locomotion, allowing spontaneous shifts in left-right coordination to occur on a step-by-step basis. However, these changes occurred alongside relatively invariable stride durations, suggesting that the disruption to hindlimb coordination occurs within the confines of a stable locomotor rhythm.

***Silencing L2-L5 interneurons disrupts hindlimb alternation independent of speed and step frequency while preserving the fundamental principles that govern locomotion***

Changes in interlimb coordination are tantamount to transition between the slower walk-trot gaits and the faster, more synchronous gallop-bound. Therefore,

we set out to determine if the observed perturbations in hindlimb coordination were associated with stepping speed. First, we compared the transformed phase values to the corresponding speeds for collapsed control and $DOX^{ON}$ time points, respectively (Figure 9b) and found no association between silencing-induced changes in hindlimb coordination and speed, with a correlation coefficient of 0.13 (Figure 9b). This result was substantiated when we analyzed the individual time points, the averaged datasets, and the irregular steps only (yellow) (Figure 14, supplementary to Figure 9). Importantly, approximately 67% of these irregular steps occurred at speeds less than 90 cm/s, a velocity where the alternating gaits typically predominate in the adult rat[1] (Figure 14, supplementary to Figure 9). We also examined the step frequency (number of steps/second) which usually increases with speed. It is at greater step frequencies that the more synchronous gaits typically occur[17]. When we compared the silencing-induced changes in hindlimb alternation to step frequency, we once again saw no meaningful correlation (Figure 9c). The individual time point comparisons corroborated these findings (data not shown). In that vein, we also saw no associations between silencing-induced changes in hindlimb coordination and various gait parameters (Figure 14, supplementary to Figure 9; Table 5, Table 6). Therefore, silencing L2-L5 interneurons alters hindlimb coordination independent of locomotor speed and step frequency.

Due to the unexpected dissociation between changes in hindlimb coordination and step frequency/speed, we wanted to determine if other principal features that govern locomotion were also affected. During stepping, the limbs are

coordinated in both space and time. This allows us to quantify locomotion using a set of spatiotemporal parameters, or gait indices, which include stride length, stance duration, swing duration, and stride time[12,13]. Importantly, these parameters change with speed in a stereotypic, well-characterized manner (Figure 9d,g)[12,109]. Silencing L2-L5 interneurons did not alter the primary spatiotemporal gait indices of step frequency (Figure 9e, right panel), stride length (Figure 9f)[12,109], stride and swing times (Figure 9g-h, left panel), and stance duration (Figure 9i). Some animals did not step at velocities greater than 90 cm/s at control time points, preventing a statistical comparison between the two speed categories (Figure 9i, top left vs right). Nonetheless, the pattern and magnitude of change in swing-stance durations were similar (data not shown). When we focused on the dispersion of the irregular hindlimb steps, it became apparent that the silencing-induced changes to alternation occurred over a relatively broad range of speeds, step frequencies, and spatiotemporal indices. This further supports the notion that the perturbations to hindlimb alternation are not reflective of the traditional gaits[17]. All together, these data suggest that silencing L2-L5 interneurons disrupts hindlimb alternation independent of speed and step frequency and while preserving key stepping characteristics that are fundamental to locomotion.

***L2-L5 interneurons are a bilaterally distributed pathway with sparse local projections throughout the rostral lumbar spinal cord***

To detect the eTeNT.EGFP-positive terminals in the caudal lumbar cord, animals were sacrificed on DOX2$^{ON}$-D5 and cross-sections of L4-L5 spinal segments were co-stained with anti-NeuN (Figure 10a-c) to label neurons and anti-

GFP to amplify the endogenous eTeNT.EGFP. Immunoreactive eTeNT.EGFP-positive terminals were found in close apposition to somata and primary dendrites of neurons in the ventral gray matter (Figure 10a$_{i}$). Rotating the neurons in three-dimensions confirmed that eTeNT.EGFP-positive terminals surrounded the somata (Figure 10a$_{ii}$), with patterns suggestive of complex branching (Figure 10b$_{i-ii}$). Isotype controls showed little-to-no EGFP signal (Figure 10c). We also processed the thoracic spinal cord as an additional negative control and saw no EGFP immunoreactivity (data not shown).

The projection patterns of L2-L5 interneurons in the adult rat are unknown. We performed a series of tracing experiments to explore the anatomy through which L2-L5 interneurons may exert their functional role(s). We repeated the original L5 injections using FluoroEmerald and FluoroRuby to retrogradely label L2-L5 interneurons (Figure 10d,e). Thereafter, the L2 segment was dissected, cleared, imaged using light sheet fluorescence microscopy (LSFM)[100], and unbiased counts were performed (Figure 10f-h; Figure 15, supplementary to Figure 10). Even though silencing L2-L5 interneurons disrupts left-right (contralateral) alternation while preserving intralimb (ipsilateral) coordination, quantitative analysis revealed no significant difference in the number of ipsi- and contralateral-projecting interneurons, indicating that this pathway is bilaterally distributed (Figure 10f-g).

One explanation for the disruption in left-right alternation is that L2-L5 interneurons may have collaterals near their somata throughout the rostral lumbar spinal cord, an area critical for central pattern generation[35,37,38,43,101,110]. Previous

studies in the isolated spinal cord of the neonatal rodent showed that descending commissural interneurons have collaterals within a segment of their somata[52,54, 50]. Therefore, we hypothesized that L2-L5 interneurons would have dense projections locally within the rostral lumbar cord. To test this, we first retrogradely-labelled L2-L5 interneurons with cholera toxin beta subunit (CTB) conjugated to AlexaFluor-594/-647 (Figure 10i,k). Next, we unilaterally-injected CTB AlexaFluor-488 into the L1 segment (Figure 10i,j), allowing us to determine if the local projections were ipsi- or contralateral to the L2-L5 somata (Figure 10n).

Once again, we saw many L2-L5 interneurons within the intermediate gray matter (Figure 10l,m) with no significant difference between the ipsi- and contralateral subtypes (data not shown). Of the labeled L2-L5 interneurons, few had resident collaterals (Figure 10m,o). More local projections arose from the contralateral-L2-L5 interneurons as compared to the ipsilateral (Figure 10p). These collaterals were also primarily commissural in nature (Figure 10r), representing the most abundant projection pattern observed (Figure 15, supplementary to Figure 10). Alternatively, the ipsilateral-projecting L2-L5 interneurons primarily had local collaterals ipsilateral to their somata (Figure 10q). This purely ipsilateral pathway constituted the second-largest projection pattern observed (Figure 15, supplementary to Figure 10). Notwithstanding, the proportion of L2-L5 interneurons with at-level projections appears to be small. Collectively, these data illustrate that the majority of L2-L5 interneurons lack local projections in the rostral segments of the lumbar cord with only 12% having at-level projections that anatomically connect the two sides of the spinal cord.

## Discussion

Rhythm and pattern are precisely controlled by the hindlimb locomotor circuitry[21]. Together, these features change with speed in a stereotypic fashion[17]. This is a fundamental principle of locomotion[7]. We show here that a discrete component of stepping, left-right alternation, can be manipulated without influencing the other central features. This key finding is the focus of our discussion below.

Reversible silencing of spinal interneurons reveals that left-right alternation can be discretely manipulated independent of rhythm. There are five crucial findings that support this concept. The first is also the most obvious: effective locomotion continued during silencing. If L2-L5 interneurons were a part of the rhythm generating circuitry, silencing would have greatly impeded or even prevented the animals' ability to step. Second, the hindlimb:forelimb step ratio remained 1:1. This indicates that all four limbs stepped equally with no missteps or double-steps, "mistakes" that would have affected the overall rhythm. Third, the changes in hindlimb alternation were not associated with step frequency or speed. As a function of speed, an increase in step frequency occurs along with changes in gait-specific coordination patterns (out-of-phase to in-phase)[17]. Fourth, the step-by-step shifts in left-right coordination occurred alongside invariable changes in stride time, a defining feature of rhythm[109]. Fifth, the relationship between speed and spatiotemporal (gait) indices was not affected. These findings suggest that within a stable locomotor rhythm, silencing L2-L5 interneurons has affected patterned left-right movements. Moreover, the silencing did not affect the other

pattern of stepping: intralimb coordination. From these data, where do we place L2-L5 interneurons within the locomotor hierarchy? We propose that L2-L5 interneurons should be considered part of the left-right pattern formation layer[111] where they help to secure left-right alternation on a step-by-step basis during overground locomotion. This places them functionally "below" the rhythm generating circuitry and suggests that they distribute temporal information caudally from the rostral lumbar segments.

These results are in stark contrast to our hypothesized role for these interneurons in intralimb (flexor-extensor, multi-joint) coordination, anticipated based on previous studies that utilized *in vitro* neonatal rat and mouse spinal cords[56-58]. These electrophysiological studies explored the intrinsic properties, firing patterns, and synaptic output of commissural L2-L5 interneurons. Based primarily on the timing of their activity and output onto L4/5 motoneurons during drug-induced locomotor-like activity these interneurons were assigned putative roles in the flexor-extensor aspects of pattern formation. In turn, this was the framework on which we set out to assess their functional role in the mature, freely behaving rat. Our findings clearly illustrate the importance of taking hypotheses formed at the cellular and network levels and testing them at the systems level. However, significant caveats remain in the network-to-systems approach used here. Most notably, we cannot reconcile why, at most, 30% of the hindlimb steps were disrupted. This may reflect a practical limitation of the dual-virus silencing system and/or the probability that functional populations of interneurons are unlikely to be purely segmentally defined, anatomically. It is also possible that we

observed the most severe phenotype possible in our model given that the full ensemble of pathways that secure left-right coordination remains unknown.

Another unexpected result was the striking contrast between stepping and swimming. Swimming is primarily a bipedal (hindlimbs) locomotor task that is characterized by highly stereotypic rhythmic, left-right alternation[93] and flexion-extension durations that are distinct from those of stepping[112,113]. During swimming, the limbs are unloaded, which greatly reduces signaling from Golgi tendon organs, a sensory system that typically conveys information about dynamic loading of the limbs[112]. The extension phase is dramatically reduced as compared to stepping[112] and while the duration of limb flexion is similar between the two behaviors, muscle recruitment patterns are distinct[113]. Therefore, while stepping and swimming patterns likely arise from similar or overlapping neural pathways, they represent different locomotor programs[112]. In light of these differences, we cannot say that the lack of a phenotype during silencing reflects a lack of involvement of L2-L5 interneurons in hindlimb alternation during swimming. However, it is abundantly clear that the effects of silencing L2-L5 interneurons are pronounced during stepping and inconspicuous during swimming.

Using reversible silencing of spinal interneurons as a tool, we have revealed that a core component of the locomotor pattern can be selectively and reversibly manipulated without disrupting the other core features of stepping. The changes observed illustrate the nervous system's ability to adapt to a significant, but discrete perturbation. Therefore, the observed continuum of walking-to-hopping likely reflects the system's strategy to maintain effective stepping given the internal

and external constraints associated with that particular behavior[114]. Furthermore, changing the behavioral conditions from stepping to swimming exposes how the functional importance of distinct pathways can be powerfully modulated by a reconfiguration of the whole system. Altogether, these data illustrate a striking freedom in an otherwise precisely-controlled system, a phenomenon dependent on the behavioral context.

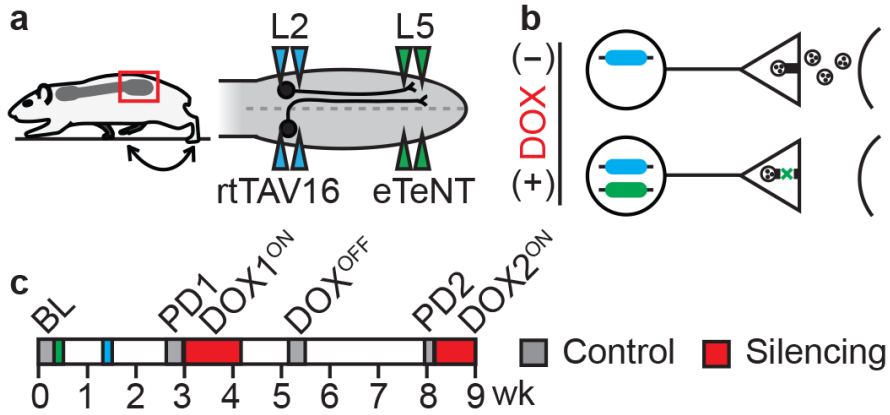


**Figure 4. Experimental Design To Conditionally Silence L2-L5 Interneurons In The Freely Behaving Adult Rat.**

(**a**) In the lumbar spinal cord, L2 neurons with ipsilateral or contralateral projections to L5 were targeted for conditional silencing. Bilateral injections of AAV2-CMV-rtTAV16 (blue triangles) and HiRet-TRE-EGFP.eTeNT (green) were performed at L2 and L5, respectively. (**b**) In the presence of doxycycline (DOX) only double infected neurons conditionally express eTeNT (bottom panel; adapted from Kinoshita *et al*. 2012). eTeNT is transported to the terminal field where it prevents synaptic vesicle release thereby silencing neurotransmission. (**c**) Behavioral assessments were performed at four control time points (Baseline, BL; Pre-DOX1, PD1; $DOX^{OFF}$; Pre-DOX2, PD2) and during two rounds of $DOX^{ON}$ silencing separated by a one month washout ($DOX1^{ON}$ days 3,5,8 and $DOX2^{ON}$ days 3 and 5).

*Figure 5*

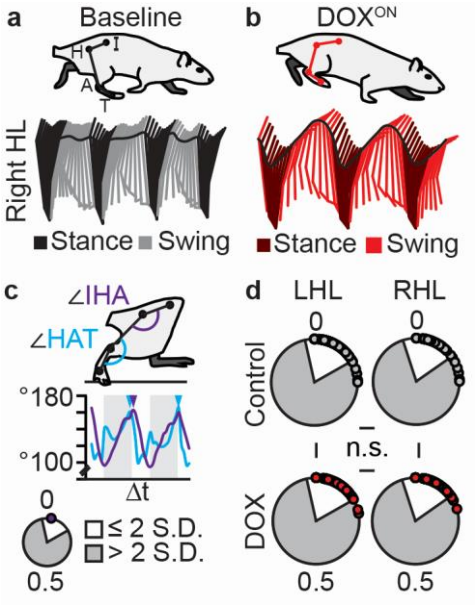


**<u>Figure 5</u>. L2-L5 Interneurons Are Dispensable For Intralimb Coordination During Locomotion.**

(**a**) Intralimb movements described by the excursion of the iliac crest (I), hip (H), ankle (A), and toe (T). Shown below is a representative two-dimensional stick-figure of stepping kinematics at control time points. (**b**) Silencing L2-L5 interneurons significantly increased vertical movements in the hip (black horizontal trace; data not shown) while preserving normal intralimb kinematics (refer to Figure 11). (**c**) Analysis of proximal (IHA) and distal (HAT) hindlimb joint angles (top panel). Peak angular excursions (middle panel, triangles; shaded region=stance phase) were used to calculate intralimb coordination (circular graph, white inset=normal variability at control time points). (**d**) Intralimb coordination between the proximal and distal hindlimb joint angles remained intact. Individual circles=intralimb coordination value for one stride (n=30/time point). Collapsed CON and DOX$^{ON}$ time points shown. LHL=left hindlimb; RHL=right hindlimb. All

comparisons in (**d**) were p>0.5, Watson's non-parametric two-sample $U^2$ test; LHL: Control vs $DOX^{ON}$ $U^2$=0.04232; RHL: CON vs $DOX^{ON}$ $U^2$=-0.13874; CON: LHL vs RHL $U^2$=-0.00653; $DOX^{ON}$: LHL vs RHL $U^2$=0.01623).

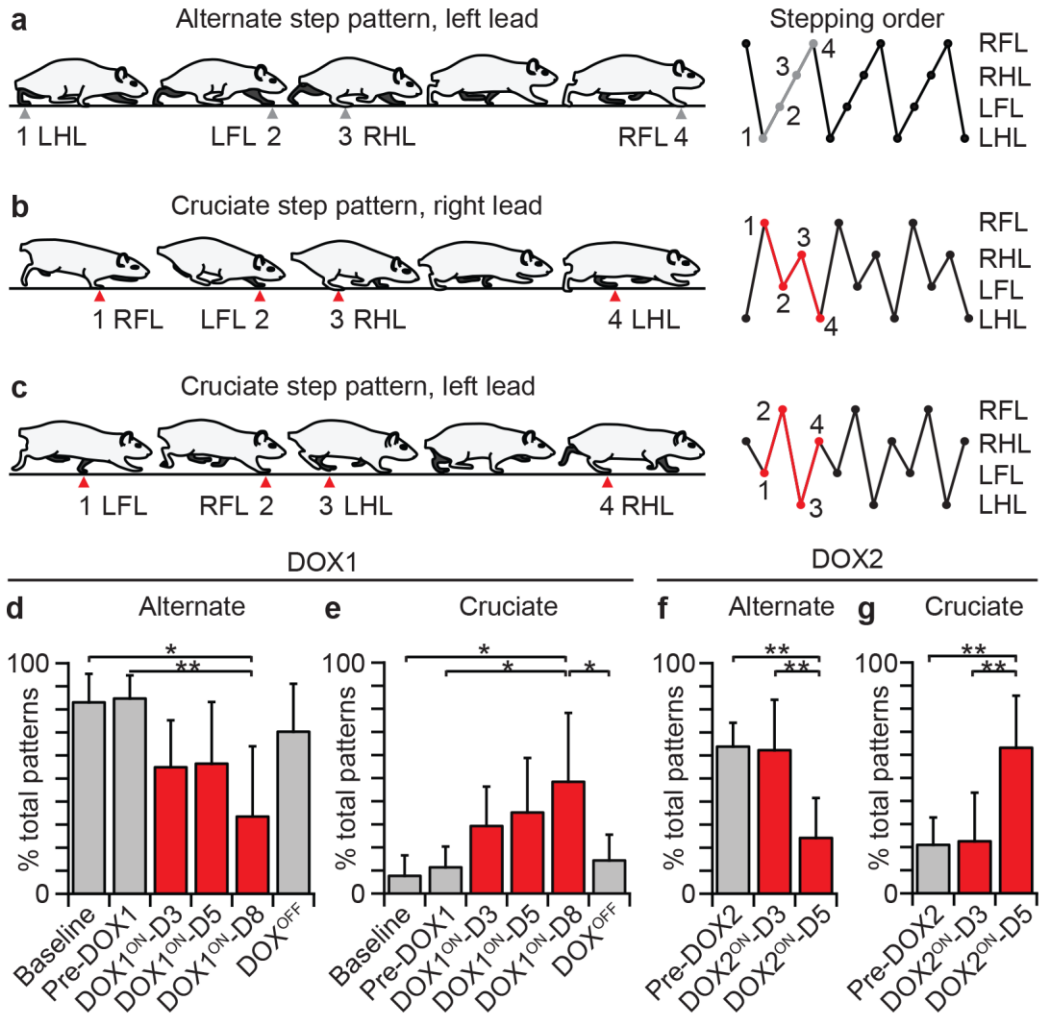


**Figure 6. Silencing L2-L5 Interneurons Altered The Locomotor Step Sequence Pattern.**

(**a-c**) Schematics of alternate and cruciate step sequence patterns as defined by footfall order (right panels). The alternate pattern predominates at control time points (**d**, Baseline: 83.0±13.5%; Pre-DOX1: 82.3±14.8%). Silencing L2-L5 interneurons changed the pattern from alternate to cruciate (**d-e**, $DOX1^{ON}$-D8: 33.5±30.4% alternate, 48.4±29.8% cruciate as compared to 7.7±8.9% and 11.4±9.0% at Baseline and Pre-DOX1, respectively). This was reversed by DOX

removal and replicated one month later (**f-g**). (*p≤0.05; **p≤0.01; repeated measures analysis of variance (ANOVA) and Tukey honest significant difference (HSD) *post hoc* t-test; data are mean ± S.D.; n=47-66 step sequence patterns/time point) (LHL=left hindlimb, RHL=right hindlimb, LFL=left forelimb, RFL=right forelimb).

*Figure 7*

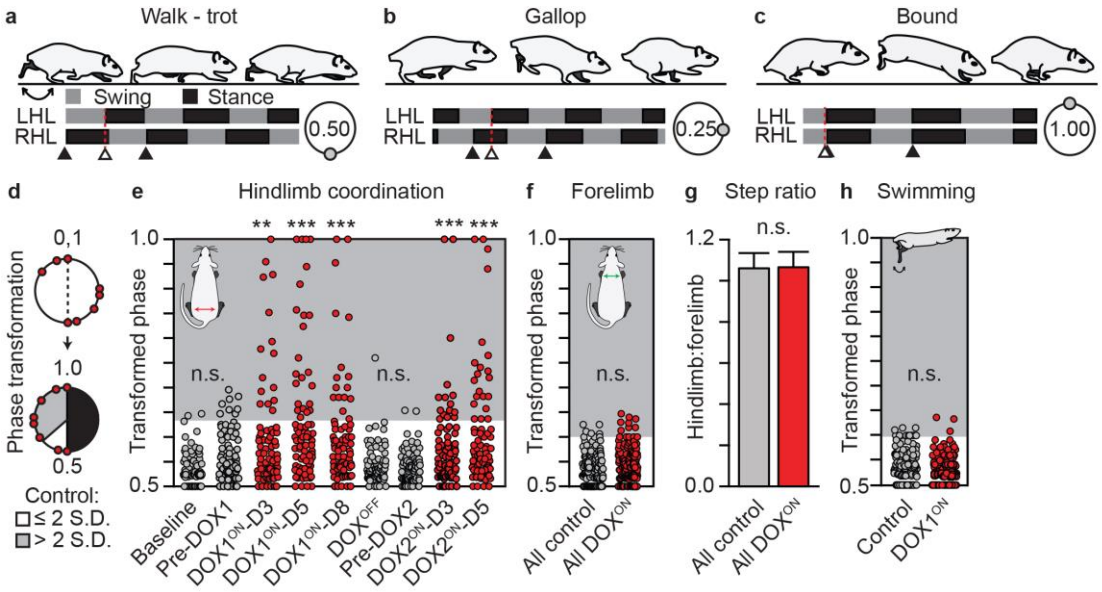


**Figure 7. Silencing L2-L5 Interneurons Selectively Disrupts Left-Right Hindlimb Alternation During Overground Stepping.**

(**a-c**) Stereotypic locomotor gaits with representative swing-stance graphs and characteristic left-right hindlimb coordination values (shown in circular plots, see methods for detail). (**d**) Schematic illustrating phase transformation (see methods for detail). Shaded area denotes any coordination value beyond normal variability observed (>2 S.D.) at control time points. Each circle represents one step cycle (n=84/time point). (**e**) Silencing L2-L5 interneurons significantly increased the proportion of steps that deviated beyond normal variability observed at control time points. Removing DOX restored alternation and silencing one month later repeated the effects (Baseline, n=3/84 vs $DOX1^{ON}$, n=15/84, 24/84, 17/84; Pre-DOX2, n=2/84 vs $DOX2^{ON}$, n=15/84, 21/84; **p≤0.01, ***p≤0.001; Binomial Proportion (B.P.) Test; group data shown [N=6]). Control time points were not significantly

different from each other (data not shown). (**f**) Left-right forelimb alternation was not perturbed (p=0.08; B.P. test). (**g**) No differences were observed in the hindlimb:forelimb stepping index (p=0.86, two-sample t-test). (**h**) Left-right hindlimb alternation persisted during swimming (n=80 stroke cycles/time point; p=0.20, B.P. test).

*Figure 8*

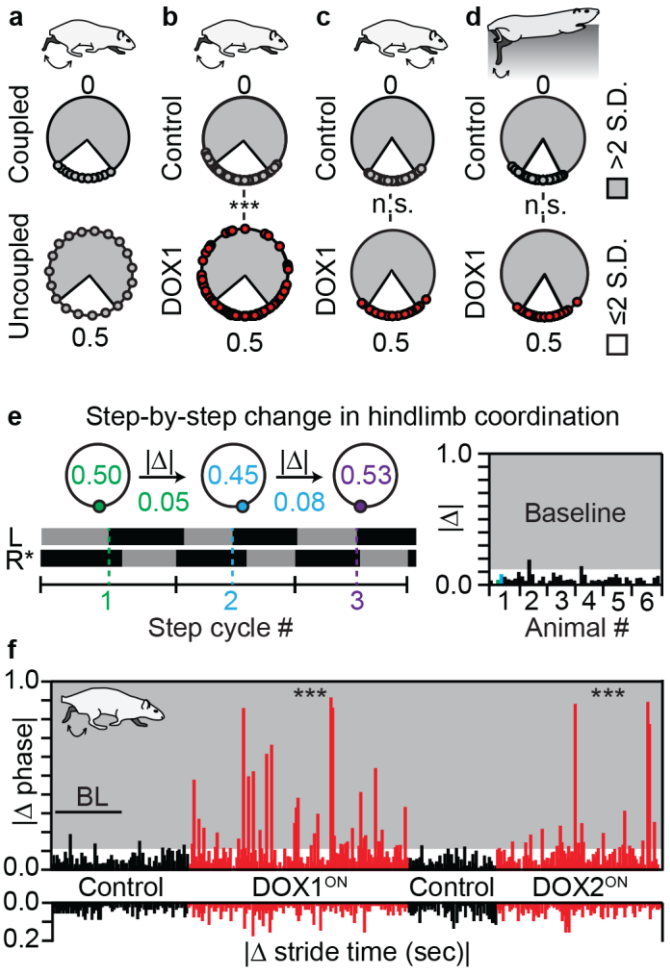


**<u>Figure 8</u>. Silencing L2-L5 Interneurons Partially Uncouples The Hindlimbs, Significantly Increasing The Step-By-Step Variability In Left-Right Coordination.**

(**a**) Coupling and complete uncoupling schematics (white inset=normal variability observed at control time points). (**b**) Silencing L2-L5 interneurons significantly decreased phases concentrated at alternation during hindlimb stepping as compared to Control (Baseline + Pre-DOX1; ***p<0.001; $U^2$=0.59762; Watson's $U^2$ test). Forelimb stepping (**c**) and hindlimb swimming (**d**) remained clustered at alternation (see Supplementary Tables 1-2) (n=84 steps/time point or n=80

strokes/time point). (**e**) Example of swing-stance graph illustrating analysis of consecutive strides within one locomotor bout to determine the step-by-step (absolute) change in left-right coordination (*reference). Individual bars represent |change| in left-right coordination, per step, for each animal across all time points (right panel, e.g. Baseline, |change| in coordination between steps 1-to-2 and 2-to-3 highlighted in green and blue, respectively). Shaded region indicates per step changes in coordination beyond control variability. (**f**, top panel) Silencing L2-L5 interneurons significantly increased step-by-step variability in hindlimb coordination (Baseline+Pre-DOX1 vs $DOX1^{ON}$, n=3/80 vs 38/136; $DOX^{OFF}$+Pre-DOX2 vs $DOX2^{ON}$, n=2/53 vs 21/100; ***p<0.001, B.P. Test; group data shown [N=6]). The hindlimbs stepped with relatively consistent stride durations (bottom panel).

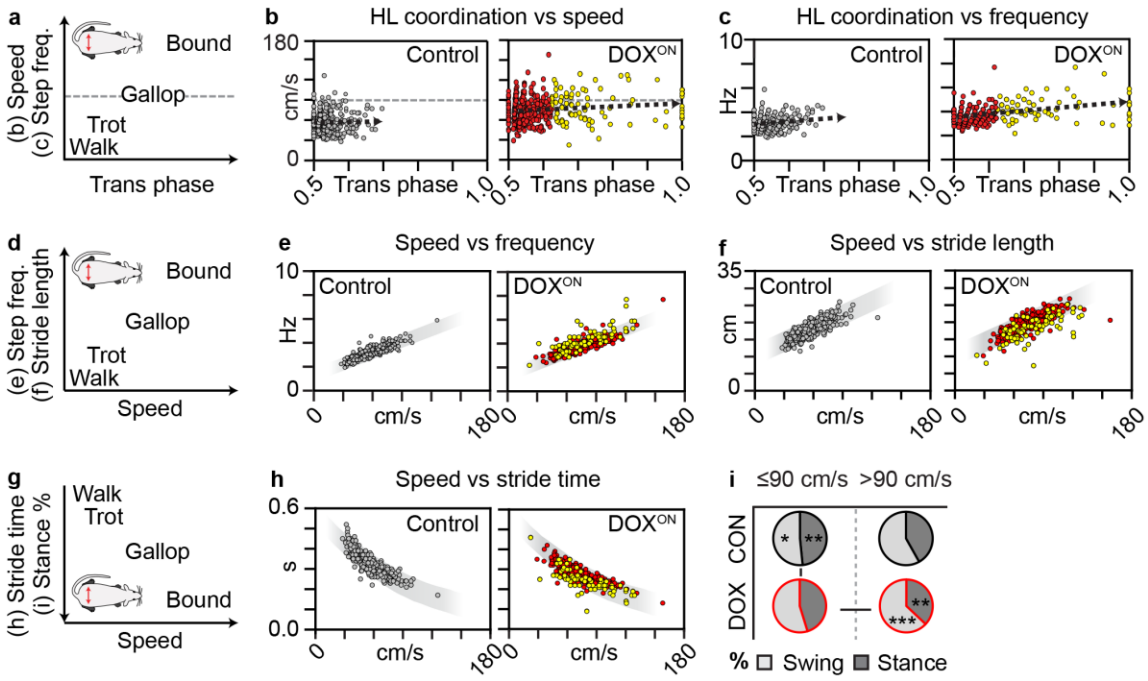


**<u>Figure 9</u>. Silencing L2-L5 Interneurons Disrupts Hindlimb Alternation Independent Of Speed And Step Frequency While Preserving Salient Features That Govern Locomotion.**

(**a**) Schematic illustrating the general relationship between speed/step frequency and locomotor gaits. Dashed gray line indicates reported transition between the alternating trot and asynchronous gallop in the adult rat. (**b**) Silencing-induced changes in hindlimb coordination did not correlate with increased speed (Control, $r_S$=-0.01; DOX$^{ON}$, $r_S$=0.13, Spearman Rank; see Figure 14) nor increased step frequency (**c**, Control: $r_S$=0.04; DOX$^{ON}$: $r_S$=0.33). (**d,g**) Schematics indicating the general relationship between speed and various spatiotemporal gait indices. Silencing L2-L5 interneurons does not affect these stereotypic associations, including speed vs step frequency (**e**, CON $r_S$=0.87; DOX $r_S$=0.83), stride length

(**f**, CON $r_S$=0.81; DOX $r_S$=0.78), stride time (**h**, CON $r_S$=-0.87; DOX $r_S$=-0.83), and the relative decrease in stance duration (**i**, Control vs $DOX^{ON}$: *p<0.05, **p<0.01, independent t-test; $DOX^{ON}$ speed comparisons: **p<0.01, ***p<0.001, paired t-test) (red=phases ≤2 S.D. control mean; yellow=phases >2 S.D. control mean; Control: n=336 steps; $DOX^{ON}$: n=420; shaded region=95% prediction interval for control; group data shown [N=6]).

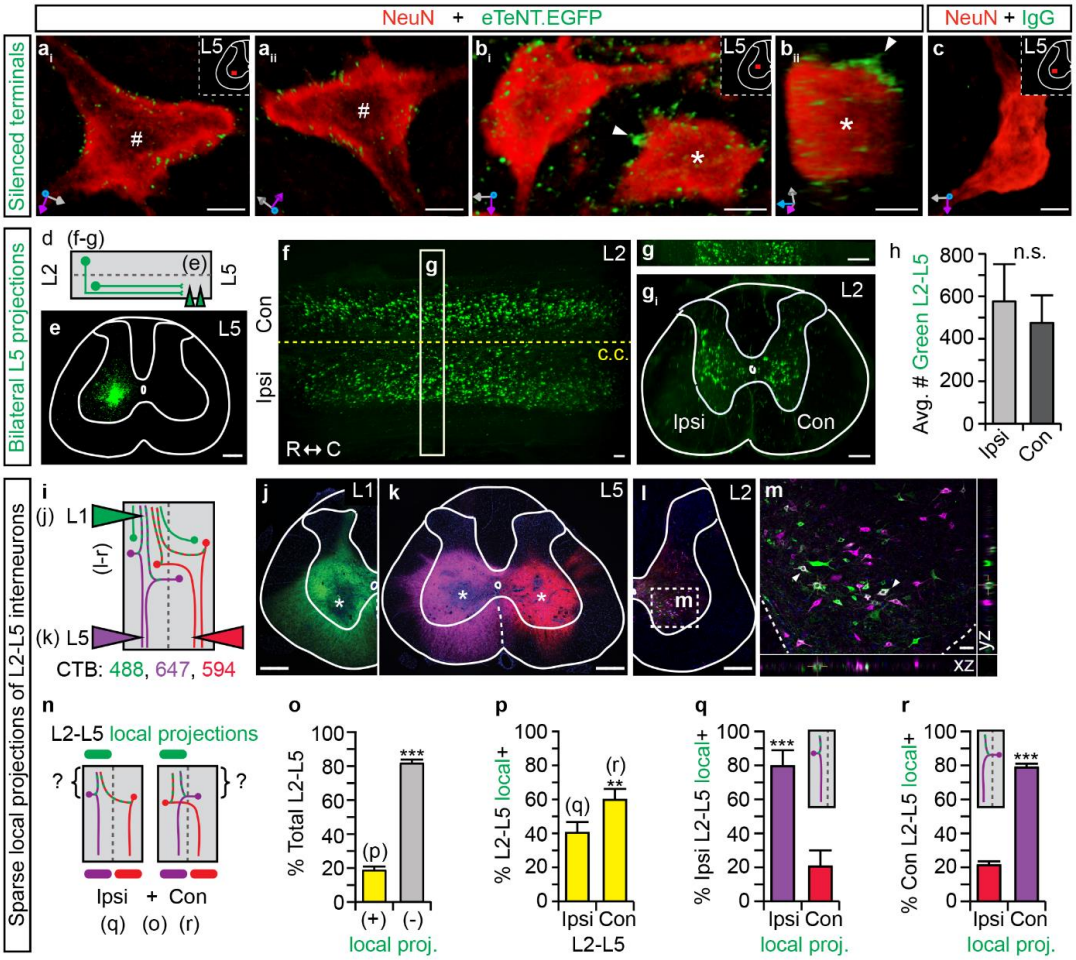


**Figure 10. eTeNT.EGFP⁺ Putative Terminals And Anatomical Characterization Of The L2-L5 Interneurons.**

(**a-b**) Volumetric three-dimensional renderings show eTeNT.EGFP⁺ terminals closely apposed to somata and primary dendrites (#,* indicate same neuron rotated, xyz axes shown in gray/magenta/blue; scale=10 µm). (**c**) Isotype control. (**d**) Light sheet fluorescence microscopy experimental design with representative L5 injection site shown in (**e**). (**f**) Retrogradely-labeled L2-L5 interneurons in isolated and cleared L2 segment (C.C. = central canal; R-C = rostral-caudal). (**g**) 100 µm cross-section. (**h**) Absolute counts of ipsi- and contralateral L2-L5 interneurons (**h**, p=0.47; independent t-test; see Figure 15). (**i**) Experimental

design to quantify L2-L5 local projections with representative injection sites shown in (**j**,**k**, *tracer bolus). (**l**,**m**) Confocal images of double-labelled L2-L5 interneurons (**d-m**, co-localization in orthogonal xz/yz, scale=100 µm). (**o-r**) Quantification of L2-L5 projections shown in (**n**) (**p≤0.01; ***p≤0.001; one-way ANOVA with Tukey's HSD; data are mean ± S.D.; N=5).

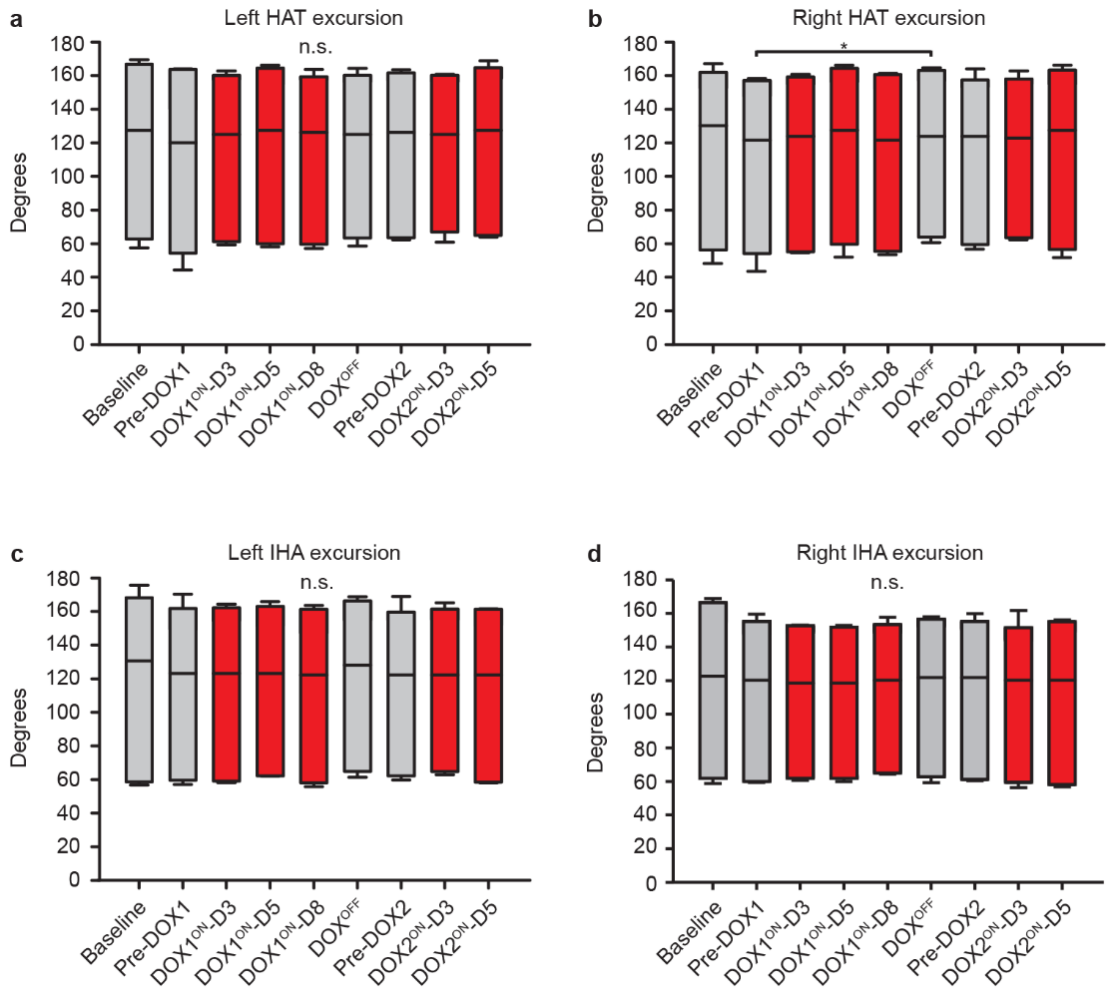


**<u>Figure 11</u>. Silencing L2-L5 Interneurons Does Not Affect Hindlimb Range-Of-Motion.**

The excursion of the left (**a**) and right (**b**) distal hindlimb joint angles (hip-ankle-toe, HAT) at control time points was not significantly different from $DOX^{ON}$. Right hindlimb HAT excursion at $DOX^{OFF}$ was significantly increased compared to Pre-DOX1 (*p<0.05; mixed model ANOVA and Bonferroni *post hoc* t-test). There was no change in the (**c**) left or (**d**) right proximal hindlimb joint angular excursion (iliac crest-hip-ankle, IHA) (black lines denote mean joint excursion).

*Figure 12*

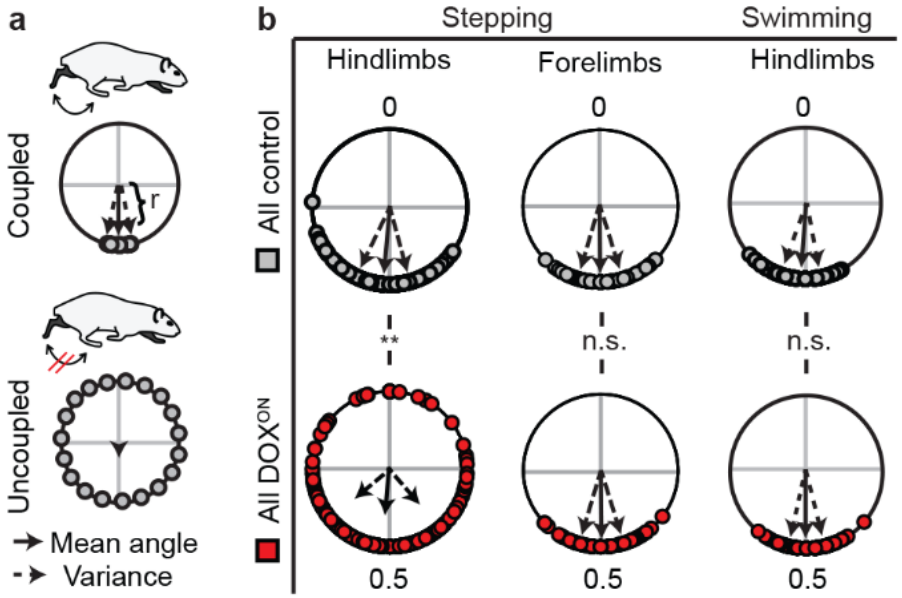


**<u>Figure 12</u>. Silencing L2-L5 Interneurons Partially Uncouples The Hindlimbs During Stepping While Forelimb Stepping And Hindlimb Swimming Remain Intact.**

(**a**) Schematics illustrating phase dispersion (*r*) and circular variance (dashed-arrows). Circles represent individual step or swim cycles. (**b**, left panel) Silencing significantly increased dispersion (r=0.94 vs 0.73; **p<0.01) and variance (±20.51º vs ±45.92º; ***p<0.001; All control, n=336 steps; All $DOX^{ON}$, n=420 steps; group data shown [N=6]). Stereotypic forelimb stepping (middle panel, r=0.96 vs 0.95, variance=±17.20º vs ±18.89º; each p>0.5) and hindlimb swimming (right panel, r=0.97 vs 0.98, variance=±15.06º vs ±12.76º; each p>0.5; Control [Baseline, PD1, $DOX^{OFF}$], n=320 strokes; All $DOX1^{ON}$, n=240 steps) remained intact (averages analyzed using one-way ANOVA followed by Tukey's *post hoc* t-test; see Table 4 for non-parametric two-sample $U^2$ comparisons). Group data shown (N=6).

*Figure 13*

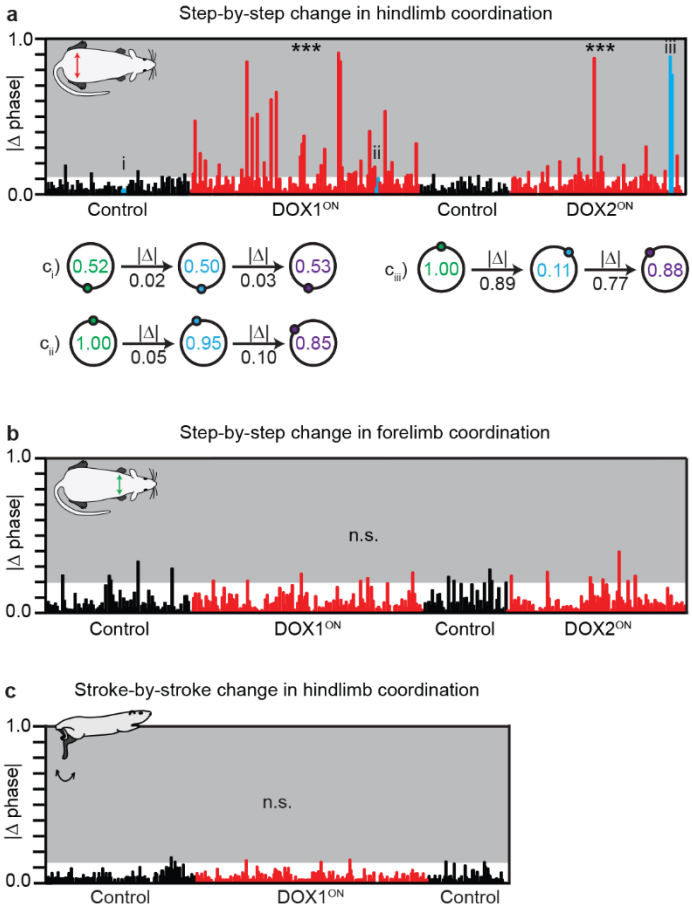


**<u>Figure 13</u>. Conditional Silencing Did Not Alter Step-By-Step Changes In Forelimb Coordination Nor Stroke-By-Stroke Changes In Hindlimb Coordination.**

(**a**) Representative examples of step-by-step changes in hindlimb coordination (**i-iii**, blue lines) from one animal (data previously shown in Figure 8). (**b**) Silencing L2-L5 interneurons does not affect the variability in the step-by-step forelimb coordination (Control [BL, PD1, $DOX^{OFF}$]: 93.1% vs $DOX1^{ON}$: 94.4%, p=0.48, Binomial Proportion Test). (**c**) Similar results were found for stroke-by-stroke changes in hindlimb coordination during swimming (Control [BL, PD1, $DOX^{OFF}$]:

94.7% vs DOX1$^{ON}$: 97.9%; p=0.10) (shaded region denotes step-by-step changes >2 S.D. from respective control means).

*Figure 14*

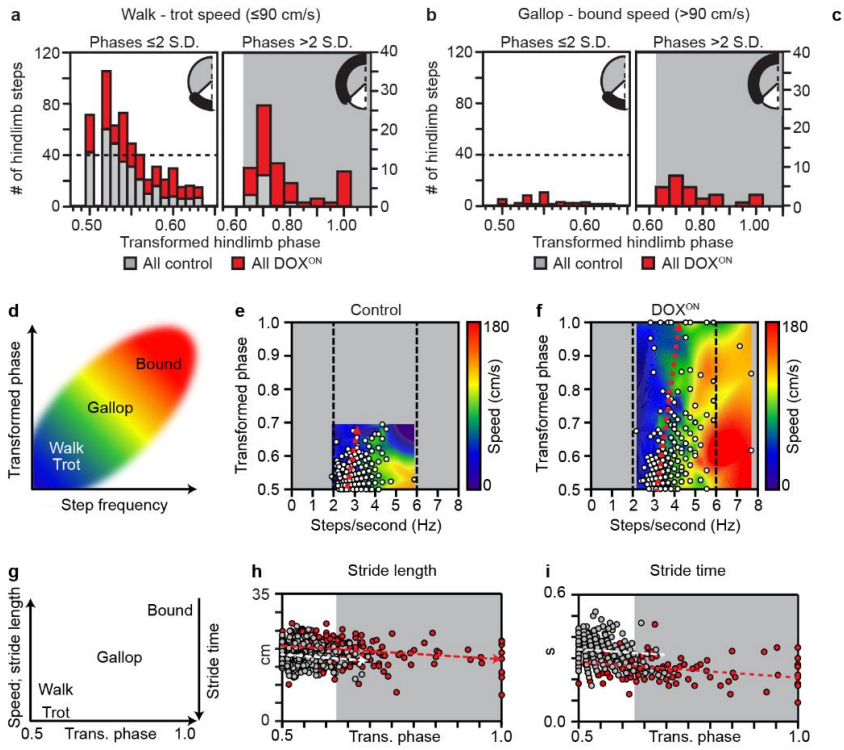


| Time point | r value | p value |
|---|---|---|
| Baseline | -0.023 | 0.965 |
| Pre-DOX1 | -0.677 | 0.140 |
| DOX1$^{ON}$-D3 | 0.455 | 0.365 |
| DOX1$^{ON}$-D5 | -0.468 | 0.349 |
| DOX1$^{ON}$-D8 | -0.082 | 0.878 |
| DOX$^{OFF}$ | 0.613 | 0.196 |
| Pre-DOX2 | -0.367 | 0.475 |
| DOX2$^{ON}$-D3 | 0.001 | 0.999 |
| DOX2$^{ON}$-D5 | 0.097 | 0.855 |
| All >2 S.D. | 0.005 | 0.980 |

**<u>Figure 14</u>. Silencing-Induced Changes In Hindlimb Coordination Did Not Correlate With Speed Nor Gait-Related Indices.**

(**a**) Left panel shows the frequency distribution of hindlimb coordination values within the control variability (right inset; 0.50-0.63) that occurred at ≤90 centimeters/second, a locomotor velocity where the limbs typically alternate in a walk or trot gait. Right panel shows the frequency at which phases >0.63, including synchrony at 1.0, occur at a speed where alternation usually prevails (shaded region denotes phases beyond control variability). (**b**) Frequency distribution of hindlimb phases at gallop-to-bound speeds (>90 cm/sec). (**c**) Summary of Pearson correlations between averaged phase vs speed, per time point (Bonferroni adjustment for multiple comparisons was performed to reduce the likelihood of Type I errors). (**d,g**) Inter-relationship between various gait indices. (**e,f**) Step

frequency-phase relationship (white circles) mapped onto speed contour plot (see methods for detail). Silencing-induced changes in hindlimb coordination did not correlate with increased step frequency. (**h**) Similarly, changes to hindlimb coordination did not correlate with increased stride length (Control, $r_S$=-0.068 in dashed white line; $DOX^{ON}$, $r_S$=-0.125 in dashed red line; Spearman Rank correlation) nor decreased stride time (**i**, Control $r_S$=-0.036; $DOX^{ON}$ $r_S$=-0.338).

**a**

| | Ipsilateral L2-L5 INs | | | Contralateral L2-L5 INs | | |
|---|---|---|---|---|---|---|
| Animal ID | F.E. | F.R. | F.E.+F.R. | F.E. | F.R. | F.E.+F.R. |
| 1 | 772 | 355 | 1,127 | 623 | 302 | 925 |
| 2 | 434 | 243 | 677 | 378 | 211 | 589 |
| 3 | 522 | 285 | 807 | 423 | 235 | 658 |
| Total | 1,728 | 883 | 2,611 | 1,424 | 748 | 2,172 |
| % of total | 54.82 | 54.14 | 54.59 | 45.18 | 45.86 | 45.41 |

F.E.=FluoroEmerald; F.R.=FluoroRuby

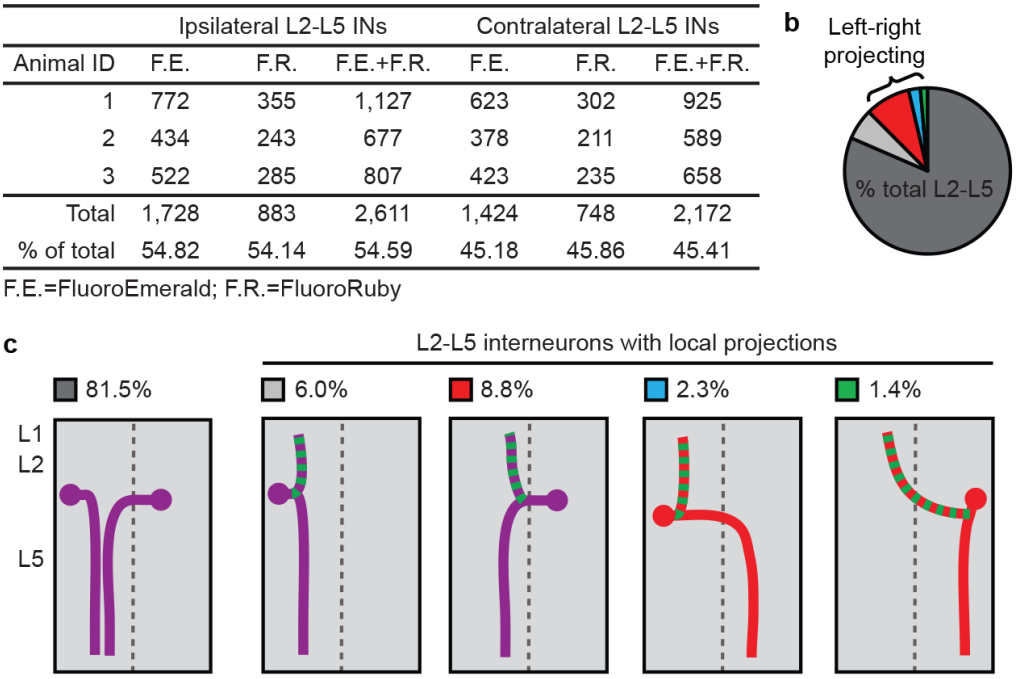


**Figure 15. The Majority Of L2-L5 Interneurons Lack Local Projections In The Rostral Lumbar Spinal Cord.**

(**a**) Data shown are absolute cell counts and percent total of L2 interneurons with ipsilateral or contralateral projections to spinal L5 following bilateral injections of FluoroEmerald (F.E.) and FluoroRuby (F.R.). No significant difference was found between ipsi- and contralateral L2-L5 interneurons (total ipsilateral vs total contralateral: p>0.4; independent t-test between means of equal variance). (**b**,**c**) Summary of the L2-L5 projection patterns observed following triple tracer (CTB) injections. Of the total L2-L5 interneurons labelled at L2 following bilateral L5 injections, approximately 80% did not have local projections within one (rostral) segment of their cell body (dark gray, 81.49±2.36%). Almost 20% of the L2-L5

interneurons had projections within one segment of their cell body (18.51±2.36%). Of this proportion, approximately 12.5% had direct projections between the left and right sides of the spinal cord (**c**, red, blue, and green). Data shown represents the proportions of projection patterns observed relative to percent total L2-L5 interneurons that were labelled.

**<u>Table 3</u>. Silencing L2-L5 Interneurons Functionally Uncouples The Left And Right Hindlimbs During Overground Stepping.**

Using the non-parametric two-sample $U^2$ test, we tested the null hypothesis that the two samples (e.g. Baseline vs DOX1$^{ON}$-D5) came from two populations with the same directions (in other words, degree of concentration or dispersion). This is an indication of whether the limbs are coupled (phases concentrated in same direction) or uncoupled (phases are dispersed). Silencing the L2-L5 interneurons significantly decreased the concentration of the phase values (reduced clustering at 0.5) and caused an increased dispersion throughout the coordination range. This suggests the hindlimbs became functionally uncoupled during overground locomotion. (Critical value of Watson's $U^2_{(0.05,\infty,\infty)} = 0.1869$; Appendix D, Table D.44)[19].



*Table 3*

| | | p value | $U^2$ value |
|---|---|---|---|
| Baseline vs | Pre-DOX1 | p>0.50 | -0.13369 |
| | DOX1$^{ON}$-D3 | 0.05<p<0.10 | 0.16895 |
| | DOX1$^{ON}$-D5 | **0.002<p<0.005** | 0.33339 |
| | DOX1$^{ON}$-D8 | 0.10<p<0.20 | 0.13157 |
| | All-DOX1$^{ON}$ | **p<0.001** | 0.56176 |
| | DOX$^{OFF}$ | p>0.5 | 0.07047 |
| Pre-DOX1 vs | DOX1$^{ON}$-D3 | 0.20<p<0.50 | 0.08912 |
| | DOX1$^{ON}$-D5 | **0.01<p<0.02** | 0.24507 |
| | DOX1$^{ON}$-D8 | **0.02<p<0.05** | 0.21514 |
| | All-DOX1$^{ON}$ | **p<0.001** | 0.59762 |
| | DOX$^{OFF}$ | p>0.50 | 0.00498 |
| | Pre-DOX2 | p>0.50 | 0.01499 |
| Baseline + Pre-DOX1 vs | All-DOX1$^{ON}$ | **p<0.001** | 0.59762 |
| Pre-DOX2 vs | DOX$^{OFF}$ | p>0.50 | 0.07400 |
| | DOX2$^{ON}$-D3 | **0.002<p<0.005** | 0.31224 |
| | DOX2$^{ON}$-D5 | **p<0.001** | 0.39267 |
| | All-DOX2$^{ON}$ | **p<0.001** | 1.29965 |

**Table 4. The Conditional Silencing Of L2-L5 Interneurons Does Not Uncouple The Forelimbs During Stepping Nor The Hindlimbs During Swimming.**

Following methods described above, the null hypothesis was not rejected for time point comparisons of forelimb stepping and hindlimb swimming. Silencing the L2-L5 interneurons did not change the concentration of the phase values at 0.5. Note that in hindlimb swimming, Baseline was significantly different from $DOX^{OFF}$ wherein the phases were more clustered at 0.5. (Critical value of Watson's $U^2_{(0.05,\infty,\infty)} = 0.1869$; Appendix D, Table D.44)[19].

*Table 4*

| | | | p value | $U^2$ value |
|---|---|---|---|---|
| Forelimb stepping | Baseline vs | Pre-DOX1 | p>0.50 | 0.01735 |
| | | $DOX1^{ON}$-D3 | p>0.50 | 0.03821 |
| | | $DOX1^{ON}$-D5 | p>0.50 | -0.03716 |
| | | $DOX1^{ON}$-D8 | p>0.50 | 0.06999 |
| | | All-$DOX1^{ON}$ | p>0.50 | 0.00771 |
| | | $DOX^{OFF}$ | p>0.50 | 0.02585 |
| | Pre-DOX1 vs | $DOX1^{ON}$-D3 | p>0.50 | 0.02560 |
| | | $DOX1^{ON}$-D5 | p>0.50 | 0.03907 |
| | | $DOX1^{ON}$-D8 | p>0.50 | 0.02254 |
| | | All-$DOX1^{ON}$ | p>0.50 | 0.07072 |
| | | $DOX^{OFF}$ | p>0.50 | 0.03725 |
| Hindlimb swimming | Baseline vs | Pre-DOX1 | p>0.50 | 0.02585 |
| | | $DOX1^{ON}$-D3 | p>0.50 | -0.96664 |
| | | $DOX1^{ON}$-D5 | p>0.50 | -0.54443 |
| | | $DOX1^{ON}$-D8 | p>0.50 | -0.48521 |
| | | All-$DOX1^{ON}$ | p>0.50 | -1.62815 |
| | | $DOX^{OFF}$ | **0.02<p<0.05** | 0.20163 |
| | Pre-DOX1 vs | $DOX1^{ON}$-D3 | p>0.50 | -1.3616 |
| | | $DOX1^{ON}$-D5 | p>0.50 | -0.79496 |
| | | $DOX1^{ON}$-D8 | p>0.50 | -0.92183 |
| | | All-$DOX1^{ON}$ | p>0.50 | -2.69285 |
| | | $DOX^{OFF}$ | p>0.50 | 0.07581 |

**Table 5. Disruption In Hindlimb Phase Did Not Correlate With Speed-Related Gait Parameters.**

Time point comparisons showed hindlimb phase did not significantly correlate with speed-associated gait measures such as stance, swing, and stride time as well as stride distance. All phase values >2 S.D. also did not significantly correlate with speed-related gait measures (averaged data; Pearson correlation with the Bonferroni adjustment for multiple comparisons to reduce the likelihood of Type I errors).

*Table 5*

| | | | p value | $U^2$ value |
|---|---|---|---|---|
| Forelimb stepping | Baseline vs | Pre-DOX1 | p>0.50 | 0.01735 |
| | | $DOX1^{ON}$-D3 | p>0.50 | 0.03821 |
| | | $DOX1^{ON}$-D5 | p>0.50 | -0.03716 |
| | | $DOX1^{ON}$-D8 | p>0.50 | 0.06999 |
| | | All-$DOX1^{ON}$ | p>0.50 | 0.00771 |
| | | $DOX^{OFF}$ | p>0.50 | 0.02585 |
| | Pre-DOX1 vs | $DOX1^{ON}$-D3 | p>0.50 | 0.02560 |
| | | $DOX1^{ON}$-D5 | p>0.50 | 0.03907 |
| | | $DOX1^{ON}$-D8 | p>0.50 | 0.02254 |
| | | All-$DOX1^{ON}$ | p>0.50 | 0.07072 |
| | | $DOX^{OFF}$ | p>0.50 | 0.03725 |
| Hindlimb swimming | Baseline vs | Pre-DOX1 | p>0.50 | 0.02585 |
| | | $DOX1^{ON}$-D3 | p>0.50 | -0.96664 |
| | | $DOX1^{ON}$-D5 | p>0.50 | -0.54443 |
| | | $DOX1^{ON}$-D8 | p>0.50 | -0.48521 |
| | | All-$DOX1^{ON}$ | p>0.50 | -1.62815 |
| | | $DOX^{OFF}$ | **0.02<p<0.05** | 0.20163 |
| | Pre-DOX1 vs | $DOX1^{ON}$-D3 | p>0.50 | -1.3616 |
| | | $DOX1^{ON}$-D5 | p>0.50 | -0.79496 |
| | | $DOX1^{ON}$-D8 | p>0.50 | -0.92183 |
| | | All-$DOX1^{ON}$ | p>0.50 | -2.69285 |
| | | $DOX^{OFF}$ | p>0.50 | 0.07581 |

**Table 6. Hindlimb Phase Versus Gait After Controll[illegible]or Speed.**

Part correlations were performed, where the relationship between phase and gait (e.g., stance time) was measured after controlling for the effect of speed on that gait variable. Hindlimb phase significantly correlated with stride distance at DOX1$^{ON}$-D5 only. This represents approximately 2.8% of the total phase versus gait comparisons analyzed. All hindlimb phase values >2 S.D. did not significantly correlate with gait (averaged data; Part correlation with Bonferroni correction for multiple comparisons).

*Table 6*

| | Stance time | | Swing time | | Stride time | | Stride length | |
|---|---|---|---|---|---|---|---|---|
| | $r_{y(2\cdot1)}$ value | p value | $r_{y(2\cdot1)}$ value | p value | $r_{y(2\cdot1)}$ value | p value | $r_{y(2\cdot1)}$ value | p value |
| Baseline | 0.663 | 0.223 | 0.766 | 0.131 | 0.862 | 0.060 | 0.842 | 0.073 |
| Pre-DOX1 | -0.414 | 0.323 | 0.645 | 0.051 | 0.306 | 0.487 | 0.246 | 0.582 |
| DOX1$^{ON}$-D3 | 0.025 | 0.965 | -0.544 | 0.274 | -0.801 | 0.342 | -0.753 | 0.071 |
| DOX1$^{ON}$-D5 | -0.700 | 0.110 | -0.809 | 0.261 | -0.858 | 0.054 | -0.867 | **0.027** |
| DOX1$^{ON}$-D8 | -0.961 | 0.072 | -0.463 | 0.430 | -0.669 | 0.215 | -0.809 | 0.095 |
| DOX$^{OFF}$ | -0.327 | 0.488 | 0.014 | 0.978 | -0.284 | 0.553 | -0.267 | 0.579 |
| Pre-DOX2 | 0.633 | 0.206 | 0.045 | 0.939 | 0.599 | 0.241 | 0.534 | 0.312 |
| DOX2$^{ON}$-D3 | -0.966 | 0.072 | -0.557 | 0.329 | -0.852 | 0.067 | -0.883 | 0.423 |
| DOX2$^{ON}$-D5 | -0.915 | 0.243 | -0.744 | 0.146 | -0.840 | 0.072 | -0.930 | 0.180 |
| **All phases >2 S.D.** | -0.039 | 0.827 | -0.258 | 0.148 | -0.140 | 0.436 | -0.162 | 0.368 |

# CHAPTER III

# LONG ASCENDING PROPRIOSPINAL NEURONS: A FLEXIBLE, CONTEXT-SPECIFIC INTER-ENLARGEMENT NETWORK FOR LEFT-RIGHT ALTERNATION

## Introduction

Locomotion is a fundamental behavior that allows animals to move in order to satisfy their needs, whether it is searching for food, escaping predators, or simply traversing through various environments. While the expression of locomotion starts within supraspinal centers, it is the spinal circuitry that ultimately effects patterned limb movements[21]. Indeed, the isolated spinal cord devoid of all supraspinal and sensory inputs can produce motor patterns indicative of stepping[115].

Stepping is defined by two principal features: rhythm and pattern[25]. Rhythm is the master regulator of locomotion, defining the underlying frequency at which all movements occur[116]. Pattern is the expression of this rhythm, taking the form of both intralimb and interlimb coordination[25]. Together, these core features of locomotion are produced by neuronal networks that are collectively called the central pattern generator (CPG)[25]. Within the spinal cord, the cervical and lumbar enlargements serve as CPG hubs that govern fore- and hindlimb stepping,

respectively[110,115,117]. Therefore, it is the neural circuitry within these enlargements that expresses patterned limb movements that are indicative of the locomotor gaits[17]. In addition to coordinating the actions at each girdle independently, quadrupedal mammals must also coordinate between them[118-120]. Two intraspinal pathways are anatomically well-suited to facilitate forelimb-hindlimb coordination: the long descending and long ascending propriospinal neurons[115,118,119,121,122].

Long descending propriospinal neurons (LDPNs) reside within the cervical enlargement and send projections caudally to innervate the lumbar enlargement[123-126]. Initial electrophysiological studies performed in the cat suggested that this descending system is critically involved in postural control as it relays proprioceptive inputs from the head and neck down to the hindlimb motor pools[125]. A recent study by Ruder and colleagues further elaborated on these findings[127]. Here, they showed that the selective ablation of cervico-lumbar projections resulted in diminished “coherent locomotion.” Specifically, animals had postural instability, a reduction in the maximum speed during overground stepping, and impaired interlimb coordination at increased velocities on the treadmill[127]. These studies suggest that the descending, inter-enlargement system is primarily involved in maintaining postural control, and to some extent interlimb coordination, but perhaps only when the animal is pushed to step faster.

Long ascending propriospinal neurons (LAPNs) are the “reciprocal” pathway to LDPNs with their cell bodies residing in the lumbar enlargement and their terminal field throughout the cervical enlargement[123,126,128]. This heterogeneous pathway is comprised of ipsilateral and commissural projections

that provide excitatory as well as inhibitory inputs onto neurons throughout the cervical gray matter, including motor neurons[121,123,126,129-131]. What role this pathway plays during locomotion remains unknown. Here, we set out to determine the consequences of silencing this ascending inter-enlargement network during overground locomotion in the alert and behaving adult rat. In light of the anatomical underpinnings of this neural circuit, we hypothesized that silencing LAPNs would disrupt hindlimb-forelimb coordination during overground locomotion.

**Materials and methods**

Experiments were performed in accordance with the Public Health Service Policy on Humane Care and Use of Laboratory Animals, as well as the Institutional Animal Care and Use and Institutional Biosafety Committees at the University of Louisville. These experiments utilized the Kentucky Spinal Cord Injury Research Center Neuroscience core facilities that are supported by P30 GM103507.

A total of N=37 adult, female, Sprague-Dawley rats (200-220g) were used in this study. Animals were housed two per cage under 12 hour light:dark cycle with *ad libitum* food and water. Power analysis of previous silencing experiments revealed that N=6 was sufficient to detect a significant difference with 90-99% power. Data shown represent two separate experiments, each N=6 and N=7. Experiments were performed in a staggered fashion separated by one month. Therefore, while the first group was undergoing DOX2 testing the second group was performing DOX1 testing. No significant differences were detected between the two groups. Data shown are from the total N=13.

***Viral vector production***

Dr. Tadashi Isa and colleagues generously provided the plasmid vectors[80]. The HiRet-TRE-EGFP.eTeNT and AAV2-CMV-rtTAV16 viral vectors were built following previously described methods[89,90] with viral titers of $1.6x10^7$ vp/ml and $4.8x10^{12}$ vp/ml, respectively.

***Intraspinal injections to double infect L2-C6 interneurons***

N=13 rats were anesthetized with sodium pentobarbital (50 mg/kg, i.p.) and received a C6-C7 laminectomy to expose spinal C6. Clamps were applied to the spinous processes to stabilize the vertebral column. Intraspinal injections were performed following previously described methods[123]. A total of four HiRet-TRE-EGFP.eTeNT injections were performed. Injections were bilateral with 0.5 µl per site, separated by1.5 mm rostrocaudally. Each injection targeted the intermediate gray matter (0.6 mm mediolateral, 1.3 mm dorsoventral) and were given in two, 0.25 µl boluses. Three minute incubations after each injection were allotted to facilitate viral uptake. After the last injection, the incision site was sutured in layers with surgical staples applied to close the wound. Animals received standard post-operative care, including gentamicin (20 mg/kg, s.c.), glycopyrrolate (0.02 mg/kg, s.c.), and lactated Ringer's solution (10 c.c, s.c.). Prophylactic doses of gentamicin continued for 7 days and buprenorphine was given every 12 hours for the first 48 hours post-surgery for pain management (10mg/kg, s.c.). Voluntary bladder control recovered within 24 hours post-surgery.

One week later, animals were re-anesthetized with ketamine:xylazine (80 mg/kg:4 mg/kg, i.p.) and received a T12 laminectomy to expose spinal L2.

Following the injection protocol used at the cervical spinal cord, animals received four injections of AAV2-CMV-rtTAV16 (0.6 mm mediolateral, 1.5 mm dorsoventral). After the incision site was closed, Yohimbine was given to reverse the effects of xylazine (0.1 mg/kg; i.m.). Standard post-operative care was followed with staples removed 7-10 days post-surgery. Post-surgery baseline testing began one month later.

***Experimental timeline***

Doxycycline hydrochloride (DOX, 15 mg/ml) was dissolved in sucrose water (3%) and provided *ad libitum* for 5-8 days. Approximate consumption volumes were recorded and replenished daily. Behavioral testing was performed prior to intraspinal injections (Baseline), post-surgery/pre-DOX administration (Pre-DOX1), during DOX ($DOX1^{ON}$D1-D8), and one week post-DOX ($DOX^{OFF}$). Testing was repeated one month later (Pre-DOX2, $DOX2^{ON}$D1-D5) to assess the reproducibility of functional changes. N=6 animals underwent vehicle control testing as well (4 days of sucrose water followed by behavioral testing). $Control^{All}$ reflects the combined data from the following time points: Baseline, Pre-DOX1, $DOX^{OFF}$, and Pre-DOX2. Although no significant differences were detected between the Sugar control and all other control time points, we excluded this time point from the $Control^{All}$ grouping as the drinking solutions were different. $DOX^{All}$ reflects the combined data from the following time points (unless otherwise noted): $DOX1^{ON}$D3, -D5, -D8 and $DOX2^{ON}$D3, and -D5.

Animals were acclimated to stepping walkway prior to Baseline acquisition. All stepping behavior analyzed was spontaneous and volitional. Animals did not

receive positive or negative reinforcement training. The order in which animals were tested was random. It was impossible to fully blind experimenters to the study due to the overt changes in behavior during control versus $DOX^{ON}$ time points. However, raters were blinded to animal-specific behavior across time points and behavioral tasks.

Each animal served as its own control throughout the study. The justification for this approach are as follows: (1) surgeries are unique for each animal with regard to proportion of total L2-C6 interneurons silenced, (2) the silencing technique endows inherent variability in transgene expression across animals, and (3) each animal has unique behavioral characteristics (ipso facto, inter-animal variability). Data shown are control versus experimental ($DOX^{ON}$) time point comparisons for the total N=13.

***Three-dimensional hindlimb kinematics and intralimb coordination***

Hindlimb kinematic analyses were performed following previously described methods[92,132]. To summarize, prior to Baseline we marked the skin overlying the anterior rim of the pelvis (iliac crest; I), head of the greater trochanter (hip; H), lateral malleolus of the ankle (A), and the metatarsophalangeal joint of the toe (T). This allowed us to describe hindlimb movements with three segments (I-H, H-A, A-T) and two angles (I-H-A, H-A-T). High speed (100 frames/second) video recordings were performed as animals freely stepped in a custom built plexiglass walkway tank. Videos were acquired from two sagittal and one ventral viewpoints. Recordings were analyzed using MaxTraq, MaxMate, and MaxTraq3D software (Innovision Systems; MI, USA).

A minimum of two stepping passes (8-10 stride cycles) per hindlimb (left and right) were analyzed for each animal across all time points. Locomotor bouts that were analyzed met the following criteria: (1) animals stepped for approximately three-fourths the length of the tank, which is one meter, (2) animals stepped continuously with no distracted behavior, (3) there were minimal lateral deviations during stepping, and (4) were representative of each animal's overall behavior at that specific time point.

The mean peak, trough, and excursions of the proximal (iliac crest-hip-ankle angle, IHA) and distal (hip-ankle-toe angle, HAT) hindlimb segments were analyzed for each limb, respectively, across all time points. Data shown in Figure 22 are the mean ± S.D. for N=13 at $Control^{All}$ and $DOX^{All}$ time points, respectively. Individual time point data is shown in Figure 30 (supplementary to Figure 22). To calculate intralimb coordination between the two joint angles, the time of peak IHA was divided into the peak-to-peak HAT cycle time. These values (ranging from 0 to 1) were plotted on a circular graph (Figure 22) wherein 0 denotes normal coordinated movements between the limb segments.

***Volitional overground gait analyses***

The timing of paw contacts and lift offs were analyzed from ventral recordings. Following the previously defined criteria, a minimum of four passes (or approximately 8 step cycles) were analyzed per animal across time points.

To quantify interlimb coordination, the initial contact time of the one limb was divided into the length of time for one complete stride cycle of a reference limb. This coordination (or phase) value, which ranges from 0 to 1, describes the

temporal relationship between the limbs. Phase values are plotted on a circular graph wherein 0/1 indicates in-phase (synchrony) movements while 0.5 denotes out-of-phase (alternation). For example, hindlimb coordination was calculated by dividing the time of left limb initial contact into the right limb stride cycle duration. Similar approaches were taken to calculate left-right forelimb coordination (right reference), ipsilateral hindlimb-forelimb coordination (hindlimb reference), and diagonal hindlimb-forelimb coordination (hindlimb reference).

Freely stepping animals present with two main concerns regarding analysis of interlimb coordination. First, there is inter- and intra-animal variability in lead limb during stepping. To account for these variances, we normalized the circular 0-1 phase data by transforming it to a linear scale. For limbs that typically move in-phase during the walk-trot gait (e.g. diagonal hindlimb-forelimb), coordination values >0.5 were converted to the reciprocal <0.5. Limbs that typically move out-of-phase (e.g. left-right hindlimbs), coordination values <0.5 were converted to the reciprocal >0.5. Therefore, limb pairs that stereotypically move simultaneously are now plotted on a scale of 0.0 (normal in-phase) to 0.5 (out-of-phase) and pairs that move alternatingly are now on a scale of 0.5 (normal out-of-phase) to 1.0 (in-phase).

The second concern regarding freely stepping animals is the natural variability in relative “accuracy” or precision of coordination. To quantify silencing-induced changes in interlimb coordination beyond this normal variability observed, we calculated the average coordination value for all control time points for each limb pair. From this value we next set a control threshold (average + 2 standard

deviations). Any value that is below this threshold can be attributed to normal variability observed during overground stepping while any value above is considered “irregular” or altered. The proportion of phases beyond this control threshold were compared across time points for the limb pairs.

To determine the magnitude change in interlimb coordination during silencing (Figure 18), we first calculated each animal’s number of altered steps (>2 S.D. beyond control average) for $Control^{All}$ and $DOX^{All}$ time points for the following limb pairs: right and left forelimb, right and left hindlimb, right homolateral limb pair (hindlimb-to-forelimb), and right hindlimb-left forelimb pair (note: only DOX data is shown). After calculating the total number of altered steps for each animal, we then calculated each animal’s percent of total disrupted steps that were observed in left-right limb pairs or hindlimb-forelimb.

The group peak effects were calculated as follows. First, we determined the $DOX^{ON}$ time point that each animal showed peak changes to interlimb coordination. Thereafter, we stratified the animals into either DOX1 or DOX2 categories and then performed the comparisons (see statistics section below). One animal did not show changes in left-right hindlimb coordination (Figure 18, black circles), but did have silencing-induced perturbations to left-right forelimb and contralateral hindlimb-forelimb coordination.

To determine if there was a “preferred” altered coupling pattern expressed during silencing (Figure 26), we calculated the frequency of disrupted steps for the whole group that fell within discrete ranges of left-right coordination values (e.g., [≤0.05], [>0.05,≤0.10], [>0.10, ≤0.15], etc; raw 0-1 phase values). The frequency

is expressed as a percent of the total altered coupling patterns observed (top panel: forelimbs; bottom panel: hindlimbs). We then calculated the regression of x (binned phase ranges) on y (frequency of observation for each bin) to determine the line of best fit and compare the slopes between the "forelimb quadrants" (top lefts versus right slopes) and "hindlimb quadrants" (bottom left versus right slopes). There was no preferred coupling pattern in the altered hindlimb steps. The forelimbs did have two preferred coupling patterns during silencing. These preferred patterns were closely juxtaposed to the control threshold ([>0.40, ≤0.45], [>0.65, ≤0.70]) and were not significantly different from each other.

Per-step changes in interlimb coordination were calculated from raw 0-1 phase values (Figure 19). These data reflect the absolute difference in coordination with each step for all animals across all time points. Any value >2 S.D. from the control mean change is plotted in the shaded area (hindlimb mean=0.043, S.D.>0.113; forelimb mean=0.066; S.D.>0.131). To determine the proportion of steps that had per-stride changes of ≤0.1 versus >0.1, we first calculated each animal's total number of steps where the per-step change in coordination was between 0.0-0.10 or >0.10 ($Control^{All}$ and $DOX^{All}$, respectively). Then, from each animal's grand total of steps analyzed, we determined what percent had per-step changes in coordination that were ≤0.1 or >0.1. Data shown are comparing the group averages ± S.D. (bars) with individual averages overlaid on top (circles). The ratio of hindlimb-to-forelimb steps taken was calculated following previously described methods[133]. Data shown are from calculating each animal's stepping index at $Control^{All}$ and $DOX^{All}$ time points, respectively.

Phase-frequency polar plots were created in SigmaPlot (Figure 20) with each concentric circle set to 2 Hz increments (inner most: 0 Hz, outer most: 10 Hz). All steps analyzed ($Control^{All}$, N=480; $DOX^{All}$, N=600) were plotted for the raw left-right coordination value and its associated step frequency value. The dashed circle denotes a 5 Hz threshold at which virtually all $Control^{All}$ steps fell within (forelimbs: 99.8% all steps; hindlimbs: 100%). Yellow circles denote individual steps that deviated beyond control variability for the forelimbs and hindlimbs, respectively. Data were compared for the circular dispersion as described below (statistics section).

The underlying rhythm indices were analyzed as follows (Figure 20). For the mean stride frequency and durations, we first established that there was no significant side effects during $Control^{All}$ and $DOX^{All}$ time points, respectively. Thereafter, we calculated each animal's $Control^{All}$ and $DOX^{All}$ average stride duration and frequency to then between the time points for the fore- and hindlimbs, respectively. We also compared between the limb pairs for $Control^{All}$ and $DOX^{All}$ as well (bars: group mean ± S.D.; circles: individual means). Regression and slope analyses were also performed (comparing CON vs DOX) on the following comparisons: left versus right forelimb stride duration, left versus right forelimb stride frequency, left versus right hindlimb stride duration, left versus right hindlimb stride frequency, forelimb versus hindlimb stride duration, and forelimb versus hindlimb stride frequency. The inter-girdle comparisons had the left and right limb pairs averaged together before hindlimb versus forelimb analyses.

We also calculated each animal's average stance and swing durations as well as stride length for the left and right limb pairs (fore- and hindlimbs, respectively) across all time points. Group comparisons were made for Control$^{All}$ versus DOX$^{All}$ with and without speed as a co-variate (Figure 21). Regression and slope analyses were performed as described above. To compare the proportion of steps that occurred at speeds ≤90 cm/s versus >90 cm/s, we binned the steps into speed ranges and calculated each animal's average for all DOX$^{ON}$ steps as well as for the altered steps alone.

***Balance, posture, and trunk control assessments***

Base of support

We assessed balance, posture, and trunk control through a series of "intensity" graded tasks. First, we analyzed the base of support during overground locomotion. We focused our analyses to the hindlimbs alone as this is where the major propulsive forces for locomotion are generated. To do this, we used a three-point angle analyses to quantitatively describe the rotation of the hind paws at initial contact (point 1: area between shoulder blades, 2: groin, 3: hind paw position at initial contact). We chose to use the initial contact instead of lift off as there is some normal rotation of the paw as weight is differentially transferred to the hindlimb throughout the stance phase. To quantitatively describe paw rotations on a step-by-step basis, digitized all three points (1 [between shoulder blades] – 2 [groin] – 3 [base of paw]) thereby creating an angle. The degree of paw rotation could then be used to quantitatively describe the base of support. The left and right hindlimbs were analyzed individually.

Ladder

Next, we quantified the animals' ability to effectively traverse a ladder with fixed-spacing rungs (Columbus Instruments)[134,135] (Figure 23). Behavioral testing was performed at Baseline, Pre-DOX1, DOX1$^{ON}$-D4, DOX1$^{ON}$-D8, DOX$^{OFF}$, Pre-DOX2, DOX2$^{ON}$-D4, and DOX2$^{ON}$-D5. Each animal received five stepping trials. The total number of footfalls were calculated for the left and right hindlimbs, respectively, for each animal across the time points. We then calculated the each animal's average number of foot slips during the Control and DOX time points listed above. After determining no statistical difference between the left and right hindlimbs, we combined the trials for the left and right limbs and determined each animal's average for Control and DOX, respectively. Statistics were performed on the group means (bars: average ± S.D.; circles: individual means overlaid). There was one outlier in the data set (red circle; >4 S.D.). Excluding the outlier from analyses did not change the results (Control mean: 3.33±2.4 with outlier, 2.70±1.02 without outlier; both $p<0.001$ when compared to DOX [1.09±0.54]).

Beam

We also assayed each animals' ability to maintain balance, posture, and trunk control while stepping on a 1.8 cm wide beam[136] (Figure 23). Animals traversed the beam for three trials during the following time points: Baseline, Pre-DOX1, DOX1$^{ON}$-D3, DOX1$^{ON}$-D5, DOX1$^{ON}$-D8, DOX$^{OFF}$, Pre-DOX2, DOX2$^{ON}$-D3, and DOX2$^{ON}$-D5. We calculated the total number of foot slips from each trial per animal per time point for the left and right hindlimbs, respectively. After detecting no significant difference between the left and right sides, we combined the trials

for both hindlimbs and calculated the average for Control and DOX, respectively, for each animal. Statistics were performed on the group means. There were three outliers in the data set (one animal at Control and DOX, a second animal at DOX). When we excluded these animals from the beam dataset, we saw similar results (including outliers: $Control^{All}$: 4.38±3.07 vs $DOX^{All}$: 5.46±3.38; p=0.27; excluding outliers: 3.55±2.34 vs 4.4±2.54; p=0.41).

Spontaneously-evoked rearing events

Sagittal recordings of animals in the stepping chamber were analyzed for volitional rearing (Figure 23). We defined rearing as when the animal fully supported itself on its hindlimbs only (grooming events excluded). We defined the onset of rearing as when the animal removed its last forepaw from the ground (removal of all digits). The completion of the rearing event was defined as when the forepaw returned to the ground. As such, we quantified all spontaneously expressed rearing events based on both frequency and duration. To stratify the rearing events based on the level of forepaw support, we documented the onset times of when the forepaw contacted the side of the plexiglass chamber, came into visual focus, and demonstrated weight bearing through spreading of fingertips and postural adjustments. The completion of forepaw support was defined as when the paw was removed from the glass as seen by postural movements, blurring of the hand, and narrowing of the fingertips. As such, we could define the degree of forepaw support by both frequency and duration of the events. Any event where the forepaws were out the field of view were excluded from analysis.

Trunk angle during swimming

In what we consider to be the most challenging task for maintaining trunk control, we assessed the angle at which the animals held their bodies relative to the water (this principal is illustrated in Figure 23). Using four-point angle analysis, we were able to measure the angle of the trunk on a stroke-by-stroke basis throughout the swimming pass (points 1 and 2: water surface [left and right extremes of the videos], 3: iliac crest; 4: hip). Data shown from Pre-DOX1 and DOX1$^{ON}$-D5 with a total of N=3,892 and 3,981; N=4,866 and N=5,654 trunk angles analyzed, respectively, for left and right sides. Data shown are the group means ± S.D.

***Quantitative analyses of volitionally-expressed locomotor gaits***

In order to interpret our silencing data with respect to the traditional locomotor gaits, we had to devise a strategy that would allow us to record and quantify animals that volitionally expressed the higher frequency gaits (e.g., gallop, bound) during overground stepping. To do this, we built a custom “long tank” with the following dimensions (length x width x height): 305 cm, 30.5 cm, and 14 cm. The tank was supported by three A-frame sawhorses. Four high speed video cameras (200 Hz) were evenly spaced below the tank, all mounted to a wooden block.

N=12 naïve adult female Sprague Dawley rats (200-220 g) were used to generate normal gait data. Animals were handled by the experimenters (“gentling”) and exposed to food reward three to four days before being introduced to the tank. After the initial introduction phase where the animals explored the tank, they

underwent positive reinforcement training to ensure that they consistently and repeatedly stepped across the entire length of the track (no pauses, hesitations, or bouts of exploration). Animals were trained twice a day for one week and once a day for the following week prior to the start of video acquisition. To train the animals, we performed the following regimen. First, two experimenters were positioned at either end of the tank. To start, one trainer would create a sound (gently tapping the side of the tank or lightly rubbing two gloved fingers back and forth). Animals typically stepped towards the side of the stimuli where they received a food reward. Thereafter, the second experimenter would provide auditory stimuli and the animal would turn around to fully traverse the tank again to receive another food reward. No food reward was given if the animal did not successfully complete one pass start to finish.

Data shown are from seven separate recording sessions that were spread out over a fourth month period. Food rewards were not given during the video recording sessions. However, the experimenters did provide the auditory stimuli that the animals were accustomed to during training. Videos were acquired at 200 frames per second with approximately four to six stepping passes recorded per animal per time point. In order to “stitch” together the multiple cameras such that all steps could be accounted for across the length of the tank, we used the following strategy. First, we arranged the cameras such that the fields of view (FOV) overlapped (e.g. camera 1-2, 2-3, 3-4). We placed two markers (between the first and second as well as the third and fourth cameras) to use as points of reference during video analysis. These points were copied to all videos such that the

stepping coordinates were integrated across the four individual files acquired (one per camera). Using these strategies, we had no missing frames or steps when animals stepped between the different FOVs. In order to prevent or “subtract out” digitization of steps that fell within two FOVs, we created a series of inter-camera markers throughout the length of the tank. We measured the distance between the start of the tank to each of these markers and quantified these points during video analysis. Thereafter, we developed a custom macro that would detect these digitized inter-camera markers to then filter out the “extra digitizing” between two overlapping FOVs. These processes were also repeated for cameras three and four. Each camera has a 5 cm scale visible, allowing us calibrate the video files using the MaxTRAQ scale feature. Within our macro, we created a pixel-to-cm conversion factor that allowed us to reliably measure the various spatiotemporal indices of locomotion. Altogether, this experimental design allowed us to stitch together multiple videos for seamless step analyses.

Our silencing experiments were performed separate from the long tank, stereotypic gait study. There are two key justifications for performing these studies separately. First, in the long tank paradigm, we used food reward as a tool to encourage the animals to volitionally express the faster gaits. These gaits are volitional in the sense that the animals are not placed on a treadmill and “forced” to step a fast rates of speed. During silencing, we did not want to confound our results by “encouraging” the expression of distinct coupling patterns. Instead, we wanted to assess how the nervous system would intrinsically respond to the functional loss of LAPNs without influence from the experimenters. Second, it is

unknown if the underlying neural circuitry that governs the two behavioral conditions (normal expression without training versus positive reinforcement training via food reward) are similar or different. How could we interpret the silencing-induced changes in interlimb coordination if the animals also received training to express different coupling patterns (e.g. gaits)? Therefore, we opted to keep the two groups separate (silencing group vs long tank gait group). Instead, we used the long tank stereotypic gait data as a conceptual framework to help us interpret our silencing dataset.

Our defining criteria for the distinct locomotor gaits are based off of previously described coupling patterns[17]. In our analyses, we did not distinguish between the two alternating gaits: walk (three limbs in contact with the ground) and trot (two limbs in contact with the ground at any moment).

***Swim phase analysis***

After stepping assessments, the walkway tank was filled with 7-8 inches of water and swim assessments were performed following previously described methods[93]. Briefly, a high-speed camera was placed 18 inches in front of the tank to record animals as they swam towards an exit ramp. A minimum of 4 passes per side (left and right) were analyzed per animal per time point following criteria described above. Each pass was approximately 6 complete stroke cycles. To determine the hindlimb phase relationship during swimming, peak downward extension of the left and right hindlimb toes were digitized. The time of peak downward extension of the left toe was divided into the length of time for one complete stroke cycle of the right hindlimb (refer to Figure 31). These values,

ranging from 0 to 1, were transformed as described above and the proportion of phase values >2 S.D. from the control threshold were compared across time points.

***Viral tissue processing and EGFP.eTeNT immunohistochemistry***

Following terminal assessments, animals were sacrificed at $DOX2^{ON}$-D5 with an overdose of sodium pentobarbital. Animals were transcardially perfused with 0.1 M PBS (pH 7.4) followed by 4% paraformaldehyde (PFA). Thereafter, spinal cords were dissected, post-fixed in 4% PFA for 1 to 3 hours, and transferred to 30% sucrose for 3-4 days at 4ºC. The cervical and lumbar injection sites were dissected, embedded in tissue freezing medium, cryosectioned at 30 µm in 5 sets, and stored at -20ºC.

Immunofluorescent detection of EGFP.eTeNT-positive terminals at C6 was performed following previously described methods[137]. Antibodies used include the following: rabbit anti-GFP (abcam ab290, dilution of 1:5,000) and guinea pig anti-NeuN (Millipore ABN90P, dilution of 1:500). Negative controls include non-immune sera matched for protein concentration and dilution (donkey anti-rabbit IgG; Jackson ImmunoResearch #711-005-152, dilution of 1:5,000). Secondary antibodies were used at a dilution of 1:200 and included the following: anti-rabbit AlexaFluor 488 and -guinea pig AlexaFluor 594 (Jackson Immunoresearch). Images were captured on an Olympus FluoView 1000 confocal microscope using the oil immersion 100x objective with 488, 594, and 647 lasers. Z-stacks acquired ranged from 53-68 slices with each optical step 0.4 µm in depth. Raw .oif files were imported into Amira 3D software for volumetric rendering and three-dimensional

rotation to assess density and distribution of EGFP.eTeNT-positive terminals throughout the gray matter.

Neurons were detected using the Millipore IHC Select DAB kit (DAB500, Millipore). The protocol designed for the kit was followed apart from the following modifications. Slides were warmed at 66ºC for 30 minutes, post-fixed in 4% PFA for one hour at 4ºC, and then briefly rinsed in 0.1 M PBS. The blocking, secondary antibody, and streptavidin HRP steps were 30 minutes in duration. The chromagen reaction lasted 10 minutes. Primary antibodies used included rabbit anti-GFP at 1:40,000 to amplify endogenous eTeNT.EGFP signal and a concentration and dilution-matched isotype control (donkey anti-rabbit IgG; Jackson ImmunoResearch #711-005-152, dilution of 1:40,000). Images were taken on a Nikon Eclipse microscope using a Spot RT CCD digital camera with the DIA-ILL filter at 4x, 10x, 20x, and 40x magnifications.

***Statistical analyses***

Statistical analyses were performed using the SPSS v22 software package from IBM. Additional references for various analyses were also used[103-107,138]. Differences between groups were deemed statistically significant at $p \leq 0.05$. Two-tail p values are reported.

The Binomial Proportion Test was used to detect significant differences in the proportion of coordination values beyond control threshold for the raw (not shown) and transformed interlimb coordination data of various limb pairs. It was also used to detect a significant group peak effect (DOX1 vs DOX2), per-step changes in left-right coordination and stride durations (beyond control thresholds),

the interaction between altered coupling patterns, testing for the preferred “altered” forelimb coupling pattern during silencing, and the stroke-by-stroke changes in hindlimb coordination as well as stroke cycle durations (beyond control variability).

Circular statistics performed on the stepping inter- and intralimb coordination datasets as well as the swimming hindlimb coordination data[103]. We primarily used the non-parametric two-sample $U^2$ test for the following rationale. Typically, parametric tests are performed to determine whether the data has a uniform distribution[103,138]. Importantly, these analyses are based on strict assumptions that the distribution is restricted to two patterns: uniform or unimodal[103,138]. Our data do not fit these criteria (e.g. differences in lead limb and natural intra- and inter-animal variability in interlimb coordination). Moreover, the various control time points (Baseline, Pre-DOX1, $DOX^{OFF}$, Pre-DOX2) do not have unimodal distributions with the exact same degree of concentration. Therefore, we used non-parametric two-sample $U^2$ test. This tests the null hypothesis that two time points have the same concentration (or phasic direction). The length of vector *r* denotes the amount of concentration of phases in a single direction[37]. The average *r* value was calculated for all control and $DOX^{ON}$ time points, respectively, and compared using the independent t-test between means of equal variance. This approach was also used to detect significant differences in the amount of circular variance in the coordination date (angular deviation, value *s*).

Spearman Rank correlations were performed on the speed versus spatiotemporal gait indices for the forelimbs and hindlimbs during $Control^{All}$ and

$DOX^{All}$, respectively. These comparisons included speed versus stance, swing, and stride durations as well as the stride length and frequency.

Regression analyses to compare the slopes for the lines of best fit were performed on the speed versus spatiotemporal gait indices datasets ($Control^{All}$ vs $DOX^{All}$ for forelimbs and hindlimbs, respectively, as well as between the limb pairs). Regression and slope analyses were also performed to test for preferred coupling patterns in the altered stepping datasets as well as comparing the left versus right fore- and hindlimb step frequency and durations as well as comparing between the two girdles.

Mixed model analysis of variance (ANOVA) Bonferroni post hoc *t-tests* were used to detect a significant difference in the peak, trough, and excursion of the proximal and distal hindlimb segments for range-of-motion analyses.

Repeated measures ANOVA with speed as a co-variate were used when comparing $Control^{All}$ vs $DOX^{All}$ stride, swing, and stance durations for the fore- and hindlimbs as well as between the girdles. Sidák *post hoc* t-tests were used when appropriate.

Multivariate analysis of variance (MANOVA) with speed as a co-variate followed by Sidák *post hoc* t-tests were used when comparing the mean stride frequencies and durations for $Control^{All}$ vs $DOX^{All}$ for the fore- and hindlimbs as well as between the two girdles. These analyses were also used when comparing the average stride durations of the left and right forelimbs and hindlimbs, respectively, over time (9 total time points, excluding Sugar control) as well as within the individual time points.

Repeated measures ANOVA without speed as a co-variate were performed when comparing the mean stride durations between the fore- and hindlimbs within the individual time points.

Paired t-tests were used to detect significant differences in: (1) the magnitude change in interlimb coordination during silencing, (2) the proportion of steps with per-stride changes that were ≤0.1 or >0.1, (3) the hindlimb:forelimb step index, (3) when comparing the percent of $DOX^{ON}$ steps that were ≤90 cm/s versus >90 cm/s as well as (4) for the altered steps alone, (5) when comparing the base of support, (6) average number of foots slips on the ladder (7) and beam (8), (9) the frequency and (10) duration of spontaneously expressed rearing events, (11) the trunk angle during swimming, and (12) when comparing the swing-stance durations within speed categories of ≤90 cm/s or >90 cm/s for the fore- and hindlimbs, respectively, at $Control^{All}$ and $DOX^{All}$.

Levene's Test for Equality of Variances were performed to test for a normal distribution within the interlimb coordination datasets. Notably, at control time points (e.g. Baseline) the coordination data has a non-normal distribution as phase values will naturally concentrate towards one value (e.g. 0.5 for left-right alternation in the hindlimbs).

## Results

### *Silencing LAPNs selectively disrupts contralateral hindlimb-forelimb movements while preserving ipsilateral hindlimb-forelimb coordination during overground locomotion*

To test this hypothesis, we used a dual virus system originally developed by Dr. Tadashi Isa and colleagues that permits the functional dissection of anatomically-defined pathways independent of cell-specific promoters[80]. Using this system, we targeted both ipsilateral and commissural LAPNs for conditional silencing in the adult rat spinal cord. We performed bilateral injections of HiRet-TRE-eTeNT.EGFP ("eTeNT") and AAV2-CMV-rtTAV16 at the caudal cervical and rostral lumbar enlargements, respectively (Figure 16a). In double infected neurons, *ad libitum* doxycycline (DOX) induces eTeNT expression within the cell body (Figure 16b). eTeNT is then anterogradely transported to the terminal field where it suppresses neurotransmission through the blockade of synaptic vesicle exocytosis (Figure 16b, bottom panel). Longitudinal assessments were performed over three and a half months (Figure 16c) with a total of five control time points (gray) and two rounds of conditional silencing (red) that were separated by a one month washout period. We also performed a vehicle control to account for the effects of sucrose water consumption on locomotor behaviors (DOX is dissolved in 3% sucrose solution; "Sugar control," SC). A total of N=13 female Sprague Dawley rats were used in this silencing study with each animal serving as its own control (see methods for rationale).

Before we begin to tease out the effects of silencing LAPNs on hindlimb-forelimb coordination, we first need to consider the normal temporal relationship between the pelvic and shoulder girdles during stereotypic locomotion. There are two patterns of hindlimb-forelimb movements: ipsilateral and contralateral. Ipsilateral hindlimb-forelimb coordination describes movements of limbs on the same side of the body (Figure 17a, e.g. red=right hindlimb-forelimb movements). Contralateral hindlimb-forelimb movements describe the diagonal stepping patterns observed across the two girdles (e.g., blue=left hindlimb-right forelimb). Together with the left-right movements observed at each girdle, these coordination patterns are the defining features of the classic locomotor gaits (Figure 17a-c) (Figure 24, supplementary to Figure 17).

Interlimb coordination is expressed as a ratio and is calculated by dividing the initial contact time of one limb by the stride time of a reference limb[17]. For example, to measure ipsilateral hindlimb-forelimb coordination, the initial contact time of the right forelimb (Figure 17a, RFL, dashed red line, open red triangle) is divided by the stride time of the right hindlimb (RHL, filled red triangles=start/end of one complete stride cycle). These phase values, which range from 0 to 1, are plotted on a circular graph to illustrate the interlimb coordination for distinct limb pairs (Figure 17a-c, circular graphs). In the slower gaits such as walk and trot, ipsilateral hindlimb-forelimb movements are out-of-phase, or alternating (Figure 17a, circular graph, red near 0.5; Figure 24, supplementary to Figure 17). Conversely, contralateral hindlimb-forelimb movements are in-phase, or synchronous (Figure 17a, blue near 0/1). As animals increase their speed and

switch from a walk-trot to gallop gait, contralateral hindlimb-forelimb movements undergo a phase shift to where the limbs are moving with increased overlap (Figure 17b, dashed blue box, phase plot=0.25/0.75; Figure 24, supplementary to Figure 17) as compared to strict out-of-phase movements. Ipsilateral hindlimb-forelimb movements continue to move out-of-phase (red at 0.5). At maximal speeds animals switch to the full bound wherein both ipsi- and contralateral hindlimb-forelimb movements are out-of-phase (Figure 17c, circular plot, red/blue=0.5; Figure 24, supplementary to Figure 17).

In this study, we focused on exploring the functional consequences of silencing LAPNs during overground locomotion. This task presents with unique challenges, including but not limited to inter- and intra-animal differences in preferred lead limb as well as intrinsic variability in interlimb coordination[12]. Therefore, to determine how silencing affects hindlimb-forelimb coordination beyond these normal variances, we performed a series of phase transformations and control thresholding. First, to account for the influence of differing lead limbs, we transformed the raw ipsilateral and contralateral hindlimb-forelimb phase values (Figure 17d, f). As ipsilateral hindlimb-forelimb movements are typically out-of-phase, we converted any phase value that was from 0 to 0.5 to its reciprocal 0.5 to 1 value (Figure 17d). Therefore, interlimb coordination values concentrated at 0.5 indicate normal alternating movements while values at 1 denote synchronous stepping of the ipsilateral limbs, a trait of the pacing or racking gait[119]. The converse phase transformation was performed for the contralateral hindlimb-forelimb movements such that phase values range from 0 (normal, in-phase

movements for the walk-trot gait) to 0.5 (out-of-phase movements for the bound gait) (Figure 17f). After controlling for the variability in preferred lead limb, we next wanted to define a set of criteria upon which we could decipher between normal variability associated with overground stepping and the silencing-induced changes. To do this, we calculated the average coordination value of the four control time points (BL, PD1, DOFF, PD2) for each limb pair, respectively. Thereafter, we set the coordination value that was two standard deviations beyond this mean as the “control threshold.” Any phase value that is below this threshold represents steps that fell within normal variability associated with overground locomotion (Figure 17d-g, plotted in white regions). Phase values above this threshold, which are plotted in the shaded region, indicate that the stepping behaviors observed deviated beyond normal behaviors observed at control time points.

At control time points, we saw that the ipsilateral and contralateral hindlimb-forelimb pairs were moving in stepping patterns indicative of the walk-trot gait (Figure 17e,g) (Video 3). This is shown by the preponderance of steps that were out-of-phase for the ipsilateral limbs (Figure 17e, steps at 0.5 and within control variability) and the in-phase movements of the contralateral limbs (Figure 17g, steps at 0.0 and within control levels). When we silenced LAPNs, the locomotor walk-trot gait was disrupted. Instead, we saw the emergence of a spectrum of stepping behaviors that ranged from mild perturbations in hindlimb alternation to synchronous-like movements at the fore- and hindlimbs, respectively (Video 4).

Interestingly, these overt changes in the stepping behaviors explicitly affected one form of hindlimb-forelimb coordination. Apart from one stepping pass were we saw evidence of pacing (DOX1$^{ON}$-D5 [D1D5], red circles near 1.0), silencing LAPNs did not affect the out-of-phase ipsilateral hindlimb-forelimb movements (Figure 17e). This is shown schematically in Figure 17i (red triangles). In contrast, we saw a significant disruption in contralateral hindlimb-forelimb movements (Figure 17g, right hindlimb-left forelimb shown). Instead of the limbs moving in-phase or at a slight phase-shift (within control variability), we saw a range of coordination values that encompassed in-phase movements, to asynchronous gallop-like movements (Figure 17b, blue = 0.25/0.75), all the way to out-of-phase movements (Figure 17c, 0/1) which were reflective of bounding (Figure 17i, blue triangles). These perturbations were observed for both pairs of contralateral hindlimbs and forelimbs (data not shown for the left hindlimb-right forelimb pair). Removing DOX from the drinking water restored normal contralateral hindlimb-forelimb movements and silencing one month later reproduced the effects (Figure 17g, D$^{OFF}$ through D2D5). Notably, giving animals sucrose water (vehicle control) did not change their interlimb coupling patterns, indicating that the changes observed are attributed to the silencing of LAPNs. Collectively, these data suggest that silencing ipsi- and commissural LAPNs selectively disrupts one pattern of hindlimb-forelimb coordination (contralateral) while preserving the other (ipsilateral).

***Silencing LAPNs profoundly affects left-right alternation as compared to hindlimb-forelimb coordination***

Although silencing LAPNs did alter hindlimb-forelimb coordination, it is clear that left-right alternation of the fore- and hindlimbs was profoundly affected (Video 5). Therefore, we set out quantify these perturbations observed within each girdle, respectively.

During control time points, left-right alternation predominated at the shoulder (Figure 18b, forelimbs) and pelvic (Figure 18c, hindlimbs) girdles (gray circles concentrated at 0.5 and within control variability). This is indicative of a walk-trot gait where the two limbs are moving out-of-phase relative to one another (Figure 18a, bottom panel) (Figure 24, supplementary to Figure 18). Silencing LAPNs significantly disrupted this stepping pattern. Once again, we saw a spectrum of coordination values where the left-right fore- and hindlimbs were moving out-of-phase (alternation, 0.5) all the way to in-phase synchronous stepping (0/1) (Figure 18b,c). Together with changes observed in hindlimb-forelimb coordination, it is clear that silencing LAPNs leads to the emergence of an interlimb coupling continuum. These data suggest that reversibly removing this pathway from the otherwise intact system unmasks incredible freedom to the locomotor circuitry, allowing the limbs to adopt a breadth of coupling patterns.

To tease out which coupling pattern was most affected, we compared the magnitude of silencing-induced changes between the various limb pairs. It is clear that silencing LAPNs profoundly affected left-right movements at each girdle as compared to hindlimb-forelimb coordination (Figure 18d). Furthermore, when we

examined the interaction of all affected coupling patterns, we saw that the significant majority of disrupted hindlimb-forelimb movements were associated with left-right perturbations, but not vice versa (Figure 25, supplementary to Figure 18). These results suggest that the primary consequence of silencing this inter-enlargement pathway was the disruption to intra-girdle coupling, not the anticipated inter-girdle movements.

Another surprising result was that it appears as though the silencing effects become more pronounced over time. When we identified the specific $DOX^{ON}$ time point at which each animal showed peak changes in interlimb coordination, we saw that the significant majority had maximal disruption to left-right hindlimb stepping during the second round of silencing (DOX2, one month after DOX1) (Figure 18e). Similar trends were observed in both left-right forelimb and contralateral hindlimb-forelimb coordination, although they did not reach statistically significant levels. Complementary to this "additive" effect we observed when comparing $DOX1^{ON}$ to $DOX2^{ON}$, we also observed a "ramping up" effect. Specifically, the proportion of altered steps significantly increased from one time point to next (e.g., $DOX2^{ON}$-D3 to $DOX2^{ON}$-D5; $p<0.01$).

Together, these data reveal that silencing LAPNs profoundly affects left-right coordination. Due to these overt changes, we believe that the disruptions to hindlimb-forelimb coordination are likely a "byproduct" of the affected left-right movements. Moreover, the effects of silencing LAPNs did not "wash out" over time. Instead, the disruptions became more severe. This suggests that the locomotor

circuitry could not compensate for the functional loss of LAPNs as if it could, then the effects would have been masked.

The emergence of an apparent coordination continuum raises an interesting question: are these new coupling patterns the result of spontaneously-evoked shifts in left-right coordination? Or do they represent stable, albeit altered patterns of stepping that are now possible due to the limbs no longer being “fixed” in alternation?

***The silencing-induced perturbations to interlimb coordination represent stable, albeit irregular coupling patterns that are expressed within a fixed locomotor cycle***

To answer this question, we explored the dynamic coordination between the limbs on a step-by-step basis (Figure 19a-b, untransformed data). Within each individual stepping pass, we first determined the phase relationship between the left and right limbs for each stride taken (Figure 19a, step cycles 1-3 with right limb as reference). Thereafter, we calculated the absolute change in phase between two successive steps taken (Figure 19b, absolute changes shown in red and blue). These step-by-step changes in left-right coordination were then plotted for each step taken, per animal, across all time points. Any per-step change in coordination that deviated beyond control variability is plotted in the shaded region. The results shown are from left-right forelimb and hindlimb coordination, respectively (similar results were found for hindlimb-forelimb, data not shown).

Prior to silencing, we saw small fluctuations in step-by-step coordination (Figure 19c,e, black vertical bars). This indicates that the limbs were stepping with

relatively high fidelity, indicative of a steady-state coupling pattern (left-right alternation). Surprisingly, the silencing-induced disruptions to left-right alternation were not due to spontaneous shifts in coordination. This is shown by the apparent lack of overt changes in step-by-step coordination (red bars within control variability). Instead, we saw that the significant majority of $DOX^{ON}$ steps actually had very minor (≤0.1) per-step changes in left-right coordination, for both the forelimbs (Figure 19d) and hindlimbs (Figure 19f), respectively. Not only were these per-stride changes in coordination minor, but so were the step-by-step changes in stride duration, an indicator of the underlying locomotor rhythm (Figure 19c,e, bottom panels).

When we looked at the stepping relationship between all four limbs (Figure 19g, hindlimb:forelimb step index), we saw that silencing did not alter this salient feature of locomotion (Figure 19h). All limbs stepped equally within one stride cycle (no double or missteps). Therefore, despite the significant perturbations silencing introduced to the left-right forelimb, left-right hindlimb, and contralateral hindlimb-forelimb movements, the overall locomotor cycle remained in a fixed 1:1 relationship.

Altogether, these data suggest that silencing LAPNs “releases the system” from strict alternation, allowing the limbs to express a breadth of coupling patterns that are maintained with great fidelity. Importantly, these diverse coupling patterns do not affect a principle feature of locomotion, the hindlimb:forelimb relationship. This raises a key question: is the master regulator of stepping, the rhythm

generator, similarly impervious to the profoundly altered interlimb coupling schema?

***The underlying locomotor rhythm remains intact during silencing-induced disruptions to interlimb coordination***

Rhythm generation can be described by two underlying features of locomotion: stride duration and step frequency[116]. Moreover, these features are inextricably associated with interlimb coordination[17]. When animals switch from a walk-trot gait (alternation coupling pattern) to that of gallop-bound (synchrony), there is a concomitant increase in the underlying step frequency and decrease in stride duration[17] (Figure 28, supplementary to Figure 20). Therefore, do the perturbations we observe in interlimb coordination cause overt changes to step frequency as well? This would indicate that not only does silencing LAPNs disrupt the locomotor pattern (interlimb coordination), but it also affects the rhythm.

To address this question, we plotted the interlimb coordination data against the corresponding step frequency for all steps analyzed (N=480 for Control, N=600 for DOX). The yellow circles denote the silencing-induced “irregular” coupling patterns expressed in the forelimbs and hindlimbs, respectively.

At Control time points, both the left-right forelimbs and hindlimbs primarily stepped in an alternating pattern (Figure 20a-b, left panels, circles concentrated at 0.5). These steps almost exclusively occurred within a 2-5 Hz frequency range. The conditional silencing of LAPNs functionally uncoupled the limbs at each girdle respectively, as seen by the significant increase in phasic dispersion around the polar plot (Figure 20a-b, right panels; refer to Table 7 for summary of individual

time point comparisons). Interestingly, even though silencing “released the system” from strict left-right alternation, the overwhelming majority of steps still fell within the 2-5 Hz frequency range (N=555/600 and N=572/600 for forelimbs and hindlimbs, respectively). Even when we compared the mean frequencies of the “normal” DOX steps to that of the altered we saw no significant difference (data not shown). Once again, it appears as though the underlying rhythm persists, regardless of the coupling patterns expressed. This led us to systematically examine both stride frequency and duration, our two indices for the underlying rhythm generation during overground locomotion.

We first set out to determine if the overall stride frequency and duration were different between $Control^{All}$ and $DOX^{All}$ time points for the fore- and hindlimbs, respectively (Figure 20c,g). When we compared the mean stride frequency between $Control^{All}$ and $DOX^{All}$ at each girdle (Figure 20c, top=forelimbs, bottom=hindlimbs), we saw no significant difference. Moreover, there was no significant difference between the girdles, indicating that the step frequencies of the hindlimbs were not different from that of the forelimbs. Comparing the overall stride durations yielded the same results (Figure 20g; refer to Figure 27, supplementary for Figure 20, for individual time point comparisons). These comparisons were performed with speed as a co-variate as it has a predictable influence on our indices of interest. When we ran all these analyses without controlling for the effects of speed, we again saw no significant differences (Figure 27, supplementary for Figure 20). Together, these data reveal that the overall fore-

and hindlimb stride frequency and duration, with and without controlling for the effects of speed, were not affected during silencing.

To increase the resolution of our analyses, we gated our comparisons to the individual limbs at each girdle, respectively (Figure 20d-e, h-i). We plotted the rhythm indices of the left limb against that of the right for all steps taken as well as the average of each animal across the four control and five silencing time points. After performing regression analyses and comparing the slopes of the lines-of-best-fit between $Control^{All}$ and $DOX^{All}$ (left versus right forelimb, left versus right hindlimb), we saw no significant differences. Similarly, no differences were detected when we compared between the two girdles (hindlimb versus forelimb, Figure 20f) as well as when we focused our analyses on the irregular steps alone (Figure 27, supplementary for Figure 20). To conclude, silencing LAPNs disrupts the pattern, but the rhythm persists. If one principal feature of locomotion continues despite the altered coupling patterns, do other salient features of locomotion prevail as well?

***Silencing LAPNs reversibly disrupts temporal limb coupling while preserving the fundamental relationship between speed and the spatiotemporal features of limb movements***

Locomotion is characterized by coordinated limb movements through both space and time. These spatiotemporal parameters, which include the rhythm indices, stride length, as well as stance and swing durations, change with speed in a stereotypic, well-defined manner[12,13,109] (Figure 28, supplementary to Figure 21). This relationship is a central feature that governs locomotion. Therefore, we

set out to determine if the silencing LAPNs altered this relationship as a consequence of the significant disruptions to interlimb coordination.

First, we plotted the various spatiotemporal indices against speed for the fore- and hindlimbs respectively (Figure 21, forelimbs top row; hindlimbs bottom). We then performed regression analyses to compare the slopes for the lines of best fit between $Control^{All}$ and $DOX^{All}$. Similar to the preservation of the underlying rhythm, the fundamental relationship between speed and stride duration, frequency, and length remained intact. We did notice a slight, but significant change in slope between $Control^{All}$ and $DOX^{All}$ for the speed versus stride length comparisons of fore- and hindlimbs, respectively (each $p<0.05$). Notwithstanding, the trend line is still linear indicating that the association persists. Similar results were found when we analyzed the stance and swing durations (Figure 29, supplementary for Figure 21).

In addition to comparing the dynamic relationship between speed and the spatiotemporal indices, we also compared the mean stride, stance, and swing durations between $Control^{All}$ and $DOX^{All}$ for the fore- and hindlimbs, respectively (Figure 21d). The silencing-induced disruptions to interlimb coordination did not affect these underlying features of the step cycle. Moreover, there were no differences observed between the hind- and forelimbs as well. Collectively, these data suggest that the defining features of the step cycle persist, a result that makes sense in light of the intact locomotor rhythm.

One of the primary functional consequences of ablating cervico-lumbar projections was the inability to step at faster rates of speed[127]. Clearly, silencing

LAPNs does not recapitulate that finding as our animals have the capacity to step at speeds upwards of 150 cm/s (Figure 21a-c). In addition to the reduced maximum speeds, a second key finding from the irreversible ablation of cervico-lumbar projections was that the expression of impaired interlimb coordination required faster rates of speed during treadmill stepping. Here, we show that the significant majority of $DOX^{ON}$ steps were at speeds ≤90 cm/s during overground locomotion. Moreover, if we analyzed the silencing-induced "irregular" steps alone, we saw that increased speed was not a requirement for the expression of the altered coupling patterns (Figure 21f). These data illustrate that silencing LAPNs reversibly disrupts interlimb coordination independent of speed, speed-dependent spatiotemporal indices, and the underlying locomotor rhythm.

Altogether, we have shown that we can selectively manipulate one defining feature of central pattern generation: interlimb coordination. Moreover, this manipulation is incredibly discrete as all other spatiotemporal aspects of limb movement appear to be inextricably intact. However, there is another form of patterned limb movement that is also governed by the central pattern generator: intralimb coordination. Therefore, does silencing LAPNs disrupt both patterns of limb movement (inter- and intra-) or is it exquisitely tuned to one (interlimb)?

***Intralimb coordination persists during silencing-induced perturbations to interlimb coordination***

To answer this question, we focused on two key features of intralimb coordination: range-of-motion and temporal coordination between the proximal and distal limb segments. We gated these analyses to the hindlimbs as this is

where the major propulsive forces for locomotion are generated[27-29] and where silencing LAPNs exerted its most profound effects (data not shown).

First, we marked the skin overlying the iliac crest, hip, ankle, and toe in order to describe the hindlimb movement using three segments (illustrated in Figure 22a) and two angles (Figure 22c). At Control time points, animals stepped with normal coordinated flexor-extensor actions across the joints as shown by the characteristic excursions of the limb segments (Figure 22a$_{i\text{-}ii}$, refer to Figure 30, supplementary for Figure 22, for quantitation). Silencing LAPNs caused a slight, but significant change in the overall peak-to-trough excursion of the proximal-to-distal hindlimb segments, likely due to the biomechanics of the hindlimbs moving in synchrony as illustrated in Figure 22b$_i$ (e.g., lift off to weight acceptance) and kinematically in Figure 22b$_{ii}$.

We next examined the coordination between the proximal and distal hindlimb joint angles on a step-by-step basis during locomotion (Figure 22c-f). To do this, we analyzed the time of peak proximal angular excursion (Figure 22d, blue) with respect to peak-to-peak distal angular excursion cycle time (Figure 22d, purple). These values, ranging from 0 to 1, are then plotted on a circular graph wherein 0 indicates normal, coordinated movements between the limb segments. Here, we saw that silencing LAPNs did not disrupt this temporal coordination for both the left and right hindlimbs (Figure 22e-f). Together, these data show that in spite of the significant perturbations to interlimb coordination, intralimb movements remain intact.

***Silencing LAPNs does not affect the capacity to maintain balance, posture, and trunk stability***

Ruder and colleagues showed that ablating cervico-lumbar projections in the mouse spinal cord resulted in postural instability during overground locomotion, uneven stepping routes, shorter distances per locomotor bout, and reduced maximum speeds (as described above)[127]. To draw further parallels between these two inter-enlargement studies, we set out to determine if silencing LAPNs similarly affected balance and postural control.

First, we examined the base of support during overground locomotion by measuring the external rotation of the hind paws on a step-by-step basis (see methods for detail). Animals typically have a relatively narrow base of support (illustrated in Figure 23a). In conditions with increased postural instability (e.g. spinal cord injury), the paws become externally rotated and the base of support widens[139]. Conditional silencing of LAPNs did not affect this postural index (Figure 23b).

We next challenged the animals' ability to maintain balance and posture by testing them on the ladder and beam walk tasks (Figure 23c). Here, animals must maintain effective postural control in order to accurately place their limbs on fix-spaced rungs or traverse a narrow beam that is 1.8 cm wide. Once again, we saw no impediments to balance and posture during silencing as the average number of footfalls was not significantly greater during silencing.

A task that is likely more challenging is rearing. Here, the animals must have sufficient balance and postural control such that when they plant their hindlimbs,

they are able to elevate their trunk and upper body safely (Figure 23d). The efficacy of this action can be stratified further by the amount of forepaw support required to maintain balance (0 forepaws=”high” control, 2 forepaws=”low” control). Silencing LAPNs did not affect the overall frequency of spontaneously-evoked rearing events (Figure 23e). We even saw a significant increase in the duration at which the animals stood on their hindlimbs alone, highlighting the overall stability these animals maintained during silencing (Figure 23f).

Finally, we asked whether animals could maintain effective trunk control when all limbs were fully unloaded during swimming. In this bipedal task, the body is almost parallel to the surface of the water. The head, neck, and proximal portion of the back remain above water while the distal body and tail are just below[140]. To quantitatively describe the body angle relative to the water surface, we performed a four-point angle analysis using the positional markers shown in Figure 23g. Using this approach to measure postural stability on a stroke-by-stroke basis, we saw no silencing-induced defects in the animals’ ability to maintain an acute trunk angle (Figure 23g, right panel). From this this series of stability-challenging tasks, it is clear that silencing LAPNs does not affect the overall balance and postural control. These data reveal an interesting dichotomy between what role the lumbo-cervical and cervico-lumbar projection pathways might play in motor behaviors.

Within the vein of functional dichotomies, our swimming analysis revealed a striking result: the silencing-induced perturbations to left-right coordination during stepping were unequivocally abolished when the animals swam (Video 6).

Therefore, not only does silencing LAPNs disrupt interlimb coordination, but it might do so in a task-dependent manner.

## Discussion

### *Long ascending propriospinal neurons: a flexible, task-specific inter-enlargement network for quadrupedal alternation*

Here, we have shown that silencing LAPNs significantly disrupts three patterns of interlimb movements: left-right forelimb, left-right hindlimb, and contralateral hindlimb-forelimb coordination. What emerged from these perturbations was a coordination continuum that spanned from out-of-phase limb movements (alternation) all the way to strict in-phase synchrony. When we examined how these altered coordination patterns were dynamically expressed, we saw that they reflected stable, steady-state coupling mechanisms between the various limb pairs. Moreover, these newly expressed coupling patterns occurred independent of the underlying rhythm, intralimb coordination, speed, and speed-dependent spatiotemporal gait indices. It appears as though by silencing LAPNs, we have released the constraints of the system such that it no longer strictly adheres to rhythmic, left-right alternation. Instead, the limbs were able express a breadth of coupling patterns with incredible fidelity, but all within the confines of a stable locomotor rhythm. Strikingly, when the behavioral context is changed (stepping to swimming) the silencing-induced effects are immediately abolished. Therefore, the functional importance of this pathway is likely gated towards the task at hand.

***The immutable ipsilateral actions***

Interestingly, it appears as though ipsilateral movements were impervious to silencing as homolateral hindlimb-forelimb coordination as well as intralimb coordination were unaffected. The lack of changes in intralimb coordination are not entirely surprising as this patterned movement is likely secured through segmental interneuronal networks[25]. However, the persistence of the stereotypic, out-of-phase movements of the homolateral limb pairs was surprising. This was the only coupling pattern that escaped silencing-induced perturbations. Interestingly, similar results were found when the cervico-lumbar projections were ablated[127]. What makes this even more intriguing is that there is a well-documented, "substantial" ipsilateral ascending projection that interconnects the lumbo-cervical circuitry[121,129,130]. Moreover, electrophysiological interrogations of inter-CPG coupling mechanisms reveal that it is primarily through the ipsilateral, excitatory projections that the lumbar CPG entrains the cervical[115]. In an effort to better understand how the homolateral limb pairs typically perform, we referred back to our long tank, normal gait data. Here, it is clear that the ipsilateral limb pairs simply do not adopt an in-phase coupling relationship, even at speeds upwards of 300 cm/s (Figure 28). Perhaps this patterned movement is "hard-wired" through the intervening thoracic circuitry in addition to long spinal projections. This could help "lock" the limbs in an out-of-phase (or slight phase-shift) relationship to secure dynamic stability across the girdles. Indeed, the pacing (or racking) gait where the limbs step in lateral couplets is rarely expressed[119,141], plausibly due to these

stabilization issues. Notwithstanding, it is clear that silencing the ipsilateral LAPNs does not influence the ipsilateral hindlimb-forelimb movements.

***The functional dichotomy of reciprocal inter-enlargement pathways***

While the cervico-lumbar projection pathways investigated by *Ruder et al* and the lumbo-cervical pathway studied here can be considered "anatomical reciprocals," current evidence suggests they are not functional reciprocals[127]. It is important to note that these disparate results could be attributed to the fundamental differences in the two approaches. Here, we conditionally and reversibly silenced anatomically-defined long ascending projections in naïve adult rat. By contrast, Ruder and colleagues investigated the functional role of transcriptionally-specified neurons that have cell bodies in the cervical enlargement and projections throughout the lumbar segments through irreversible genetic ablations[127]. After taking into account these distinct differences in experimental approach, what does this functional dichotomy mean with regard to how the inter-enlargement system effects locomotion?

Perhaps the LDPNs are involved in discrete forms of locomotion that require more supraspinal influence. In support of this notion, these cervico-lumbar projection neurons have also been shown to have ascending supraspinal projections[142]. Interestingly, the LDPNs receive reciprocal synaptic inputs from these higher motor centers in return[127]. It is clear that this pathway also densely innervates the intervening thoracic circuitry[127], likely a contributing factor to the issues with postural control following their selective ablation. Moreover, Ruder *et al* showed that when you push the animal to step faster, perhaps beyond its

comfort or capacity due to their postural deficits, then the stepping pattern breaks down. Therefore, it is likely that LDPNs participate in a more meticulous form of stepping wherein they operate within a supraspinal feedback loop to then distribute patterned information throughout the entire neuraxis.

LAPNs, on the other hand, clearly do not contribute to maintaining postural control and they profoundly lack lumbar and thoracic projections (data not shown). Instead, they appear to project directly to the cervical enlargement. Therefore, it makes sense that these neurons are a key pathway in distributing left-right, temporal information from the hindlimbs to secure forelimb coordination. It is the hindlimbs that generate the major propulsive forces during locomotion[27-29]. As such, perhaps LAPNs function as primary pattern distributing network when the hindlimbs are required to generate locomotor behaviors immediately and powerfully. Therefore, it is through this inter-enlargement network that both precision and power are endowed to quadrupedal stepping.

*Figure 16*

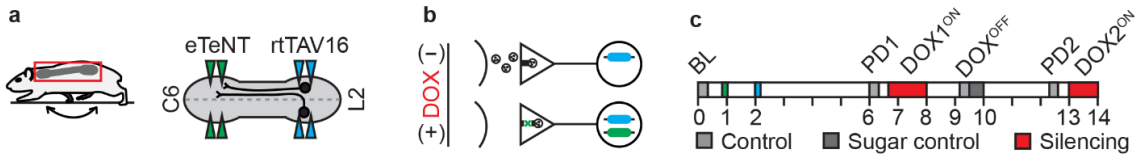


**Figure 16. Experimental design to conditionally silence long ascending propriospinal neurons (LAPNs) in the adult rat spinal cord.**

(**a**) In the spinal cord of N=13 adult female Sprague Dawley rats, bilateral injections of HiRet-TRE-eTeNT.EGFP ("eTeNT") and AAV2-CMV-rtTAV16 ("rtTAV16") were performed in the caudal cervical enlargement (C6) and rostral lumbar enlargement (L2), respectively. (**b**) *Ad libitum* doxycycline (DOX) induces eTeNT expression to suppress neurotransmission at the terminal field in double-infected long ascending propriospinal neurons. (**c**) Functional testing was performed prior to injections (BL=Baseline), post-injections (PD1=Pre-DOX1), during one week of $DOX^{ON}$ silencing (D1D3, D1D5, D1D8=$DOX1^{ON}$-D3, -D5, -D8), and one week post-DOX (DOFF=$DOX^{OFF}$). Testing was repeated one month later (PD2=Pre-DOX2, D2D3, D2D5=$DOX2^{ON}$-D3, -D5). In N=6 animals, a vehicle control was performed ("Sugar control",S.C.). $Control^{All}$=BL, PD1, DOFF, and PD2. $DOX^{All}$=D1D3, D1D5, D1D8, D2D3, and D2D5.

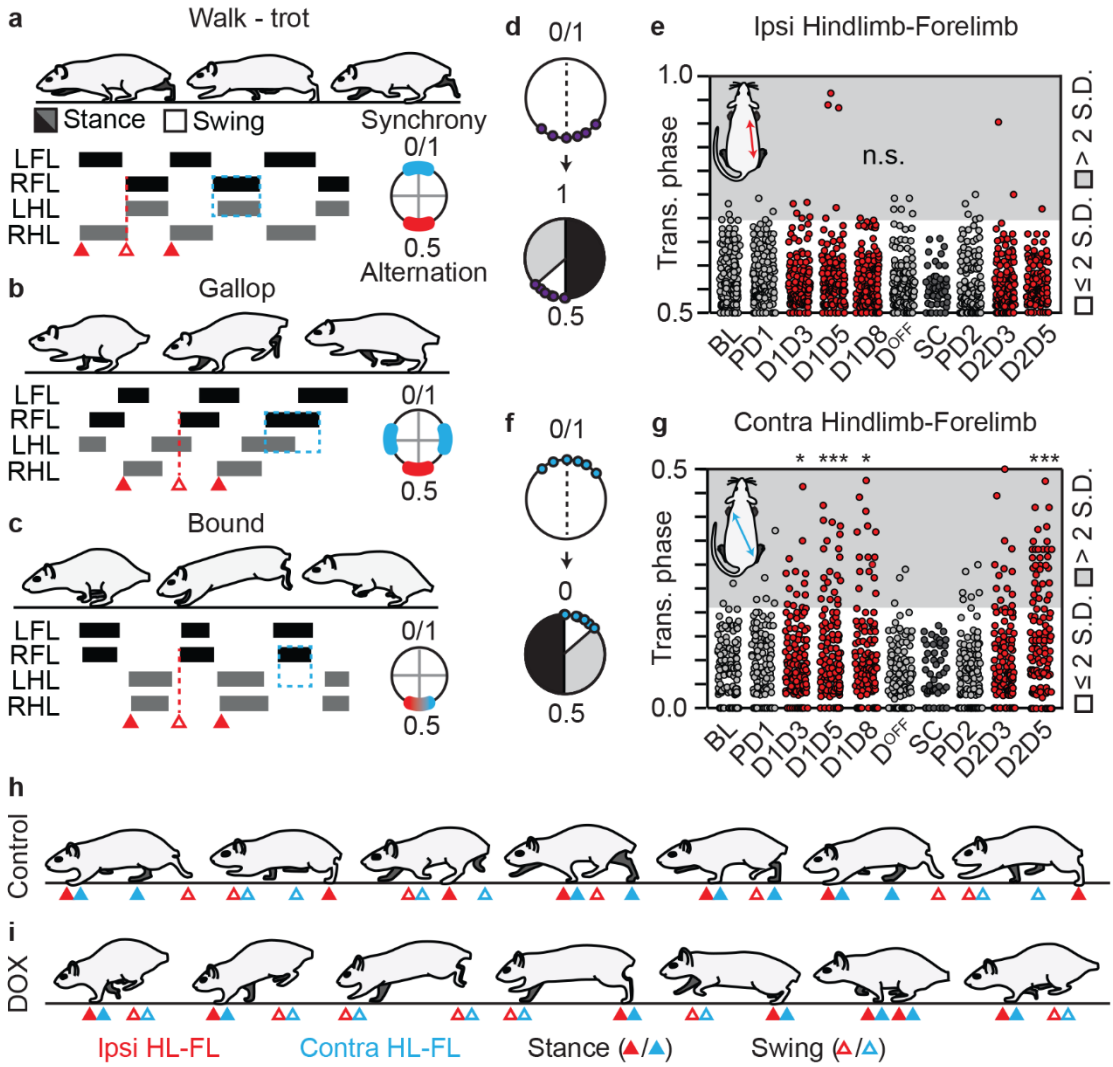


**<u>Figure 17</u>. Silencing LAPNs Selectively Disrupts Contralateral Hindlimb-Forelimb Coordination While Preserving Ipsilateral Hindlimb-Forelimb Alternation.**

(**a-c**) Stereotypic locomotor gaits with representative swing-stance graphs and interlimb coordination patterns (0/1=in-phase/synchronous limb movements; 0.5=out-of-phase/alternating movements). Red triangles denote one step cycle for ipsilateral right hindlimb-forelimb (stance=filled; swing=open). Dashed blue boxes highlight contralateral hindlimb-forelimb movements for the various gaits (**a**,

overlap=in-phase/synchrony; **b**, partial overlap=phase shift/asynchronous; **c**, out-of-phase/alternation). (**d**) Transformation of interlimb coordination values to control for lead limb and natural variability in coordination during stepping (convert 0-0.5 to 0.5-1.0). White area denotes normal variability observed at control time points. Shaded region indicates variability beyond control levels. (**e**) Silencing LAPNs did not disrupt ipsilateral hindlimb-forelimb alternation during overground locomotion. (**f**) Contralateral hindlimb-forelimb coordination values were transformed from 0-1 to 0.0-0.5. (**g**) Silencing LAPNs significantly disrupted contralateral hindlimb-forelimb coordination. This effect was reversible upon DOX removal (DOFF) and reproducible one month later (PD2, D2D3, D2D5). (**h-i**) Schematics illustrating stepping behaviors observed at control time points and during $DOX^{ON}$ silencing of LAPNs. Red=ipsilateral hindlimb-forelimb; blue=contralateral hindlimb-forelimb. Filled triangles=stance; open triangles=swing. (N=120 steps/time point; S.C. N=60).

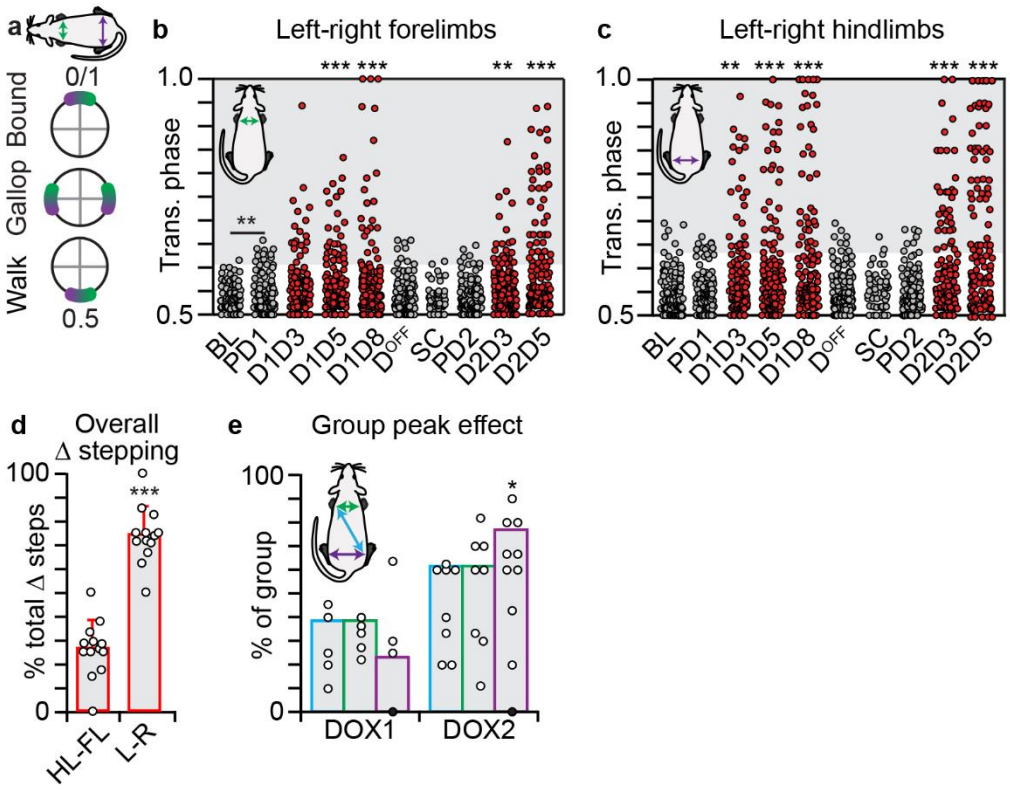


**<u>Figure 18</u>. Silencing LAPNs Disrupts Left-Right Alternation At The Pelvic And Shoulder Girdles.**

(**a**) Gait-associated coupling patterns for left-right forelimb (green) and hindlimb coordination (red). Silencing LAPNs disrupts left-right forelimb (**b**) and hindlimb alternation (**c**), respectively. (**d**) The disruption to left-right alternation (fore- and hindlimbs) was significantly greater than that of hindlimb-forelimb (ipsi- and contralateral) coordination (73.8±11.8% vs 26.2±11.8% of all irregular steps; $p<0.001$, paired t-test). (**e**) Significantly more animals had peak disruptions to hindlimb alternation during DOX2 as compared to DOX1 (23.08% vs 76.92%; $p=0.0012$, B.P. test; bars=percent of total group; circles=individual percent). While more animals showed peak disruption to contra hindlimb-forelimb and left-right forelimb movements during DOX2 (61.5%; N=8/13), it was not statistically

significant as compared to DOX1 (38.5%; N=5/13; p=0.20). Shaded circle denotes animal that did not show changes beyond control variability in hindlimb coordination (albeit 10% change in contralateral hindlimb-forelimb and 22.2% change in left-right forelimb coordination).

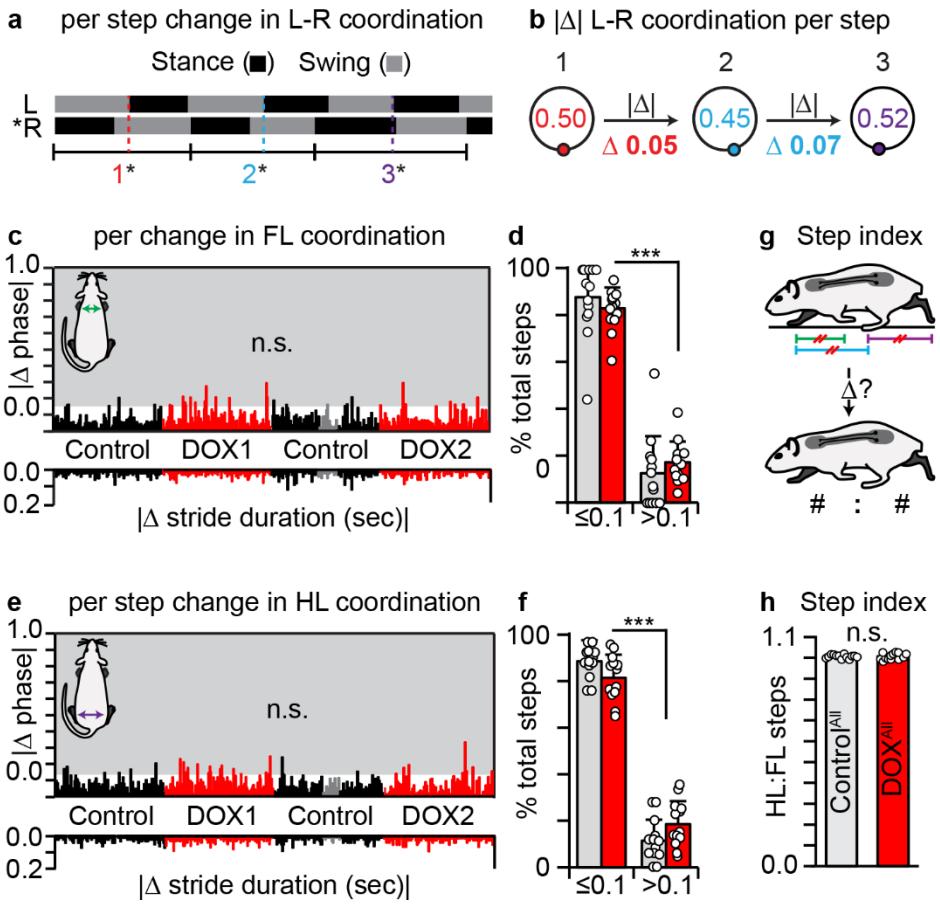


**Figure 19. The Silencing-Induced Perturbations To Left-Right Coordination Reflect Altered, Albeit Steady-State Coupling Patterns That Are Expressed Within A Fixed Locomotor Cycle.**

(**a**) Example of swing-stance graph demonstrating the analysis of consecutive step cycles within one locomotor bout to calculate absolute step-by-step change in left-right coordination (*reference limb). Individual bars (**b**, right panel) represent per step change in coordination (left, e.g. 0.05, 0.07). (**c**) Silencing LAPNs did not significantly increase the step-by-step variability in left-right forelimb coordination beyond control levels (BL+PD1: n=110/110 vs $DOX1^{All}$: n=163/165; p=0.16, z=1.42; $D^{OFF}$+PD2: n=95/95 vs DOX2: n=94/95; p=0.31, z=1.01; B.P. test). (**d**) The

significant majority of per-step changes for $Control^{All}$ and $DOX^{All}$ fell within 0.10 as compared to >0.10 ($Control^{All}$: 87.51±15.84% vs 12.49%±15.84%, p=1.96e-06; $DOX^{All}$: 82.86±8.84% vs 17.14%±8.84%, p=1.40e-08, paired t-test; bars=group mean; circles=individual mean). There was no significant difference between $Control^{All}$ and $DOX^{All}$ for phase changes ≤0.10 or >0.10, respectively (each p=0.44). (**e**) Similarly, silencing did not affect the per-step variability in hindlimb coordination beyond control levels (BL+PD1: n=114/114 vs $DOX1^{All}$: n=165/166; p=0.32, z=1.00; $D^{OFF}$+PD2: n=108/108 vs DOX2: n=84/84; p=0.31, z=1.01; B.P. test) with the significant majority of steps falling within ≤0.10 as compared to >0.10 for both $Control^{All}$ (**f**, 88.55±9.05% vs 11.45%±9.05%, p=2.96e-09) and $DOX^{All}$ (81.45±9.05% vs 9.89%±9.05%, p=7.98e-08). No significant difference was detected between the $Control^{All}$ and $DOX^{All}$ time points for phase changes ≤0.10 or >0.10, respectively (each p=0.06). Per-step changes in stride duration were similarly not affected (**c,e**). (**g**) The changes observed in contralateral hindlimb-forelimb, left-right forelimb, and left-right hindlimb coordination (**g**, top panel) did not affect the overall ratio of hindlimb-to-forelimb steps taken (**g**, bottom panel; **h**, $Control^{All}$: 1.008±0.009 vs $DOX^{ALL}$: 1.008±0.016; p=0.97, paired t-test; bars=group mean ± S.D.; circles=individual mean).

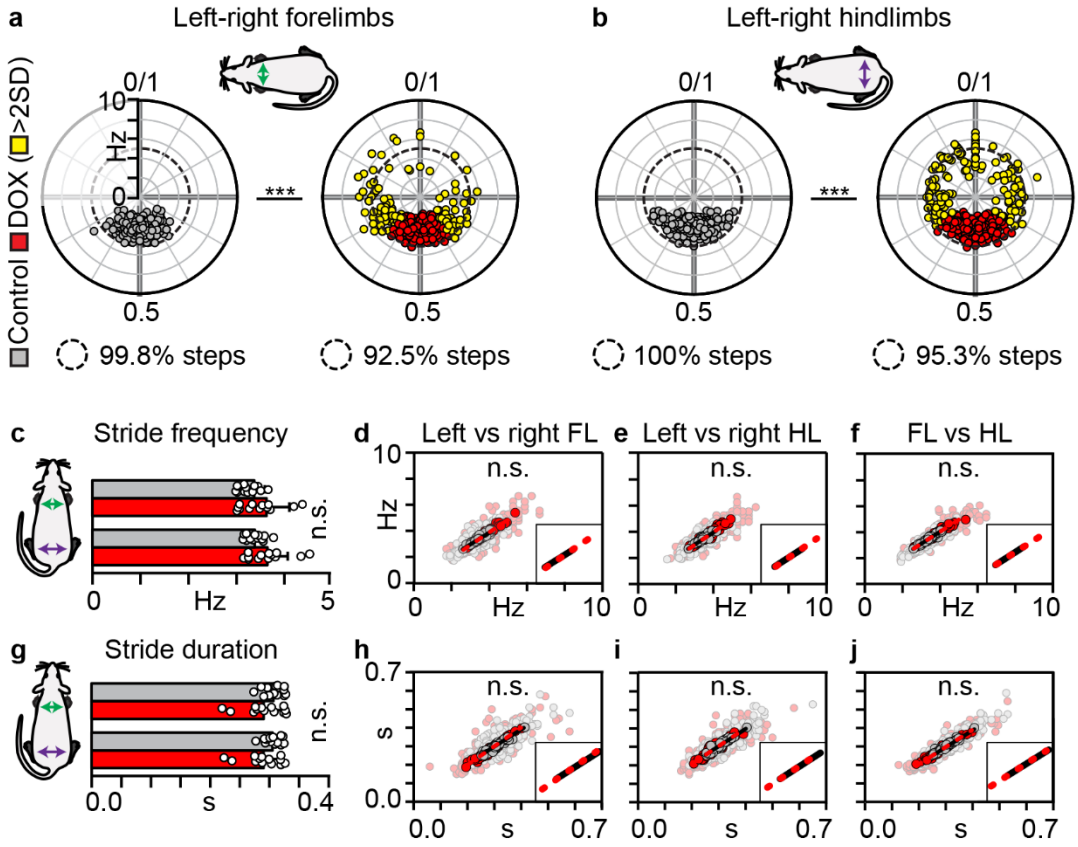


**<u>Figure 20</u>. Silencing LAPNs Uncouples The Left-Right Stepping Pattern Separate From The Underlying Locomotor Rhythm.**

(**a,b**) Phase-frequency polar plots for the fore- and hindlimbs at Control$^{All}$ and DOX$^{All}$, respectively. Each concentric circle=2Hz (dashed line=5Hz). Yellow=DOX$^{ON}$ irregular steps. Silencing LAPNs significantly increased the dispersion of left-right phase data for the fore- (**a**, $U^2$=0.672; ***p<0.001, Watson's non-parametric two-sample $U^2$ test) and hindlimbs (**b**, $U^2$=1.446; ***p<0.001) as compared to Control$^{All}$. (**c**) No differences were detected when comparing mean stride frequencies between Control$^{All}$ and DOX$^{All}$ for the fore- and hindlimbs, respectively (top=FLs, Control$^{All}$: 3.39±0.22Hz vs DOX$^{All}$: 3.65±0.45Hz, p=0.98; bottom=HLs, Control$^{All}$: 3.39±0.19Hz vs DOX$^{All}$: 3.65±0.42Hz, p=0.92, mixed

model ANOVA with speed as a co-variate, Sidák *post hoc* t-tests). (**g**) Similar results were found when comparing mean stride durations (FLs: $Control^{All}$: 0.31±0.02s vs $DOX^{All}$: 0.29±0.03s, p=0.52; HLs: $Control^{All}$: 0.30±0.01s vs $DOX^{All}$: 0.29±0.03s, p=0.52; $Control^{All}$ FLs vs HLS: p=0.34; $DOX^{All}$ FLs vs HLs: p=0.10). $DOX^{All}$ stride frequency slopes (dashed red line) were not significant different from $Control^{All}$ (black) when comparing left vs right forelimb (**d**, CON: 0.98 vs DOX: 0.90, t=-1.31 and p=0.19) and hindlimb (**e**, CON: 0.99 vs DOX: 0.94, t=-1.17 and p=0.24) as well as between the two girdles (**f**, CON: 0.917 vs DOX: 0.921, t=-1.06 and p=0.29). $DOX^{All}$ stride duration slopes were not significant different from $Control^{All}$ when comparing left vs right forelimb (**h**, CON: 0.91 vs DOX: 0.99, t=1.56 and p=0.12) and hindlimb (**i**, CON: 0.96 vs DOX: 0.94, t=1.06 and p=0.29) as well as between the two girdles (**j**, CON: 0.93 vs DOX: 0.91, t=1.09 and p=0.28) (**d-j**, statistics reported from averaged datasets, which are shown superimposed onto raw data).

*Figure 21*

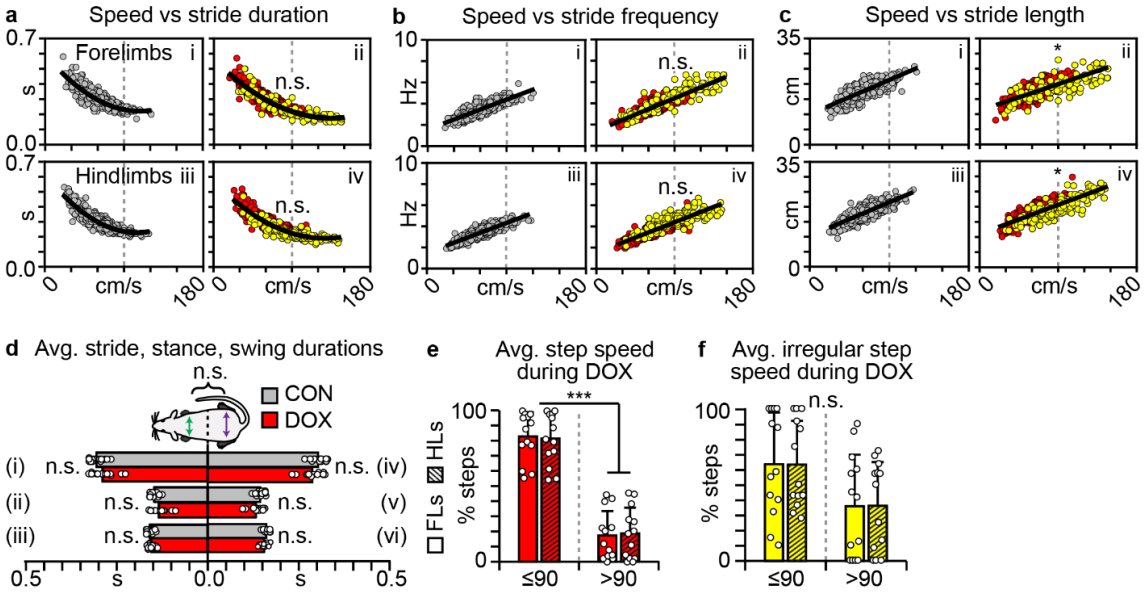


**<u>Figure 21</u>. Silencing LAPNs Disrupts Alternation At The Shoulder And Pelvic Girdles While Preserving Key Stepping Features That Are Fundamental To Locomotion.**

(**a-c**) The relationship between speed and spatiotemporal parameters remained intact during silencing, albeit with a slight but significant change in stride length (dashed line=transitional zone between trot and gallop) [1]. (**a-i,ii**, speed vs stride duration: Control$^{All}$: 0.032 vs DOX$^{All}$: 0.034; t=-1.68, p=0.09) (**a-iii,iv**, Control$^{All}$: 0.031 vs DOX$^{All}$: 0.032; t=-1.64, p=0.10) (**b-i,ii**, speed vs stride frequency: Control$^{All}$: -6.95E-3 vs DOX$^{All}$: -5.75E-3; t=-0.34, p=0.74) (**b-iii,iv**, Control$^{All}$: -7.53E-3 vs DOX$^{All}$: -5.99E-3; t=-0.75, p=0.46) (**c-i,ii**, speed vs stride length: Control$^{All}$: 0.126 vs DOX$^{All}$: 0.097; t=2.18, p=0.03) (**c-iii,iv**, Control$^{All}$: 0.126 vs DOX$^{All}$: 0.107; t=2.42, p=0.02). Slopes [lines of best fit] were compared after calculating the regression of x on y. (**d**) Silencing LAPNs did not significantly change mean forelimb stride duration (**i**, Control$^{All}$ vs DOX$^{All}$, p=0.41; repeated

measures ANOVA with speed as a co-variate), stance duration (**ii**, p=0.60), or swing duration (**iii**, p=0.32). Similar results were found at the hindlimbs (**iv**, p=0.38; **v**, p=0.14; **vi**, p=0.78). No significant differences were detected between the fore- and hindlimbs for each measure, respectively (FL vs HL: stride, p=0.64; stance, p=0.15; swing, p=0.48; limb*time: stride, p=0.22; stance, p=0.56; swing, p=0.34). (**e**) The significant majority of $DOX^{ON}$ steps taken by the forelimbs (solid bars) and hindlimbs (shaded) were at speeds ≤90 cm/s (FLs: ≤90cm/s [82.70±16.18%] vs >90cm/s [17.30±16.18%], p=9.63E-06; HLs: ≤90cm/s [81.30±16.97%] vs >90cm/s [18.70±16.97%], p=2.35E-05; both speeds, FL vs HL: p=0.14; paired t-tests). (**f**) Analyzing the silencing-induced altered steps alone revealed that they did not predominantly occur at these faster speeds (FLs: ≤90cm/s [63.90±34.02%] vs >90cm/s [36.10±34.02%], p=0.17; HLs: ≤90cm/s [63.59±28.87%] vs >90cm/s [36.41±28.87%], p=0.12; both speeds, FL vs HL: p=0.92). (bars=group mean ± S.D.; circles=individual mean).

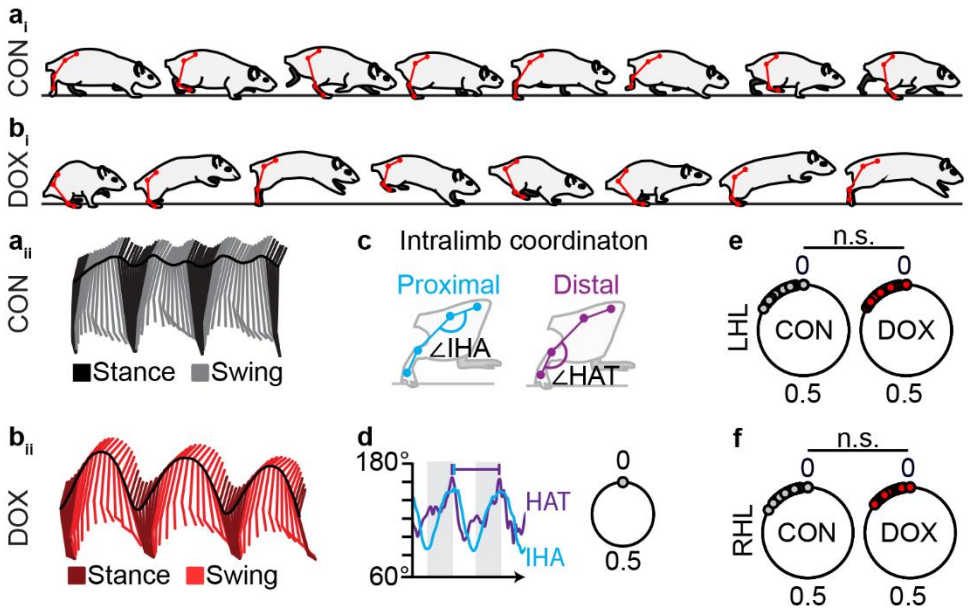


**<u>Figure 22</u>. Intralimb Coordination Persists Despite The Significant Disruption To Interlimb Coordination.**

Illustrations of stepping behaviors at control time points (**$a_i$**) and during silencing (**$b_i$**) with hindlimb movements shown in red. The kinematic stick figures of **$a_i$** and **$b_i$** are shown in **$a_{ii}$** and **$b_{ii}$**, respectively. (**c-d**) Per-step, onset times of peak IHA excursion (blue) relative to duration of peak-to-peak HAT excursions (purple) were used to calculate intralimb coordination. Values were plotted on circular graph (right panel) wherein 0 denotes normal, in-phase coordination of the proximal and distal limb segments. Silencing LAPNs did not disrupt intralimb coordination of the left (**e**, $p>0.5$, $U^2=-0.0595$, Watson's non-parametric two-sample $U^2$ test; N=166 intralimb cycles from Baseline+Pre-DOX1) or right hindlimbs during stepping (**f**, $p>0.5$, $U^2=0.0039$; N=178 intralimb cycles DOX1; critical $U^2=0.1896$).

*Figure 23*

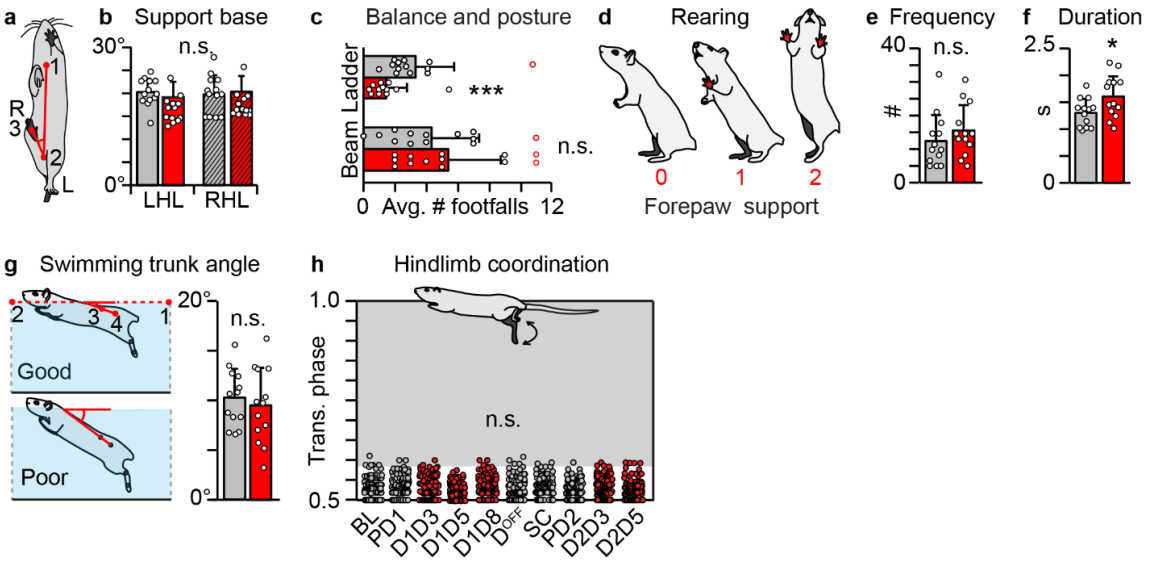


**<u>Figure 23</u>. Silencing LAPNs Does Not Affect The Animal's Capacity To Maintain Balance, Posture, And Trunk Stability.**

(**a**) Three-point angle analysis to measure base of support of the hindlimbs (point 1: area between shoulder blades; 2=groin; 3=hind paw position at initial contact). (**b**) Silencing LAPNs did not increase external rotation in the left (LHL: 20.23±3.00° vs 19.13±3.38° for Baseline [N=166 angles] and D1D5 [N=178], respectively; p=0.31) and right hindlimbs (RHL: 19.76±4.19° vs 20.37±3.39°; p=0.62). No significant differences were observed between the left-right hindlimbs (CON, p=0.72; DOX, p=0.39). (**c**, top panel) Average number of foot slips during ladder stepping is significantly reduced during silencing ($Control^{All}$: 3.33±2.4 vs DOX [D1D4/D1D8/D2D4/D2D5]: 1.43±1.33; p=0.0002). (**c**, lower panel) There was no significant change in the average number of foot slips on the 1.8 cm wide beam ($Control^{All}$: 4.38±3.07 vs $DOX^{All}$: 5.46±3.38; p=0.27). Excluding the outliers (red circles) yielded similar results (see methods). Spontaneously expressed rearing was analyzed, including the extent of forepaw support (0, 1, or 2 paw contacts).

(**e**) There was no difference in the average frequency of rearing events between Control$^{All}$ and DOX$^{All}$ (7.62±4.89 vs 9.46±4.74, p=0.29). (**f**) The average duration of rearing was significantly greater during DOX$^{All}$ (1.92±0.47s vs 1.56±0.31s, p=0.045). (**g**, left) Schematic illustrating the four-point angle analysis (points 1 and 2=water surface; point 3=iliac crest; point 4=hip) used to measure trunk angle during swimming. Silencing did cause trunk instability during swimming (PD1: 10.23±2.87° vs D1D5: 9.49±3.78°; p=0.18). Angles were calculated throughout the stroke cycle (N=7,873 total at PD1 10,520 at D1D5; left and right hindlimbs combined). (**h**) Silencing did not disrupt left-right hindlimb alternation during swimming (N=130 stroke cycles/time point; Control$^{All}$ [N=518/520 normal stroke cycles] vs DOX$^{All}$ [N=650/650], p=0.16, Binomial Proportion test. All data shown had no side differences detected. Average of left and right hindlimbs shown for N=13 at time points specified unless otherwise stated. Paired t-tests were used in (**b,c,e-g**). Circles=individual means. Bars=group mean ± S.D.

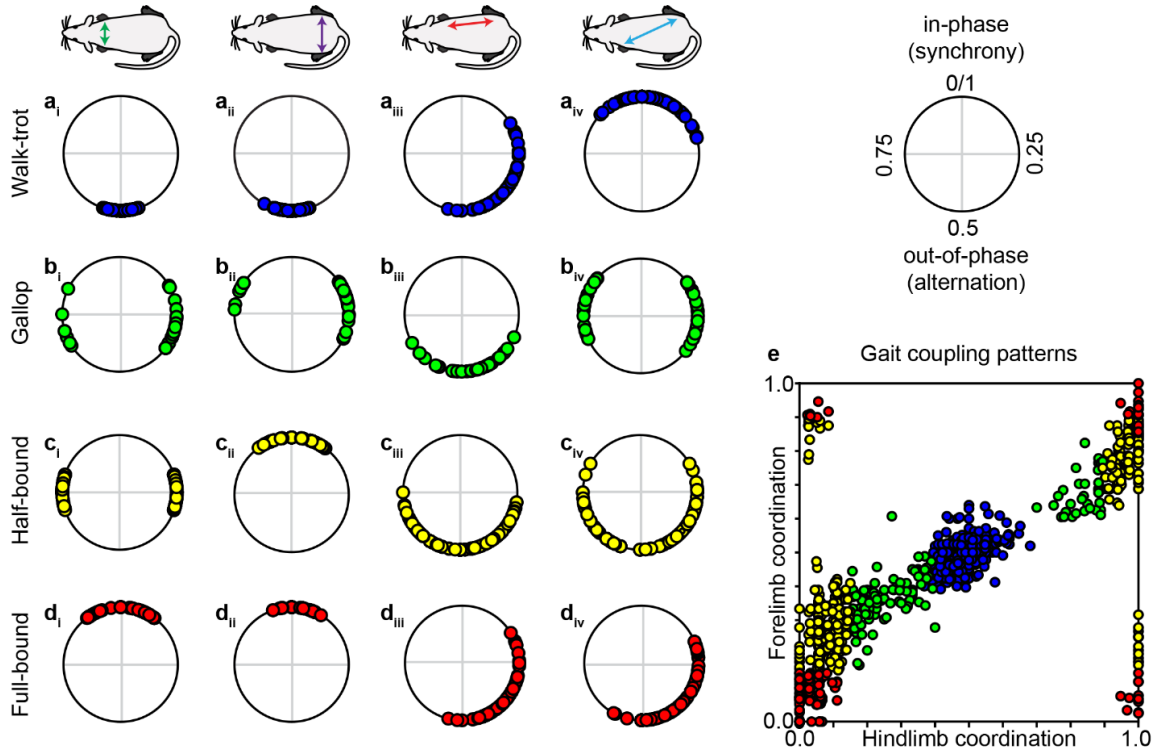


**<u>Figure 24</u>. Traditional Coupling Patterns For Volitionally-Expressed, Speed-Dependent Gaits.**

Data shown are from N=12 naïve, adult, female Sprague Dawley rats that volitionally stepped overground in a custom-built long tank runway (see methods for detail). The coupling patterns for the various limb pairs (column 1: forelimbs; 2: hindlimbs; 3: ipsilateral hindlimb-forelimb; 4: contralateral hindlimb-forelimb) are shown for the stereotypic locomotor gaits (**a**, walk-trot; **b**, gallop; **c**, half-bound; **d**, full-bound). In-phase, synchronous movements have a coupling index of 0 or 1 while strict, out-of-phase movements have a coordination value of 0.5 (top right panel). (**e**) The coupling patterns observed at the hindlimbs and forelimbs are plotted against each other to demonstrate the linear relationship of gait switches with increasing speed (refer to Figure 28).

*Figure 25*

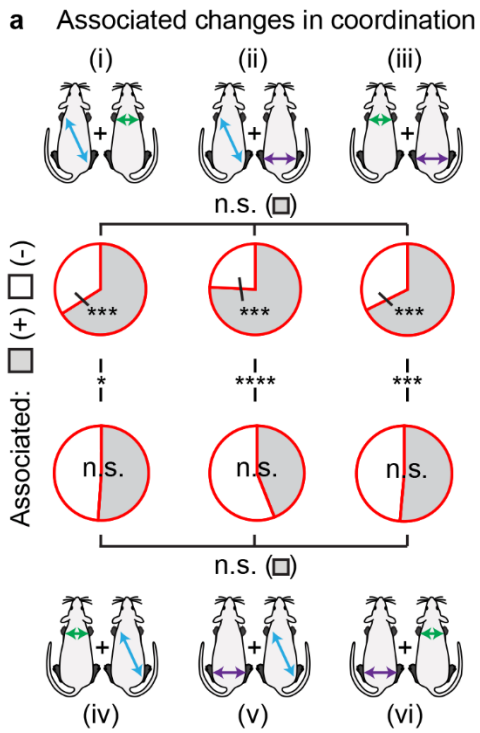


**<u>Figure 25</u>. The Silencing-Induced Defects In Contralateral Hindlimb-Forelimb Movements Are Likely A Byproduct Of The Overt Changes To Left-Right Alternation At The Pelvic And Shoulder Girdles, Respectively.**

(**a**) The interaction between different coupling patterns was examined to determine if the silencing-induced perturbations in one limb pair were associated with altered stepping at another (e.g., **i**, changes in contralateral hindlimb-forelimb coordination were concomitant with changes in left-right forelimb coordination). A positive association (shaded region) indicates that changes observed at the limb pairs of interest occurred concomitantly within one complete locomotor step cycle (all four limbs stepped once). A negative association (white region) denotes no association. Data shown are focused on the silencing-induced irregular stepping patterns. (**i**) The significant majority of irregular contralateral hindlimb-forelimb steps were

concomitant with irregular left-right forelimb steps (66.0% [68/103] vs 34.0% [35/103]; p<.001; z=4.85, Binomial Proportion [B.P.] test). Similar results were found when we examined left-right hindlimb coordination (**ii**, 75.7% [78/103] vs 24.3% [25/103]; p<.001; z=8.61) as well as changes observed in left-right forelimb coordination that were concomitant with changes in left-right hindlimb (**iii**, 67.7% [90/133] vs 32.3% [43/133]; p<0.001; z=6.16). There was no significant difference in the preponderance at which the various irregular coupling pattern interactions occurred (top bracket, comparing shaded insets, [**i**] vs [**ii**], p=0.12, z=1.54; [**i**] vs [**ii**], p=0.79, z=0.27; [**ii**] vs [**iii**], p=0.17, z=1.38). Examining the inverse relationship for the various limb pairs (e.g. **iv**, changes in left-right coordination that were concomitant with changes in contralateral hindlimb-forelimb coordination) revealed no significant differences (bottom pie charts, [**iv**], 51.1% vs 48.9%; p=0.71; [**v**], 48.6% vs 51.4%; p=0.60; [**vi**], 51.4% vs 48.6% p=0.60). Once again, there was no significant difference in the preponderance at which the various irregular coupling pattern interactions occurred (bottom bracket, data not shown).

*Figure 26*

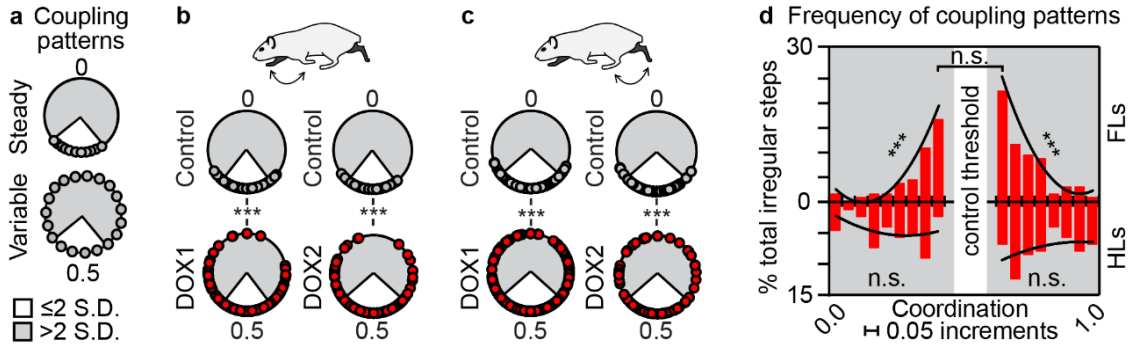


**<u>Figure 26</u>. Silencing LAPNs Functionally Uncouples The Left-Right Limb Pairs At The Girdles, Allowing The Hindlimbs To Adopt Any Coupling Pattern While The Forelimbs Maintain A Preferred, Albeit Altered Phase Relationship.**

(**a**) Schematics illustrating steady coupling patterns (concentrated) vs variable (dispersed). Silencing LAPNs functionally uncouples the left-right forelimbs (**b**; left panel: Baseline+Pre-DOX1 vs $DOX1^{All}$; $p<0.001$, $U^2=0.4255$; right panel: $D^{OFF}$+Pre-DOX2 vs $DOX2^{All}$; $p<0.001$, $U^2=0.5621$; Watson's non-parametric two sample-test) and left-right hindlimbs (**c**, left panel: $p<0.001$, $U^2=05533$; right panel: $p<0.001$, $U^2=1.4458$), transforming the steady stepping pattern (phases clustered at 0.5 and within control variability [white inset]) into a variable one (spread from 0-1 [shaded region]). (**d**) Frequency of irregular left-right forelimb (top) and left-right hindlimb (bottom) coupling patterns (phase range 0-1, 0.05 bin increments; e.g. frequency of [0 to ≤0.05], [>0.05 to ≤0.10], etc). Regression analyses revealed the presence of "preferred" irregular forelimb coupling patterns (reject null hypothesis that slope for line of best fit was flat) (top left: $p=0.0049$, $t=4.049$; right: $p=0.0030$, $t=-4.820$). The two predominant irregular forelimb coupling patterns (X,

Y; both juxtaposed to the control threshold) were n.s. from one other (p=0.22; z=1.22; B.P. test). There was no preferred irregular hindlimb coupling pattern (bottom left: p=0.38; t=0.937; right: p=0.31; t=-1.114).

*Figure 27*

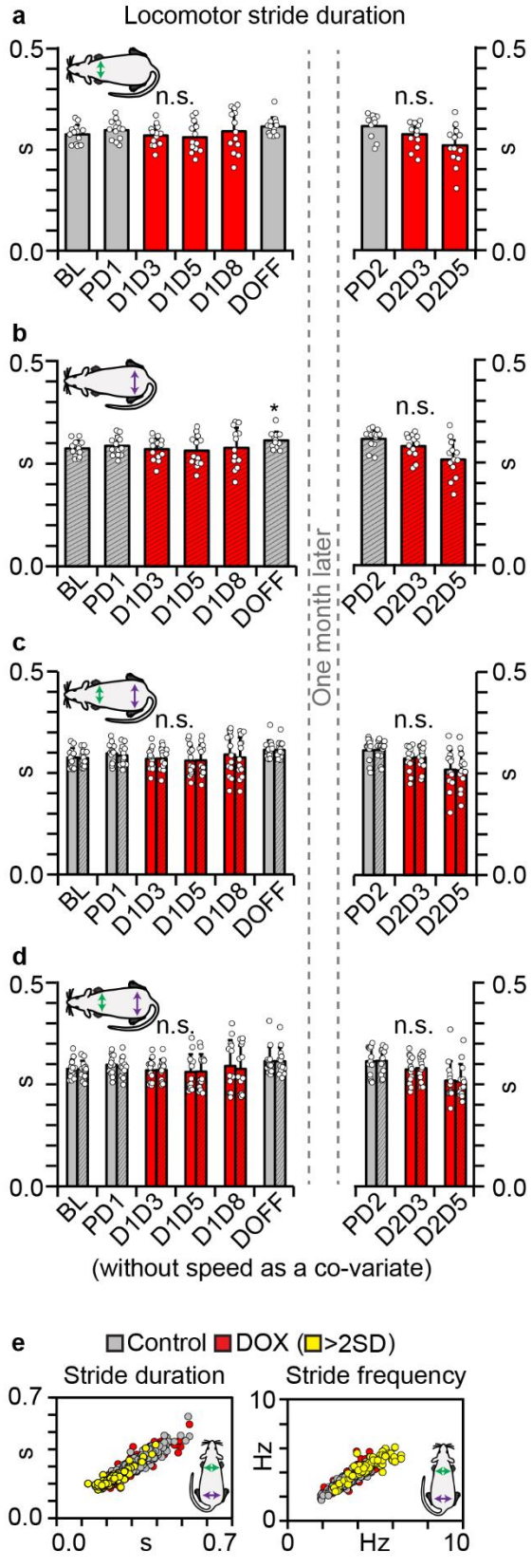
a
Locomotor stride duration
b
c
d
n.s.
*
0.5
0.0
s
BL
PD1
D1D3
D1D5
D1D8
DOFF
PD2
D2D3
D2D5
One month later
(without speed as a co-variate)
e
Control
DOX (>2SD)
Stride duration
Stride frequency
0.7
Hz
10

**Figure 27. Silencing LAPNs Does Not Affect The Forelimb, Hindlimb, Nor The Hindlimb-Forelimb Stride Durations During Overground Locomotion.**

(**a**) The mean stride duration of the forelimbs (average of left and right) was not altered during conditional silencing of LAPNs (multivariate analysis of variance [MANOVA] with speed as co-variate; bars=group predicted means ± S.D.; circles=individual means). (**b**) While there was a slight, but significant increase in hindlimb mean stride duration at DOFF as compared to BL ($p=0.027$; MANOVA with Sidák post hoc *t-test*), no significant differences were detected during DOX silencing of LAPNs. (**c**) When comparing the mean stride durations between the fore- and hindlimbs within time points, no significant differences were observed. (**d**) Similar results were obtained when the effects of speed on fore- and hindlimb stride durations were not controlled (repeated measures ANOVA). (**e**) Forelimb vs hindlimb stride duration (left panel) and frequency (right panel) for all analyzed steps are shown, including $Control^{All}$ (gray), $DOX^{All}$ (red), and DOX-induced irregular steps as defined by an altered phase relationship (yellow).

*Figure 28*

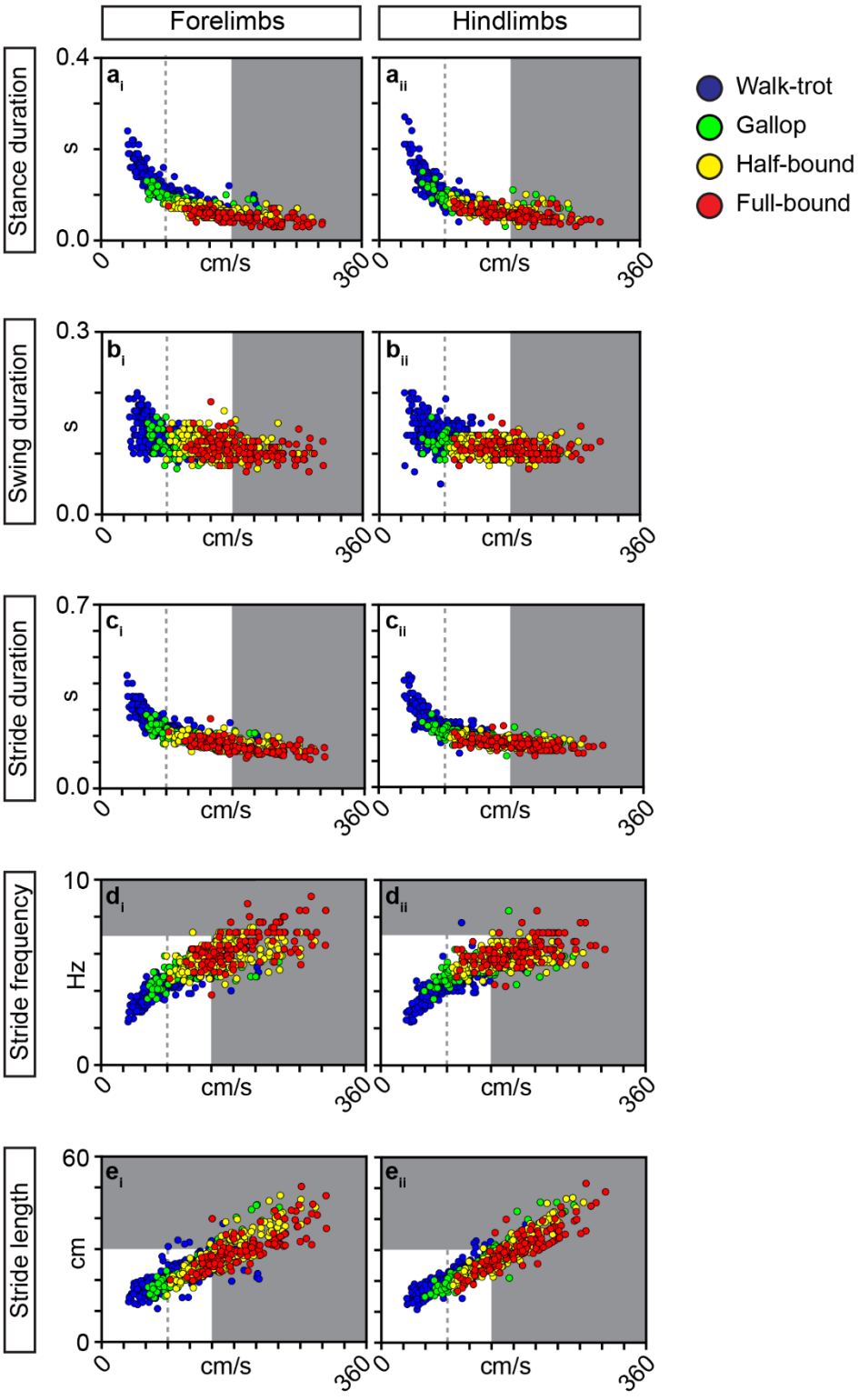
Forelimbs
Hindlimbs
Walk-trot
Gallop
Half-bound
Full-bound
Stance duration
Swing duration
Stride duration
Stride frequency
Stride length
s
Hz
cm
cm/s
0
360
0.4
0.0
0.3
0.7
10
60
a_i
a_ii
b_i
b_ii
c_i
c_ii
d_i
d_ii
e_i
e_ii

**Figure 28. Speed-Spatiotemporal Index Relationships For Stereotypic Locomotor Gaits.**

The fundamental relationship between speed and the various spatiotemporal gait indices are shown for the forelimbs (left column) and hindlimbs (right column), respectively. The relationships analyzed include speed versus stance duration (**a**), swing duration (**b**), stride duration (**c**), stride frequency (**d**), and stride length (**e**). We did not distinguish between the walk gait (three limbs in contact with the ground) and that of trot (two limbs in contact with ground at any moment)[17]. Dashed vertical line denotes transitional zone between trot and gallop[1] while the shaded region indicates speed ranges not observed in the silencing experimental group.

*Figure 29*

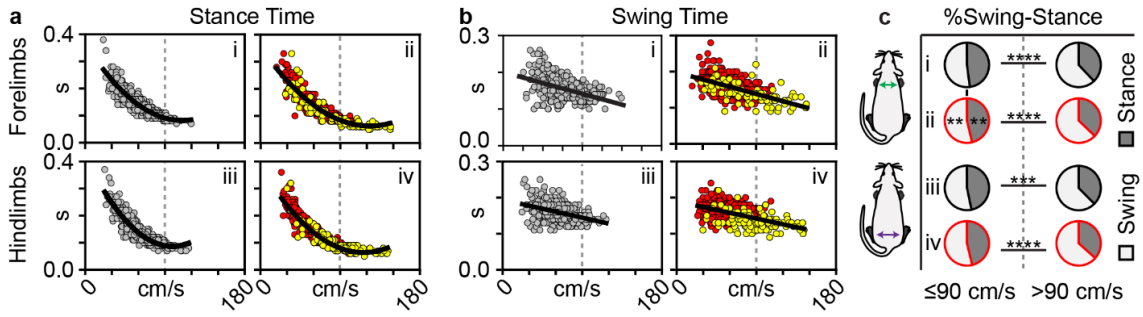


**<u>Figure 29</u>. The Silencing-Induced Perturbations To Interlimb Coordination Do Not Affect The Underlying Relationship Between Speed And Swing-Stance Durations, Principle Features That Govern Locomotion.**

A central aspect of locomotion is that as animals increase their stepping speed, the relative stance duration will decrease[7]. Swing duration will also decrease, but to a considerably lesser extent[7]. Silencing long ascending propriospinal neurons did not disrupt this characteristic feature as stance time predictably decreased as speed increased for both the forelimbs and hindlimbs, respectively (**a**, Forelimbs: [**i**] Control$^{All}$ $r_S$=0.87, $R^2$=75.69%; [**ii**] DOX$^{All}$ $r_S$=0.87, $R^2$=75.69%; Hindlimbs: [**iii**] Control$^{All}$ $r_S$=0.87, $R^2$=75.69%; [**iv**] DOX$^{All}$ $r_S$=0.87, $R^2$=75.69%; Spearman Rank correlation). When we compared the slopes for the lines of best fit after calculating the regression of x on y, we saw no significant difference between Control$^{All}$ and DOX$^{All}$ for the fore- and hindlimbs, respectively (data not shown). As anticipated, speed weakly correlated with swing time (**b**, Forelimbs: [**i**] Control$^{All}$ $r_S$=-0.43, $R^2$=18.2%; [**ii**] DOX$^{All}$ $r_S$=-0.59, $R^2$=35.3%; Hindlimbs: [**iii**] Control$^{All}$ $r_S$=-0.39, $R^2$=15.1%; [**iv**] DOX$^{All}$ $r_S$=-0.53, $R^2$=27.7%). Notwithstanding, the slopes were not different when comparing Control$^{All}$ vs DOX$^{All}$ for the fore- and hindlimbs, respectively (data not shown). (**c**) The relative percent of swing (light gray) and

stance (dark gray) durations were analyzed as they relate to speed. The following comparisons were made for the forelimbs: (**i**) Control$^{All}$ ≤90 cm/s vs >90 cm/s; (**ii**) DOX$^{All}$ ≤90 cm/s vs >90 cm/s; and Control$^{All}$ vs DOX$^{All}$ at ≤90 cm/s (left panel of [**i**] vs [**ii**]). Not all animals stepped at speeds >90cm/s. Statistical comparisons were performed on a subset of the total group (as indicated) wherein animals stepped at >90cm/s for at least two DOX$^{ON}$ time points. The results as follows: (**i**) Control$^{All}$ forelimb relative %stance [N=7/13]: 48.35±1.49% at ≤90 cm/s vs 37.49±1.85% at >90cm/s; p=1.67E-05; %swing: 51.65±1.49% at ≤90 cm/s vs 62.51±1.85% at >90cm/s; p=1.67E-05. (**ii**) DOX$^{All}$ forelimb relative %stance [N=10/13]:45.69±2.24% at ≤90 cm/s vs 37.12±2.24% at >90cm/s; p=1.25E-06; %swing: 54.31±2.24% at ≤90cm/s vs 62.83±2.24% at >90cm/s; p=1.25E-06. (**i** vs **ii**) The %stance and %swing for Control$^{All}$ vs DOX$^{All}$ at ≤90cm/s were significantly different (p=0.01, respectively). Comparisons were performed in the hindlimbs as well with the following differences detected: (**iii**) Control$^{All}$ hindlimb relative %stance [N=7/13]: 46.56±2.12% at ≤90 cm/s vs 36.95±1.82% at >90cm/s; p=0.0002; %swing: 53.44±2.12% at ≤90 cm/s vs 63.05±1.82% at >90cm/s; p=0.0002. (**iv**) DOX$^{All}$ hindlimb relative %stance [N=9/13]:45.75±2.08% at ≤90 cm/s vs 36.51±1.54% at >90cm/s; p=9.27E-09; %swing: 54.24±2.08% at ≤90cm/s vs 63.49±1.54% at >90cm/s; p=9.27E-09. (**iii** vs **iv**) The %stance and %swing for Control$^{All}$ vs DOX$^{All}$ at ≤90cm/s were not significantly different (each p=0.25; paired and independent t-tests were performed for within and between time point comparisons, respectively). (yellow=phases >2 S.D. control mean; Control: n=336 steps; DOX$^{ON}$: n=420). **p≤0.01, ***p≤0.005, ****p≤0.001).

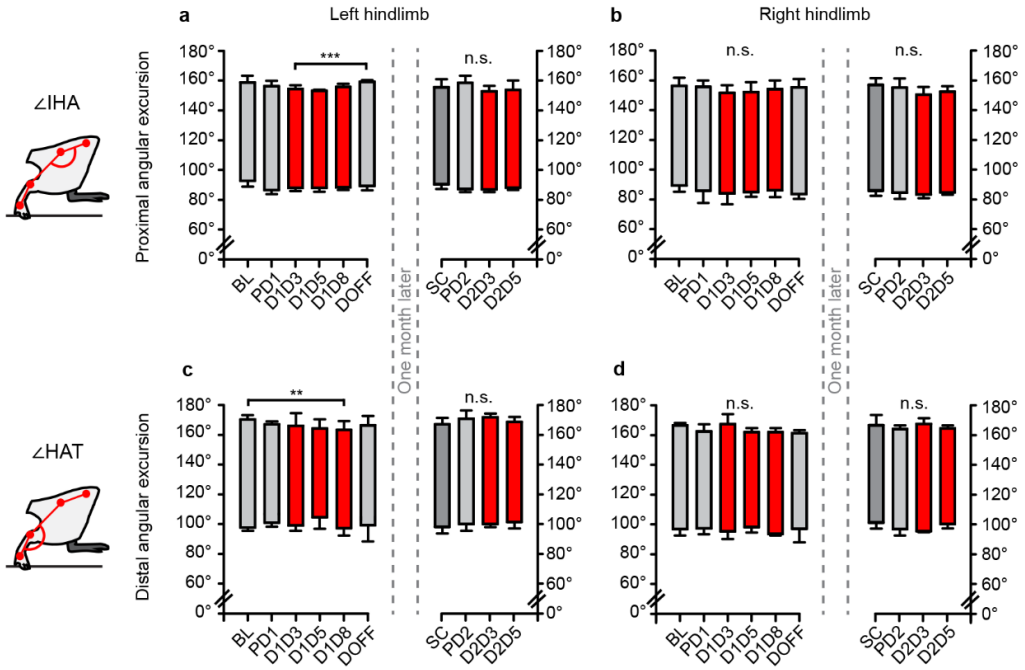


**<u>Figure 30</u>. Hindlimb Range-Of-Motion Is Preserved During Conditional Silencing Of LAPNs.**

(**a,b**) Peak-to-trough excursion of the proximal hindlimb segments (iliac crest-hip-ankle angle, IHA) is not profoundly affected by the conditional silencing of LAPNs. The excursion of the proximal left hindlimb segments was slightly, but significantly reduced at D1D3 (58.59±7.93°) as compared to $D^{OFF}$ (64.98±3.84°) ($p=0.004$). No changes were observed in the right hindlimb. (**c**) Similarly, a slight but significant decrease was observed in the excursion of the distal left hindlimb segments (hip-ankle-toe angle, HAT) at D1D5 (52.42±6.45°) as compared to BL (62.53±4.65°) ($p=0.007$). (**d**) No changes were observed in the distal segments of the right hindlimb. Data shown are mean peak-to-trough excursions of the proximal and distal limb segments ± S.D. Mixed model ANOVA with Bonferroni post hoc *t-tests* were performed.

*Figure 31*

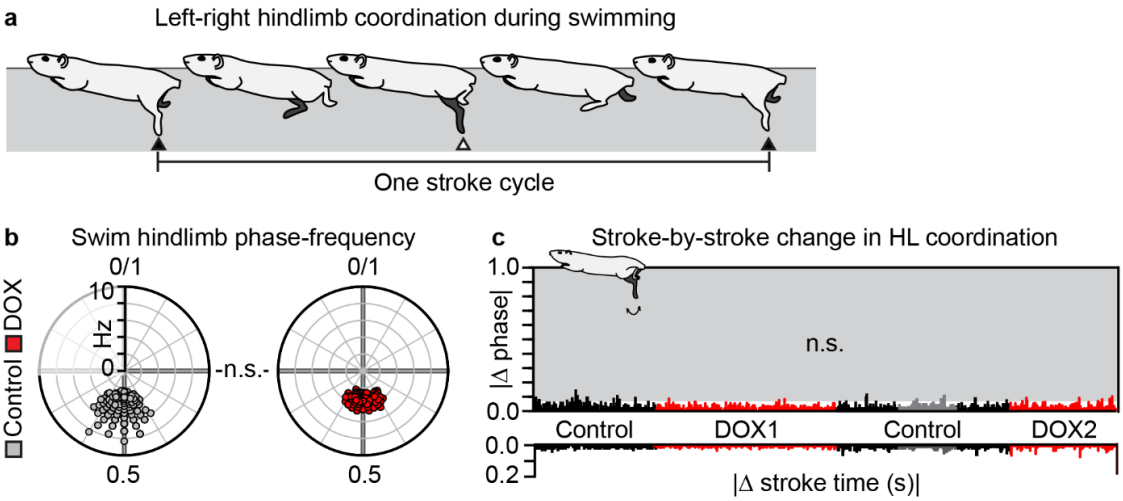


**<u>Figure 31</u>. Silencing LAPNs Does Not Disrupt Left-Right Hindlimb Coordination During Swimming.**

(**a**) Schematic illustrating left-right hindlimb coordination during swimming. Peak-to-peak downward extension of the hindlimb (filled triangles) determined the stroke cycle duration. The latency within this reference stroke cycle that the opposite hindlimb had peak downward extension (open triangle) was used to determine the left-right coordination value on a stroke-by-stroke basis. (**b**) Hindlimb swim phase-frequency circular plots for Control (BL+PD1) and DOX1$^{All}$, respectively. Silencing LAPN did not cause significant dispersion in the left-right phase relationship ($U^2$=-24.1698; p>0.5 with Watson's non-parametric $U^2$ test). (**c**) The stroke-by-stroke change in left-right hindlimb coordination and stroke cycle duration were not affected by LAPN silencing.

*Figure 32*

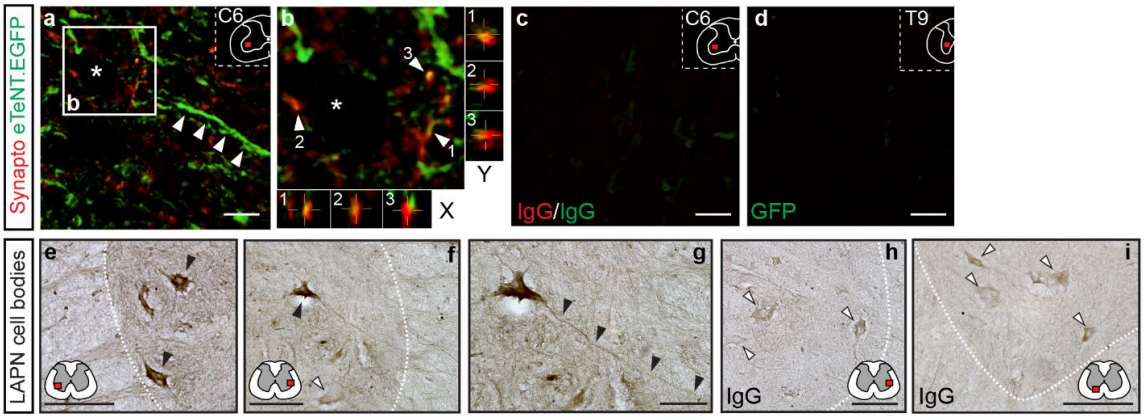


**Figure 32. Immunohistochemical Detection Of Silenced LAPNs.**

(**a**) Within the intermediate gray matter of the C6 segment (inset, upper right), putatively silenced eTeNT.EGFP+ terminals were amplified with anti-GFP (green). Arrow denote axonal branches. Asterisk denotes “ghost border” where neuron would reside. (**b**) Enlargement of (**a**), showing co-localization of eTeNT.EGFP with synaptophysin shown in red (x,y cross-sections). (**c**) Negative control showed little-to-no staining (note some endogenously-expressed, non-amplified eTeNT.EGFP will be present). (**e**) Putatively silenced LAPNs (black triangles) are detected at L2 in the intermediate gray matter (DAB-amplified anti-GFP). (**f-g**) Emerging axon from eTeNT-expressing LAPN that projects to white matter (black triangles). Non-double infected resident neurons do not express eTeNT.EGFP (white triangles). (**h-i**) Isotype control shows little-to-no eTeNT.EGFP expression.

**Table 7. Silencing LAPNs Functionally Uncouples The Left And Right Limb Pairs At Each Girdle While Preserving Hindlimb-Forelimb Coordination.**

To determine whether silencing functionally uncouples the limb pairs, we performed Watson's non-parametric two-sample $U^2$ tests[103]. The null hypothesis is that two samples (e.g. BL vs D1D8) came from two populations with the same direction (the degree of concentration of dispersion in the coordination data)[103]. Silencing LAPNs significantly decreased the concentration of the left-right forelimb and left-right hindlimb phase data (reduced clustering at 0.50), indicating the limbs became functionally uncoupled. Ipsilateral hindlimb-forelimb movements remained functionally coupled. Contralateral hindlimb-forelimb movements were primarily unaffected, apart from a significant effect detected at $DOX2^{ON}$-D5 (D2D5) as compared to Pre-DOX2 (PD2). (Critical value of Watson's $U^2_{(0.05,\infty,\infty)} = 0.1869$; Appendix D, Table D.44).



*Table 7*

| | | Left-right Forelimbs | | Lef-right Hindlimbs | | Contra Hindlimb-Forelimb | | Ipsi Hindlimb-Forelimb | |
|---|---|---|---|---|---|---|---|---|---|
| | | p value | $U^2$ | p value | $U^2$ | p value | $U^2$ | p value | $U^2$ |
| BL vs | PD1 | 0.1<p<0.2 | 0.1199 | p>0.5 | -0.0759 | p>0.5 | 0.0176 | 0.2<p<0.5 | 0.0103 |
| | D1D3 | **0.01<p<0.02** | 0.2654 | 0.1<p<0.2 | 0.1298 | p>0.5 | 0.0638 | 0.2<p<0.5 | 0.0125 |
| | D1D5 | **0.02<p<0.05** | 0.2073 | **0.02<p<0.05** | 0.2262 | 0.05<p<0.10 | 0.1696 | p>0.5 | -0.0423 |
| | D1D8 | **0.001<p<0.002** | 0.3615 | **0.02<p<0.05** | 0.1906 | p>0.5 | 0.0678 | p>0.5 | -0.0302 |
| | DOX1 | **p<0.001** | 0.9516 | **p<0.001** | 0.5622 | p>0.5 | -0.6823 | p>0.5 | -0.6392 |
| | DOFF | p>0.5 | 0.0387 | p>0.5 | -0.1514 | 0.2<p<0.5 | 0.1092 | p>0.5 | 0.0488 |
| | SC | p>0.5 | 0.0145 | p>0.5 | 0.0259 | p>0.5 | -0.0362 | p>0.5 | 0.1228 |
| PD1 vs | D1D3 | p>0.5 | -0.0049 | 0.05<p<0.1 | 0.1716 | p>0.5 | 0.0312 | p>0.5 | -0.0438 |
| | D1D5 | p>0.5 | 0.0183 | **0.02<p<0.05** | 0.1987 | 0.2<p<0.5 | 0.1040 | p>0.5 | -0.0902 |
| | D1D8 | 0.2<p<0.5 | 0.0897 | **0.01<p<0.02** | 0.2507 | p>0.5 | 0.0557 | p>0.5 | -0.0499 |
| | DOFF | p>0.5 | 0.0469 | **0.02<p<0.05** | 0.2235 | p>0.5 | 0.0394 | p>0.5 | 0.0274 |
| BL + PD1 vs | DOX1 | **p<0.001** | 0.4255 | **p<0.001** | 0.5533 | p>0.5 | -0.1901 | p>0.5 | -0.8575 |
| PD2 vs | D2D3 | 0.1<p<0.2 | 0.1400 | **p<0.001** | 0.4337 | 0.1<p<0.2 | 0.1335 | p>0.5 | -0.0626 |
| | D2D5 | 0.1<p<0.2 | 0.1473 | **0.01<p<0.02** | 0.2399 | 0.05<p<0.10 | 0.1656 | p>0.5 | -0.1099 |
| | DOX2 | **0.02<p<0.05** | 0.1973 | **p<0.001** | 0.4881 | **0.002<p<0.005** | 0.3370 | p>0.5 | -0.2236 |

# CHAPTER IV

# DISCUSSION

## Salient findings from spinal interneuron silencing

### *L2 projection pathways: left-right pattern distributors*

While previous studies suggest that L2-L5 interneurons facilitate crossed flexor-extensor coordination[57,59] and LAPNs likely mediate hindlimb-forelimb coordination during locomotion[115,121,131,143], it is clear that the primary role of these L2 projection pathways is the distribution of left-right temporal information. The striking similarities in silencing these two pathways is very intriguing as they project to incredibly disparate parts of the spinal cord. Even their cell bodies are closely intermingled, but anatomically distinct. This is especially clear when we retrogradely labeled both pathways and visualized the entire L2 segment using light sheet fluorescence microscopy (unpublished data, **Error! Reference source ot found.**). What is it about L2 that makes these distinct pathways key contributors in the distribution of temporal coordination?

L2 is one of the rostral segments within the lumbar enlargement, which has been shown to contain the necessary neuronal circuitry to produce hindlimb stepping[7]. As such, the hindlimb central pattern generating circuitry is often thought

to lie within the lumbar spinal cord. However, the specific rostrocaudal distribution throughout this caudal neuraxis has been greatly contested[25].

Two hypotheses have been put forth as it relates to the specific location of the hindlimb CPG: (1) the functional rhythm generating networks are distributed throughout the lumbar spinal cord, but with a rostrocaudal excitability gradient[31-39] or (2) the primary rhythmogenic core is confined to the rostral segments alone[110,144]. Regardless of where the hindlimb stepping rhythm is produced, it is clear that the proximal lumbar segments play a key role in generating hindlimb movements[145,146]. The cell bodies of our L2-L5 interneurons and LAPNs both reside within this critical area.

Thankfully, there appears to be little disagreement as to where within the gray matter the CPG-related neurons reside[25]. Activity-labeling, electrophysiological, and microlesion studies all show that this circuitry is concentrated in the intermediate and ventral gray matter (laminae VII, VIII, and X)[33,37,40-43]. Once again, our pathways of interest reside primarily within these laminae[123,128,147].

In light of the critical role the rostral lumbar circuitry plays in the expression of hindlimb stepping and the anatomical underpinnings of the pathways studied here (L2 resident cell bodies that are concentrated in the intermediate gray matter), we propose that these L2 projection pathways distribute temporal information necessary for interlimb coordination during overground locomotion. Specifically, we propose that these pathways are constituents of interlimb pattern formation

layer, distinct from intralimb and separate from the rhythm generation, within the lumbar central pattern generating circuitry.

***Silencing left-right pattern distributors leads to a coordination continuum***

Alternation is the preferred coupling pattern during locomotion. It is the default mode for many species[1-7]. Here, when we silence key distributors of that temporal information, the pattern changes. But do the observed coupling continua reflect the pattern "breaking down" or does silencing "release the temporal constraints" such that the limbs can now express new patterns? Or does the continua reflect an incomplete "knockout" of all L2-L5 interneurons or LAPNs? This "differential knockout" is discussed in detail in the Limitations and Alternative Approaches section of Chapter Four. Here, I will focus on discussing two plausible mechanisms for the coupling continuum: a broken pattern or released constraint.

The coupling continuum: a broken pattern

If we entertained the idea that the left-right pattern "breaks down" during silencing, then we would anticipate seeing corrective responses from the otherwise intact circuitry. From a teleological perspective, the locomotor circuitry "wants to fix what is broken." This could account for the strikingly disparate results we observed in the step-by-step changes in left-right coordination between the two studies (Figure 34). When we silenced L2-L5 interneurons, we saw large changes in per-step coordination (Figure 34, bottom panel, red spikes). However, silencing LAPNs did not influence this dynamic coordination. While we put forth the idea that these changes in per-stride coordination indicate spontaneous shifts in left-right coupling, it could also reflect the spinal circuitry attempting to "fix" or compensate

for the irregular patterns. In support of this concept are two observations. First, the forelimbs continued to alternate throughout the expression of these irregular hindlimb coupling patterns. Therefore, these animals are actively stepping with normal, left-right forelimb alternation but highly atypical hindlimb coupling. And when you watch these animals step, the only word that comes to mind when describing their behavior is “awkward” (Video 7). If not awkward, then surely “effortful” as it seems like the animal is “trying to fix” these strange stepping patterns expressed in the hindlimbs. Our second piece of data that supports the idea that silencing L2-L5 interneurons “breaks down" the left-right pattern is that silencing-induced perturbations to hindlimb coordination are attenuated one month later during DOX2. As such, the otherwise intact circuitry could compensate for or “fix” these patterns. Repeated silencing of LAPNs, on the other hand, makes the perturbations to interlimb coordination more profound.

Therefore, if the left-right coupling continuum observed is due to a “broken pattern,” then it appears as though only L2-L5 interneuron silencing supports this hypothesis.

The coupling continuum: released temporal constraints

An alternative consideration for the underlying mechanism of the coupling continuum is a “released constraint” from the alternating, left-right pattern. Released constraint, but still within the boundaries of maintaining a stable locomotor rhythm. In support of this hypothesis is data generated from silencing LAPNs. Here, there appears to be no attempt to “fix” or compensate for the altered stepping patterns expressed. Indeed, the changes become more profound over

time and the relative fidelity with which these patterns are expressed on a step-by-step basis suggests they are a steady-state coupling pattern. However, it is clear that data generated from the L2-L5 study does not fully support this hypothesis.

Altogether, it seems likely that there are disparate mechanisms of action going on. If the L2-L5 continuum is the reflection of a “broken pattern” that the locomotor circuitry is actively trying to fix, then this could signify functional redundancy within the lumbar neural circuitry. Therefore, L2-L5 interneurons constitute one of many lumbar-enriched pathways that contributes to left-right coordination during stepping. Alternatively, it appears as though the coupling continuum observed from silencing LAPNs reflects the release of the left-right limb pairs from strict, out-of-phase movements. Therefore, silencing this ascending inter-enlargement network endows the circuitry with the flexibility and freedom to express a breadth of coupling patterns with great fidelity. Peculiarly, the overall changes from silencing LAPNs are more profound than that of the L2-L5 interneurons, but the animals actually appeared “more coordinated.” To conclude, even though the end result of silencing is a left-right coordination continuum, it is likely due to a differential response of the nervous system to the manipulation.

**Silencing task-dependency: context is key**

While the majority of our analyses focused on quantifying changes observed during overground locomotion, it became clear to us that there was a second story building, one that was more nebulous, but very intriguing. Throughout our studies, we saw that the “behavioral context” exerted a profound influence on the expression of the silencing phenotype. Specifically, it appears as though

certain tasks overrode the silencing effects. In this section, I will highlight two conditions where we saw apparent context-dependent modulation of the silencing phenotype. At the end, I will briefly discuss how these task-dependent observations feed into our emerging hypothesis of the multifunctional reorganization of the lumbar central pattern generator.

***Stepping versus swimming***

The most striking result from our studies is also our strongest argument for how the behavioral context appears to gate the expression of the silencing phenotype. Regardless of the pathway we silenced, the disruptions to interlimb coordination during stepping were immediately abolished when the animals swam. What is it about swimming that modulates the silencing effects we observed overground so profoundly?

To address this question, we first need to consider the fundamental differences between stepping and swimming. The obvious disparity between the two is the environment in which these behaviors are expressed. During stepping, the limbs are actively loaded throughout discrete phases of the step cycle[148]. It is this sensory and proprioceptive feedback (in conjunction with inputs from the muscle spindles about dynamic changes in muscle length) that powerfully modulates the transitions between swing and stance during stepping. Swimming, on the other hand, has drastically reduced load applied to the limbs due to the animal's inherent buoyancy in water[112]. Therefore, the overall contributions from load sensors (group Ib, Golgi tendon organs) to patterned limb movement is profoundly different from that in stepping[113].

While these two behaviors are fundamentally different, swimming is often thought to be a “simpler” form of locomotion[149] that shares both similarities and differences with stepping[112]. Akin to stepping, there are two phases in the hindlimb swim cycle: the power stroke and return stroke[112]. Power stroke is “equivalent” to the stance phase where limb extensors are active. However, unlike stepping, the limb extensors are maximally driven in a single, synchronous burst (co-activation of hip, knee, and ankle extensors)[112]. These peak forces, along with full extension of the knee and ankle (due to no opposing ground reaction forces), increases the relative surface area of the hindlimb that can be used to generate thrust for forward propulsion. There is no equivalent for this motor action in normal stepping[112]. Moreover, while return stroke shares a similar pattern of limb flexor burst duration and latency to that of swing phase during stepping[112], the muscle groups are activated in a sequential manner such that one flexor group is recruited throughout the entire swim cycle. This feature is qualitatively distinct from patterns of activation observed during overground locomotion[112]. Therefore, while both behaviors will take the form of rhythmic left-right alternation in the hindlimbs, the underlying neural mechanisms that govern it are strikingly different. Whether or not there is differential involvement of supraspinal centers between the two tasks is unknown.

Therefore, it comes as no surprise regarding the difficulties we faced in reconciling the disparate effects silencing had on stepping versus swimming. Nonetheless, there are three plausible mechanisms of action that could explain these results. First, these pathways are weakly involved in left-right coordination during swimming, potentially due to cutaneous and/or load-related inputs gating

their involvement. A second, albeit parsimonious, explanation is that swimming could have a fundamentally different neuro-ensemble from stepping such that the L2 projection pathways are not active during the task. And finally, perhaps these pathways are active during swimming, but other neural circuitry compensates thereby masking the effects. It is particularly challenging to interpret the involvement of LAPNs in swimming as forelimbs (and therefore hindlimb-forelimb coordination) are not involved in this task apart from occasional steering. What role would an inter-enlargement pathway serve when the task is almost entirely bipedal? To begin to address these questions, we must first determine whether or not these pathways are even active during swimming. This could be addressed through a relatively straightforward experiment where L2-L5 interneurons and LAPNs are first retrogradely labeled with fluorescent tract tracers. After retrograde transport to back-label the neurons, animals would then receive multiple swim sessions immediately before sacrifice. The *post hoc* detection of the labeled neurons that co-express c-fos, an immediate early gene that denotes cellular activity, could help determine whether or not the neurons are active during the task[150]. Until then, we have no way of knowing whether L2-L5 interneurons or LAPNs are a part of the “hindlimb swim ensemble” for left-right alternation.

Despite our inability to fully interpret these data, the swimming phenotype was very intriguing to us. Unlike stepping, swimming simply “looked automated.” There seemed to be a “preset” frequency and phase relationship at which the hindlimbs cycled. It was as if the locomotor circuitry underwent a profound functional reorganization, switching from the flexible, dynamic system we observed

during overground locomotion to a fixed motor ensemble. This was not the only instance where we saw an apparent functional reorganization of the locomotor circuitry. Indeed, even the “type” of stepping behavior profoundly shaped the silencing phenotype.

***“Going from A to B” leads to C, the coordination continuum***

We realized very quickly during our studies that not all stepping behaviors are alike. For example, if an animal appeared to step in a “directed” mode (“going from A to B”), we saw significant perturbations to limb coupling. This is clearly demonstrated in videos where the initiation of locomotion is captured on camera (Video 8). In these examples, you can see the animal initially look around, turn its head towards the end tank, and then start stepping with a significantly altered coupling pattern. However, if that same animal locomoted in an outwardly “exploratory,” non-directed mode (e.g. snout-down) then the silencing phenotype was essentially abolished (Video 9).

We attempted to quantify these apparent behavioral differences by analyzing overt exploratory passes in which the animals stepped continuously with minimal-to-no hesitations while its snout was pointed towards the ground. These preliminary results revealed that when an animal was “snout-down stepping” (“exploring”), then the silencing phenotype was reversed (Figure 35). The animals essentially reverted back to the normal coupling patterns observed at control time points. While intriguing, we fully acknowledge the tenuous nature of these analyses, especially with regards to the relatively subjective definition of exploratory behavior as well as the influence speed could have on shaping the

phenotype (e.g., non-exploratory stepping could be faster than exploratory, thus leading to a change in coupling patterns). Therefore, we analyzed both modes of stepping (exploratory vs non-exploratory) at a fixed speed range of 23-90 cm/s (max snout-down stepping was 92 cm/s) (Figure 36). Even after we took into account the speed at which the animals stepped, we still saw a difference between the two stepping modes and whether or not silencing had an influence of hindlimb coordination. While these data are preliminary and require additional analyses, it appears as though the “type” or apparent mode of stepping also modulates the silencing phenotype. Why would this snout-down, exploratory stepping behavior mask the silencing-induced effects?

We do not know what the animal is actually doing during these “snout-down” stepping events. Are they actively whisking and/or sniffing? Whisking is an interesting sensory-motor task where the facial vibrissae rhythmically move back and forth to spatially and tactilely explore objects and surfaces[151]. During locomotion, the vibrissae essentially scan ahead of the animal[152,153], establishing localization in the forward direction but not the transverse[154,155]. Widespread neural activity throughout various cortical structures suggests this task has high cognitive drive. Indeed, the following structures have been shown to be active: the trigeminal ganglion, posterior medial nucleus of the thalamus, primary vibrissa somatosensory cortex, and primary vibrissa motor cortex[156-161]. And while whisking behaviors concomitantly emerge with locomotion during development, how these two systems are fundamentally interconnected still remains poorly understood[151]. Therefore, I will focus this discussion on the dynamic interactions between the

olfactory and locomotor systems as the integration of these modules has been mapped out in greater detail.

If the animals truly are sniffing during these snout-down locomotor bouts, then this could reflect a functional reorganization of the network to where an olfactory-motor circuit drives the spinal locomotor circuitry. This sensory-motor functional ensemble is not unheard of. It is widely recognized that animals will express motor behaviors in response to an odor stimulus. This phenomena has been documented in fish[162], lamprey[163], rats[164], and even humans[165]. Moreover, this olfactory-motor response is expressed incredibly early in life. Hours old rat pups could elicit rhythmic, locomotor-like movements when presented with a piece of home-cage bedding while suspended in a sling[164]. Most surprising was that these locomotor-like movements were in an alternating pattern with a 1:1 or 1:2 fixed relationship.

The apparent conservation and fidelity of these olfactory-motor responses led Dubuc and colleagues to identify the underlying neural mechanisms that govern this sensory-motor behavior[166,167]. Specifically, what pathways link the olfactory system to that of the locomotor? Using the sea lamprey model, they revealed that olfactory input is relayed from the medial olfactory bulb to the posterior tuberculum, a structure in the caudal diencephalon that is exquisitely involved in sensory-motor control[168]. Projections from the posterior tubercle are then relayed to the mesencephalic locomotor region, or “the locomotor command center”[168,169]. From here, mesencephalic locomotor neurons project to the reticular formation, where they activate reticulospinal neurons to then drive the spinal

circuitry. Not only could these snout-down locomotor bouts implicate an olfactory-motor relay onto the spinal circuitry, but there could also be modulatory effects through the vestibulospinal tract. Here, the vestibulospinal system (medial and lateral projections) collectively modulates muscle tone, balance and posture, head and eye coordination, as well as spatial orientation[170]. This system influences the spinal circuitry through direct projections onto neurons residing in the intermediate gray matter (medial tract innervates cervical segments, lateral tract runs along the entire length of the spinal cord)[170]. These studies, as well as others, highlight how various supraspinal centers, as well as the dynamic interactions between them, can powerfully shape and modulate spinal generated locomotion.

These “snout-down” observations were just one example of an apparent “top-down” behavior that reversed the stepping perturbations. We also noticed that the silencing effects were masked when animals were actively looking about their environment while they stepped. Again, whether this is due to the speed at which the animals stepped or if it reflected another “top-down” behavior where the animal was forming an internal map of its external environment (active involvement of the ventral hippocampus and nucleus accumbens) remains unknown[171-174]. Nonetheless, it appears as though there are differential gating mechanisms at play. Ones that endow the expression of the silencing phenotype as well as override its effects. What could account for these intriguing “context is key” observations?

***The multi-functional reconfiguration of the central pattern generator: "top-down versus bottom-up" locomotion***

We propose that conditional silencing has unmasked a context-driven, top-down bottom-up reconfiguration of the lumbar central pattern generator. These effects are revealed through silencing L2 projection pathways as they likely operate at the interface between the two modules (Figure 37).

First, let us consider the "bottom-up" context. From our observations, if an animal "wanted to go from A to B," left-right coordination was significantly disrupted, but only during conditional silencing of the L2 projection pathways. What does this "directed, A to B" stepping indicate about the status of underlying neural circuitry that governs this particular behavior? We propose that in this specific context, the CNS calls upon these L2 projection pathways immediately, and robustly, to effect the desired action. The "functional demand" is high for L2-L5 interneurons and/or LAPNs to distribute the temporal information throughout the neuraxis (Figure 37, panel $b_i$). Therefore, when these neurons are not functionally available to do so, the consequences are profound (Figure 37, panel $b_{ii}$). On this conjecture, the L2-L5 interneurons and LAPNs receive direct, monosynaptic input from supraspinal structures. Indeed, the ventral gray matter is known to receive dense supraspinal input[175]. As such, it is no surprise that when we mapped the known terminal innervation zones of various supraspinal centers onto where the L2-L5 and LAPN cell bodies reside, we see potential overlap between the two (Figure 38). Therefore, there could be a direct link between the descending command signals for "go" and the L2 temporal distribution networks studied here.

However, when the context changes, such as the sensory-driven locomotor behaviors during “snout-down” stepping, the neural circuitry functionally reorganizes into a “top-down module.” Here, the functional demand for L2-L5 interneurons and/or LAPNs is much lower as the task does not demand for the immediate distribution of temporal information throughout the neuraxis. As such, the functional loss of the L2 projection pathways does not affect the expression of the desired behavior as these pathways contributed very little to its expression in the first place (or many other pathways are involved in the task, thus offsetting the silencing effects) (Figure 37, panel c). Or perhaps the L2 projection pathways are not involved in expressing the desired action at all, a potential explanation as to why silencing an inter-enlargement pathway (LAPNs) does not influence a purely bipedal task (swimming, Figure 37, panel d).

We do not suggest that these “top-down” and “bottom-up” functional modules are mutually exclusive. Instead, we believe these context-dependent observations highlight how the locomotor network reconfigures itself to fit the needs of the task. This concept is within the vein of the modular organization hypothesis for left-right coordination, where discrete pathways are recruited in a speed-dependent manner to secure alternation. Here, we show that the reorganization is likely not dependent on speed, but instead the task at hand.

To conclude, the locomotor circuitry could be considered a “hard-wired” system based on the discrete anatomical interconnections between various neurons[176]. However, at any given time the strength of these connections can be modulated through changes in synaptic strength and/or cellular excitability. This

salient feature endows the entire system with flexibility to reconfigure itself, allowing different neuronal ensembles to be recruited in order to express the broad repertoire of motor behaviors. Moreover, the dynamic inputs from proprioceptive and/or exteroceptive sources can powerfully modulate the system, even on "functional ensembles" that are otherwise unchanging/intact. We believe our data from the conditional silencing of L2 projection pathways nicely illustrates this principle.

## Limitations and alternative approaches

In this section, I will address four key limitations in our study. First, I will discuss the likely incomplete penetrance of silencing all L2-L5 interneurons and all LAPNs from a technical and functional perspective. Next, I will address the issues we had in detecting the absolute number of neurons that were double infected. Thereafter, I will outline the inherent limitations in dissecting the role of all ipsilateral versus all commissural projections as well as the excitatory versus inhibitory subtypes. To conclude, I will highlight how poorly we understand where these networks fit into the overall locomotor connectome and why this knowledge is key for interpretation of our data. Throughout these sections, I will put forth several experiments that could potentially address these limitations.

### *Incomplete penetrance in the conditional silencing of L2-L5 interneurons and LAPNs*

Technical considerations

From a purist perspective, to truly appreciate the functional significance of a discrete pathway all of its neural constitutents should be manipulated

(genetically, virally, or otherwise). As such, one major criticism of our work is that the approach used here does not permit a systematic dissection of the L2-L5 and LAPN pathways. Specifically, we cannot conditionally silence all L2 neurons that have L5 projections or all LAPNs whose cell bodies in the lumbar cord have cervical projections. And while we have replicability across time points (DOX1 vs DOX2) and between animals for the behavioral phenotype, an issue that is often raised is what proportion of the total pathway we ultimately infected.

Studies previously performed in our laboratory have shown that following cervical injections (at different levels) with retrograde tract tracers, LAPNs were distributed throughout the entire lumbar neuraxis[123]. If the cervical injections were performed more rostrally, then the relative distribution and number of LAPNs labeled was different. Anatomical studies performed in the cat showed similar results[128]. Therefore, despite the somewhat diffuse nature of these nuclei the preponderance of LAPNs appears to reside in the rostral segments[123,128]. This was the rationale behind our targeted injections at spinal L2. Surprisingly, the rostrocaudal spread of L2-L5 interneurons remains unknown in the adult rat, although studies in embryonic rats indicate they are relatively confined to the rostral segments[52,54].

Therefore, to target the “entire” pathway we would have to perform bilateral, serial injections along the entire length of the lumbar spinal cord (LAPNs) or confined to the rostral segments (L2-L5 interneurons). To compound the issue further, we do not know to what extent the AAV2 viral vector spreads rostrocaudally. Answering this question requires *in situ* hybridization to detect

rtTAV16 expression. This proved impossible as not only do we not have the probes designed to detect rtTAV16, but also due to the fact that our spinal cord tissue was cryosectioned at 30 µm. *in situ* hybridizations usually requires sections of 8 to 10 µm thick[177]. As such, the number of injections required for sufficient infection could be relatively few (virus has diffuse spread) or considerably high (restricted spread). Therefore, not only could animals require a substantial volume of virus that would likely cause a profound immune response[178], but the laminectomy and injections themselves could cause irreversible locomotor deficits as the lumbar spinal cord has been shown to be critically involved in generating hindlimb stepping[146].

It seems improbable that the $Tet^{On}$ technique will allow us to have complete penetrance such that all neurons that comprise our pathways of interest are double-infected. The only approach that likely affords greater penetrance would be to genetically ablate these neurons in the mouse spinal cord (see “Bridging the gap” section of Discussion).

Functional considerations

The fact that we cannot unequivocally silence all L2-L5 interneurons or all LAPNs raises a serious question: does this incomplete penetrance account for the phasic dispersion we observed in interlimb coordination (the “left-right coordination continuum)? Alternatively, are the changes observed a “byproduct” of the incomplete penetrance or the true functional readout, regardless of the relative proportion we silenced? While directly answering this question is likely impossible, generating the following data would provide more context such that we could better interpret the results generated from our studies.

If we graded the penetrance we achieved from silencing L2-L5 interneurons and LAPNs as “medium,” then one might speculate that we observed a spectrum of coupling patterns because we did not “knockout” enough of the pathway. Therefore, the animals could not default (or switch) to the more conventional coupling patterns (e.g. gallop, bound) and instead were left with adopting a “hybrid” or spectrum of left-right phase relationships. If this is true, then silencing a significantly greater (or lesser) proportion of the pathway would tip the balance such that animals defaulted to more typical coupling patterns (Figure 39). These data would suggest that L2-L5 interneurons and LAPNs do play gait-specific roles in locomotion, a significant deviation from our emerging hypotheses.

To address this issue, we would keep the lentiviral vector injections consistent across all groups. However, we would then vary the number of AAV2 injection sites in an attempt to gate the relative proportion of neurons that are silenced (Figure 39). Data shown in this dissertation were generated from animals that received two sets of bilateral injections (a total of four injections) that were separated by 1.5 mm rostrocaudally. As such, the “low” silencing effects group would receive one set of injections (bilaterally) while the “high” effects group would receive three to four sets of injections. If the magnitude and pattern of silencing-induced changes observed was not different between the groups (especially the “medium” versus “high”), this would support our idea that the changes we observed were the true functional readout and not a byproduct of a differential “knockout.” However, if these proposed experiments reveal silencing-affected steps that cluster at discrete coupling patterns (such as gallop or bound for the “high” effects

group), this would suggest that the coupling continua we observed were likely a byproduct of an incomplete knockout. And while increasing the number of injection sites could effectively reduce the variability observed in interlimb coordination (e.g., steps concentrated at gallop or bound), this approach could also yield infections of “off-target, non-specific” neurons. Moreover, these infected neurons could be functionally unrelated to our L2 projection pathways of interest thereby confounding our interpretation of the perceived consequences from silencing.

Ultimately, it is likely that we did not silence all L2 interneurons that project to L5 or C6. Therefore, under these conditions of “incomplete” silencing we observed a breadth of coupling patterns in interlimb coordination. Despite this incomplete silencing, these data are still interpretable based on three key findings. First, the effects were highly specific as we observed no overt changes to intralimb coordination (L2-L5 and LAPN studies), no perturbations to ipsilateral forelimb-hindlimb movements (LAPN), and the silencing effects were clearly context-specific (L2-L5 and LAPN studies). Second, all animals showed a silencing-induced phenotype from both studies (N=19 animals). Third, the silencing-induced changes to interlimb coordination were reversible and reproducible one month later. These robust observations detected across both studies provides strong support that we can still appreciate the functional significance of these pathways during overground locomotion, even if there was incomplete penetrance of conditional silencing.

***What proportion of the total pathway did we conditionally silence?***

In the vein of incomplete penetrance, another major criticism of our studies is that we currently do not know the absolute number of L2-L5 interneurons and LAPNs that we silenced. Ideally, we would know how many neurons were silenced in each animal such that we could correlate the magnitude of phenotypic changes observed to the number of neurons silenced. The $Tet^{On}$ constructs are designed to address this as any neuron that expresses eTeNT.EGFP can be detected *post hoc* using immunohistochemical techniques[80]. However, this was exceptionally challenging. The technical issues described below have greatly impacted the fidelity with which we believe absolute counts of eTeNT.EGFP-expressing spinal neurons could be performed.

One plausible explanation for our technical issues was that viral titers we produced were lower as compared to that used by the developers of the $Tet^{On}$ system[80]. Here, we produced the lenti- and adeno-associated viral titers of $1.6 \times 10^7$ viral particles (vp)/ml and $4.8 \times 10^{12}$ vp/ml, respectively. Alternatively, Kinoshita and colleagues produced titers as high as $7.5 \times 10^{11}$ copies/ml and $2.0 \times 10^{13}$ vp/ml[80]. Our lower titers could have affected the overall expression of eTeNT.EGFP that was induced *in vivo*, thereby making *post hoc* detection of the fusion protein more difficult in the spinal cords.

Another key technical issue that still needs to be resolved is developing an optimal protocol for tissue preservation to detect eTeNT.EGFP consistently and reproducibly. In the L2-L5 interneuron study, we processed the tissue following our normal protocol where the animals were transcardially perfused with phosphate-

buffered saline (PBS, pH 7.4) followed by 4% paraformaldehyde (PFA). The harvested spinal cords were then post-fixed overnight in 4% PFA followed by cryopreservation in 30% sucrose solution. However, this protocol made the histological detection of eTeNT.EGFP-positive neurons problematic. When we attempted to amplify the eTeNT.EGFP signal by staining for GFP, it became clear that our signal-to-noise ratio was poor. We could not reliably identify double-infected neurons above the background noise, potentially due both low transgene expression as described above and/or excessive cross-linking of the antigenic sites such that the anti-GFP antibody could not effectively bind to its epitope[179]. In support of the latter, we were able to detect double-infected cell bodies with greater resolution with we adopted a “light fixation” protocol (LAPN study) wherein the spinal cords were briefly post-fixed for one to three hours followed by cryopreservation. Using heat-induced epitope retrieval techniques improved the antigenicity of our L2-L5 spinal cord tissue, but not to the level at which absolute counts could be performed definitively. Interestingly, our immunohistochemical detection of putatively silenced terminals was considerably less cumbersome by comparison, potentially due to the high concentration of eTeNT.EGFP signal in a small cellular structure.

Finally, the buffers and detergents used during immunohistochemical detection of eTeNT.EGFP also proved to be an issue. Our routinely used buffer and detergent for staining is Tris-buffered saline (TBS) as well as Triton x-100 in concentrations ranging from 0.1%-0.3%. Through innumerable trial and error sessions, it became apparent that TBS and triton are counter-productive for our

staining needs. Instead, it appears as though PBS in combination with or complete absence of more gentle detergents such as Tween-20 or saponin (0.05-0.1%) yielded more consistent and reliable results.

Should robust immunohistochemical detection of the double-infected cell bodies prove to be technically unfeasible, one might postulate that an approximation of the number of neurons silenced could be inferred through intraspinal tract tracing experiments. To do this, the lenti- and AAV2 injection protocols would be repeated, but using fluorescent tracers instead of the viral vectors such that any neuron that co-expresses both tracers would “mimic” a double-infected cell body. But even this relatively simple approach has a significant limitation: the uptake mechanisms and diffusion properties between fluorescent tracers and viral vectors are profoundly different. The lentivirus is a pseudotyped HIV-1 vector designed for enhanced uptake at the terminal field (via its fusion of rabies virus glycoprotein [extracellular and transmembrane domains] with cytoplasmic domain of vesicular stomatitis virus)[80-83]. Alternatively, the fluorescently-conjugated cholera toxin beta subunit tracer is taken up by binding to the monosialoanglioside receptor (GM1)[180]. The AAV2 virus is neurotropic and infects the cell bodies through cell surface glycan binding (heparin sulfate proteoglycan for serotype 2)[181] while the anterograde tracer biotinylated dextran amine (BDA ) labels cell bodies through an unknown mechanism, although it is likely endocytotic in nature[182]. Due to the disparate nature between viral infections and tracer uptake, using tracer data as a “stand in” or approximation for double-infected cell bodies is non-ideal, if not inappropriate.

In light of these technical issues regarding tissue preservation, epitope detection, the inability to reliably approximate viral infection numbers through tract tracing, and the desire to have absolute counts to correlate back to behavior, it is unequivocally essential to develop an optimal protocol for tissue processing and immunohistochemistry. Performing a pilot study where fixation (e.g. PFA, glutaraldehyde, formalin, fresh-frozen), buffers (PBS or TBS of varying acidities), detergents (Tween-20, Triton x-100, digitonin, or saponin of varying percentages), and primary antibodies (mouse, rabbit, chicken, goat anti-GFP of varying concentrations) are systematically tested is required, at a minimum, to address this issue. In hindsight, these conditions should have been standardized before behavioral experiments were performed. However, our initial proof-of-concept study was silencing L2-L5 interneurons. As such, we did not have the opportunity to determine the optimal conditions before functional testing.

***What are the functional contributions of the pathway subtypes: ipsilateral versus commissural, excitatory versus inhibitory?***

Silencing data from both studies revealed an intriguing dichotomy: contralateral limb movements (left-right fore- and hindlimbs, diagonal hindlimb-forelimb) are selectively impaired while ipsilateral movements (intralimb coordination, homolateral limb pairs) are unaffected. This raises an interesting question: what functional roles do the commissural versus ipsilateral subpopulations play during locomotion, in particular the ipsilateral pathways?

At first blush, addressing these questions appears relatively straightforward. Unilateral viral vector injections would silence the ipsilateral pathways while

bilateral injections would target the commissural subpopulations (Figure 40). However, only one set of the ipsilateral (e.g. left L2 interneurons that project to left L5) or commissural (e.g. left L2 interneurons that project to right L5) subtypes can be studied. In these experiments, we would effectively be studying a subset (left L2-L5 interneurons) of a subset (ipsilateral L2-L5 interneurons, left and right sides). Because we would be silencing a considerably small fraction of neurons in the otherwise intact locomotor circuitry, the potential for functional compensation is likely high. Indeed, even Kinoshita *et al* showed compensatory effects mediated through indirect, intact circuits using the same $Tet^{On}$ system used here[80]. Therefore, it is likely that the effects of silencing "one subset of a subset" could be masked by the intact, complementary subset or through other relevant circuits.

Therefore, to address what role the ipsilateral or commissural pathways play, we would need to combine the $Tet^{On}$ system with another technique that endows pathway-specific manipulations independent of cell-specific promoters. One approach would be to combine $Tet^{On}$ silencing with DREADDS, which are "Designer Receptors Exclusively Activated by Designer Drugs"[183,184]. This is a chemogenic approach where proteins are engineered to interact with non-endogenous, small, drug-like compounds. These "designer drugs" act as chemical actuator that can be programed to increase or decrease neural activity remotely[184]. As such, we could employ a Cav-Cre mediated approach wherein we induce recombination to express DREADD inhibitors on one side of the spinal cord in conjunction with $Tet^{On}$ silencing on the opposite side (Figure 40c, left; refer to Figure 41 below for detail on Cav-Cre). Apart from concerns regarding differential

"silencing" mechanisms, there is an insurmountable issue with this approach: we would essentially produce "hybrid commissural" neurons that express a combination of both systems (Figure 40c, right). What impact this could have on cell viability or functionality is unknown. It seems impossible, at the moment, to silence all ipsilateral (or commissural) projections. Moreover, there is no way for us to determine the functional role of excitatory versus inhibitory L2-L5 interneurons and LAPNs in adult rats. These questions would have to be addressed in the transgenic mouse model. Ultimately, the best approach would be to computationally model these networks. Using this technique, one could "reverse engineer" the *in vivo* observations by differentially removing the excitatory and inhibitory inputs (both ipsi- and commissural) to determine which permutations mimicked the phenotype.

***How do L2-L5 interneurons and LAPNs fit into the overall locomotor circuitry?***

Anatomy of the L2-L5 interneurons and LAPNs in the adult rat are poorly understood

While we have explored in some detail the anatomical underpinnings of the silencing effects, the precise projection patterns of these neurons in the adult rat are still unknown. This is a serious concern because any terminal, regardless of its location, will have eTeNT-mediated VAMP2 cleavage to prevent neurotransmission. How can we interpret the functional consequences of silencing a "L2-C6" pathway if these neurons also have projections throughout the lumbar and thoracic neuraxis in additional to cervical segments? A rigorous anatomical

study is required to understand “the full scope” to which L2-L5 interneurons and LAPNs integrate into the nervous system.

Dissecting the complexity of the pathway projections in the rat spinal cord is technically challenging, but potentially feasible using a combinatorial viral vector approach optimized for synaptic labeling (Figure 41, refer to legend for simplified and detailed workflows). First, we would need to retrogradely deliver Cre recombinase to our neurons of interest using Cav-Cre viral constructs[185]. In this system, Cre is retrogradely delivered to neurons through the canine adenovirus (serotype 2) which efficiently transduces axon terminals[185-187]. Therefore, Cav-Cre would be injected at L5 to retrogradely infect L2-L5 interneurons and at C6 for the LAPNs. Thereafter, at the level of the Cre-infected cell bodies we would perform injections using the AAV2-flex-SynTag viral constructs[127]. This construct has double-inverted-orientation-LoxP flanked sites that expression of fluorescently-tagged synaptic proteins following Cre-mediated recombination. Studies show that efficient Cre-mediated recombination to induce the expression of fluorescently-tagged synaptic proteins originating from the double-infected neurons takes approximately two weeks[127]. Using this approach, we would be able to detect both the synaptic arborization profiles and axonal projection patterns throughout the entire neuraxis for each pathway. Therefore, we could determine whether these neurons project to various motor neuron pools, other spinal segments, or supraspinal centers.

Anticipated projection patterns of L2-L5 interneurons

Based on our initial triple-tracer anatomy experiments, we do not anticipate seeing dense terminal innervation within the rostral lumbar segments derived from L2-L5 interneurons. However, the dual-virus technique described here affords superior resolution in uncovering projection patterns. If we did observe L2-L5 interneuron collaterals throughout the rostral lumbar segments this would greatly influence the interpretation of our functional data. We propose that left-right coordination is disrupted during silencing due to the loss of rostro-caudal distribution of key temporal information. If L2-L5 interneurons do have dense collaterals locally, then this could be the primary mechanism as to why left-right coordination was disrupted as the rostral lumbar segments are profoundly involved in central pattern generation[25]. Nonetheless, we anticipate these anatomy experiments will reveal dense synaptic innervation throughout the caudal lumbar segments.

Anticipated projection patterns of LAPNs

Following a series of unpublished double-tracer experiments, we revealed that LAPNs appear to lack local projections throughout the lumbar enlargement (Figure 42). These results are unexpected as this pathway plays a key role in coordinating temporal information between left-right hindlimbs and left-right forelimbs. The apparent lack of dense innervation throughout the lumbar spinal cord makes reconciling the changes to left-right hindlimb coordination challenging. Moreover, disparate from the apparent dense innervation long descending

propriospinal neurons provide throughout the thoracic segments[127], we show that long ascending neurons appear to not have substantive projections here.

We did not observe double-labeled neurons following dual tracer injections at the cervical and thoracic segments, respectively (Figure 42). It is important to note that these were not systematic dissections and that using the more sensitive dual virus technique could reveal projection patterns that were otherwise below the threshold for detection with standard fluorescent tracers. If the proposed experiments uncover projection patterns throughout the lumbar segments, this could account for the profound effects silencing had on hindlimb coordination. However, if they also revealed synaptic projections throughout the thoracic segments then this raises interesting questions as to why balance, posture, and trunk stability were not affected during silencing. Nonetheless, we anticipate that these experiments will uncover dense innervation throughout the cervical segments onto neurons in laminae VII, VIII, and X.

***How do L2-L5 and LAPNs fit into the locomotor connectome?***

We frequently emphasize that our functional data are interpreted with respect to “the otherwise intact locomotor circuitry.” However, the anatomical integration of these pathways into the locomotor connectome, both on a macrocircuit and microcircuit scale, is unknown. Not only could this information provide great anatomical context as to why we observed the silencing phenotypes, but it could also provide information as to why certain tasks were amenable to disrupted coordination while others were not (e.g., non-exploratory vs exploratory behavior). Deciphering where L2-L5 interneurons and LAPNs fit with the locomotor

macrocircuit would require the use of trans-synaptic tracers (e.g. pseudorabies virus), a technique that is notoriously challenging for interpretation[188]. Therefore, I will focus this discussion on how to dissect the microcircuit architecture of both pathways.

To probe the microcircuit integration of L2-L5 interneurons and LAPNs, we need to dissect their input-output organizational structure. This is possible using the TRIO approach ("tracing the relationship between input and output")[185,188], a technique that is illustrated in Figure 43. Using this tracing technique, we could map the inputs of neurons from "region 1" that synapse onto L2 neurons in "region 2" which then project to "region 3" (Figure 43a).

First, we would need to create "starter" neurons. Starter cells gate the selective infection and monosynaptically-restricted spread of glyco-deleted rabies virus. Here, our starter cells would either be the L2-L5 interneurons or the LAPNs (Figure 43b). To create these starter cells, we would need to double-infect the neurons with two Cre-dependent AAVs. The first is AAV2-FLEx$^{loxP\text{-}TC}$ (Figure 43b, red construct). "TC" denotes the TVA-mCherry fusion protein[189]. The second Cre-dependent construct is AAV-FLEx$^{loxP\text{-}G}$ (Figure 43b, light green construct). This construct encodes for the rabies G-protein, a requirement for trans-synaptic spread. Therefore, our starter "L2" neurons would be dually infected with two Cre-recombinase-activated constructs. The transgenes (TVA-mCherry; G-protein) would only be expressed following Cre-loxP driven FLEx-switch recombination.

The next step is where we would decide which pathway, L2-L5 or L2-C6, we wished to focus on for dissecting the input-output architecture. This is due to

the fact that we would deliver Cav-Cre at the level of the terminal field. Cav-Cre would then retrogradely transported back to the double-infected cell body where it would induce FLEx-switch Cre-recombination. Therefore, if we wanted to dissect the L2-L5 microcircuit, we would inject Cav-Cre at L5. If we wanted to dissect the LAPN microcircuit, we would inject at C6 (shown in Figure 43c). In the dual-infected L2 starter neurons, Cre would now be expressed. This would lead to FLEx switch recombination which would produce both TVA-mCherry and rabies G-protein (Figure 43d).

In the final step, we would target the starter neurons with a rabies virus that is EnvA-pseudotyped (envelope protein from avian ASLV type A virus), glycoprotein-deficient (requires trans-complementation), and GFP expressing ("RV*d*G") (Figure 43e). The EnvA-pseudotyping selectively targets the infection only to starter L2 neurons that express the TVA receptor. As such, our L2 neurons would now express mCherry and GFP (ultimately fluoresce yellow). Because these starter neurons express rabies G-protein, the RV*d*G virus can replicate and spread trans-synaptically ("trans-complementation"). Therefore, input neurons that synapse onto the starter neurons would be infected and express GFP. However, these input neurons do not express the rabies G-protein (were not infected with AAV-FLEx$^{loxP\text{-}G}$). As such, the rabies spread would be restricted to monosynaptic connections only. Therefore, using this technique, we could tease out the input pathways onto our pathways of interest was well as where they project to and synapse on.

Despite the relative elegance of this system, working with viral tracers presents unique technical limitations. Most obvious is that rabies virus expression will ultimately kill the neurons. Studies show that following neuronal infection, the cells are still detectable for up to 14 days post-injection[190]. However, their viability as assessed by electrophysiological techniques becomes questionable after 12 days[191]. The second most important limitation relates to the overall efficiency of the labelling. Notably, under most conditions only a fraction of the "true" total inputs onto starter neurons will be labelled[188]. As outlined by the developers of the system, this could be due numerous reasons, including: (1) poor expression levels of the rabies G-protein in the starter neurons, (3) an insufficient number of pseudotyped-rabies virus particles that ultimately infect the starter neurons, or (3) the length of time required for monosynaptic spread before the neuron starts to die[188]. Notwithstanding, this is currently the only technique that allows us to map out the local microcircuit of these neurons.

**Bridging the gap: the deep divide between developmental and functional modules**

The genetic models of locomotor circuitry have identified key pathways that secure left-right coordination in a speed-dependent manner[61]. So, where does our silencing data fit within this framework? Simply put: it does not. In this section, I will re-address the genetically-dissected functional organization of the left-right coordinating circuitry, illustrate why our data does not fit easily into this model, put forth "plausible" experiments that could bridge this gap, and conclude with a functional model that could account for our data with respect to the genetic studies.

### *The V0 class: primary mediators of left-right alternation*

Initial studies that investigated the role of V0 interneurons involved the deletion of *Dbx1* (developing brain homeobox 1), which is the fate-determining transcription factor expressed in the progenitor pools that ultimately give rise to V0 interneurons[75,192]. Therefore, in these mice, the loss of the Dbx1 gene prevents the development of all types V0 interneurons (note, three subtypes have been identified thus far). In the isolated neonatal spinal cords of these Dbx1-null mice, drug induced locomotor-like activity produced periods of left-right synchronous activity interspersed with normal alternation[68] (Figure 44b). Kiehn extended these findings, showing these synchronous events were also observed *in vivo* when V0 interneurons were selectively ablated early in development through the expression of diphtheria toxin A (Dbx1-DTA mice; V0-deleted mice)[17]. Bound was the only gait these animals could express across all speeds analyzed[17]. However, what roles do the excitatory and inhibitory subtypes play during locomotion? Talpalar and colleagues demonstrated that it the excitatory subtype (V0v) governs alternation at high frequencies. When this subclass is removed, the trot gait is abolished while the slower alternating gait (walk) and the more synchronous gaits (gallop, bound) are preserved (Figure 44c)[17,69]. Therefore, the inhibitory V0d interneurons secure left-right alternation at lower frequencies. Computational modelling supports the notion that inhibitory V0d and excitatory V0v interneurons are recruited in an ascending order as the stepping speed increases[74]. However, the V0 interneurons

are not the only class that have been implicated in securing left-right coordination during locomotion.

***The V2a subclass: a facilitator of fast-paced alternation***

Of special interest is the work from the Harris-Warrick group. In their transgenic mouse model (strain: ICR/BL6/129), the wild-type mice trot at all speeds and step frequencies (Figure 44d)[66,67]. Therefore, these mice normally do not gallop or bound. This is not uncommon as certain strains of mice do not deviate beyond an alternating gait[14]. When Crone *et. al.* ablated the excitatory V2a interneurons, the mice could no longer preserve left-right alternation at high rates of speed and step frequencies (Figure 44e). As such, removing these neurons from the spinal cord caused the animals to gallop where they would normally alternate. Interestingly, these V2a neurons project ipsilaterally onto the excitatory V0v interneurons[66,193-195]. The anatomical underpinning of this pathway suggests that while they likely contribute to alternation at all speeds, the V2a-V0v circuit drives left-right alternation at higher frequencies. This hypothesis has been computationally validated[74].

***The genetic model for left-right coordination***

These studies, along with extensive computational modelling[74,196-198], have led to the modular organization hypothesis illustrated in Figure 44 (panel f). Here, V0d neurons secure left-right alteration of the limbs at reduced speeds and step frequencies. Therefore, this pathway is recruited during the walking gait, where animals are stepping slowly with three limbs in contact with the ground at any given

moment[17]. As speed increases, the V0v-V2a circuit is recruited to secure the limbs in the trot pattern where they act as struts with only two pairs contacting the ground at any given moment. Together, these are the alternation networks that secure left-right coordination at low-to-moderate speeds and step frequencies. The molecular identity of the gallop or bound pathways, ones that synchronize the left and right sides of the body, are unknown[61], but the hypothesis is that these alternation networks are either suppressed or overridden during these tasks.

***The division: reconciling our data with the genetic models***

It is quite challenging trying to reconcile our data with that of the genetic literature, both from the technical approaches used (refer back to Chapter One for detail), functional readouts (*in vitro* versus *in vivo*, overground stepping versus treadmill-based locomotion), and underlying anatomy of the pathways that were investigated. Nonetheless, let us highlight the similarities and differences between the two.

Similar to that described in the V0-null mice, we observed synchronous or synchronous-like movements at speeds and step frequencies where these patterns are normally not expressed. However, unlike the V0-nulls, we did not observe a “switch” or “default” to the synchronous patterns. Instead, we observed a spectrum of left-right coordination values, which could be due to a differential “knockout” of the pathways we silenced (see Limitations section for more detail) (Figure 45b). When we compare our results to that of the V2a literature, there are similarities in that ablating the V2a neurons endows the locomotor system with

“new” coupling patterns it normally would not express (mice that could only alternate at all speeds can now gallop at fast-paced locomotion). However, the expression of the gallop gait was predicated on the animals stepping at fast rates of speed, a phenomenon we did not observe in either of our studies. Indeed, we saw coupling patterns indicative of a full bound at 60 cm/s when rats typically bounded at over 200 cm/s (long tank study). Moreover, how can we reconcile the V2a data in light of the fact that these mice normally do not express gallop or bound when those are a part of our rats’ normal gait repertoire?

Both approaches present with unique technical considerations when interpreting the functional consequence of the manipulations performed (refer back to Chapter One for genetic pitfalls). It is also important to note that we have not directly tested whether silencing L2-L5 interneurons or LAPNs affects the expression of the faster gaits. As such, we do not know if silencing these pathways results in the “loss” of gallop or bound at speeds at which they normally should occur (Figure 45**c**). To do this, we would need to train the animals to volitionally express these gaits during overground stepping. What effects a positive reinforcement training paradigm could have on the neural ensembles involved in the normal expression of locomotion (e.g. context is key), let alone during silencing, could prove to be challenging in interpretation. Where does that leave us in our reconciliation of the silencing data with that of the genetic literature? There is a pressing need to fit our data within these current models. What experiments do we need to perform in order to bridge this divide?

***Building the bridge***

To bridge this gap, we would first have to "unequivocally" demonstrate which genetically-encoded V-class series the mature L2-L5 interneurons and LAPNs represent in the adult mouse spinal cord. While this idea is simple in conception, its poses incredible technical challenges.

The genes that mark the various spinal progenitor domains and/or early post-mitotic V-class subtypes are quickly downregulated during embryogenesis[199]. Therefore, the litany of transcription factor-specific Cre-driver lines are unusable postnatally. To circumnavigate this issue we would have to use a combinatorial approach developed by Arber and colleagues, making use of both genetic and viral technologies[200] to "lock" the expression of these transient markers in post-natal neurons.

First, we would breed our "transcription factor of interest" Cre-line with a transgenic mouse whose pan-neuronal *Tau* locus conditionally expressed Flp recombinase ($Tau^{lox\text{-}STOP\text{-}lox\text{-}FLP\text{-}INLA}$)[200]. The progeny from this breeding pair would have permanent expression of both nls-LacZ and Flp recombinase in neurons that were born from the progenitor domain of interest.

Next, in the double transgenic mice, we would perform intraspinal injections of a double-inverted-orientation-FRT-flanked adeno-associated virus[127]. The delivery of this virus induces expression of green fluorescent protein in the Cre-positive neurons whose transient transcription factors were permanently "locked." Therefore, any mature neuron derived from the progenitor domain of interest is

now green. Not only would we have to perform intraspinal AAV injections to induce recombination for LacZ expression, but this must be combined with a fluorescently-tagged retrograde tracer. Because our pathways of interest are anatomically-defined through tract tracing, we must also retrogradely-label the neurons and look for co-expression of both the tracer and LacZ. Thankfully, Ruder *et. al*. revealed that the lumbo-cervical projection neurons (a plausible correlate for the long ascending propriospinal neurons) are primarily derived from the V0-Dbx1 and/or V2-Shox2 progenitor domains[127]. Therefore, we would only have to perform the aforementioned experiments for the L2-L5 pathway alone. However, these experiments are purely anatomical and do not address any functional role(s) the pathway could play during locomotion. Separate experiments would be required to address this question.

Ultimately, the interpretation of these experiments is predicated on two key assumptions. First, that developmental modules specify functional modules. Second, there is a discrete transcription factor that specifies every L2 neuron that projects to either L5 or C6. Ruder *et. al.* clearly demonstrated that lumbo-cervical neurons (a likely corollary of LAPNs) are not derived from one genetically-encoded domain[127]. Moreover, studies have shown there are clear differences in developmental versus functional modules of select, genetically-encoded neurons[77,78]. Taken together, it is obvious that any approach to functionally manipulate discrete circuits comes with inherent limitations.

### *Finding a happy medium*

Clearly, the lengths to which we would need to go in order to bridge this divide are insurmountable, at least for the unforeseeable future. Even if our data do not fit into the current genetic frameworks, we believe we have exposed a very complementary feature to this fixed (modular) system: intrinsic flexibility.

A modular system where specific coupling patterns are expressed at relatively fixed ranges of speeds and step frequencies makes perfect sense from an energy economy standpoint. Rhythmic, left-right alternation is incredibly efficient at conserving energy during locomotion[1]. During the first half of the stance phase when the animal is slowing down and rising up, forward kinetic energy is converted to potential energy. When the animal then begins to “fall” and speed up during the latter half of the stance phase, the potential energy is converted to forward kinetic energy[201]. This “alternating” energy transfer reduces the energetic costs of locomotion by up to 75%[1,202]. Therefore, it comes as no surprise that alternation is the most commonly expressed coupling pattern across numerous species, ranging from insects to mammals[1-7]. Consequently, when animals step at increasing rates of speed, not only do the interlimb coupling patterns change but the overall biomechanics of locomotion will adjust as well in order to conserve energy. These adjustments include stride lengthening due to movements of the torso as well as the incorporation of aerial phases into the stride cycle (no limbs in contact with ground)[1], a mechanism animals to increase their speed even further. Therefore, it makes sense that the limbs would be moving in synchrony as the

animals are effectively springing from their hindlimbs onto their forelimbs with incredible force at high rates of frequency. When these synchronous movements are coupled with the underlying biomechanical adjustments, animals are able to convert and recover their forward kinetic energy from both elastic strain (muscles) and gravitational potential energies (bound through the air)[201].

From our work, we believe we have uncovered the intrinsic capacity of the spinal cord to express a key complementary feature to this fixed, modular system: inherent flexibility and adaptability. Pattern generating circuits have been shown to be capable of "extreme reorganization," a property nicely illustrated in the stomatogastric network of decapod crustaceans[203,204]. Studies show that this circuitry can be reorganized to produce a breadth of different behaviors, but variations of the same type of behavior can also be expressed through network reconfigurations. This parallels nicely with our "context is key" findings, where silencing affects left-right alternation during "directed" stepping but not during exploratory locomotion or swimming.

Therefore, perhaps the modular organization of locomotor circuitry is key for how stepping patterns are initiated, and perhaps to some extent maintained. However, it is the flexible system that regulates stepping on a moment-by-moment basis. Indeed, the flexibility of control is "the basis for decision-making in the nervous system…the very essence of what animals must do throughout their daily lives"[204]. We do not believe these fixed and flexible coupling systems are mutually exclusive (Figure 46). Instead, we suggest they are both key regulators for

effective locomotion. Together, they endow the spinal cord with incredible precision, efficiency, and adaptability in how it orchestrates locomotion, both at its onset and on a moment-by-moment basis.

## Clinical significance

We have shown that the L2-L5 interneurons and LAPNs participate in one fundamental aspect of locomotion: interlimb coordination. But do these pathways sub-serve any meaningful role in bipedal locomotion for humans? Before discussing the translational implications of these findings, we must first address one fundamental question: are the neural control mechanisms of interlimb coordination in human locomotion similar to that of a quadrupedal mammal? While directly answering this question is impossible, several studies have provided evidence which suggests that the functional organization of bipedal interlimb coordination is similar to that of the quadrupedal mammal[205]. The pertinent results of these studies are summarized below.

### *Interlimb coordination of the lower extremities*

Much like quadrupedal mammals, bipedal stepping requires exquisitely timed coordination between muscles of the left and right lower extremities[205] such that the initiation of swing in one limb is predicated on the other limb being in stance[206-210]. This coordination between the left and right lower extremities is tightly regulated such that if a perturbation to gait occurs, there is an immediate bilateral response[211]. The short latency of these bilateral electromyography (EMG) responses suggests that this coordinating action between the two limbs is secured

at the level of the spinal cord. Although these features are tightly controlled, they are also flexible such that when stepping on a split-belt treadmill of two different speeds the lower extremities will still perform in a "cooperative manner"[205]. Therefore, even though the activity of one limb will influence the spatiotemporal stepping features of the other, effective stepping persists[212-215].

***Interlimb coordination of the upper and lower extremities***

Similar to quadrupedal mammals, humans also have long projection neurons that couple the cervical and lumbar enlargements[216,217]. While the upper extremities are typically not involved in producing the forward motions required for bipedal stepping, they are still temporally coordinated with the lower extremities as seen during swimming, crawling, and walking[218]. The expression of these coordinated movements is similar between infants[208,209,212], adults[206,207], and quadrupedal mammals[7], suggesting a common neuronal control mechanism between bipedal and quadrupedal locomotion[205]. Indeed, numerous limb reflex facilitation/inhibition and EMG studies have demonstrated plausible neuronal coupling between the two spinal enlargements in humans[219-221].

Although arm swing is temporally coordinated with the legs during stepping (e.g., right leg in stance, left arm swung forward), the current hypothesis is that this is primarily facilitated through passive forces[222]. From this perspective, arm swing acts as an "elastic linkage" between the shoulder and pelvic girdles, regulating the dynamic stability of the whole body and dampening trunk torsion during locomotion[223,224].

### *Context-specific gating of interlimb coordination*

Interestingly, it appears as though this functional coupling between the cervical and lumbar enlargements is task-specific[205]. When a mechanical impulse is applied to one leg, either at the middle or end of the stance phase while walking, a bilateral arm response is evoked in the deltoid and triceps muscles, respectively[205,225]. Electrical stimulation of the distal tibial nerve, a mixed fiber that innervates the skin and plantar foot muscles, also evokes similar responses in the arm muscles during stepping[225]. However, if the same mechanical stimulus is applied to the leg during sitting (while writing) or standing (with volitional arm swinging), no responses in the arms could be evoked. These results suggest that this ascending inter-enlargement pathway becomes "gated by the activity of the central pattern generator during walking," indicating that the coupling mechanisms between the two enlargements are flexible and context-specific[205]. From this perspective, bipeds can effectively switch from global motor actions such as stepping to more refined tasks like writing[225].

Collectively, these studies suggest that some of the underlying neural mechanisms that secure interlimb coordination for bipedal locomotion are likely shared with quadrupeds[205,226]. If these neural mechanisms are indeed conserved, what role could L2-L5 interneurons and LAPNs serve in bipedal locomotion?

### *Putative functional role(s) of L2-L5 interneurons in bipedal locomotion*

While most quadrupedal mammals have a repertoire of gaits with various coupling patterns (e.g. left-right alternation for walk-trot, left-right synchrony for

bound, etc), humans essentially have two alternating gaits, walking and running[227]. As such, the significance of maintaining well-organized coordination between the left and right legs cannot be understated. Any deficit could have profound effects on locomotion. And while the walking and running gaits are both characterized by out-of-phase coupling between the left and right legs, there are still underlying changes between the spatiotemporal gait indices and speed similar to what we observe in the quadrupeds. Specifically, with increasing speed the stance duration decreases and the stride length increases, all while the limbs continue to step alternatingly[227,228]. Therefore, not only does bipedal locomotion require effective left-right coordination for the walking and running gaits, but also across the full spectrum of speed-spatiotemporal relationships. We speculate that a "bipedal correlate" of L2-L5 interneurons could constitute one pathway in a repertoire of lumbar networks that governs left-right coordination of the lower extremities. Our results indicating that this lumbar pathway helps secure left-right coordination across a range of speed-spatiotemporal relationships provides some support for this idea.

***Putative functional role(s) of LAPNs in bipedal locomotion***

Speculating on the functional significance of LAPNs in normal bipedal locomotion is considerably more interesting. We showed that silencing this ascending inter-enlargement pathway in quadrupedal mammals significantly affects three patterns of interlimb coordination: left-right hindlimbs, left-right forelimbs, and contralateral hindlimb-forelimb movements. Therefore, in a context

where all four limbs are engaged in providing forward propulsive movements, distributing left-right temporal information from the hindlimbs to the forelimbs by way of LAPNs appears to be a key requirement for normal locomotion. We speculate that this ascending, inter-enlargement pathway facilitates these coupling patterns in bipeds as well, but in a highly task-specific manner.

First, we propose that LAPNs could participate in interlimb coordination during developmental stages prior to acquisition of bipedal stepping. Because babies are crawling on all four limbs, we propose that this pathway might play similar roles as to what we observed in our quadrupedal animal model. Therefore, coordination between the left-right lower and upper extremities, respectively, as well as between the contralateral limb pairs could be facilitated through these neurons. This idea is supported by the fact that the basic coordination patterns observed between infants and quadrupedal mammals are very similar (diagonal interlimb coupling between the girdles)[229,230]. Moreover, this pathway could also contribute to the expression of quadrupedal crawling behaviors in adult bipeds.

Following the transition from quadrupedal crawling to bipedal stepping, what functional role(s) could LAPNs serve? It is clear that “uncoupling” the two girdles (bind the arms to prevent their coordinated swing with the legs) does not perturb the coordination of the legs during stepping[231]. However, preventing this coupling between the arms and legs comes at the cost of increased trunk rotation and horizontal displacement of the limbs as well as an overall increase in the energy expenditure[231,232]. As such, LAPNs could plausibly help secure

coordination between the upper and lower extremities in order to facilitate a more energy efficient form stepping in the non-disabled populations.

***Role of propriospinal neurons in functional recovery following spinal cord injury***

Spinal cord injury (SCI) is a devastating neurological condition where communication between the spinal cord and supraspinal centers are profoundly altered. To date, exogenous approaches used to restore severed connections have had very limited success[233]. It appears as though the injured central nervous system has a poor regenerative capacity[234,235]. Therefore, there has been a push to explore for endogenous approaches to enhance functional recovery, primarily through spared pathways that could serve as potential neural substrates for functional recovery[236].

Since the 1960's and 1970's, scientists have suggested that the propriospinal system could play an important role in functional recovery after SCI[237,238]. Propriospinal neurons, a term which loosely describes any neuron whose cell body and terminal field reside entirely within the spinal cord, are an ideal candidate system to promote functional recovery due to their sheer number, location, inter-segmental projection patterns, as well as their ability to activate and coordinate the locomotor circuitry[236]. Both the L2-L5 interneurons and ascending inter-enlargement neurons studied here are propriospinals.

Particular interest has been focused on the long propriospinal systems as the axons of these pathways reside in the lateral most quadrants of the white

matter, an area often spared following contusive spinal cord injury[239]. Indeed, Stelzner and colleagues have shown through a series of anatomical tract tracing experiments that long descending propriospinal neurons survive post-SCI[240,241]. We also found that the axons LAPNs were spared following a mid-thoracic contusive injury (unpublished data, Figure 47), an anatomical finding substantiated by previous work done in our lab that illustrates these ascending projections remain functional as assessed by electrophysiological interrogations (described in "LAPNs and locomotor recovery following SCI")[242]. While both inter-enlargement systems appear to be spared following SCI, the significant majority of studies have focused on the long descending projections, in part due to the landmark paper described below.

In 2004, Bareyre and colleagues showed that spared long descending propriospinal neurons are involved in the formation of *de novo* circuits that facilitate transmission caudal to spinal lesions[243]. Following a thoracic hemisection, severed corticospinal tract axons formed new synapses onto resident long descending propriospinals. These neurons, whose axons were spared, bypassed the lesion and synapsed onto motor neurons. Moreover, any synapses that formed onto propriospinal neurons which did not span the lesion were ultimately lost, suggesting that these *de novo* bridges are maintained through an activity-dependent mechanism. Courtine *et al* extended these results, showing that locomotor recovery could occur if rostrocaudal staggered spinal lesions occurred at temporally-distinct times, but not when the lesions were simultaneous[244]. This

suggests that the propriospinal neurons within the intervening segments of the staggered hemisections can undergo functional plasticity to facilitate locomotor recovery, but only if given the time to do so. Together, these studies illustrate that the propriospinal circuitry is an effective substrate for functional recovery, but in an activity- and time-dependent fashion. This leads us to our next question: what role(s) could L2-L5 interneurons and LAPNs play in functional recovery following spinal cord injury?

### *L2-L5 interneurons and locomotor recovery following SCI*

Nearly 90% of all clinical cases of spinal cord injury occur above the level of the lumbar segments (National Spinal Cord Injury Statistical Center, the University of Alabama at Birmingham). Therefore, it is likely that the "human equivalent" of this pathway is spared in most patients. In animal models where the lumbar spinal cord is functionally isolated from the rest of the nervous system (complete thoracic transection), weight-supported hindlimb stepping can be re-gained following intensive treadmill training[245-247]. Therefore, the lumbar circuitry has the intrinsic capacity to be retrained through activity-based therapies. We speculate that L2-L5 interneurons are likely a key pathway involved in the recovery of hindlimb stepping following SCI.

### *LAPNs and locomotor recovery following SCI*

We have shown that the axons of this long projection pathway reside in the lateral most quadrants of the white matter funiculi[123], an area that is often preserved following contusive SCI (Figure 47). As such, LAPN axons are likely

intact (Figure 47). Previous studies performed in our laboratory as well as others support this hypothesis. Using an electrophysiological assessment (magnetically-evoked inter-enlargement response, MIER), bilateral EMG responses in the triceps muscles could be detected following stimulation of hip afferents post-SCI[242,248]. Therefore, not only are LAPNs likely spared anatomically, but also functionally. Altogether, these studies suggest that LAPNs likely pose as a neural substrate capable of facilitating functional recovery following SCI.

It is clear from our silencing experiments that LAPNs are a key regulator in coordinating the actions of all four limbs. While the coordination of “all four limbs” is not critical for effective stepping in non-disabled populations (as they have the capacity to offset any torsional effects), it could play a profound role in patients whose balance and posture are severely impaired[249]. Indeed, studies have shown that active incorporation of arm swing during treadmill training actually enhances the muscle activity in the legs[250,251].

The intrinsic capacity for functional recovery after spinal cord is thought to be possible through the engagement of the central pattern generating circuitry[252,253]. Here, we have identified two key pathways within that circuitry that profoundly influence interlimb coordination and are anatomically positioned to be spared in the significant majority of clinical SCI cases. As such, these L2 projection pathways likely represent key substrates for recovery. Ongoing studies are directly testing this hypothesis. We believe that with the $Tet^{On}$ silencing system used here, we can now systematically identify the key neural substrates of functional recovery.

With this knowledge, activity-based therapies can be designed to engage these substrates not just for improving locomotion, but also quality of life.

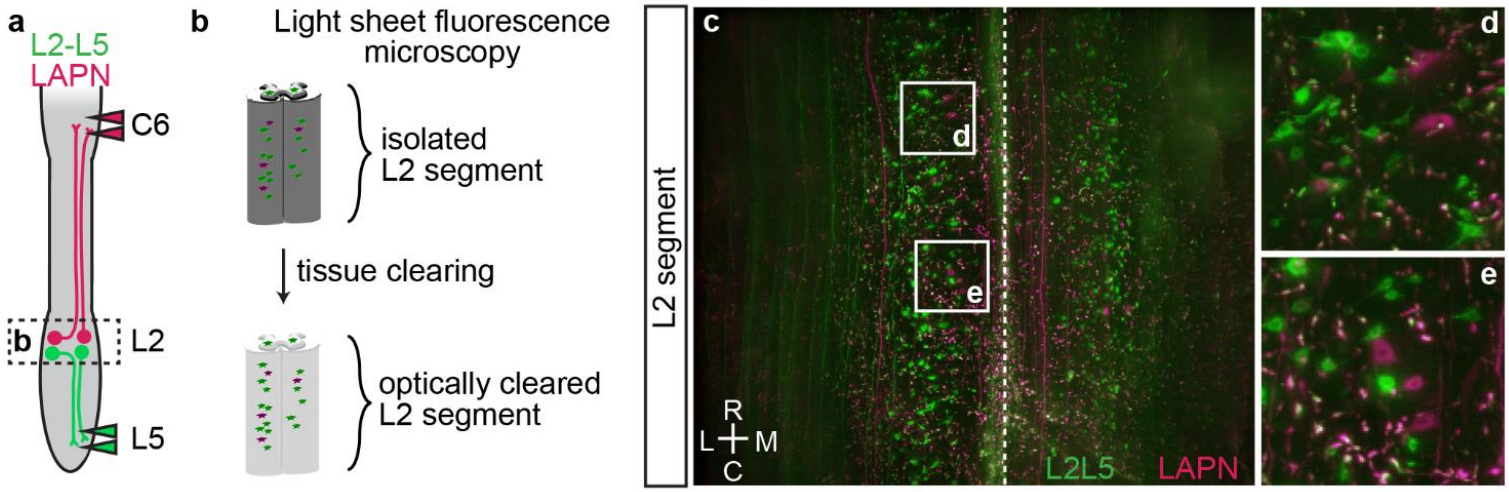


**Figure 33. L2-L5 interneurons and LAPNs are anatomically-distinct pathways that distribute left-right patterning information.**

(**a**) Retrograde tracer labelling of L2-L5 interneurons (green) and LAPNs (magenta) followed by (**b**) light sheet fluorescence microscopy reveals that (**c**) both pathways have cell bodies at L2 that are intermingled with one another, but anatomically distinct.

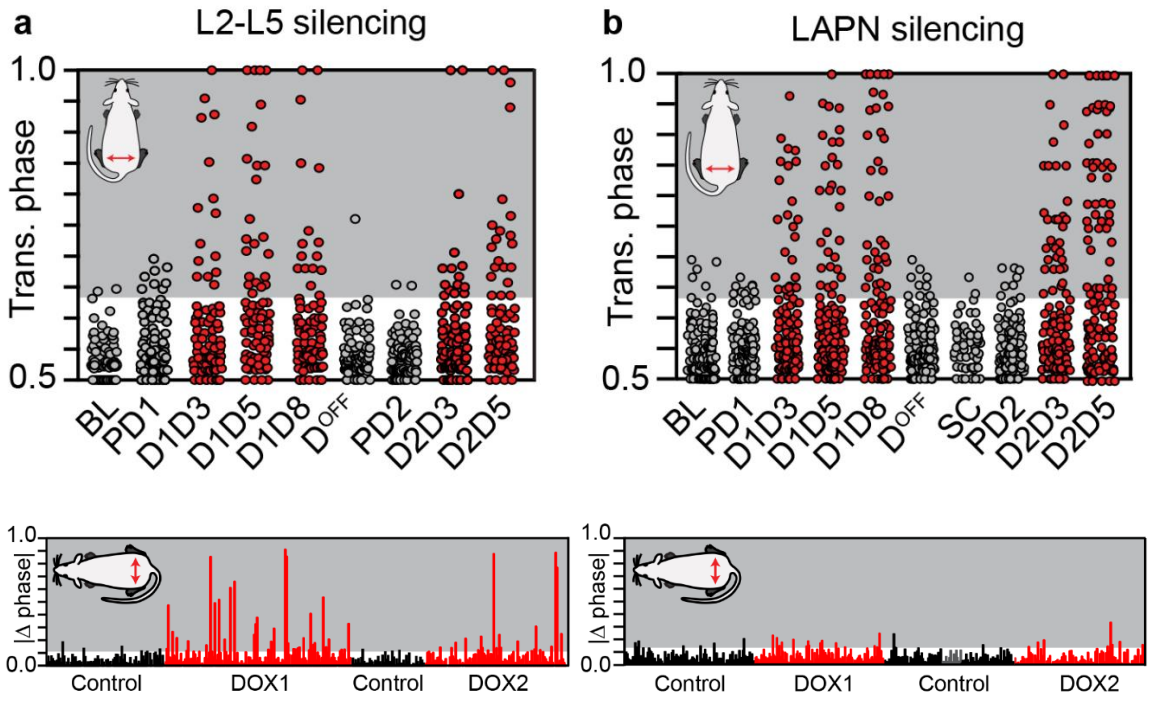


**<u>Figure 34</u>. Comparing the functional consequences of silencing L2-L5 interneurons versus LAPNs in left-right hindlimb coordination.**

Comparison of changes in left-right hindlimb coordination observed during (**a**) L2-L5 silencing and (**b**) LAPN silencing with per-step changes in coordination shown below.

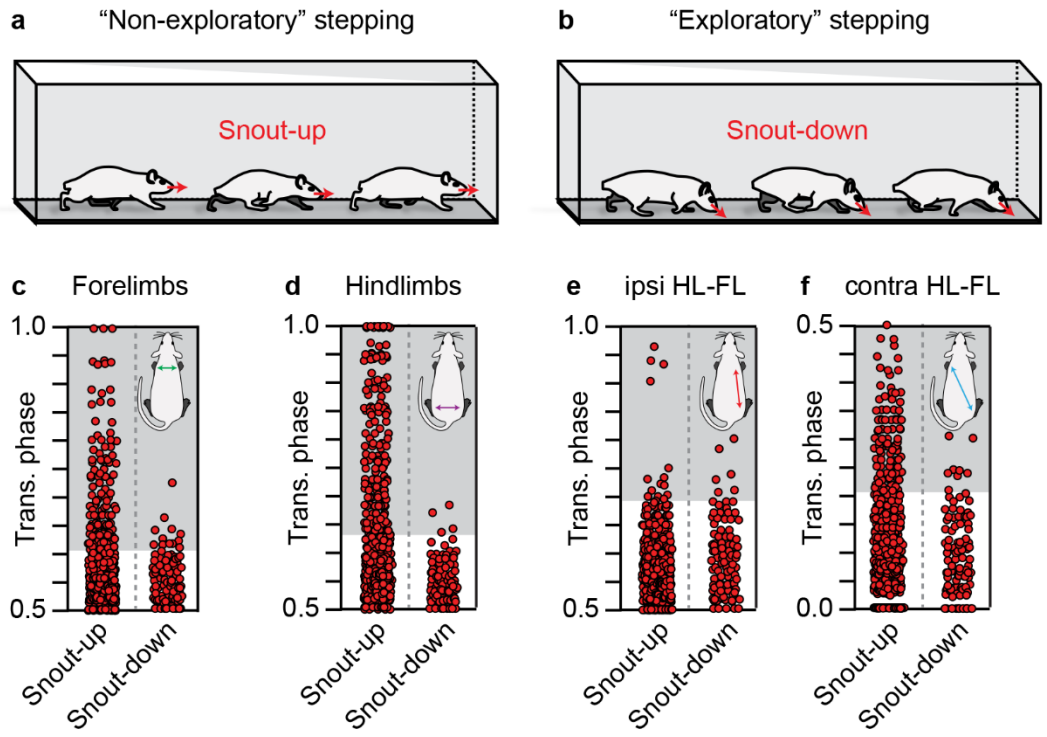


**Figure 35. Silencing LAPNs disrupts interlimb coordination during select “modes” of stepping.**

(**a**) “Non-exploratory stepping” is defined as the animal stepping with its “snout up.” (**b**) Alternatively, “exploratory stepping” is defined as stepping where the animal’s snout is pointed downwards (“snout-down”). During non-exploratory stepping, silencing LAPNs disrupts (**c**) left-right forelimb, (**d**) left-right hindlimb, and (**f**) contralateral hindlimb-forelimb coordination during locomotion. (**e**) Ipsilateral hindlimb-forelimb coordination was not affected by silencing.

*Figure 36*

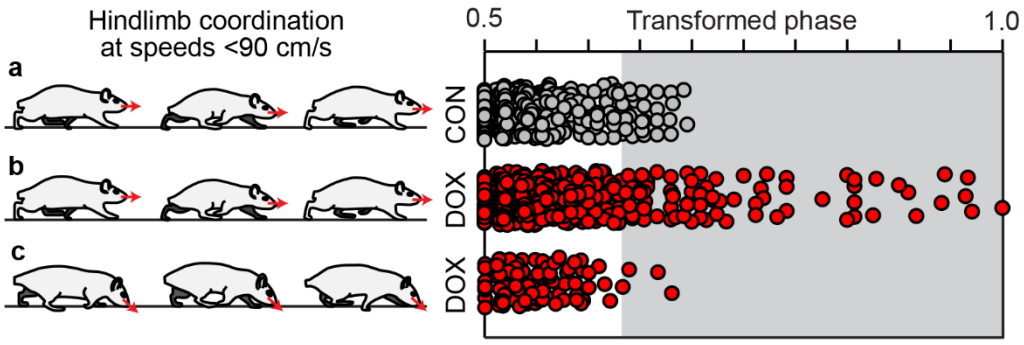


**Figure 36. At speeds less than 90 cm/s, the silencing-induced effects on hindlimb coordination are still modulated by the apparent stepping mode.** Steps that occurred under 90 cm/s were analyzed for changes in interlimb coordination during (**a**) Control non-exploratory stepping, (**b**) $DOX^{ON}$ non-exploratory stepping, and (**c**) $DOX^{ON}$ exploratory stepping. Even after taking into account the speeds at which the animals stepped, the apparent stepping mode appears to still modulate the silencing effects.

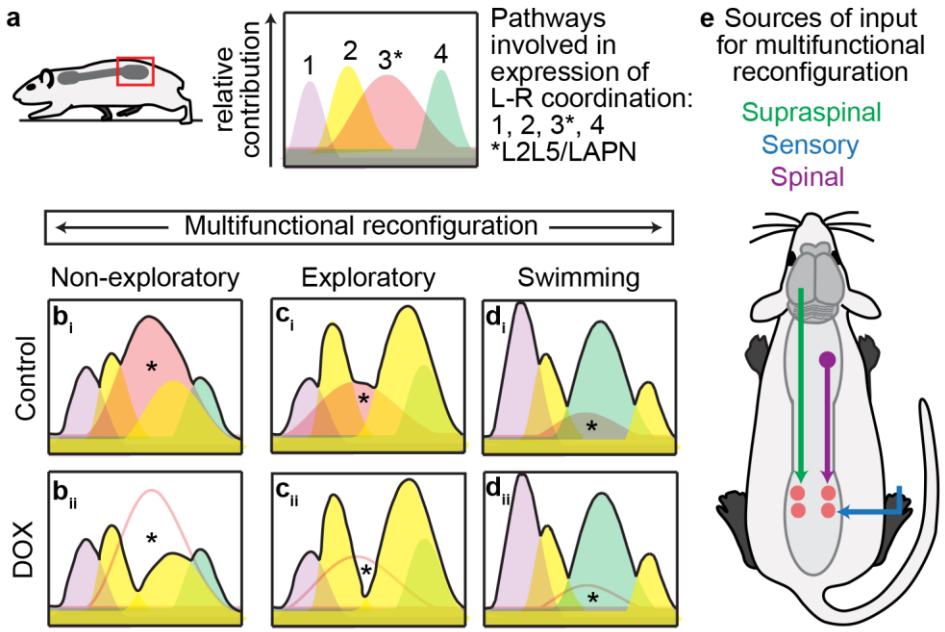


**Figure 37. Schematic illustrating the principles behind a multifunctional reconfiguration of the central pattern generating circuitry.**

Within the lumbar CPG (**a**), a collection of various neural pathways are likely involved in the expression of a particular behavior (e.g. left-right alternation). Here, each color represents a different pathway with red denoting the L2-L5 interneurons and LAPNs. The vertical scale denotes the perceived relative contribution or "functional importance" of each pathway to effect its physiological role during select behavioral contexts. (**b-d**) Multifunctional reorganization of the lumbar CPG in three behavioral contexts: directed/non-exploratory stepping (**b**), exploratory stepping (**c**), and swimming (**d**). The black traces denote the overall "functional landscape," which is determined by the physiological demand of the various color-coded pathways. During non-exploratory, directed stepping at Control time points

(**b**$_{i}$), the L2-L5 interneurons and LAPNs are key contributors to controlling left-right alternation (asterisk, high red peak). As such, during DOX$^{ON}$ silencing (**b**$_{ii}$), the functional loss of these pathways profoundly changes the “functional landscape” leading to significant disruptions to interlimb coordination. During exploratory stepping (**c**$_{i}$), the functional demand for L2-L5 interneurons and LAPNs is minor (asterisk, moderate peak). Therefore, during silencing (**c**$_{ii}$), the functional loss of these pathways does not profoundly change the functional landscape as the key pathways that secure left-right coordination in this task are intact (yellow pathways). (**d**) During swimming, the involvement of L2-L5 interneurons and LAPNs could be negligible (asterisk, small peak). Therefore, their functional loss during silencing (**d**$_{ii}$) does not affect left-right coordination as other pathways are the primary facilitators for hindlimb alternation (purple, blue pathways). Ultimately, we do not suggest that the neural pathways that participate in the expression of the various behaviors (directed versus exploratory stepping, swimming) are mutually exclusive from one another. (**e**) Moreover, we propose that the perceived multifunctional reconfiguration likely reflects the modulatory effects derived from supraspinal, spinal, and sensory sources.

*Figure 38*

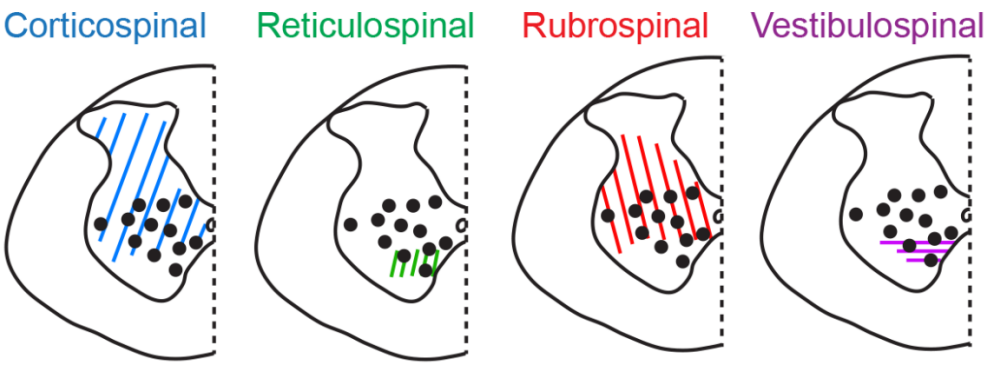


**Figure 38. L2-L5 and LAPN cell bodies reside within laminae that receive direct supraspinal innervation.**

Schematics illustrating the documented terminal innervation zones from supraspinal centers throughout the lumbar gray matter[175]. Black circles denote location of L2-L5 and LAPN cell bodies. Overlaying the location of these cell bodies onto the terminal field map suggests that L2-L5 and/or LAPNs are positioned to potentially receive direct supraspinal input.

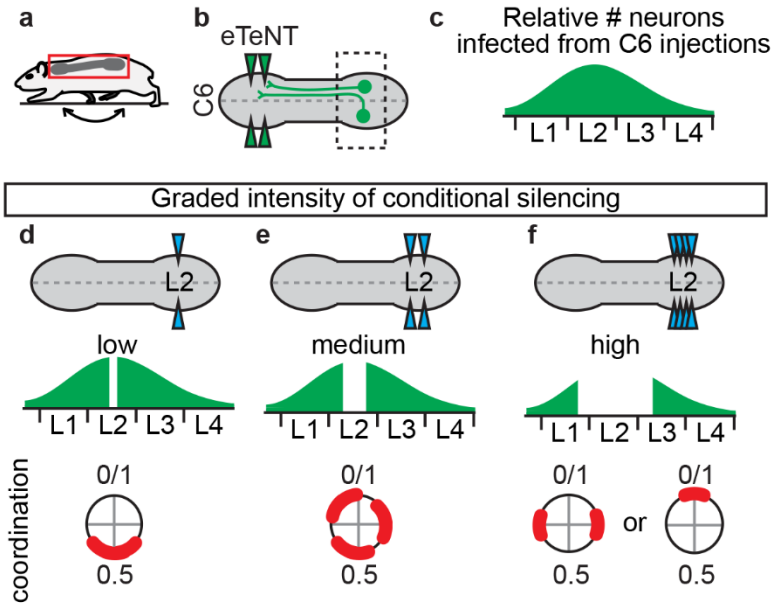


**<u>Figure 39</u>. Experimental design to gate the relative "penetrance" of L2 spinal neuron silencing in order to determine its role in the expression of the left-right coordination continuum.**

(**a**) Example experiments designed for silencing LAPNs. (**b**) The C6 lenti-eTeNT injections will be identical across all groups, thereby infecting a similar proportion of LAPNs throughout the lumbar cord (**c**). This distribution of lent- eTeNT infected LAPNs will be differentially targeted for double-infection with AAV2-rtTAV16 (low, medium, high double-infection groups). (**d**) Low silencing effects group as defined by one set of AAV2-rtTAV16 injections (top panel) to double infect a smaller portion of the pathway (middle panel). The anticipated results would be very mild perturbations to left-right coordination (bottom panel, increased variability about 0.5, which denotes alternation). (**e**) Medium silencing effects group, which is defined by two sets of injections at L2 (top panel) to doubly-infect "half" of the L2

projection pathways (middle panel). If half of the pathway is silenced, then this could yield differential coupling patterns (bottom panel). (f) High silencing effects group, which is defined by multiple (3-4) sets of injections throughout rostrocaudal L2 (top panel) to double infect all L2 projection pathways (middle panel). If the coupling continuum observed is due to a differential “knockout” of L2 pathways, then the “high” effects group should not show a continuum. Instead, the limbs would “switch” or “default” to other coupling patterns (bottom panel).

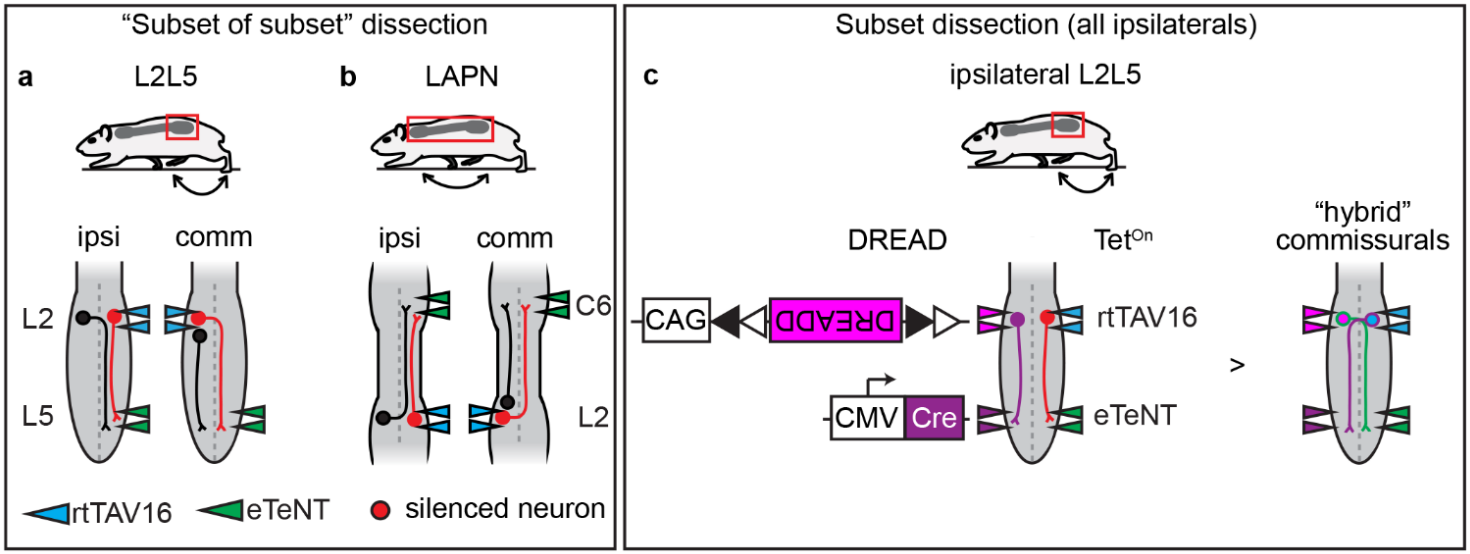




**Figure 40. Experimental design to determine the functional role(s) of ipsilateral versus commissural L2 projection pathways.**

Unilateral injections of eTeNT and rtTAV16 will double infect only one subset of ipsilateral L2-L5 interneurons (**a**, left panel, red projection) or LAPNs (**b**, left panel, red). Similarly, only one subset of commissural projections can be targeted (**a,b**, right panels, red projections). To study the effects of functionally removing all ipsilateral projections, a combinatorial approach is required (**c**, left panel, e.g. DREADDs with $Tet^{On}$). A consequence of combining two techniques are "hybrid" neurons that will be infected with both viral systems (**c**, right panel).

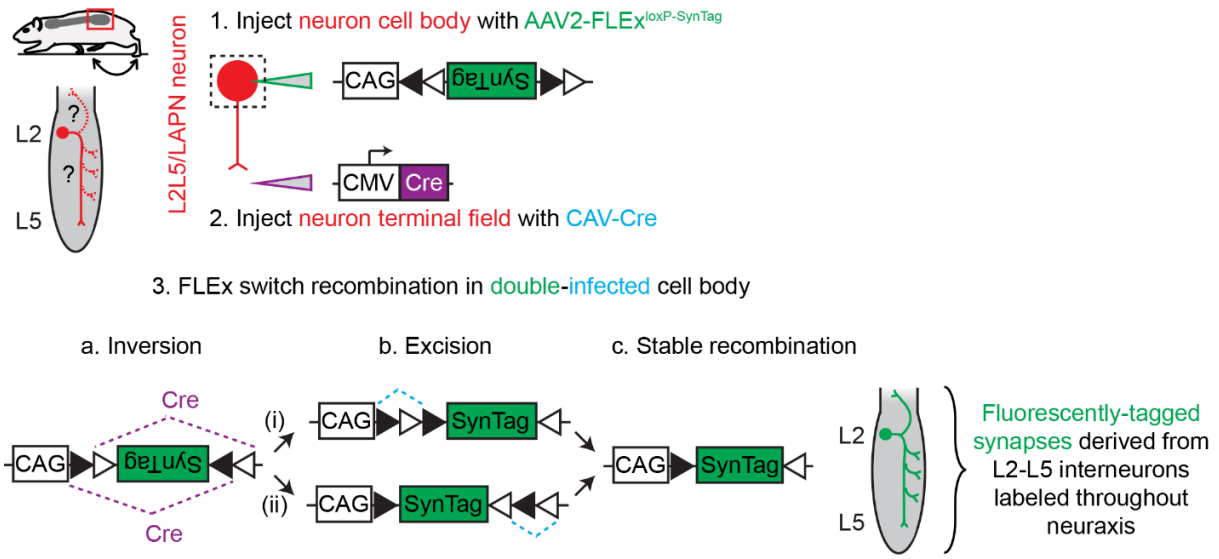


**Figure 41. Dual virus approach to detect LAPN or L2L5 (shown) synapses throughout the neuraxis.**

**Simplified workflow:** To detect the projection profile, we will double infect L2-L5 interneurons with two constructs. (**1**) A synapse-labeling (GFP) construct is injected into the cell bodies. Synapses cannot be labeled until the construct is "activated" by Cre-recombinase (inverted "SynTag"). (**2**) A second construct that expresses Cre-recombinase is delivered at the terminal field. Cre-recombinase is retrogradely transported to the cell body. In the now double infected neurons, Cre activates the synapse-labeling construct (**3**, FLEx activation). Synaptic projections derived from this double infected neuron will now express GFP (right panel). **Detailed workflow:** (**1**) First, at the level of the

cell bodies, the AAV2-FLEx$^{loxP\text{-}SynTag}$ construct is injected (green). “SynTag” is a synaptophysin-GFP fusion protein that will be expressed following recombination. (**2**) Next, at the level of the terminal field the second construct is injected: Cav-Cre (purple). “Cav” is a canine adenovirus (serotype 2) that is designed for terminal uptake. (**3**) In doubly-infected neurons, FLEx switch recombination occurs (two part system consisting of inversion [**3a**] followed by excision [**3b**] for stable recombination [**3c**]; black and white triangles denote orthogonal recombination sites, loxP and lox2272)[254]. The justification for FLEx-mediated inversion and excision is as follows[255]. “Typical” DNA inversion is based on site-specific recombination between antiparallel oriented loxP sites. However, inversion can be unstable, causing a mixture of forward and reverse configurations thereby reducing transgene expression. In FLEx switch recombination, two sets of heterotypic, antiparallel loxP-type recombination sties undergo inversion of the coding sequence (**3a** to **3b**). Following coding sequence inversion, the two sets of antiparallel loxP sites undergo excision (**3b**-**3c**). The end result will produce orthogonal recombination sites that are in opposite orientation, preventing further recombination (**3c**, black and white triangles). Constructs adapted from Atasoy *et al* 2008.

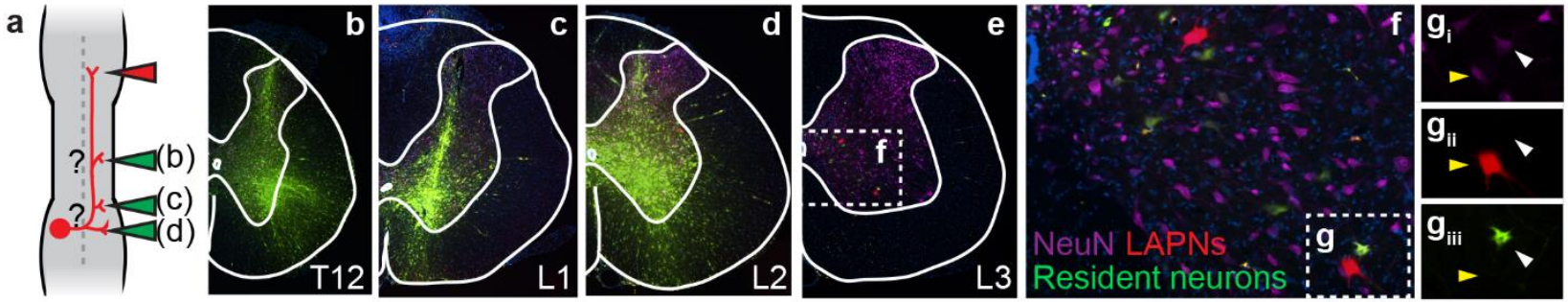


**Figure 42. LAPNs appear to lack lumbar as well as thoracic projections in the spinal cord.**

(**a**) Preliminary data shown from retrograde labeling of LAPNs (FluoroRuby) followed by injections at (**b**) T12, (**c**) L1, or (**d**) L2 with a second tracer (FluoroEmerald). Double labeling would indicate that LAPNs had local or thoracic projections in addition to the cervical. (**e**) Representative image highlighting the salient finding from all double-tracing experiments. No double-labeled LAPNs were detected. Panels (**f,g**) are close-up of (**e**). Yellow triangles emphasize that LAPNs do not co-localize with white arrows (green=resident neurons following L1 injection).

*Figure 43*

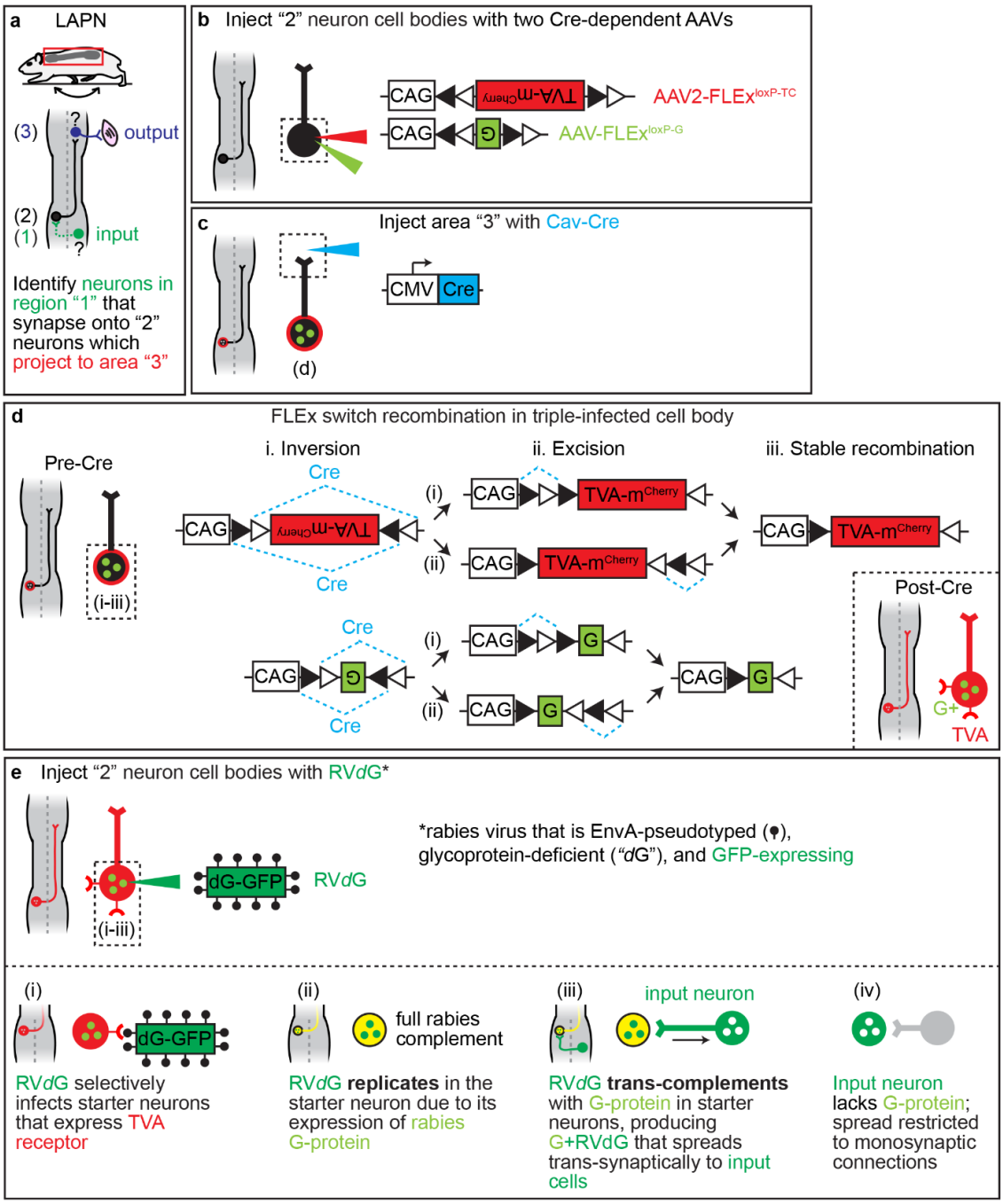


**Figure 43. Experimental design to map the input-output microcircuit architecture of the LAPNs.**

**Simplified workflow:** The goal is to detect the input neurons (**a**, green, “input”) onto LAPN neurons (**a**, black) and what neurons LAPNs synapse onto (**a**, purple, “output”). (**b**) First, LAPNs must be double-infected with two constructs (both inactive until Cre is delivered). After Cre, one construct will produce TVA (avian viral receptor that is conjugated to mCherry fluorophore, red). The second will produce glyco-protein (“G” protein needed for monosynaptic spread of rabies to label input neurons, green). (**c**) At terminal field, Cre is delivered. (**d**) In triple-infected LAPNs, Cre activates TVA and G protein expression. TVA receptor is now expressed on LAPN cell surface. G protein expressed in cell body (lower panel, “Post-Cre”). (**e**) Modified rabies is injected into triple-infected LAPN. Modified rabies does not express G-protein (cannot spread like “traditional rabies”). Modified rabies is also coated with protein that binds specifically to TVA receptor (envelope protein A; EnvA). (**$e_i$**) Only LAPNs with TVA receptor bind to and pick up modified rabies (TVA-EnvA binding). (**$e_{ii}$**) LAPN is now infected “fully complemented” rabies. The G protein (green circles) that LAPN expresses (from steps **b-d**) complements the G-deleted rabies virus. (**$e_{iii}$**) “Complemented rabies” trans-synaptically spreads, labeling input neurons. (**$e_{iv}$**) Input neuron does not express G-protein (empty circles). G-deleted rabies cannot spread further (mono-synaptic restriction). **End result:** LAPNs will be yellow (TVA-mCherry/rabies-GFP). Input neurons onto LAPNs will be green (rabies-GFP). Target (output) neurons of LAPN projections will have yellow synapses. For **detailed workflow**, refer to FLEx recombination description in Figure 41 legend.

*Figure 44*

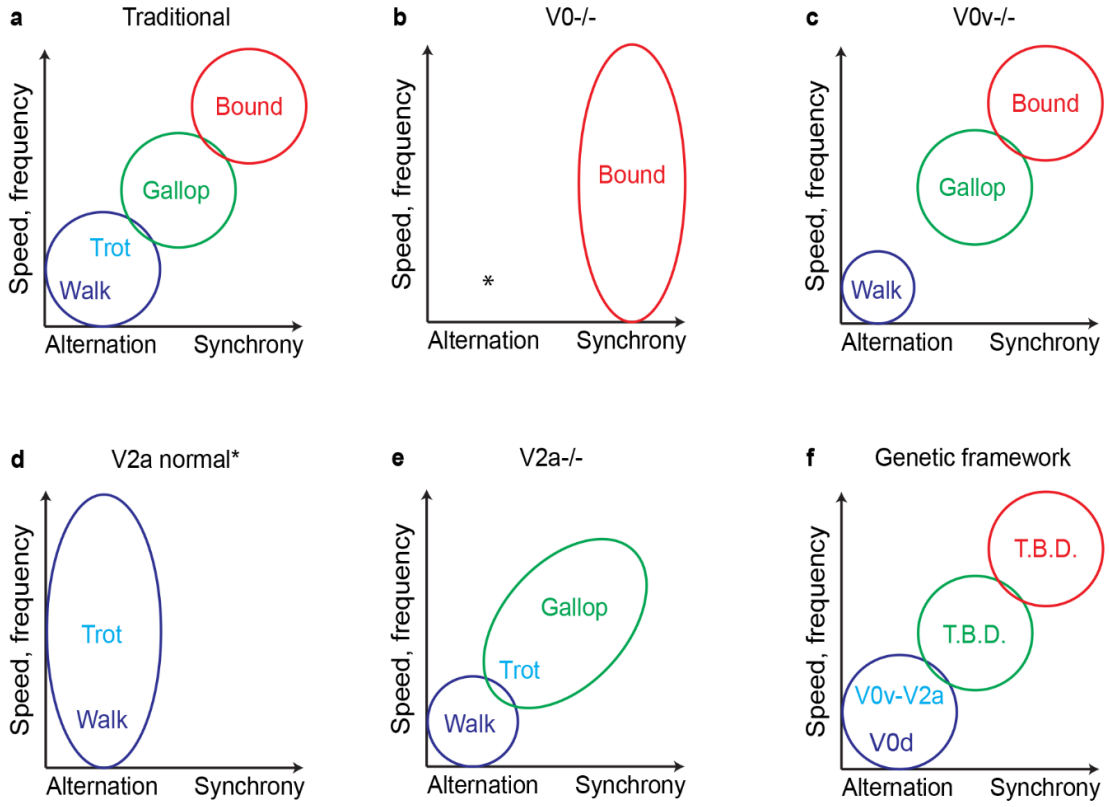


**<u>Figure 44</u>. Simplified schematics illustrating the salient findings from genetic-based dissection of alternation networks.**

(**a**) A conceptual framework for the association between increasing speed/step frequency, interlimb coupling patterns expressed, and the locomotor gaits that are described by these patterns. (**b**) The deletion of excitatory and inhibitory V0 interneurons results in left-right synchrony across all speeds and step frequencies. Bouts of alternation (*) are still observed[68]. (**c**) Deleting the excitatory V0 interneurons alone abolishes the trot gait while preserving walk, gallop, and bound[17]. (**d**) In the V2a wild-type mice, only the walk and trot gaits are normally expressed across all speeds and frequencies[67]. (**e**) The conditional deletion of V2a

interneurons caused the limbs to adopt gallop-like coupling patterns at increased speed[67]. (**f**) Schematic illustrating the modular organization hypothesis for the spinal circuitry that governs left-right alternation.

*Figure 45*

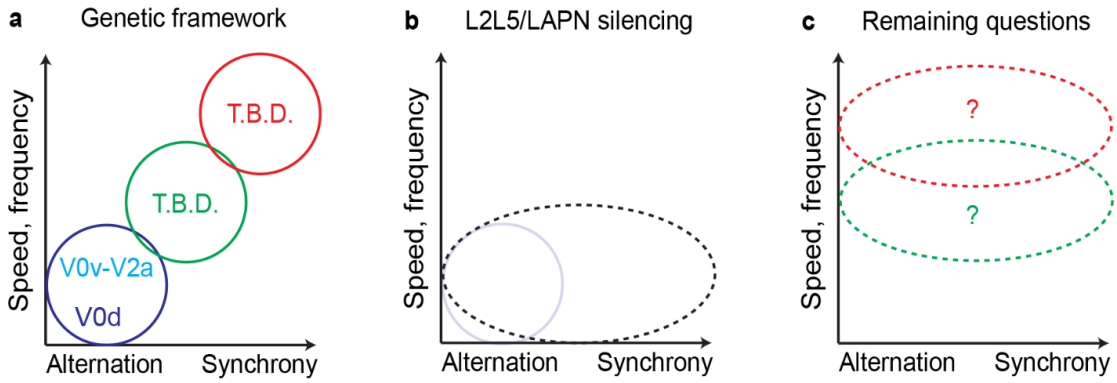


**Figure 45. Salient findings from spinal neuron silencing: a left-right coupling continuum.**

(**a**) Schematic illustrating the genetically-defined modular organization hypothesis. The V0 and V2a interneurons are recruited in a speed-dependent manner to secure the limbs in left-right alternation. (**b**) Visual representation of the salient findings from silencing L2 projection pathways. Here, the left-right limb pairs can express coupling patterns from alternation to synchrony independent of speed or frequency. (**c**) Whether or not such flexibility in left-right coupling occurs at increased speeds and frequencies (e.g., domains where gallop or bound are expressed) remains unknown.

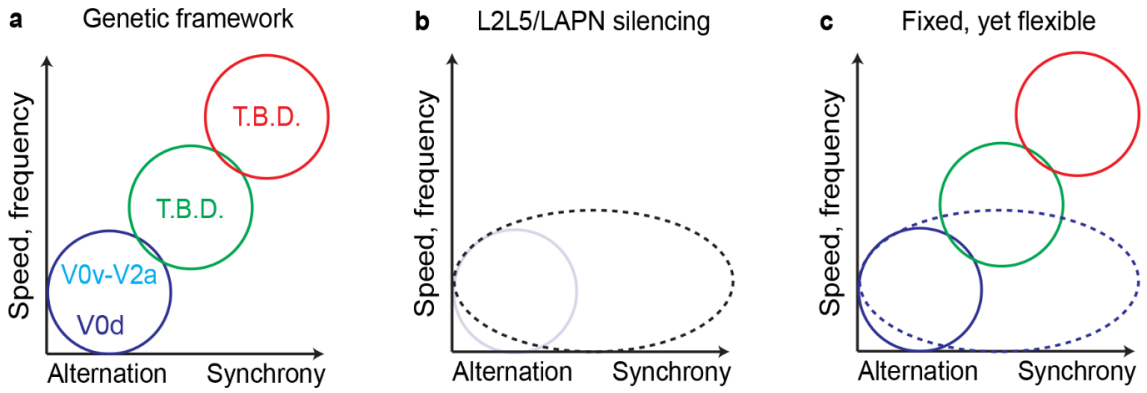


**Figure 46. Fixed, yet flexible organization of the left-right circuitry.**

(**a**) Modular organization hypothesis for left-right coordination as defined by genetic studies. (**b**) Flexible, left-right coordination continuum as revealed through reversible silencing of L2 spinal pathways. (**c**) Combined model to account for the fixed, yet flexible expression of interlimb coupling patterns with respect to speed and step frequency.

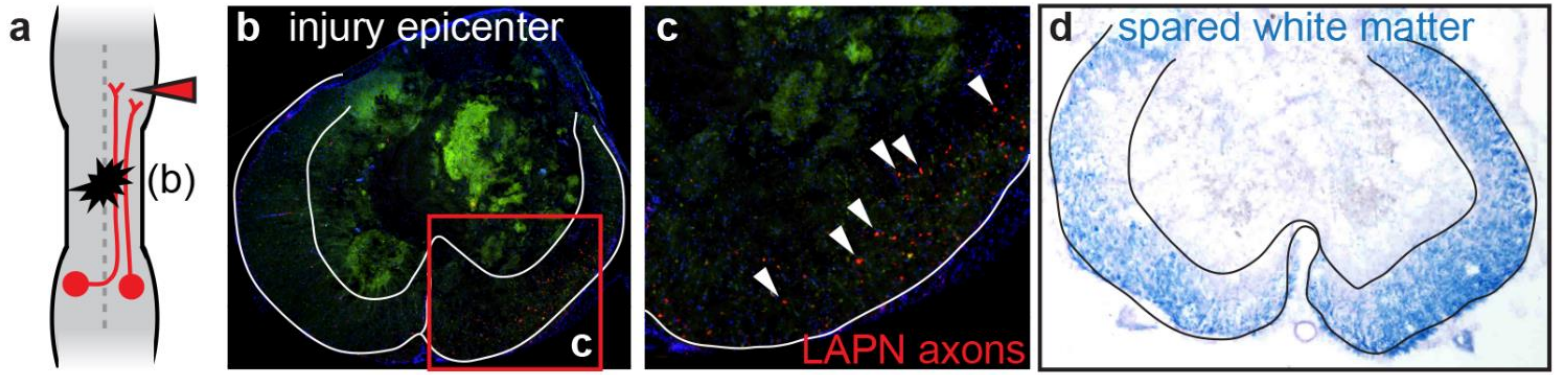


**Figure 47. Acute sparing of LAPN axons following a mid-thoracic spinal cord injury.**

(**a**) LAPNs were retrogradely labeled with FluoroRuby prior to a mild-moderate spinal cord injury at mid-thoracic levels (T9, 12.5 gcm contusion). (**b,c**) At the injury epicenter 7 days post-SCI, putatively spared LAPN axons can be detected in the ventrolateral white matter. (**d**) The lateral-most regions of the white matter funiculi are often spared chronically post-SCI, as shown by eriochrome cyanine staining for intact myelin (10 weeks post-injury).

REFERENCES


1 Muir, G. in *The Behavior of the Laboratory Rat : A Handbook with Tests* 2004-2009-2030 (Oxford University Press, 2004).

2 Cohen, A. H. & Gans, C. Muscle activity in rat locomotion: movement analysis and electromyography of the flexors and extensors of the elbow. *J Morphol* **146**, 177-196, doi:10.1002/jmor.1051460202 (1975).

3 Grillner, S. Locomotion in vertebrates: central mechanisms and reflex interaction. *Physiol Rev* **55**, 247-304 (1975).

4 Miller, S., Van Der Burg, J. & Van Der Meche, F. Coordination of movements of the kindlimbs and forelimbs in different forms of locomotion in normal and decerebrate cats. *Brain Res* **91**, 217-237 (1975).

5 Hildebrand, M. in *Neural Control of Locomotion* (ed S. Grillner R. M. Herman, P. S. G. Stein, and D. G. Stuart) (Plenum Press, 1976).

6 Dunbar, D. C., Badam, G. L., Hallgrimsson, B. & Vieilledent, S. Stabilization and mobility of the head and trunk in wild monkeys during terrestrial and flat-surface walks and gallops. *J Exp Biol* **207**, 1027-1042 (2004).

7 Grillner, S. Control of locomotion in bipeds, tetrapods, and fish. *Handbook of Physiology, The Nervous System, Motor Control* (1981).

8 Hildebrand, M. The Quadrupedal Gaits of Vertebrates: The timing of leg movements relates to balance, body shape, agility, speed, and energy expenditure. *BioScience* **39**, 766-775, doi:10.2307/1311182 (1989).

9 Koopmans, G. C. *et al.* Strain and locomotor speed affect over-ground locomotion in intact rats. *Physiol Behav* **92**, 993-1001, doi:10.1016/j.physbeh.2007.07.018 (2007).

10 Herbin, M., Gasc, J. P. & Renous, S. Symmetrical and asymmetrical gaits in the mouse: patterns to increase velocity. *J Comp Physiol A Neuroethol Sens Neural Behav Physiol* **190**, 895-906, doi:10.1007/s00359-004-0545-0 (2004).

11 Gorska, T., Bem, T., Majczynski, H. & Zmyslowski, W. Unrestrained walking in intact cats. *Brain Res Bull* **32**, 235-240 (1993).

12 Gorska, T., Zmyslowski, W. & Majczynski, H. Overground locomotion in intact rats: interlimb coordination, support patterns and support phases duration. *Acta neurobiologiae experimentalis* **59**, 131-144 (1999).

13 Gorska, T., Majczynski, H. & Zmyslowski, W. Overground locomotion in intact rats: contact electrode recording. *Acta neurobiologiae experimentalis* **58**, 227-237 (1998).

14 Herbin, M., Hackert, R., Gasc, J. P. & Renous, S. Gait parameters of treadmill versus overground locomotion in mouse. *Behav Brain Res* **181**, 173-179, doi:10.1016/j.bbr.2007.04.001 (2007).

15 Webb, A. A. & Muir, G. D. Unilateral dorsal column and rubrospinal tract injuries affect overground locomotion in the unrestrained rat. *Eur J Neurosci* **18**, 412-422 (2003).

16 Lemieux, M., Josset, N., Roussel, M., Couraud, S. & Bretzner, F. Speed-Dependent Modulation of the Locomotor Behavior in Adult Mice Reveals Attractor and Transitional Gaits. *Front Neurosci* **10**, 42, doi:10.3389/fnins.2016.00042 (2016).

17 Bellardita, C. & Kiehn, O. Phenotypic characterization of speed-associated gait changes in mice reveals modular organization of locomotor networks. *Curr Biol* **25**, 1426-1436, doi:10.1016/j.cub.2015.04.005 (2015).

18 Drew, T. & Marigold, D. S. Taking the next step: cortical contributions to the control of locomotion. *Curr Opin Neurobiol* **33**, 25-33, doi:10.1016/j.conb.2015.01.011 (2015).

19 Takakusaki, K. Neurophysiology of gait: from the spinal cord to the frontal lobe. *Mov Disord* **28**, 1483-1491, doi:10.1002/mds.25669 (2013).

20 Garcia-Rill, E. The basal ganglia and the locomotor regions. *Brain Res* **396**, 47-63 (1986).

21 Orlovskiĭ, G. N., Deliagina, T. G. & Grillner, S. *Neuronal Control of Locomotion: From Mollusc to Man*. (Oxford University Press, 1999).

22 S Grillner, a. & Wallen, P. Central Pattern Generators for Locomotion, with Special Reference to Vertebrates. *Annual Review of Neuroscience* **8**, 233-261, doi:doi:10.1146/annurev.ne.08.030185.001313 (1985).

23 Grillner, S. & Zangger, P. On the central generation of locomotion in the low spinal cat. *Exp Brain Res* **34**, 241-261 (1979).

24 Belanger, M., Drew, T. & Rossignol, S. Spinal locomotion: a comparison of the kinematics and the electromyographic activity in the same animal before and after spinalization. *Acta biologica Hungarica* **39**, 151-154 (1988).

25 Kiehn, O. Locomotor circuits in the mammalian spinal cord. *Annu Rev Neurosci* **29**, 279-306, doi:10.1146/annurev.neuro.29.051605.112910 (2006).

26 Brown, T. G. On the nature of the fundamental activity of the nervous centres; together with an analysis of the conditioning of rhythmic activity in progression, and a theory of the evolution of function in the nervous system. *J Physiol*, 18-46 (1914).

27 Muir, G. D. & Whishaw, I. Q. Complete locomotor recovery following corticospinal tract lesions: measurement of ground reaction forces during overground locomotion in rats. *Behavioural Brain Research* **103**, 45-53, doi:http://dx.doi.org/10.1016/S0166-4328(99)00018-2 (1999).

28 Demes, B. *et al.* The kinetics of primate quadrupedalism: "hindlimb drive" reconsidered. *Journal of Human Evolution* **26**, 353-374, doi:http://dx.doi.org/10.1006/jhev.1994.1023 (1994).

29 Snyder, R. C. The anatomy and function of the pelvic girdle and hindlimb in lizard locomotion. *American Journal of Anatomy* **95**, 1-45, doi:10.1002/aja.1000950102 (1954).

30 Raineteau, O. & Schwab, M. E. Plasticity of motor systems after incomplete spinal cord injury. *Nat Rev Neurosci* **2**, 263-273 (2001).

31 Bonnot, A. & Morin, D. Hemisegmental localisation of rhythmic networks in the lumbosacral spinal cord of neonate mouse. *Brain Res* **793**, 136-148 (1998).

32 Bonnot, A., Whelan, P. J., Mentis, G. Z. & O'Donovan, M. J. Locomotor-like activity generated by the neonatal mouse spinal cord. *Brain Res Brain Res Rev* **40**, 141-151 (2002).

33 Bracci, E., Ballerini, L. & Nistri, A. Localization of rhythmogenic networks responsible for spontaneous bursts induced by strychnine and bicuculline in the rat isolated spinal cord. *J Neurosci* **16**, 7063-7076 (1996).

34 Christie, K. J. & Whelan, P. J. Monoaminergic establishment of rostrocaudal gradients of rhythmicity in the neonatal mouse spinal cord. *J Neurophysiol* **94**, 1554-1564, doi:10.1152/jn.00299.2005 (2005).

35 Cowley, K. C. & Schmidt, B. J. Regional distribution of the locomotor pattern-generating network in the neonatal rat spinal cord. *J Neurophysiol* **77**, 247-259 (1997).

36 Gabbay, H., Delvolve, I. & Lev-Tov, A. Pattern generation in caudal-lumbar and sacrococcygeal segments of the neonatal rat spinal cord. *J Neurophysiol* **88**, 732-739 (2002).

37 Kjaerulff, O. & Kiehn, O. Distribution of networks generating and coordinating locomotor activity in the neonatal rat spinal cord in vitro: a lesion study. *J Neurosci* **16**, 5777-5794 (1996).

38 Kremer, E. & Lev-Tov, A. Localization of the spinal network associated with generation of hindlimb locomotion in the neonatal rat and organization of its transverse coupling system. *J Neurophysiol* **77**, 1155-1170 (1997).

39 Kudo, N. & Yamada, T. N-methyl-D,L-aspartate-induced locomotor activity in a spinal cord-hindlimb muscles preparation of the newborn rat studied in vitro. *Neurosci Lett* **75**, 43-48 (1987).

40 Cina, C. & Hochman, S. Diffuse distribution of sulforhodamine-labeled neurons during serotonin-evoked locomotion in the neonatal rat thoracolumbar spinal cord. *J Comp Neurol* **423**, 590-602 (2000).

41 Dai, X., Noga, B. R., Douglas, J. R. & Jordan, L. M. Localization of spinal neurons activated during locomotion using the c-fos immunohistochemical method. *J Neurophysiol* **93**, 3442-3452, doi:10.1152/jn.00578.2004 (2005).

42 Kjaerulff, O., Barajon, I. & Kiehn, O. Sulphorhodamine-labelled cells in the neonatal rat spinal cord following chemically induced locomotor activity in vitro. *J Physiol* **478 ( Pt 2)**, 265-273 (1994).

43 Tresch, M. C. & Kiehn, O. Coding of locomotor phase in populations of neurons in rostral and caudal segments of the neonatal rat lumbar spinal cord. *J Neurophysiol* **82**, 3563-3574 (1999).

44 Kato, M. Motoneuronal activity of cat lumbar spinal cord following separation from descending or contralateral impulses. *Cent Nerv Syst Trauma* **4**, 239-248 (1987).

45 Kjaerulff, O. & Kiehn, O. Crossed rhythmic synaptic input to motoneurons during selective activation of the contralateral spinal locomotor network. *J Neurosci* **17**, 9433-9447 (1997).

46 Beato, M. & Nistri, A. Interaction between disinhibited bursting and fictive locomotor patterns in the rat isolated spinal cord. *J Neurophysiol* **82**, 2029-2038 (1999).

47 Cazalets, J. R., Bertrand, S., Sqalli-Houssaini, Y. & Clarac, F. GABAergic control of spinal locomotor networks in the neonatal rat. *Ann N Y Acad Sci* **860**, 168-180 (1998).

48 Cowley, K. C. & Schmidt, B. J. Effects of inhibitory amino acid antagonists on reciprocal inhibitory interactions during rhythmic motor activity in the in vitro neonatal rat spinal cord. *J Neurophysiol* **74**, 1109-1117 (1995).

49 Jankowska, E., Edgley, S. A., Krutki, P. & Hammar, I. Functional differentiation and organization of feline midlumbar commissural interneurones. *J Physiol* **565**, 645-658, doi:10.1113/jphysiol.2005.083014 (2005).

50 Quinlan, K. A. & Kiehn, O. Segmental, synaptic actions of commissural interneurons in the mouse spinal cord. *J Neurosci* **27**, 6521-6530, doi:10.1523/jneurosci.1618-07.2007 (2007).

51 Bannatyne, B. A., Edgley, S. A., Hammar, I., Jankowska, E. & Maxwell, D. J. Networks of inhibitory and excitatory commissural interneurons mediating crossed reticulospinal actions. *Eur J Neurosci* **18**, 2273-2284 (2003).

52 Stokke, M. F., Nissen, U. V., Glover, J. C. & Kiehn, O. Projection patterns of commissural interneurons in the lumbar spinal cord of the neonatal rat. *J Comp Neurol* **446**, 349-359 (2002).

53 Nissen, U. V., Mochida, H. & Glover, J. C. Development of projection-specific interneurons and projection neurons in the embryonic mouse and rat spinal cord. *J Comp Neurol* **483**, 30-47, doi:10.1002/cne.20435 (2005).

54 Eide, A. L., Glover, J., Kjaerulff, O. & Kiehn, O. Characterization of commissural interneurons in the lumbar region of the neonatal rat spinal cord. *J Comp Neurol* **403**, 332-345 (1999).

55 Zhong, G., Diaz-Rios, M. & Harris-Warrick, R. M. Serotonin modulates the properties of ascending commissural interneurons in the neonatal mouse spinal cord. *J Neurophysiol* **95**, 1545-1555, doi:10.1152/jn.01103.2005 (2006).

56 Kiehn, O. & Butt, S. J. Physiological, anatomical and genetic identification of CPG neurons in the developing mammalian spinal cord. *Prog Neurobiol* **70**, 347-361 (2003).

57 Butt, S. J., Lebret, J. M. & Kiehn, O. Organization of left-right coordination in the mammalian locomotor network. *Brain Res Brain Res Rev* **40**, 107-117 (2002).

58 Butt, S. J., Harris-Warrick, R. M. & Kiehn, O. Firing properties of identified interneuron populations in the mammalian hindlimb central pattern generator. *J Neurosci* **22**, 9961-9971 (2002).

59 Butt, S. J. & Kiehn, O. Functional identification of interneurons responsible for left-right coordination of hindlimbs in mammals. *Neuron* **38**, 953-963 (2003).

60 Jessell, T. M. Neuronal specification in the spinal cord: inductive signals and transcriptional codes. *Nat Rev Genet* **1**, 20-29, doi:10.1038/35049541 (2000).

61 Kiehn, O. Decoding the organization of spinal circuits that control locomotion. *Nat Rev Neurosci* **17**, 224-238, doi:10.1038/nrn.2016.9 (2016).

62 Gosgnach, S. The role of genetically-defined interneurons in generating the mammalian locomotor rhythm. *Integr Comp Biol* **51**, 903-912, doi:10.1093/icb/icr022 (2011).

63 Dougherty, Kimberly J. *et al.* Locomotor Rhythm Generation Linked to the Output of Spinal Shox2 Excitatory Interneurons. *Neuron* **80**, 920-933, doi:http://dx.doi.org/10.1016/j.neuron.2013.08.015 (2013).

64 Zhang, J. *et al.* V1 and v2b interneurons secure the alternating flexor-extensor motor activity mice require for limbed locomotion. *Neuron* **82**, 138-150, doi:10.1016/j.neuron.2014.02.013 (2014).

65 Britz, O. *et al.* A genetically defined asymmetry underlies the inhibitory control of flexor-extensor locomotor movements. *Elife* **4**, doi:10.7554/eLife.04718 (2015).

66 Crone, S. A. *et al.* Genetic ablation of V2a ipsilateral interneurons disrupts left-right locomotor coordination in mammalian spinal cord. *Neuron* **60**, 70-83, doi:10.1016/j.neuron.2008.08.009 (2008).

67 Crone, S. A., Zhong, G., Harris-Warrick, R. & Sharma, K. In mice lacking V2a interneurons, gait depends on speed of locomotion. *J Neurosci* **29**, 7098-7109, doi:10.1523/JNEUROSCI.1206-09.2009 (2009).

68 Lanuza, G. M., Gosgnach, S., Pierani, A., Jessell, T. M. & Goulding, M. Genetic identification of spinal interneurons that coordinate left-right locomotor activity necessary for walking movements. *Neuron* **42**, 375-386 (2004).

69 Talpalar, A. E. *et al.* Dual-mode operation of neuronal networks involved in left-right alternation. *Nature* **500**, 85-88, doi:10.1038/nature12286 (2013).

70 Zhang, Y. *et al.* V3 spinal neurons establish a robust and balanced locomotor rhythm during walking. *Neuron* **60**, 84-96, doi:10.1016/j.neuron.2008.09.027 (2008).

71 Francius, C. *et al.* Identification of multiple subsets of ventral interneurons and differential distribution along the rostrocaudal axis of the developing spinal cord. *PLoS One* **8**, e70325, doi:10.1371/journal.pone.0070325 (2013).

72 Goulding, M. Circuits controlling vertebrate locomotion: moving in a new direction. *Nat Rev Neurosci* **10**, 507-518, doi:10.1038/nrn2608 (2009).

73 Zagoraiou, L. *et al.* A cluster of cholinergic premotor interneurons modulates mouse locomotor activity. *Neuron* **64**, 645-662, doi:10.1016/j.neuron.2009.10.017 (2009).

74 Shevtsova, N. A. *et al.* Organization of left-right coordination of neuronal activity in the mammalian spinal cord: Insights from computational modelling. *J Physiol* **593**, 2403-2426, doi:10.1113/JP270121 (2015).

75 Pierani, A. *et al.* Control of interneuron fate in the developing spinal cord by the progenitor homeodomain protein Dbx1. *Neuron* **29**, 367-384 (2001).

76 Callaway, E. M. A molecular and genetic arsenal for systems neuroscience. *Trends Neurosci* **28**, 196-201, doi:10.1016/j.tins.2005.01.007 (2005).

77 Borowska, J. *et al.* Functional subpopulations of V3 interneurons in the mature mouse spinal cord. *J Neurosci* **33**, 18553-18565, doi:10.1523/jneurosci.2005-13.2013 (2013).

78 Borowska, J., Jones, C. T., Deska-Gauthier, D. & Zhang, Y. V3 interneuron subpopulations in the mouse spinal cord undergo distinctive postnatal maturation processes. *Neuroscience* **295**, 221-228, doi:10.1016/j.neuroscience.2015.03.024 (2015).

79 Dunbar, D. C. Stabilization and mobility of the head and trunk in vervet monkeys (Cercopithecus aethiops) during treadmill walks and gallops. *J Exp Biol* **207**, 4427-4438, doi:10.1242/jeb.01282 (2004).

80 Kinoshita, M. *et al.* Genetic dissection of the circuit for hand dexterity in primates. *Nature* **487**, 235-238, doi:10.1038/nature11206 (2012).

81 Kato, S. *et al.* Neuron-specific gene transfer through retrograde transport of lentiviral vector pseudotyped with a novel type of fusion envelope glycoprotein. *Hum Gene Ther* **22**, 1511-1523, doi:10.1089/hum.2011.111 (2011).

82 Kato, S. *et al.* Selective neural pathway targeting reveals key roles of thalamostriatal projection in the control of visual discrimination. *J Neurosci* **31**, 17169-17179, doi:10.1523/JNEUROSCI.4005-11.2011 (2011).

83 Kato, S. *et al.* A lentiviral strategy for highly efficient retrograde gene transfer by pseudotyping with fusion envelope glycoprotein. *Hum Gene Ther* **22**, 197-206, doi:10.1089/hum.2009.179 (2011).

84 Zhou, X., Vink, M., Klaver, B., Berkhout, B. & Das, A. T. Optimization of the Tet-On system for regulated gene expression through viral evolution. *Gene Ther* **13**, 1382-1390, doi:10.1038/sj.gt.3302780 (2006).

85 Yamamoto, M. *et al.* Reversible suppression of glutamatergic neurotransmission of cerebellar granule cells in vivo by genetically manipulated expression of tetanus neurotoxin light chain. *J Neurosci* **23**, 6759-6767 (2003).

86 Gossard, J. P. *et al.* Chapter 2--the spinal generation of phases and cycle duration. *Prog Brain Res* **188**, 15-29, doi:10.1016/B978-0-444-53825-3.00007-3 (2011).

87 Hildebrand, M. Symmetrical gaits of horses. *Science* **150**, 701-708 (1965).

88 Fouad, K., Fischer, H. & Büschges, A. in *Handbook of Psychology* (John Wiley & Sons, Inc., 2003).

89 Abdellatif, A. A. *et al.* Gene delivery to the spinal cord: comparison between lentiviral, adenoviral, and retroviral vector delivery systems. *J Neurosci Res* **84**, 553-567, doi:10.1002/jnr.20968 (2006).

90 Sommer, J. M. *et al.* Quantification of adeno-associated virus particles and empty capsids by optical density measurement. *Mol Ther* **7**, 122-128 (2003).

91 Reed, W. R., Shum-Siu, A., Whelan, A., Onifer, S. M. & Magnuson, D. S. Anterograde labeling of ventrolateral funiculus pathways with spinal enlargement connections in the adult rat spinal cord. *Brain Res* **1302**, 76-84, doi:10.1016/j.brainres.2009.09.049 (2009).

92 Kuerzi, J. *et al.* Task-specificity vs. ceiling effect: step-training in shallow water after spinal cord injury. *Exp Neurol* **224**, 178-187, doi:10.1016/j.expneurol.2010.03.008 (2010).

93 Magnuson, D. S. K. *et al.* Swimming as a Model of Task-Specific Locomotor Retraining After Spinal Cord Injury in the Rat. *Neurorehabilitation and neural repair* **23**, 535-545, doi:10.1177/1545968308331147 (2009).

94 Muir, G. D. & Whishaw, I. Q. Ground reaction forces in locomoting hemi-parkinsonian rats: a definitive test for impairments and compensations. *Exp Brain Res* **126**, 307-314 (1999).

95 Muir, G. D. & Whishaw, I. Q. Red nucleus lesions impair overground locomotion in rats: a kinetic analysis. *Eur J Neurosci* **12**, 1113-1122 (2000).

96 Webb, A. A., Gowribai, K. & Muir, G. D. Fischer (F-344) rats have different morphology, sensorimotor and locomotor abilities compared to Lewis, Long-Evans, Sprague-Dawley and Wistar rats. *Behav Brain Res* **144**, 143-156 (2003).

97 Webb, A. A. & Muir, G. D. Compensatory locomotor adjustments of rats with cervical or thoracic spinal cord hemisections. *J Neurotrauma* **19**, 239-256, doi:10.1089/08977150252806983 (2002).

98 Gillis, G. B. & Biewener, A. A. Hindlimb muscle function in relation to speed and gait: in vivo patterns of strain and activation in a hip and knee extensor of the rat (Rattus norvegicus). *J Exp Biol* **204**, 2717-2731 (2001).

99 Ohri, S. S. *et al.* Deletion of the pro-apoptotic endoplasmic reticulum stress response effector CHOP does not result in improved locomotor function after severe contusive spinal cord injury. *J Neurotrauma* **29**, 579-588, doi:10.1089/neu.2011.1940 (2012).

100 Soderblom, C. *et al.* 3D Imaging of Axons in Transparent Spinal Cords from Rodents and Nonhuman Primates. *eNeuro* **2**, doi:10.1523/ENEURO.0001-15.2015 (2015).

101 Kiehn, O. & Kjaerulff, O. Distribution of central pattern generators for rhythmic motor outputs in the spinal cord of limbed vertebrates. *Ann N Y Acad Sci* **860**, 110-129 (1998).

102 Batschelet, E. in *Animal orientation and navigation* (ed K. Schmidt-Koenig S. R. Galler, G. J. Jacobs and R. E. Bellville) 61-91 (NASA, 1972).

103 Zar, J. H. *Biostatistical analysis*. (Prentice-Hall, 1974).

104 Hays, W. L. *Statistics*. (Holt, Rinehart and Winston, 1981).

105 Siegel, S. & Castellan, N. J. *Nonparametric Statistics for the Behavioral Sciences*. (McGraw-Hill, 1988).

106 Ott, L. *An Introduction to Statistical Methods and Data Analysis*. (Duxbury Press, 1977).

107 Java Applets for Power and Sample Size (2006-9).

108 Cheng, H. *et al.* Gait analysis of adult paraplegic rats after spinal cord repair. *Exp Neurol* **148**, 544-557, doi:10.1006/exnr.1997.6708 (1997).

109 Hruska, R. E., Kennedy, S. & Silbergeld, E. K. Quantitative aspects of normal locomotion in rats. *Life Sci* **25**, 171-179 (1979).

110 Cazalets, J. R., Borde, M. & Clarac, F. Localization and organization of the central pattern generator for hindlimb locomotion in newborn rat. *J Neurosci* **15**, 4943-4951 (1995).

111 McCrea, D. A. & Rybak, I. A. Organization of mammalian locomotor rhythm and pattern generation. *Brain Res Rev* **57**, 134-146, doi:10.1016/j.brainresrev.2007.08.006 (2008).

112 Gruner, J. A. & Altman, J. Swimming in the rat: analysis of locomotor performance in comparison to stepping. *Exp Brain Res* **40**, 374-382 (1980).

113 Akay, T., Tourtellotte, W. G., Arber, S. & Jessell, T. M. Degradation of mouse locomotor pattern in the absence of proprioceptive sensory feedback. *Proc Natl Acad Sci U S A* **111**, 16877-16882, doi:10.1073/pnas.1419045111 (2014).

114 Massion, J. Movement, posture and equilibrium: interaction and coordination. *Prog Neurobiol* **38**, 35-56 (1992).

115 Juvin, L., Simmers, J. & Morin, D. Propriospinal circuitry underlying interlimb coordination in mammalian quadrupedal locomotion. *J Neurosci* **25**, 6025-6035, doi:10.1523/jneurosci.0696-05.2005 (2005).

116 Guertin, P. A. The mammalian central pattern generator for locomotion. *Brain Res Rev* **62**, 45-56, doi:10.1016/j.brainresrev.2009.08.002 (2009).

117 Ballion, B., Morin, D. & Viala, D. Forelimb locomotor generators and quadrupedal locomotion in the neonatal rat. *Eur J Neurosci* **14**, 1727-1738 (2001).

118 Miller, S. & Van der Burg, J. in *Control of Posture and Locomotion* (eds R. B. Stein, K. G. Pearson, R. S. Smith, & J. B. Redford) 561-577 (Springer US, 1973).

119 Miller, S., Van Der Burg, J. & Van Der Meché, F. Coordination of movements of the hindlimbs and forelimbs in different forms of locomotion in normal and decerebrate cats. *Brain research* **91**, 217-237 (1975).

120 Jankowska, E., Lundberg, A. & Stuart, D. Propriospinal control of last order interneurones of spinal reflex pathways in the cat. *Brain Res* **53**, 227-231 (1973).

121 Brockett, E. G., Seenan, P. G., Bannatyne, B. A. & Maxwell, D. J. Ascending and descending propriospinal pathways between lumbar and cervical segments in the rat: evidence for a substantial ascending excitatory pathway. *Neuroscience* **240**, 83-97, doi:10.1016/j.neuroscience.2013.02.039 (2013).

122 Miller, S. & van der Meché, F. G. A. Coordinated stepping of all four limbs in the high spinal cat. *Brain Research* **109**, 395-398, doi:http://dx.doi.org/10.1016/0006-8993(76)90541-2 (1976).

123 Reed, W. R., Shum-Siu, A., Onifer, S. M. & Magnuson, D. S. Inter-enlargement pathways in the ventrolateral funiculus of the adult rat spinal cord. *Neuroscience* **142**, 1195-1207, doi:10.1016/j.neuroscience.2006.07.017 (2006).

124 Ni, Y. *et al.* Characterization of long descending premotor propriospinal neurons in the spinal cord. *J Neurosci* **34**, 9404-9417, doi:10.1523/jneurosci.1771-14.2014 (2014).

125 Alstermark, B., Lundberg, A., Pinter, M. & Sasaki, S. Subpopulations and functions of long C3-C5 propriospinal neurones. *Brain Research* **404**, 395-400, doi:http://dx.doi.org/10.1016/0006-8993(87)91402-8 (1987).

126 Giovanelli Barilari, M. & Kuypers, H. G. Propriospinal fibers interconnecting the spinal enlargements in the cat. *Brain Res* **14**, 321-330 (1969).

127 Ruder, L., Takeoka, A. & Arber, S. Long-Distance Descending Spinal Neurons Ensure Quadrupedal Locomotor Stability. *Neuron* **92**, 1063-1078, doi:10.1016/j.neuron.2016.10.032 (2016).

128 English, A. W., Tigges, J. & Lennard, P. R. Anatomical organization of long ascending propriospinal neurons in the cat spinal cord. *J Comp Neurol* **240**, 349-358, doi:10.1002/cne.902400403 (1985).

129 Sterling, P. & Kuypers, H. G. Anatomical organization of the brachial spinal cord of the cat. 3. The propriospinal connections. *Brain Res* **7**, 419-443 (1968).

130 Matsushita, M. & Ueyama, T. Ventral motor nucleus of the cervical enlargement in some mammals; its specific afferents from the lower cord levels and cytoarchitecture. *J Comp Neurol* **150**, 33-52, doi:10.1002/cne.901500103 (1973).

131 Miller, S. Excitatory and inhibitory propriospinal pathways from lumbo-sacral to cervical segments in the cat. *Acta Physiol Scand* **80**, 25A-26A, doi:10.1111/j.1748-1716.1970.tb04849.x (1970).

132 Magnuson, D. S. *et al.* Swimming as a model of task-specific locomotor retraining after spinal cord injury in the rat. *Neurorehabil Neural Repair* **23**, 535-545, doi:10.1177/1545968308331147 (2009).

133 J, K. *et al.* Task-specificity vs Ceiling Effect: Step-training in shallow water after spinal cord injury. *Experimental neurology* **224**, 178-187, doi:10.1016/j.expneurol.2010.03.008 (2010).

134 Burke, D. A. & Magnuson, D. S. K. in *Animal Models of Acute Neurological Injuries II: Injury and Mechanistic Assessments, Volume 2* (eds Jun Chen, Xiao-Ming Xu, Zao C. Xu, & John H. Zhang) 591-604 (Humana Press, 2012).

135 Metz, G. A. & Whishaw, I. Q. Cortical and subcortical lesions impair skilled walking in the ladder rung walking test: a new task to evaluate fore- and hindlimb stepping, placing, and co-ordination. *Journal of neuroscience methods* **115**, 169-179 (2002).

136 Bales, J. W., Macfarlane, K. & Dixon, C. E. in *Animal Models of Acute Neurological Injuries II: Injury and Mechanistic Assessments, Volume 2* (eds Jun Chen, Xiao-Ming Xu, Zao C. Xu, & John H. Zhang) 385-396 (Humana Press, 2012).

137 Ohri, S. S. *et al.* Attenuating the endoplasmic reticulum stress response improves functional recovery after spinal cord injury. *Glia* **59**, 1489-1502, doi:10.1002/glia.21191 (2011).

138 Batschelet, E. in *NASA, Washington Animal Orientation and Navigation* 61-91 (United States, Washington, DC, United States, 1972).

139 Basso, D. M., Beattie, M. S. & Bresnahan, J. C. Graded Histological and Locomotor Outcomes after Spinal Cord Contusion Using the NYU Weight-Drop Device versus Transection. *Experimental Neurology* **139**, 244-256, doi:http://dx.doi.org/10.1006/exnr.1996.0098 (1996).

140 Šedý, J., Urdzíková, L., Jendelová, P. & Syková, E. Methods for behavioral testing of spinal cord injured rats. *Neuroscience & Biobehavioral Reviews* **32**, 550-580, doi:http://dx.doi.org/10.1016/j.neubiorev.2007.10.001 (2008).

141 Miller, S., Van Der Burg, J. & Van Der Meché, F. G. A. Locomotion in the cat: Basic programmes of movement. *Brain Research* **91**, 239-253, doi:http://dx.doi.org/10.1016/0006-8993(75)90545-4 (1975).

142 Skinner, R. D., Nelson, R., Griebel, M. & Garcia-Rill, E. Ascending projections of long descending propriospinal tract (LDPT) neurons. *Brain Res Bull* **22**, 253-258 (1989).

143 Miller, S., Reitsma, D. J. & van der Meche, F. G. Functional organization of long ascending propriospinal pathways linking lumbo-sacral and cervical segments in the cat. *Brain Res* **62**, 169-188 (1973).

144 Bertrand, S. & Cazalets, J. R. The respective contribution of lumbar segments to the generation of locomotion in the isolated spinal cord of newborn rat. *Eur J Neurosci* **16**, 1741-1750 (2002).

145 Magnuson, D. S. *et al.* Functional consequences of lumbar spinal cord contusion injuries in the adult rat. *J Neurotrauma* **22**, 529-543, doi:10.1089/neu.2005.22.529 (2005).

146 Magnuson, D. S. *et al.* Comparing deficits following excitotoxic and contusion injuries in the thoracic and lumbar spinal cord of the adult rat. *Exp Neurol* **156**, 191-204, doi:10.1006/exnr.1999.7016 (1999).

147 Molenaar, I. & Kuypers, H. G. Cells of origin of propriospinal fibers and of fibers ascending to supraspinal levels. A HRP study in cat and rhesus monkey. *Brain Res* **152**, 429-450 (1978).

148 Kiehn, O. & Dougherty, K. in *Neuroscience in the 21st Century* 1209-1236 (Springer, 2013).

149 Lundberg, A. in *The Nansen Memorial Lecture V* 1-42 (1969).

150 Sheng, M. & Greenberg, M. E. The regulation and function of c-fos and other immediate early genes in the nervous system. *Neuron* **4**, 477-485 (1990).

151 Grant, R. A., Mitchinson, B. & Prescott, T. J. The development of whisker control in rats in relation to locomotion. *Developmental psychobiology* **54**, 151-168, doi:10.1002/dev.20591 (2012).

152 Mitchinson, B., Martin, C. J., Grant, R. A. & Prescott, T. J. Feedback control in active sensing: rat exploratory whisking is modulated by environmental contact. *Proc Biol Sci* **274**, 1035-1041, doi:10.1098/rspb.2006.0347 (2007).

153 Arkley, K., Grant, R. A., Mitchinson, B. & Prescott, T. J. Strategy change in vibrissal active sensing during rat locomotion. *Curr Biol* **24**, 1507-1512, doi:10.1016/j.cub.2014.05.036 (2014).

154 Krupa, D. J., Matell, M. S., Brisben, A. J., Oliveira, L. M. & Nicolelis, M. A. Behavioral properties of the trigeminal somatosensory system in rats performing whisker-dependent tactile discriminations. *J Neurosci* **21**, 5752-5763 (2001).

155 Knutsen, P. M., Pietr, M. & Ahissar, E. Haptic object localization in the vibrissal system: behavior and performance. *J Neurosci* **26**, 8451-8464, doi:10.1523/jneurosci.1516-06.2006 (2006).

156 Szwed, M., Bagdasarian, K. & Ahissar, E. Encoding of vibrissal active touch. *Neuron* **40**, 621-630 (2003).

157 Yu, C., Derdikman, D., Haidarliu, S. & Ahissar, E. Parallel thalamic pathways for whisking and touch signals in the rat. *PLoS biology* **4**, e124, doi:10.1371/journal.pbio.0040124 (2006).

158 Fee, M. S., Mitra, P. P. & Kleinfeld, D. Central versus peripheral determinants of patterned spike activity in rat vibrissa cortex during whisking. *J Neurophysiol* **78**, 1144-1149 (1997).

159 Curtis, J. C. & Kleinfeld, D. Phase-to-rate transformations encode touch in cortical neurons of a scanning sensorimotor system. *Nat Neurosci* **12**, 492-501, doi:10.1038/nn.2283 (2009).

160 Ahrens, K. F. & Kleinfeld, D. Current flow in vibrissa motor cortex can phase-lock with exploratory rhythmic whisking in rat. *J Neurophysiol* **92**, 1700-1707, doi:10.1152/jn.00020.2004 (2004).

161 Hill, D. N., Curtis, J. C., Moore, J. D. & Kleinfeld, D. Primary motor cortex reports efferent control of vibrissa motion on multiple timescales. *Neuron* **72**, 344-356, doi:10.1016/j.neuron.2011.09.020 (2011).

162 Selset, R. & Doving, K. B. Behaviour of mature anadromous char (Salmo alpinus L.) towards odorants produced by smolts of their own population. *Acta Physiol Scand* **108**, 113-122, doi:10.1111/j.1748-1716.1980.tb06508.x (1980).

163 Dubuc, R. *et al.* Initiation of locomotion in lampreys. *Brain Res Rev* **57**, 172-182, doi:10.1016/j.brainresrev.2007.07.016 (2008).

164 Fady, J. C., Jamon, M. & Clarac, F. Early olfactory-induced rhythmic limb activity in the newborn rat. *Brain Res Dev Brain Res* **108**, 111-123 (1998).

165 Varendi, H. & Porter, R. H. Breast odour as the only maternal stimulus elicits crawling towards the odour source. *Acta paediatrica (Oslo, Norway : 1992)* **90**, 372-375 (2001).

166 Derjean, D. *et al.* A novel neural substrate for the transformation of olfactory inputs into motor output. *PLoS biology* **8**, e1000567, doi:10.1371/journal.pbio.1000567 (2010).

167 Daghfous, G., Green, W. W., Alford, S. T., Zielinski, B. S. & Dubuc, R. Sensory Activation of Command Cells for Locomotion and Modulatory Mechanisms: Lessons from Lampreys. *Front Neural Circuits* **10**, 18, doi:10.3389/fncir.2016.00018 (2016).

168 Vernier, P. & Wullimann, M. F. in *Encyclopedia of Neuroscience* (eds Marc D. Binder, Nobutaka Hirokawa, & Uwe Windhorst) 1404-1413 (Springer Berlin Heidelberg, 2009).

169 Jordan, L. M., Liu, J., Hedlund, P. B., Akay, T. & Pearson, K. G. Descending command systems for the initiation of locomotion in mammals. *Brain Res Rev* **57**, 183-191, doi:10.1016/j.brainresrev.2007.07.019 (2008).

170 Martini, F. & Nath, J. L. *Anatomy & physiology*. 2nd ed. edn, xxxi, 935, [83] pages : color illustrations ; 29 cm (Benjamin Cummings, 2010).

171 Mogenson, G. J. & Wu, M. Effects of administration of dopamine D2 agonist quinpirole on exploratory locomotion. *Brain Research* **551**, 216-220, doi:http://dx.doi.org/10.1016/0006-8993(91)90935-O (1991).

172 Lee, R.-S., Koob, G. F. & Henriksen, S. J. Electrophysiological responses of nucleus accumbens neurons to novelty stimuli and exploratory behavior in the awake, unrestrained rat. *Brain Research* **799**, 317-322, doi:http://dx.doi.org/10.1016/S0006-8993(98)00477-6 (1998).

173 Fink, J. S. & Smith, G. P. Mesolimbicocortical dopamine terminal fields are necessary for normal locomotor and investigatory exploration in rats. *Brain Res* **199**, 359-384 (1980).

174 Grillner, S., Georgopoulos, A. & Jordan, L. (Citeseer, 1997).

175 Paxinos, G. in *The Rat Nervous System* (Academic, 1995).

176 Collins, J. J. & Richmond, S. A. Hard-wired central pattern generators for quadrupedal locomotion. *Biological Cybernetics* **71**, 375-385, doi:10.1007/bf00198915 (1994).

177 Jordan, C., Friedrich Jr, V. & Dubois-Dalcq, M. Developing Mouse Spinal Cord. (1989).

178 Nayak, S. & Herzog, R. W. Progress and Prospects: Immune Responses to Viral Vectors. *Gene therapy* **17**, 295-304, doi:10.1038/gt.2009.148 (2010).

179 Thavarajah, R., Mudimbaimannar, V. K., Elizabeth, J., Rao, U. K. & Ranganathan, K. Chemical and physical basics of routine formaldehyde fixation. *Journal of Oral and Maxillofacial Pathology : JOMFP* **16**, 400-405, doi:10.4103/0973-029X.102496 (2012).

180 Lencer, W. I. & Tsai, B. The intracellular voyage of cholera toxin: going retro. *Trends in biochemical sciences* **28**, 639-645, doi:10.1016/j.tibs.2003.10.002 (2003).

181 Murlidharan, G., Samulski, R. J. & Asokan, A. Biology of adeno-associated viral vectors in the central nervous system. *Frontiers in Molecular Neuroscience* **7**, 76, doi:10.3389/fnmol.2014.00076 (2014).

182 Reiner, A. *et al.* Pathway tracing using biotinylated dextran amines. *Journal of neuroscience methods* **103**, 23-37, doi:http://dx.doi.org/10.1016/S0165-0270(00)00293-4 (2000).

183 Dobrzanski, G. & Kossut, M. Application of the DREADD technique in biomedical brain research. *Pharmacological Reports* **69**, 213-221, doi:http://dx.doi.org/10.1016/j.pharep.2016.10.015 (2017).

184 Roth, B. L. DREADDs for Neuroscientists. *Neuron* **89**, 683-694, doi:10.1016/j.neuron.2016.01.040 (2016).

185 Schwarz, L. A. *et al.* Viral-genetic tracing of the input-output organization of a central noradrenaline circuit. *Nature* **524**, 88-92, doi:10.1038/nature14600 http://www.nature.com/nature/journal/v524/n7563/abs/nature14600.html#supplementary-information (2015).

186 Salinas, S. *et al.* CAR-associated vesicular transport of an adenovirus in motor neuron axons. *PLoS pathogens* **5**, e1000442, doi:10.1371/journal.ppat.1000442 (2009).

187 Soudais, C., Laplace-Builhe, C., Kissa, K. & Kremer, E. J. Preferential transduction of neurons by canine adenovirus vectors and their efficient retrograde transport in vivo. *Faseb j* **15**, 2283-2285, doi:10.1096/fj.01-0321fje (2001).

188 Callaway, E. M. & Luo, L. Monosynaptic Circuit Tracing with Glycoprotein-Deleted Rabies Viruses. *The Journal of Neuroscience* **35**, 8979-8985, doi:10.1523/JNEUROSCI.0409-15.2015 (2015).

189 Watabe-Uchida, M., Zhu, L., Ogawa, S. K., Vamanrao, A. & Uchida, N. Whole-brain mapping of direct inputs to midbrain dopamine neurons. *Neuron* **74**, 858-873, doi:10.1016/j.neuron.2012.03.017 (2012).

190 Wickersham, I. R. *et al.* Monosynaptic restriction of transsynaptic tracing from single, genetically targeted neurons. *Neuron* **53**, 639-647, doi:10.1016/j.neuron.2007.01.033 (2007).

191 Osakada, F. *et al.* New rabies virus variants for monitoring and manipulating activity and gene expression in defined neural circuits. *Neuron* **71**, 617-631, doi:10.1016/j.neuron.2011.07.005 (2011).

192 Moran-Rivard, L. *et al.* Evx1 is a postmitotic determinant of v0 interneuron identity in the spinal cord. *Neuron* **29**, 385-399 (2001).

193 Dougherty, K. J. & Kiehn, O. Functional organization of V2a-related locomotor circuits in the rodent spinal cord. *Ann N Y Acad Sci* **1198**, 85-93, doi:10.1111/j.1749-6632.2010.05502.x (2010).

194 Zhong, G. *et al.* Electrophysiological characterization of V2a interneurons and their locomotor-related activity in the neonatal mouse spinal cord. *J Neurosci* **30**, 170-182, doi:10.1523/jneurosci.4849-09.2010 (2010).

195 Dougherty, K. J. & Kiehn, O. Firing and cellular properties of V2a interneurons in the rodent spinal cord. *J Neurosci* **30**, 24-37, doi:10.1523/jneurosci.4821-09.2010 (2010).

196 Rybak, I. A., Dougherty, K. J. & Shevtsova, N. A. Organization of the Mammalian Locomotor CPG: Review of Computational Model and Circuit

Architectures Based on Genetically Identified Spinal Interneurons(1,2,3). *eNeuro* **2**, doi:10.1523/ENEURO.0069-15.2015 (2015).

197 Molkov, Y. I., Bacak, B. J., Talpalar, A. E. & Rybak, I. A. Mechanisms of left-right coordination in mammalian locomotor pattern generation circuits: a mathematical modeling view. *PLoS Comput Biol* **11**, e1004270, doi:10.1371/journal.pcbi.1004270 (2015).

198 Rybak, I. A., Shevtsova, N. A. & Kiehn, O. Modelling genetic reorganization in the mouse spinal cord affecting left-right coordination during locomotion. *J Physiol* **591**, 5491-5508, doi:10.1113/jphysiol.2013.261115 (2013).

199 Alaynick, W. A., Jessell, T. M. & Pfaff, S. L. SnapShot: spinal cord development. *Cell* **146**, 178-178.e171, doi:10.1016/j.cell.2011.06.038 (2011).

200 Pivetta, C., Esposito, M. S., Sigrist, M. & Arber, S. Motor-circuit communication matrix from spinal cord to brainstem neurons revealed by developmental origin. *Cell* **156**, 537-548, doi:10.1016/j.cell.2013.12.014 (2014).

201 Cavagna, G. A., Heglund, N. C. & Taylor, C. R. Mechanical work in terrestrial locomotion: two basic mechanisms for minimizing energy expenditure. *The American journal of physiology* **233**, R243-261 (1977).

202 Heglund, N. C., Cavagna, G. A. & Taylor, C. R. Energetics and mechanics of terrestrial locomotion. III. Energy changes of the centre of mass as a function of speed and body size in birds and mammals. *J Exp Biol* **97**, 41-56 (1982).

203 Sillar, K. Dynamic Biological Networks: the Stomatogastric Nervous System. *Trends in Neurosciences* **16**, 198-199, doi:10.1016/0166-2236(93)90153-D.

204 Katz, P. S. Neurons, networks, and motor behavior. *Neuron* **16**, 245-253 (1996).

205 Dietz, V. Do human bipeds use quadrupedal coordination? *Trends Neurosci* **25**, 462-467 (2002).

206 Dietz, V. Human neuronal control of automatic functional movements: interaction between central programs and afferent input. *Physiol Rev* **72**, 33-69 (1992).

207 Dietz, V. Neurophysiology of gait disorders: present and future applications. *Electroencephalogr Clin Neurophysiol* **103**, 333-355 (1997).

208 Yang, J. F., Stephens, M. J. & Vishram, R. Transient Disturbances to One Limb Produce Coordinated, Bilateral Responses During Infant Stepping. *Journal of Neurophysiology* **79**, 2329-2337 (1998).

209 Pang, M. Y. & Yang, J. F. The initiation of the swing phase in human infant stepping: importance of hip position and leg loading. *J Physiol* **528 Pt 2**, 389-404 (2000).

210 Pang, M. Y. & Yang, J. F. Interlimb co-ordination in human infant stepping. *J Physiol* **533**, 617-625 (2001).

211 Dietz, V., Quintern, J., Boos, G. & Berger, W. Obstruction of the swing phase during gait: phase-dependent bilateral leg muscle coordination. *Brain Res* **384**, 166-169 (1986).

212 Thelen, E., Ulrich, B. D. & Niles, D. Bilateral coordination in human infants: stepping on a split-belt treadmill. *Journal of experimental psychology. Human perception and performance* **13**, 405-410 (1987).

213 Prokop, T., Berger, W., Zijlstra, W. & Dietz, V. Adaptational and learning processes during human split-belt locomotion: interaction between central mechanisms and afferent input. *Exp Brain Res* **106**, 449-456 (1995).

214 Erni, T. & Dietz, V. Obstacle avoidance during human walking: learning rate and cross-modal transfer. *The Journal of Physiology* **534**, 303-312, doi:10.1111/j.1469-7793.2001.00303.x (2001).

215 Dietz, V., Zijlstra, W. & Duysens, J. Human neuronal interlimb coordination during split-belt locomotion. *Exp Brain Res* **101**, 513-520 (1994).

216 Nathan, P. W., Smith, M. & Deacon, P. Vestibulospinal, reticulospinal and descending propriospinal nerve fibres in man. *Brain* **119 (Pt 6)**, 1809-1833 (1996).

217 Nathan, P. W. & Smith, M. C. Long descending tracts in man. I. Review of present knowledge. *Brain* **78**, 248-303 (1955).

218 Wannier, T., Bastiaanse, C., Colombo, G. & Dietz, V. Arm to leg coordination in humans during walking, creeping and swimming activities. *Exp Brain Res* **141**, 375-379, doi:10.1007/s002210100875 (2001).

219 Zehr, E. P. & Chua, R. Modulation of human cutaneous reflexes during rhythmic cyclical arm movement. *Exp Brain Res* **135**, 241-250, doi:10.1007/s002210000515 (2000).

220 Zehr, E. P. & Kido, A. Neural control of rhythmic, cyclical human arm movement: task dependency, nerve specificity and phase modulation of cutaneous reflexes. *The Journal of Physiology* **537**, 1033-1045, doi:10.1111/j.1469-7793.2001.01033.x (2001).

221 Zehr, E. P., Komiyama, T. & Stein, R. B. Cutaneous reflexes during human gait: electromyographic and kinematic responses to electrical stimulation. *J Neurophysiol* **77**, 3311-3325 (1997).

222 Meyns, P., Bruijn, S. M. & Duysens, J. The how and why of arm swing during human walking. *Gait & posture* **38**, 555-562, doi:10.1016/j.gaitpost.2013.02.006 (2013).

223 Wu, Y. *et al.* Effect of active arm swing to local dynamic stability during walking. *Hum Mov Sci* **45**, 102-109, doi:10.1016/j.humov.2015.10.005 (2016).

224 Pontzer, H., Holloway, J. H. t., Raichlen, D. A. & Lieberman, D. E. Control and function of arm swing in human walking and running. *J Exp Biol* **212**, 523-534, doi:10.1242/jeb.024927 (2009).

225 Dietz, V., Fouad, K. & Bastiaanse, C. M. Neuronal coordination of arm and leg movements during human locomotion. *European Journal of Neuroscience* **14**, 1906-1914, doi:10.1046/j.0953-816x.2001.01813.x (2001).

226 Dietz, V. & Michel, J. Human bipeds use quadrupedal coordination during locomotion. *Ann N Y Acad Sci* **1164**, 97-103, doi:10.1111/j.1749-6632.2008.03710.x (2009).

227 Cappellini, G., Ivanenko, Y. P., Poppele, R. E. & Lacquaniti, F. Motor patterns in human walking and running. *J Neurophysiol* **95**, 3426-3437, doi:10.1152/jn.00081.2006 (2006).

228 Nilsson, J., Thorstensson, A. & Halbertsma, J. Changes in leg movements and muscle activity with speed of locomotion and mode of progression in humans. *Acta Physiol Scand* **123**, 457-475, doi:10.1111/j.1748-1716.1985.tb07612.x (1985).

229 Freedland, R. L. & Bertenthal, B. I. Developmental Changes in Interlimb Coordination: Transition to Hands-and-Knees Crawling. *Psychological Science* **5**, 26-32, doi:10.1111/j.1467-9280.1994.tb00609.x (1994).

230 Ledebt, A. & Bril, B. Acquisition of upper body stability during walking in toddlers. *Developmental psychobiology* **36**, 311-324 (2000).

231 Marks, R. The effect of restricting arm swing during normal locomotion. *Biomed Sci Instrum* **33**, 209-215 (1997).

232 Umberger, B. R. Effects of suppressing arm swing on kinematics, kinetics, and energetics of human walking. *Journal of Biomechanics* **41**, 2575-2580, doi:http://dx.doi.org/10.1016/j.jbiomech.2008.05.024 (2008).

233 Tetzlaff, W. *et al.* A systematic review of cellular transplantation therapies for spinal cord injury. *J Neurotrauma* **28**, 1611-1682, doi:10.1089/neu.2009.1177 (2011).

234 Houle, J. D. & Tessler, A. Repair of chronic spinal cord injury. *Experimental Neurology* **182**, 247-260, doi:http://dx.doi.org/10.1016/S0014-4886(03)00029-3 (2003).

235 Fawcett, J. Repair of spinal cord injuries: where are we, where are we going? *Spinal cord* **40**, 615-623, doi:10.1038/sj.sc.3101328 (2002).

236 Flynn, J. R., Graham, B. A., Galea, M. P. & Callister, R. J. The role of propriospinal interneurons in recovery from spinal cord injury. *Neuropharmacology* **60**, 809-822, doi:10.1016/j.neuropharm.2011.01.016 (2011).

237 Jane, J. A., Evans, J. P. & Fisher, L. E. AN INVESTIGATION CONCERNING THE RESTITUTION OF MOTOR FUNCTION FOLLOWING INJURY TO THE SPINAL CORD. *J Neurosurg* **21**, 167-171, doi:10.3171/jns.1964.21.3.0167 (1964).

238 Selzer, M. E. Mechanisms of functional recovery and regeneration after spinal cord transection in larval sea lamprey. *J Physiol* **277**, 395-408 (1978).

239 Basso, D. M. Neuroanatomical substrates of functional recovery after experimental spinal cord injury: implications of basic science research for human spinal cord injury. *Physical therapy* **80**, 808-817 (2000).

240 Conta, A. C. & Stelzner, D. J. Differential vulnerability of propriospinal tract neurons to spinal cord contusion injury. *J Comp Neurol* **479**, 347-359, doi:10.1002/cne.20319 (2004).

241 Conta Steencken, A. C. & Stelzner, D. J. Loss of propriospinal neurons after spinal contusion injury as assessed by retrograde labeling. *Neuroscience* **170**, 971-980, doi:10.1016/j.neuroscience.2010.06.064 (2010).

242 Beaumont, E., Onifer, S. M., Reed, W. R. & Magnuson, D. S. Magnetically evoked inter-enlargement response: an assessment of ascending propriospinal fibers following spinal cord injury. *Exp Neurol* **201**, 428-440, doi:10.1016/j.expneurol.2006.04.032 (2006).

243 Bareyre, F. M. *et al.* The injured spinal cord spontaneously forms a new intraspinal circuit in adult rats. *Nat Neurosci* **7**, 269-277, doi:10.1038/nn1195 (2004).

244 Courtine, G. *et al.* Recovery of supraspinal control of stepping via indirect propriospinal relay connections after spinal cord injury. *Nat Med* **14**, 69-74, doi:10.1038/nm1682 (2008).

245 Lovely, R. G., Gregor, R. J., Roy, R. R. & Edgerton, V. R. Effects of training on the recovery of full-weight-bearing stepping in the adult spinal cat. *Exp Neurol* **92**, 421-435 (1986).

246 Barbeau, H. & Rossignol, S. Recovery of locomotion after chronic spinalization in the adult cat. *Brain Res* **412**, 84-95 (1987).

247 De Leon, R. D., Hodgson, J. A., Roy, R. R. & Edgerton, V. R. Full weight-bearing hindlimb standing following stand training in the adult spinal cat. *J Neurophysiol* **80**, 83-91 (1998).

248 Cote, M. P., Detloff, M. R., Wade, R. E., Jr., Lemay, M. A. & Houle, J. D. Plasticity in ascending long propriospinal and descending supraspinal

pathways in chronic cervical spinal cord injured rats. *Front Physiol* **3**, 330, doi:10.3389/fphys.2012.00330 (2012).

249 Tester, N. J. *et al.* Device use, locomotor training and the presence of arm swing during treadmill walking after spinal cord injury. *Spinal cord* **49**, 451-456, doi:10.1038/sc.2010.128 (2011).

250 Behrman, A. L. & Harkema, S. J. Locomotor training after human spinal cord injury: a series of case studies. *Physical therapy* **80**, 688-700 (2000).

251 Visintin, M. & Barbeau, H. The effects of parallel bars, body weight support and speed on the modulation of the locomotor pattern of spastic paretic gait. A preliminary communication. *Paraplegia* **32**, 540-553, doi:10.1038/sc.1994.86 (1994).

252 Dietz, V. & Harkema, S. J. Locomotor activity in spinal cord-injured persons. *J Appl Physiol (1985)* **96**, 1954-1960, doi:10.1152/japplphysiol.00942.2003 (2004).

253 Edgerton, V. R. *et al.* Training locomotor networks. *Brain Res Rev* **57**, 241-254, doi:10.1016/j.brainresrev.2007.09.002 (2008).

254 Lee, G. & Saito, I. Role of nucleotide sequences of loxP spacer region in Cre-mediated recombination. *Gene* **216**, 55-65 (1998).

255 Schnutgen, F. *et al.* A directional strategy for monitoring Cre-mediated recombination at the cellular level in the mouse. *Nat Biotechnol* **21**, 562-565, doi:10.1038/nbt811 (2003).

# LIST OF ABBREVIATIONS AND SYMBOLS

| | |
|---|---|
| \| \| | Absolute |
| Δ | Change |
| °C | Degrees centigrade |
| µl | Microliter |
| µm | Micrometer |
| 3D | Three-dimensional |
| A | Ankle |
| AAV2 | Adeno-associated viral vector, serotype 2 |
| ANOVA | Analysis of variance |
| ASLV | Avian sarcoma leukosis virus |
| B.P. | Binomial Proportion |
| BL | Baseline |
| BL6 | C57BL/6, strain of inbred mice |
| C | Caudal |
| C.C. | Central canal |
| Cav | Canine adenovirus (serotype 2) |
| Cm/s | Centimeters per second |
| CMV | Cytomegalovirus |

| | |
|---|---|
| CON | Control |
| Con | Contralateral |
| Control$^{All}$ | Baseline, Pre-DOX1, DOX$^{OFF}$, Pre-DOX2 |
| CPG | Central pattern generator |
| CPG | Central pattern generator |
| cPPT | Central polypurine tract |
| Cre | Tyrosine recombinase enzyme; Causes recombination |
| CTB | Cholera toxin, beta subunit |
| CY5 | Cyanine dye 5 |
| D1D3 | DOX1$^{ON}$-D3 |
| D1D5 | DOX1$^{ON}$-D5 |
| D1D8 | DOX1$^{ON}$-D8 |
| D2D3 | DOX2$^{ON}$-D3 |
| D2D5 | DOX2$^{ON}$-D5 |
| DAB | 3,3' Diaminobenzidine |
| DAPI | 4',6-diamidino-2-phenylindole |
| Dbx1 | Developing brain homeobox 1 |
| DOFF | DOX$^{OFF}$ |
| DOX | Doxycycline |
| DOX$^{All}$ | DOX1$^{ON}$D3, -D5, -D8, DOX2$^{ON}$-D3, -D5 |
| DREADD | Designer Receptors Exclusively Activated by Designer Drugs |
| DTA | Diphtheria toxin A |
| EGFP | Enhanced green fluorescent protein |

| | |
|---|---|
| EMG | Electromyogram |
| EnvA | Envelope protein A |
| eTeNT | Enhanced tetanus neurotoxin, light chain |
| F.E. | FluoroEmerald |
| F.R. | FluoroRuby |
| Fig. | Figure |
| FL | Forelimb |
| FLEx | Flip-excision switch |
| Flp | Flip recombinase |
| FOV | Field of view |
| Freq. | Frequency |
| G | Glycoprotein |
| GFP | Green fluorescent protein |
| H | Hip |
| HAT | Hip-ankle-toe |
| HAT | Hip-ankle-toe angle |
| HiRet | Highly-efficient retrograde transport |
| HIV-1 | Human immunodeficiency virus, type 1 |
| HL | Hindlimb |
| HRP | Horseradish peroxidase |
| HSD | Honest significant difference |
| Hz | Hertz |
| I | Iliac crest |

| | |
|---|---|
| i.m. | Intramuscular |
| i.p. | Intraperitoneal |
| ICR | Strain of outbred mice |
| IgG | Immunoglobulin, G |
| IHA | Iliac crest-hip-ankle |
| IHA | Iliac crest-hip-ankle angle |
| Ipsi | Ipsilateral |
| KS | Kolmogorov-Smirnov |
| L | Lateral |
| L/R-IRT | Left/right inverted terminal repeat sequences |
| L2-L5 | L2 spinal interneurons that project to L5 |
| lacZ | Lactose operon, gene Z |
| LAPN | Long ascending propriospinal neurons |
| LDPN | Long descending propriospinal neuron |
| Lenti | Lentiviral vector |
| LFL | Left forelimb |
| LHL | Left hindlimb |
| loxP | Locus of crossing x over P1 |
| LSFM | Light sheet fluorescence microscopy |
| LSFM | Light sheet fluorescence microscopy |
| M | Molar |
| MANOVA | Multivariate analysis of variance |
| Me | Medial |

| | |
|---|---|
| Mg/kg | Milligram per kilogram |
| Mg/ml | Milligram per milliliter |
| MIER | Magnetically-evoked inter-enlargement response |
| Mm | Millimeter |
| n.s. | Not significant |
| NeuN | Neuronal Nuclei |
| nls | Nuclear location signal |
| PBS | Phosphate-buffered saline |
| PD1 | Pre-DOX1 |
| PD2 | Pre-DOX2 |
| PEST | Peptide sequence rich in protein (P), glutamic acid (E), serine (S), and threonine (T) |
| Proj. | Projections |
| PSI | Packing signal |
| R | Rostral |
| R-C | Rostral-caudal |
| RFL | Right forelimb |
| RHL | Right hindlimb |
| RRE | Rev response element |
| $r_S$ | Spearman rank correlation coefficient |
| rtTAV16 | Reverse tetracycline transactivator, variant 16 |
| RVdG | Rabies virus, glycol-deleted |
| s.c. | Subcutaneous |
| S.D. | Standard deviation |

| | |
|---|---|
| SC | Sugar control |
| SCI | Spinal cord injury |
| SHOX2 | Short stature homeoprotein 2 |
| SV40 pA | Simian virus 40 polyadenylation termination signal |
| SynTag | Synaptophysing-tagged to a fluorescent reporter |
| T | Toe |
| TBS | Tris-buffered saline |
| TC | TVA-mCherry fusion protein |
| $Tet^{On}$ | $Tetracycline^{On}$ |
| TexRed | TexasRed |
| Trans. | Transformed |
| TRE | Tetracycline responsive element |
| TRE | Tetracycline responsive element |
| TRIO | Tracing the relationships between input and output |
| TVA | Avian viral receptor |
| V0 | Ventrally-derived interneurons, subclass “0” |
| V1 | Ventrally-derived interneurons, subclass “1” |
| V2a | Ventrally-derived interneurons, subclass “2a” |
| V2b | Ventrally-derived interneurons, subclass “2b” |
| V3 | Ventrally-derived interneurons, subclass “3” |
| VAMP2 | Vesicle-associated membrane protein 2 |
| Vp/ml | Viral particles per milliliter |
| WPRE | Woodchuck hepatitis virus post-transcriptional regulatory element |

CURRICULUM VITA

AMANDA MARIE POCRATSKY
9203 Rockhurst Ct. Apt. 127, Louisville, KY 40299 (219) 395-4221
ampocr01@louisville.edu

## EDUCATION

University of Louisville, Louisville, KY February 2017
**Ph.D. in Anatomical Sciences and Neurobiology**
Mentors: Dr. David S.K. Magnuson & Dr. Scott R. Whittemore
Dissertation: Reversible silencing of spinal neurons unmasks a left-right coordination continuum

University of Louisville, Louisville, KY March 2013
**M.S. in Anatomical Sciences and Neurobiology**
Mentors: Dr. David S.K. Magnuson & Dr. Scott R. Whittemore
Thesis: Functional significance of ascending motor pathways

Purdue University, West Lafayette, IN May 2010
**B.S. in Neurobiology and Physiology**

## HONORS & AWARDS

Invited Plenary Speaker
Neuroscience Symposium, University of Louisville April 2016

1st place Excellence in Neuroscience Graduate Research Award
Neuroscience Day, University of Louisville April 2015

Invited Session Speaker
Society for Neuroscience Spinal Cord Plasticity in Motor Control Satellite Symposium, Invited Speaker
Washington, DC Nov. 2014

1st place Doctoral Basic Science Research Award
Travel Award Recipient
Research!Louisville, University of Louisville Sept. 2014

Graduate Student Council Travel Award Recipient
University of Louisville June 2014

Trainee Spotlight Invited Speaker
Kentucky Spinal Cord & Head Injury Research Trust Symposium
Lexington, KY May 2014

2nd Place Excellence in Neuroscience Graduate Research
Neuroscience Day, University of Louisville April 2014

Paralyzed Veterans of America & Mission Connect Poster Finalist Award
Travel Award Recipient
15th Annual International Symposium on Neural Regeneration
Pacific Grove, CA Dec. 2013

2nd Place Doctoral Basic Science Research Award
Travel Award Recipient
Research!Louisville Oct. 2013

Faculty Favorite Teaching Award Nominee
Nominated by medical students for teaching gross neuroanatomy
University of Louisville 2011

Graduate Student Fellowship
University of Louisville 2010-2017

## PUBLICATIONS

**Pocratsky, A.M.**, Burke, D.A., Morehouse, J.R., Beare, J.E., Riegler, A.S., Tsoulfas, P., Whittemore, S.R., Magnuson, D.S.K. *Silencing spinal interneurons: a continuum of walking to hopping* (Nature Comm, under revision).

**Pocratsky, A.M.**, Morehouse, J.R., Burke, D.A., Hardin, J.T., Riegler, A.S., Hainline, C.L., Beare, J.E., Whittemore, S.R., Magnuson, D.S.K. *Long ascending propriospinal neurons: a flexible, task-specific inter-enlargement network for left-right alternation* (in preparation).

## RESEARCH EXPERIENCE

**Animal models:** mouse and rat (neonatal, adult)

**Surgical technique:** stereotaxic intraspinal injections of fluorescent tracers and Biosafety Level 2 virus; hindlimb intramuscular injections; spinal cord injury (NYU and IH Impactor devices); tail vein injections; pre- and post-operative animal care; surgical micropipette fabrication

**Behavioral assessments:** Basso, Beattie, and Bresnahan (BBB) Open Field Locomotor Score; overground three-dimensional hindlimb kinematic and gait analyses; TreadScan™ treadmill-based gait analysis; swim and shallow water walking hindlimb kinematic and gait analyses; Louisville Swim Score assessment; beam walk assessment; ladder walk assessment; sensory testing (von Frey, tail flick)

**Electrophysiology:** transcranial magnetic motor evoked potentials (tcMMEP); magnetically-evoked inter-enlargement response (MIER); tail stimulation and gastrocnemius EMG recordings

**Histology:** transcardial perfusions; brain and spinal cord dissection (fresh and fixed tissues); tissue sectioning with cryostat and microtome; immunohistochemistry (direct fluorescence, indirect immunoperoxidase)

**Microscopy:** inverted (Nikon); confocal (Nikon, Olympus); multi-photon (Olympus); electron microscopy (Phillips CM10)

**Molecular biology:** DNA, RNA, and protein isolation; plasmid cloning; lentiviral and adeno-associated viral vector construct building; transfections and viral titering; *in vitro* pharmacological treatments; MTT assays; immunocytochemistry; primary CNS cell culture

**Computer software:** image analysis (Nikon Elements, Amira, ImageJ); video analysis (Innovision MaxTRAQ, MaxTRAQ 3D, MaxMATE, Windows Movie Maker); Adobe Suite; Microsoft Office Suite; statistical analyses (SPSS, SigmaPlot, GraphPad)

## SCIENTIFIC WRITING

**Manuscript reviews:** significantly contributed to peer review process for Journal of Neuroscience, Journal of Neurotrauma, Neurosurgery, and Experimental Neurology

**Research protocols:** wrote protocols for IACUC and IBC approval

**Grant preparation and review:** participated in trainee and faculty specific aims review and unfunded summary statement evaluation (12 proposals); was fully involved in the preparation of a successful Kentucky Spinal Cord and Head Injury Research Trust (KSCHIRT) proposal as well as a NIH R01, both on its initial submission and its subsequent successful A1 submission

## ABSTRACTS

**Pocratsky, A.M.**, Hardin, J.T., Morehouse, J.R., Riegler, A.S., Burke, D.A., Beare, J.E., Howard, R.M., Whittemore, S.R., Magnuson, D.S.K. (2015). *Long ascending*

*propriospinal neurons: a key pathway in left-right control.* Society for Neuroscience Abstract. Chicago, IL October 2015.

Magnuson, D.S.K., **Pocratsky, A.M.**, Whittemore, S.R. (2015). *Using in vivo conditional silencing to dissect the central pattern generator: emerging hierarchies*. Society for Neuroscience Abstract. Chicago, IL October 2015.

**Pocratsky, A.M.**, Riegler, A.S., Morehouse, J.R., Burke, D.A., Hardin, J.T., Howard, R.M., Magnuson, D.S.K., Whittemore, S.R. (2015). *Conditional silencing of adult rat spinal locomotor circuitry induces hopping*. 21st Annual Kentucky Spinal Cord & Head Injury Research Trust Symposium Abstract. Louisville, KY May 2015.

**Pocratsky, A.M.**, Hardin, J.T., Riegler, A.S., Morehouse, J.R., Burke, D.A., Howard, R.M., Magnuson, D.S.K., Whittemore, S.R. (2014). *Hopping rats: a short tale of long ascending propriospinal neurons and locomotion*. Spinal Cord Plasticity in Motor Control Satellite Symposium Abstract. 44th Society for Neuroscience Annual Meeting. Washington, DC November 2014. Selected as invited session speaker.

**Pocratsky, A.M.**, Riegler, A.S., Morehouse, J.R., Burke, D.A., Hardin, J.T., Howard, R.M., Magnuson, D.S.K., Whittemore, S.R. (2014). *Conditional silencing of adult rat spinal locomotor circuitry induces hopping*. Society for Neuroscience Abstract. Washington, DC November 2014.

**Pocratsky, A.M.**, Riegler, A.S., Morehouse, J.R., Burke, D.A., Hardin, J.T., Beare, J.E., Howard, R.M., Magnuson, D.S.K., Whittemore, S.R. (2014). *Hopping rats: a short tale of long ascending propriospinal neurons*. Research!Louisville Abstract. University of Louisville, Louisville, KY September 2014. Awarded 1st Place, Doctoral Basic Science Research.

**Pocratsky, A.M.**, Riegler, A.S., Morehouse, J.R., Burke, D.A., Hardin, J.T., Howard, R.M., Magnuson, D.S.K., Whittemore, S.R. (2014). *Conditional silencing of adult rat spinal locomotor circuitry induces hopping*. National Neurotrauma Society Abstract. San Francisco, CA June 2014.

**Pocratsky, A.M.**, Riegler, A.S., Morehouse, J.R., Burke, D.A., Hardin, J.T., Howard, R.M., Magnuson, D.S.K., Whittemore, S.R. (2014). *Conditional silencing of adult rat spinal locomotor circuitry induces hopping*. 20th Annual Kentucky Spinal Cord & Head Injury Research Trust Symposium Abstract. Lexington, KY May 2014. Trainee Spotlight Invited Speaker.

**Pocratsky, A.M.**, Riegler, A.S., Howard, R.M., Magnuson, D.S.K., Whittemore, S.R. (2013). *Selective and reversible silencing of lumbar locomotor circuitry in the adult rat spinal cord*. International Symposium on Neural Regeneration Abstract. Pacific Grove, CA December 2013. Paralyzed Veterans of America & Mission Connect Poster Finalist; Travel Award Recipient.

**Pocratsky, A.M.**, Riegler, A.S., Tsoulfas, P., Magnuson, D.S.K., Whittemore, S.R. (2013). *Long ascending propriospinal neurons lack direct connections to lumbar motor circuitry: functional implications for conditional silencing of neurotransmission during locomotion*. Research!Louisville Abstract. University of Louisville, Louisville, KY October 2013. Awarded 2nd Place, Doctoral Basic Science Research.

**Pocratsky, A.M.**, Magnuson, D.S.K., Whittemore, S.R. (2013). *Long ascending propriospinal neurons lack descending projection to the caudal lumbar enlargement*. National Neurotrauma Society Abstract. Nashville, TN July 2013.

## PROFESSIONAL ASSOCIATIONS

| | |
|---|---|
| National Neurotrauma Society Member | 2011-present |
| Society for Neuroscience Member | 2011-present |
| Graduate Student Council Representative | 2013-2015 |
| School of Medicine Representative; Faculty Forum | 2010-2011 |

## TEACHING

**School of Medicine neural systems clinical case instructor**
Small group instructor to medical students 2014-2015

**School of Medicine neuroanatomy teaching assistant and tutor**
Taught fundamentals of human neuroanatomy in gross lab 2011-2015

**Mentor undergraduate, graduate, and medical students in research**
Trained students on individualized research projects 2011-present